AFRL-RI-RS-TR-2008-118
Final Technical Report
April 2008

ADAPTIVE DIGITAL SIGNATURE DESIGN AND SHORT-DATA-RECORD ADAPTIVE FILTERING

The Research Foundation of State University of New York

APPROVED FOR PUBLIC RELEASE; DISTRIBUTION UNLIMITED.

STINFO COPY

AIR FORCE RESEARCH LABORATORY
INFORMATION DIRECTORATE
ROME RESEARCH SITE
ROME, NEW YORK

NOTICE AND SIGNATURE PAGE

Using Government drawings, specifications, or other data included in this document for any purpose other than Government procurement does not in any way obligate the U.S. Government. The fact that the Government formulated or supplied the drawings, specifications, or other data does not license the holder or any other person or corporation; or convey any rights or permission to manufacture, use, or sell any patented invention that may relate to them.

This report was cleared for public release by the Air Force Research Laboratory Public Affairs Office and is available to the general public, including foreign nationals. Copies may be obtained from the Defense Technical Information Center (DTIC) (http://www.dtic.mil).

AFRL-RI-RS-TR-2008-118 HAS BEEN REVIEWED AND IS APPROVED FOR PUBLICATION IN ACCORDANCE WITH ASSIGNED DISTRIBUTION STATEMENT.

FOR THE DIRECTOR:

/s/
STEPHEN P. REICHHART
Work Unit Manager

/s/
WARREN H. DEBANY, JR.
Technical Advisor, Information Grid Division
Information Directorate

This report is published in the interest of scientific and technical information exchange, and its publication does not constitute the Government's approval or disapproval of its ideas or findings.

REPORT DOCUMENTATION PAGE

Form Approved
OMB No. 0704-0188

Public reporting burden for this collection of information is estimated to average 1 hour per response, including the time for reviewing instructions, searching data sources, gathering and maintaining the data needed, and completing and reviewing the collection of information. Send comments regarding this burden estimate or any other aspect of this collection of information, including suggestions for reducing this burden to Washington Headquarters Service, Directorate for Information Operations and Reports, 1215 Jefferson Davis Highway, Suite 1204, Arlington, VA 22202-4302, and to the Office of Management and Budget, Paperwork Reduction Project (0704-0188) Washington, DC 20503.
PLEASE DO NOT RETURN YOUR FORM TO THE ABOVE ADDRESS.

1. REPORT DATE *(DD-MM-YYYY)*	2. REPORT TYPE	3. DATES COVERED *(From - To)*
APR 2008	Final	May 04 – Nov 07

4. TITLE AND SUBTITLE

ADAPTIVE DIGITAL SIGNATURE DESIGN AND SHORT-DATA-RECORD ADAPTIVE FILTERING

5a. CONTRACT NUMBER

5b. GRANT NUMBER
FA8750-04-2-0179

5c. PROGRAM ELEMENT NUMBER
62702F

6. AUTHOR(S)

Dimitiris A. Pados

5d. PROJECT NUMBER
IIUB

5e. TASK NUMBER
DP

5f. WORK UNIT NUMBER
04

7. PERFORMING ORGANIZATION NAME(S) AND ADDRESS(ES)
The Research Foundation of State University of New York
402 Crofts Hall
Amherst NY 14260-0001

8. PERFORMING ORGANIZATION REPORT NUMBER

9. SPONSORING/MONITORING AGENCY NAME(S) AND ADDRESS(ES)

AFRL/RIGC
525 Brooks Rd
Rome NY 13441-4505

10. SPONSOR/MONITOR'S ACRONYM(S)

11. SPONSORING/MONITORING AGENCY REPORT NUMBER
AFRL-RI-RS-TR-2008-118

12. DISTRIBUTION AVAILABILITY STATEMENT
APPROVED FOR PUBLIC RELEASE; DISTRIBUTION UNLIMITED. PA# WPAFB 08-2511

13. SUPPLEMENTARY NOTES

14. ABSTRACT

This report covers the research performed to create and develop a digital signature design analysis and development methodology that will support robust multi-user communications in rapidly changing environments. Short-data-record adaptive filtering analysis and development was also performed to support the multi-user signature design algorithms in terms of its performance in and application to multiple-input-multiple-output (MIMO) systems.

15. SUBJECT TERMS
Short data record, adaptive filtering, CDMA, multipath, auxiliary vector

16. SECURITY CLASSIFICATION OF:			17. LIMITATION OF ABSTRACT	18. NUMBER OF PAGES	19a. NAME OF RESPONSIBLE PERSON
a. REPORT	b. ABSTRACT	c. THIS PAGE			Stephen P. Reichhart
U	U	U	UU	147	19b. TELEPHONE NUMBER (*Include area code*) N/A

Contents

List of Figures

Fig. 15: TSC of proposed conditionally optimized signature set(under Case 1) against bound ($L = 16, 1 \leq N \leq 16$).

Fig. 16: TSC of proposed conditionally optimized signature set(under Case 2) against bound ($L = 14, 1 \leq N \leq 16$).

Fig. 17: TSC of proposed conditionally optimized signature set(under Case 3) against bound ($L = 15, 1 \leq N \leq 16$).

Fig. 18: TSC of proposed conditionally optimized signature set (under Case 4) against bound ($L = 17, 1 \leq N \leq 15$).

Fig. 19. (a) $\mathcal{G}_{31\times 24}$ Gold set with $ATSC = 43474212$. (b) Optimal signature set $\mathcal{S}^{opt}_{31\times 24}$ designed under Underloaded Case 3(ii) with $ATSC = (24)^2(31)^2(2(31)-1) = 33765696$.

Fig. 20. (a) $\mathcal{K}^{ss}_{15\times 2}$ small-set Kasami with $ATSC = 34220$. (b) Numerically generated $\mathcal{S}_{15\times 2}$ signature set with $ATSC = 33292$.

Fig. 21. (a) $\mathcal{K}^{ls}_{15\times 8}$ large-set Kasami with $ATSC = 441264$. (b) Optimal $\mathcal{S}^{opt}_{15\times 8}$ designed under Underloaded Case 3(ii) with $ATSC = (8)^2(15)^2(2(15)-1) = 417600$.

Fig. 22. Optimal signature set $\mathcal{S}^{opt}_{14\times 25}$ designed under Overloaded Case 2 with minimum $ATSC = (25)^2(14)^2(2(14)-1) + (2(14)-1)(3(14)-4) = 3308526$.

Fig. 23: P_D vs SINR (one-lag temporal clutter correlation 0.4).

Fig. 24: P_D vs SINR (one-lag temporal clutter correlation 0.6).

Fig. 25: TSC of $(K+1, L = 16)$ signature set.

Fig. 26: TSC of $(K+1, L = 31)$ signature set.

Fig. 27: AV, MUSIC, and MF spectra ($\theta_1 = -1^o, \theta_2 = 1^o$, SNR_1=SNR_2=7dB, $N = 50$).

Fig. 28: (a) Probability of resolution versus SNR (separation 3^o, $N = 50$). (b) Probability of resolution versus sample support (separation 3^o, SNR_1=SNR_2=0dB).

Fig. 29: (a) Probability of resolution versus SNR (separation 3^o, $N = 50$, correlation 70%). (b) Probability of resolution versus sample support (separation 3^o, SNR_1=SNR_2=5dB, correlation 70%).

Fig. 30: (a) Probability of resolution versus SNR (separation 3^o, $N = 50$, correlation 90%). (b) Probability of resolution versus sample support (separation

3^o, SNR_1=SNR_2=5dB, correlation 90%).

Fig. 31: Block-error-rate versus SNR (4-transmit-antenna system).

Fig. 32: Block-error-rate versus SNR for 4-QAM constellation (8-transmit-antenna system).

Fig. 33: Block-error-rate versus SNR for non-rectangular 8-QAM constellation and 16-QAM for the rate 3/4 code in [7] (8-transmit-antenna system).

Fig. 34: Code division MAC.

Fig. 35: Sensor Network Configuration.

Fig. 36: Net 1: One-hop, one-to-one transmission (L=16, K=8)

Fig. 37: Net 2: Two-hop, one-to-one transmission (L=16, K=8)

Fig. 38: Net 3: One-hop, two-to-one transmission (L=16, K=8)

Fig. 39: Net 4: One-hop, one-to-two transmission (L=16, K=8)

Fig. 40: Net 5: Four node configuration (two decode-and-forward nodes, L=16, K=8)

List of Tables

List of Acronyms

AMF	adaptive matched filter
ATSC	aperiodic total squared correlation
AV	auxiliary – vector
AWGN	additive white Gaussian noise
BER	bit – error – rate
BPSK	binary phase shift keying
CA – CFAR	cell averaging – constant false alarm rate
CDMA	code – division multiple – access
CFAR	constant false alarm rate
CPI	coherent processing interval
DOA	direction – of – arrival
DS – CDMA	direct – sequence code – division multiple – access
ESPRIT	estimation of signal parameters via rotational invariance techniques
FDMA	frequency – division multiple – access
GLR	generalized likelihood ratio
ISI	inter – symbol – interference
JNR	jammer – to – noise ratio
LMS	least – mean – squares
MAC	medium – access – control
MAI	multiple – access – interference
MF	matched filter
ML	maximum – likelihood
MMSE	minimum – mean – square – error
MSINR	maximum – SINR
MUSIC	multiple signal classification
NP – hard	nondeterministic polynomial – time hard
O – STBC	orthogonal space – time block codes
PAPR	peak – to – average – power ratio
PTSC	periodic (cyclic) total squared correlation
PEP	pairwise error probability
QAM	quadrature – amplitude – modulated
QO – STBC	quasi – orthogonal space – time block code
RLS	recursive least squares
SINR	signal – to – interference – plus – noise ratio
SMI	sample – matrix – inversion method
SNR	signal – to – noise ratio
TDMA	time – division multiple – access
TSC	total – squared – correlation
TWSC	total weighted squared correlation
ULA	uniform linear array
WBE	Welch – bound – equality
WSN	wireless sensor networks

I. Summary of Work

We developed a new algorithm to adaptively optimize binary and quaternary signatures for code-division multiple-access (CDMA) communications over multipath channels and/or asynchronous channel access. Using the observed signal autocorrelation matrix, the algorithm attempts to maximize, over the binary or quaternary antipodal sequence field, the signal-to-interference-plus-noise ratio (SINR) at the output of the maximum SINR linear filter. While this maximization problem is NP-hard, the algorithm is seen to produce in short polynomial time highly desirable solutions that approach in performance the theory-only complex/real-field optimal signature vectors. Signature adaptation may be carried out in either a single or a multi-user mode. Simulation studies offer direct performance comparisons with other known binary signature set designs and the theoretical complex/real-valued optimal vectors.

We derived new bounds on the periodic (cyclic) total squared correlation (PTSC) of binary antipodal signature sets for any number of signatures K and any signature length L. Optimal designs that achieve the new bounds are then developed for several (K, L) cases. As an example that arguably may be against common expectation, it is seen that neither the Gold nor the Kasami sets are PTSC optimal.

We developed a new method for the optimization of binary spreading codes under a rank-2 approximation of the inverse interference autocovariance matrix where the rank-2-optimal binary code is obtained in lower than quadratic complexity. Significant SINR performance improvement was demonstrated over the common binary hard-limited eigenvector design which was seen to be equivalent to the rank-1-optimal solution.

Our recent advances in the area of binary sequences for code-division multiplexing provide us with minimum total-squared-correlation (TSC) optimal signature sets for (almost) all signature lengths L and set sizes K. The sets are scalable as long as $K \leq L$ (underloaded systems) and non-scalable when $K > L$ (overloaded systems); in general the non-scalable case requires signature redesign/re-assignment as users enter or exit. We derive new lower bounds on the conditional TSC of overloaded binary signature sets built on fixed full-load TSC-optimal sets. Overloading is allowed to be as high as 100%. Scalable designs that achieve the new bounds are then developed. To evaluate the performance of the proposed designs, we compared the TSC of our constructions to the unconditionally minimum achievable TSC values.

We derived new bounds on the aperiodic total squared correlation (ATSC) of binary antipodal signature sets for any number of signatures K and any signature length L. We then presented optimal designs that achieve the new bounds for several (K, L) cases. As an example, we proved that the familiar Gold and (small or large) Kasami designs are not ATSC-optimal in general. The optimal

signature set designs that we provide are, in this sense, better suited for asynchronous and/or multipath code-division multiplexing applications.

We developed a binary signature design procedure to scale upwards overloaded minimum total-squared-correlation (TSC) binary signature sets. The quality of the design is measured against the recently published binary TSC bounds.

We revisited the classical problem of detecting a complex signal of unknown amplitude in colored Gaussian noise in the context of adaptive detection with limited training data via the auxiliary-vector (AV) filter estimation algorithm. Based on statistical conditional optimization criteria, the iterative AV algorithm starts from the target vector and, adding non-orthogonal auxiliary vector components, generates an infinite sequence of tests that converges to the ideal matched filter (MF) processor for any positive definite input autocorrelation matrix. Computationally, the algorithm is a simple recursive procedure that avoids explicit matrix inversion, decomposition, or diagonalization operations. When the input autocorrelation matrix is replaced by a conventional sample-average estimate, the algorithm effectively generates a sequence of MF estimators; their bias converges rapidly to zero and the covariance trace rises slowly and asymptotically to the covariance trace of the familiar adaptive matched filter (AMF). For finite data records, the generated sequence of estimators offers favorable bias/covariance balance and members of the sequence are seen to outperform in probability of detection (for any given false alarm rate) all known and tested adaptive detectors (for example AMF and the multistage Wiener filter algorithm). These issues are addressed in the context of joint space-time adaptive processing for array radar.

We developed a new subspace direction-of-arrival (DOA) estimation procedure that utilizes a non-eigenvector basis. Computation of the basis is carried out by a modified version of the orthogonal auxiliary-vector (AV) filtering algorithm. The procedure starts with the linear transformation of the array response scanning vector by the input autocorrelation matrix. Then, successive orthogonal maximum cross-correlation auxiliary vectors are calculated to form a basis for the scanner-extended signal subspace. As a performance evaluation example, our studies for uncorrelated sources demonstrated a gain in the order of 15dB over MUSIC, 7dB over ESPRIT, and 3dB over the grid-search maximum likelihood DOA estimator at probability of resolution 0.9 with a ten-element array and reasonably small observation data records. Results for correlated sources are reported as well.
An alternative form of the 8×8 two-symbol decodable quasi-orthogonal space-time block code (QO-STBC) that can be transmitted across either 4 or 8 antennas with full rate and full diversity order is presented. For the 8 transmit antenna system, we derive a new expression for the rotation angles that maximize the diversity (eigenvalue) product. In addition, we show that the previously proposed sum-eigenvalue maximization criterion for the design of rotation

angles is not relevant/applicable and we suggest, as an alternative, minimum eigenvalue maximization. Finally, working directly with the pairwise-error-probability (PEP) upper-bound expression, we obtain new true PEP-upper-bound optimal rotation angles. For 4 transmit antenna systems and correlated channel fading conditions, we modify our PEP-upper-bound to account for channel correlation. Using the new PEP-upper-bound we obtain rotation angles that maximize the diversity product and find, contrary to previous results, that the optimized angles are independent of the correlation coefficient. Simulation studies initiated herein demonstrate the advantage of using the proposed codeword across 4 transmit antennas when compared with other 4×4 QO-STBC transmission schemes. For 8 transmit antennas, the studies compare the three selected rotation angle optimization criteria (diversity product, minimum eigenvalue, PEP-upper-bound).

Finally, we considered the problem of signature waveform design for code division medium-access-control (MAC) of wireless sensor networks (WSN). In contrast to conventional randomly chosen orthogonal codes, we developed an adaptive signature design strategy under the maximum pre-detection SINR (signal to interference plus noise ratio) criterion. The proposed algorithm utilizes slowest descent cords of the optimization surface to move toward the optimum solution and exhibits, upon eigenvector decomposition, linear computational complexity with respect to signature length. Numerical and simulation studies demonstrate the performance of the proposed method and offer comparisons with conventional signature code sets.

II. Adaptive Optimization of Binary/Quaternary CDMA Signatures in Asynchronous Multipath Environments

Part of the work reported in this section, namely adaptive optimization of binary signatures, has been presented at IEEE MILCOM 2005, Atlantic City, NJ.

In direct-sequence code-division multiple-access (DS-CDMA) communication systems, multiple users/signals with individual identifying signature waveforms occupy the same channel in frequency and time. Alleviation of the resulting multiple-access-interference (MAI) problem relies on proper design of the user signatures and receivers under a separate or joint consideration.

In the past, several optimization metrics and system configurations were considered. For example, [1],[2] minimize iteratively the total-squared-correlation (TSC) of the signature set; convergence results are reported in [3]. A generalized version of the problem with a multiple base station configuration is considered in [6] and [5]. Signatures that maximize user capacity for a given signal-to-interference-plus-noise (SINR) level are sought in [6]. Under a multipath channel assumption, [7] carries out signature adaptation to maximize the SINR at the output of the RAKE-filter receivers. The same problem is considered in [8] with signature optimization over a reduced-rank vector space and minimum-mean-square-error (MMSE) receivers. Signature adaptation for multiuser MMSE minimization is described in [9].

In digital communication systems, it is necessary to have signature sets that are defined over a finite alphabet. Yet, all previous design efforts described above deal with complex (or real) field signatures. Recently, TSC-optimal *binary* signature sets were reported for nearly all signature lengths and set sizes [10]-[4]; their sum capacity is identified in [5]. The sum capacity of several other binary designs is calculated in [6].

A binary signature that has minimum sum of squared correlations with the other multiple-access signature codes is also maximum SINR optimal under MMSE filtering and synchronous, equal-power CDMA transmissions over (additive white Gaussian noise) ideal Nyquist channels. This is certainly not the case for asynchronous multiple access protocols and/or multipath channels. To the best of the knowledge of the authors, the only finite-alphabet adaptive signature optimization effort for asynchronous/multipath channels reported in the literature is [15]. In this present work, we attempt to build on and improve upon [15] working in the binary $\{\pm 1\}$ or quaternary $\{\pm 1, \pm i\}$ field. Specifically, we develop a new adaptive signature design procedure that maximizes the output SINR of the MMSE receiver filter. At nominal increase in computational cost, the proposed procedure offers significant performance improvement over [15]. In fact, as seen in the studies included herein, our designs over the restricted binary/quaternary field exhibit little performance loss in comparison with the theoretical complex-field optimal solutions.

A. Signal model

We consider a DS-CDMA system with K users and processing gain (signature length) L. The uplink (downlink) transmission from (to) user k, $k = 0, 1, \ldots, K-1$, is denoted by

$$u_k = \sum_{m=1}^{\infty} b_k(m)\sqrt{E_k}s_k\left(t - mT\right)e^{j(2\pi f_c t + \phi_k)} \tag{1}$$

where $b_k(m) \in \{-1, +1\}$ is the mth data bit (binary phase-shift-keying data modulation), E_k is the total transmission energy, and ϕ_k is the carrier phase with carrier frequency f_c; $s_k(t)$ is the normalized unit-energy user signature waveform with duration T given by

$$s_k(t) = \sum_{l=0}^{L-1} \mathbf{s}_k(l)\psi(t - lT_c) \tag{2}$$

where $\mathbf{s}_k(l),\ l = 0, 1, \ldots, L-1$, is the value of the lth chip of the spreading-code vector of the kth user ($\mathbf{s}_k$ is in $\{\pm 1\}^L$ if binary or $\{\pm 1, \pm i\}^L$ if quaternary), $\psi(t)$ is the chip waveform, and $T_c = \frac{T}{L}$ is the chip period.

The user signals propagate over multipath additive white Gaussian noise channels. The path coefficients are modeled as complex Gaussian random variables (Rayleigh amplitude and uniform phase) that are independent across paths and user signals (if uplink transmissions are considered) and remain constant during the signature adaptation period of several symbol intervals (quasi-static fading). The compound received signal due to all users after channel "processing" and carrier demodulation is given by

$$r(t) = \sum_{k=0}^{K-1} \sqrt{E_k} \sum_{m} b_k(m) \sum_{n=0}^{N-1} \alpha_{k,n} s_k\left(t - mT - nT_c - \tau_k\right) + n(t) \tag{3}$$

where N denotes the number of resolvable paths, $\alpha_{k,n},\ k = 0, 1, \ldots, K-1,\ n = 0, 1, \ldots, N-1$, is the nth path, kth user, fading coefficient, $\tau_k \in [0, T)$ is the relative delay of user k with respect to user 0 with $\tau_0 = 0$, and $n(t)$ is a complex additive white Gaussian noise (AWGN) process.

Assuming synchronization with the signal of the user of interest k, after chip-matched filtering of $r(t)$ and sampling at the chip rate over a multipath extended bit period we obtain the data vector $\mathbf{r}_k(m) \in \mathbb{C}^{L+N-1}$ of the form

$$\mathbf{r}_k(m) = \sqrt{E_k} b_k(m)\mathbf{H}_k\mathbf{s}_k + \mathbf{z}_k + \mathbf{i}_k + \mathbf{n}_k, \quad m = 1, 2, \ldots, \tag{4}$$

where $\mathbf{z}_k \in \mathbb{C}^{L+N-1}$ represents comprehensively multiple-access-interference (MAI) to user k, $\mathbf{i}_k \in \mathbb{C}^{L+N-1}$ denotes channel induced inter-symbol-interference (ISI), and $\mathbf{n}_k \in \mathbb{C}^{L+N-1}$ is a zero mean complex Gaussian noise vector with covariance matrix $E\left\{\mathbf{n}_k\mathbf{n}_k^H\right\} = \sigma^2\mathbf{I}$ ($E\{\cdot\}$ denotes statistical expectation and H is the conjugate transpose operator). In (4), $\mathbf{H}_k\mathbf{s}_k \in \mathbb{C}^{L+N-1}$ is the channel processed signature of user k where

$$\mathbf{H}_{k\,(L+N-1)\times L} = \begin{bmatrix} \alpha_{k,0} & 0 & \cdots & 0 \\ \alpha_{k,1} & \alpha_{k,0} & & \vdots \\ \vdots & \vdots & & \vdots \\ \alpha_{k,N-1} & \alpha_{k,N-2} & \cdots & 0 \\ 0 & \alpha_{k,N-1} & \cdots & 0 \\ \vdots & \vdots & & \vdots \\ 0 & 0 & \cdots & \alpha_{k,0} \\ 0 & 0 & \cdots & \alpha_{k,1} \\ \vdots & \vdots & & \vdots \\ 0 & 0 & \cdots & \alpha_{k,N-1} \end{bmatrix}. \tag{5}$$

For data bit detection purposes, we consider linear minimum-mean-square-error (MMSE) filter receivers with sign-real-part detectors,

$$\hat{b}_k = sgn\left(Re\left\{\mathbf{w}_{MMSE,k}^H \mathbf{r}_k\right\}\right), \quad k = 0, 1, \ldots, K-1, \tag{6}$$

where $\mathbf{w}_{MMSE,k} = c\mathbf{R}_k^{-1}\mathbf{H}_k\mathbf{s}_k \in \mathbb{C}^{L+N-1}$, $\mathbf{R}_k \stackrel{\triangle}{=} E\{\mathbf{r}_k\mathbf{r}_k^H\}$ and $c > 0$. The output SINR of the (maximum SINR) filter $\mathbf{w}_{MMSE,k}$ is a direct function of the binary/quaternary signature $\mathbf{s}_k$:

$$\mathrm{SINR}_{MMSE,k}(\mathbf{s}_k) = \frac{E\left\{\left|\mathbf{w}_{MMSE,k}^H(\sqrt{E_k}b_k\mathbf{H}_k\mathbf{s}_k)\right|^2\right\}}{E\left\{\left|\mathbf{w}_{MMSE,k}^H\left(\mathbf{z}_k + \mathbf{i}_k + \mathbf{n}_k\right)\right|^2\right\}} = E_k\left(\mathbf{s}_k^H\mathbf{H}_k^H\tilde{\mathbf{R}}_k^{-1}\mathbf{H}_k\mathbf{s}_k\right) \tag{7}$$

where $\tilde{\mathbf{R}}_k$ is the autocorrelation matrix of the disturbance-only part of the input vector defined by

$$\tilde{\mathbf{R}}_k \stackrel{\triangle}{=} E\left\{(\mathbf{z}_k + \mathbf{i}_k + \mathbf{n}_k)(\mathbf{z}_k + \mathbf{i}_k + \mathbf{n}_k)^H\right\}. \tag{8}$$

Viewing the pre-detection SINR expression in (7) as a function of the signature $\mathbf{s}_k$ in $\{\pm 1\}^L$ or $\{\pm 1, \pm j\}^L$ motivates a maximization search over the binary or quaternary field, respectively. In the following section, we present such an adaptive signature optimization scheme.

B. The algorithm

A rather realistic assumption for CDMA communication systems is that the ISI influence is negligible in comparison with the MAI and AWGN disturbance. In this context, we can safely approximate $\tilde{\mathbf{R}}_k$ in (8) by $\tilde{\mathbf{R}}_k \simeq E\left\{(\mathbf{z}_k + \mathbf{n}_k)(\mathbf{z}_k + \mathbf{n}_k)^H\right\}$, which makes $\tilde{\mathbf{R}}_k$ independent of $\mathbf{s}_k$ and greatly simplifies the problem of maximizing $\mathrm{SINR}_{MMSE,k}(\mathbf{s}_k)$ with respect to $\mathbf{s}_k$. The maximization criterion takes the form

$$\mathbf{s}_k = \underset{\mathbf{s}_k \in \{\pm 1\}^L \text{ or } \{\pm 1, \pm i\}^L}{argmax} \left\{\mathbf{s}_k^H\mathbf{H}_k^H\tilde{\mathbf{R}}_k^{-1}\mathbf{H}_k\mathbf{s}_k\right\} \tag{9}$$

and $\mathbf{H}_k^H \tilde{\mathbf{R}}_k^{-1} \mathbf{H}_k$ is treated as an $L \times L$ matrix term that does not involve $\mathbf{s}_k$. Since $\tilde{\mathbf{R}}_k$ is Hermitian 4positive definite by definition, $\mathbf{H}_k^H \tilde{\mathbf{R}}_k^{-1} \mathbf{H}_k$ is also Hermitian positive definite and can be Cholesky decomposed as first suggested in [15]:

$$\mathbf{A}_k^H \mathbf{A}_k = \mathbf{H}_k^H \tilde{\mathbf{R}}_k^{-1} \mathbf{H}_k \tag{10}$$

where $\mathbf{A}_k$ is an $L \times L$ upper triangular matrix.

Upon Cholesky decomposition of $\mathbf{H}_k^H \tilde{\mathbf{R}}_k^{-1} \mathbf{H}_k$, the quantity under maximization in (9) becomes

$$\mathbf{s}_k^H \mathbf{A}_k^H \mathbf{A}_k \mathbf{s}_k = \|\mathbf{A}_k \mathbf{s}_k\|^2. \tag{11}$$

Therefore, the objective is the selection of the signature (binary or quaternary) that maximizes the norm of the vector

$$\mathbf{u}_k \stackrel{\triangle}{=} \mathbf{A}_k \mathbf{s}_k = \begin{bmatrix} \mathbf{a}_{k,1} & \mathbf{a}_{k,2} & \dots & \mathbf{a}_{k,L} \end{bmatrix} \begin{bmatrix} \mathbf{s}_k(1) \\ \mathbf{s}_k(2) \\ \vdots \\ \mathbf{s}_k(L) \end{bmatrix} \tag{12}$$

where $\mathbf{a}_{k,j}$ represents the jth column of $\mathbf{A}_k$, $j = 1, \dots, L$. The norm-square in question is given by

$$\begin{aligned} \|\mathbf{u}_k\|^2 = \; & \|\mathbf{a}_{k,L}\|^2 + \|\mathbf{a}_{k,L-1}\|^2 + \ldots + \|\mathbf{a}_{k,1}\|^2 + \\ & 2Re\{\mathbf{a}_{k,L-1}^H \mathbf{a}_{k,L} \mathbf{s}_k^*(L-1)\mathbf{s}_k(L)\} + 2Re\{\mathbf{a}_{k,L-2}^H \mathbf{a}_{k,L} \mathbf{s}_k^*(L-2)\mathbf{s}_k(L)\} + \ldots + \\ & 2Re\{\mathbf{a}_{k,1}^H \mathbf{a}_{k,L} \mathbf{s}_k^*(1)\mathbf{s}_k(L)\} + 2Re\{\mathbf{a}_{k,L-2}^H \mathbf{a}_{k,L-1} \mathbf{s}_k^*(L-2)\mathbf{s}_k(L-1)\} + \\ & 2Re\{\mathbf{a}_{k,L-3}^H \mathbf{a}_{k,L-1} \mathbf{s}_k^*(L-3)\mathbf{s}_k(L-1)\} + \ldots + \\ & 2Re\{\mathbf{a}_{k,1}^H \mathbf{a}_{k,L-1} \mathbf{s}_k^*(1)\mathbf{s}_k(L-1)\} + \ldots + 2Re\{\mathbf{a}_{k,1}^H \mathbf{a}_{k,2} \mathbf{s}_k^*(1)\mathbf{s}_k(2)\} \end{aligned} \tag{13}$$

where * denotes conjugation.

The proposed algorithm works in a sequential manner assigning values to chips $\mathbf{s}_k(L), \mathbf{s}_k(L-1), \dots, \mathbf{s}_k(1)$ one at a time, in an attempt to maximize the norm in (13). Since (13) is quadratic, we can start by assigning $\mathbf{s}_k(L) = 1$ without loss of optimality. Having set $\mathbf{s}_k(L)$, the value of $\mathbf{s}_k(L-1)$ that maximizes (13) is given by

$$\begin{aligned} \mathbf{s}_k(L-1) \quad = \quad & \underset{\mathbf{s}_k(L-1) \in \{\pm 1\} \text{ or } \{\pm 1, \pm i\}}{argmax} \Big\{ Re\{\mathbf{a}_{k,L-1}^H \mathbf{a}_{k,L} \mathbf{s}_k^*(L-1)\mathbf{s}_k(L)\} + \\ & Re\{\mathbf{a}_{k,L-2}^H \mathbf{a}_{k,L-1} \mathbf{s}_k^*(L-2)\mathbf{s}_k(L-1)\} + \ldots + \\ & Re\{\mathbf{a}_{k,1}^H \mathbf{a}_{k,L-1} \mathbf{s}_k^*(1)\mathbf{s}_k(L-1)\} \Big\}. \end{aligned} \tag{14}$$

If we treat $\mathbf{s}_k(1), \dots, \mathbf{s}_k(L-2)$ as fixed unknown parameters, the value of $\mathbf{s}_k(L-1) \in \{\pm 1\}$ that maximizes (14) is

$$\mathbf{s}_k(L-1) = sgn\left\{ Re\{\mathbf{a}_{k,L-1}^H \mathbf{a}_{k,L}\} \mathbf{s}_k(L) \right\}; \tag{15}$$

the value of $\mathbf{s}_k(L-1) \in \{\pm 1, \pm i\}$ that maximizes (14) is

$$\mathbf{s}_k(L-1) = \begin{cases} sgn\left\{ Re\{\mathbf{a}_{k,L-1}^H \mathbf{a}_{k,L} \mathbf{s}_k(L)\} \right\}, & if \; \left| Re\{\mathbf{a}_{k,L-1}^H \mathbf{a}_{k,L} \mathbf{s}_k(L)\} \right| > \\ & \qquad \left| Im\{\mathbf{a}_{k,L-1}^H \mathbf{a}_{k,L} \mathbf{s}_k(L)\} \right| \\ sgn\left\{ Im\{\mathbf{a}_{k,L-1}^H \mathbf{a}_{k,L} \mathbf{s}_k(L)\} \right\} i, & otherwise. \end{cases} \tag{16}$$

We proceed similarly to calculate the values of the remaining chips $\mathbf{s}_k(L-j),\ j=2,3,\ldots,L-1$, treating the lower indexed chips $\mathbf{s}_k(1),\mathbf{s}_k(2),\ldots,\mathbf{s}_k(L-j-1)$ as unknown fixed parameters. If $\mathbf{s}_k(L-j)\ \in\ \{\pm 1\},\ \ j=2,3,\ldots,L-1$, then

$$\mathbf{s}_k(L-j)=sgn\Big\{Re\{\mathbf{a}_{k,L-j}^H\mathbf{a}_{k,L}\}\mathbf{s}_k(L)+Re\{\mathbf{a}_{k,L-j}^H\mathbf{a}_{k,L-1}\}\mathbf{s}_k(L-1)+\ldots+ Re\{\mathbf{a}_{k,L-j}^H\mathbf{a}_{k,L-j+1}\}\mathbf{s}_k(L-j+1)\Big\}; \tag{17}$$

if $\mathbf{s}_k(L-j)\ \in\ \{\pm 1,\pm i\},\ \ j=2,3,\ldots,L-1$, then

$$\mathbf{s}_k(L-j)=\begin{cases} sgn\Big\{Re\Big\{\mathbf{a}_{k,L-j}^H\mathbf{a}_{k,L}\mathbf{s}_k(L)+\mathbf{a}_{k,L-j}^H\mathbf{a}_{k,L-1}\mathbf{s}_k(L-1)+\ldots+ \mathbf{a}_{k,L-j}^H\mathbf{a}_{k,L-j+1}\mathbf{s}_k(L-j+1)\Big\}\Big\}, \\ if\ \ \Big|Re\Big\{\mathbf{a}_{k,L-j}^H\mathbf{a}_{k,L}\mathbf{s}_k(L)+\ldots+\mathbf{a}_{k,L-j}^H\mathbf{a}_{k,L-j+1}\mathbf{s}_k(L-j+1)\Big\}\Big|> \\ \quad\Big|Im\Big\{\mathbf{a}_{k,L-j}^H\mathbf{a}_{k,L}\mathbf{s}_k(L)+\ldots+\mathbf{a}_{k,L-j}^H\mathbf{a}_{k,L-j+1}\mathbf{s}_k(L-j+1)\Big\}\Big| \\ sgn\Big\{Im\Big\{\mathbf{a}_{k,L-j}^H\mathbf{a}_{k,L}\mathbf{s}_k(L)+\mathbf{a}_{k,L-j}^H\mathbf{a}_{k,L-1}\mathbf{s}_k(L-1)+\ldots+ \mathbf{a}_{k,L-j}^H\mathbf{a}_{k,L-j+1}\mathbf{s}_k(L-j+1)\Big\}\Big\}i, \quad otherwise. \end{cases} \tag{18}$$

The above sequential scheme provides the first signature, $\mathbf{s}_k^{(1)}$, in what we call the *signature candidate set*. The complete candidate set is created as follows. For binary signatures and $n=2,3,\ldots,L-1$, initialize

$$\mathbf{s}_k^{(n)}(L-n+1)=-\mathbf{s}_k^{(1)}(L-n+1)\ \text{ and }\ \mathbf{s}_k^{(n)}(j)=\mathbf{s}_k^{(1)}(j), j=L-n+2,\ldots,L, \tag{19}$$

and optimize recursively $\mathbf{s}_k^{(n)}(L-n),\mathbf{s}_k^{(n)}(L-n-1),\ldots,\mathbf{s}_k^{(n)}(1)$ by (17). For quaternary sequences and $n=2,3,\ldots,L-1$, $p=1,2,3$, initialize

$$\mathbf{s}_k^{(3(n-2)+p+1)}(L-n+1)=i^p\mathbf{s}_k^{(1)}(L-n+1)\ \text{ and }\ \mathbf{s}_k^{(3(n-2)+p+1)}(j)=\mathbf{s}_k^{(1)}(j), \quad j=L-n+2,\ldots,L, \tag{20}$$

and optimize recursively $\mathbf{s}_k^{(3(n-2)+p+1)}(L-n),\mathbf{s}_k^{(3(n-2)+p+1)}(L-n-1),\ldots,$ $\mathbf{s}_k^{(3(n-2)+p+1)}(1)$ by (18).

The described algorithm gives a set of $L-1$ candidate binary signatures or $3(L-2)+1$ quaternary signatures. Among them, we choose the one that maximizes (13).

C. Computational complexity

The computational cost to obtain the first signature of the candidate set, $\mathbf{s}_k^{(1)}$, is $O(L^3)$. At first sight, it may seem that to fill in the candidate set with $L-1$ binary signatures or $3(L-2)+1$ quaternary signatures amounts to $O(L^4)$. Yet, taking advantage of the inherent redundancy in (19) or (20) we can keep the complexity at $O(L^3)$. Consider, for example, the binary signature case and calculate the above-the-diagonal part of the $L\times L$ matrix $\mathbf{T}=Re\{\mathbf{A}_k^H\mathbf{A}_k\},\ \ T_{i,j},\ i,j=1,\ldots,L,\ i<j$. The entry $T_{i,j},\ i<j$, corresponds

to the criterion function term $Re\{\mathbf{a}_{k,i}^H \mathbf{a}_{k,j}\}\mathbf{s}_k(i)\mathbf{s}_k(j)$ in (13). Maximization of (13) is equivalent to finding an assignment for $\mathbf{s}_k(l), l = 1, \ldots, L$, that maximizes the sum of the matrix elements $\sum_{i<j} T_{i,j}$ (this problem falls under the class of *quadratic integer programming* problems which are known to be NP-hard [16]). Once $T_{i,j},\ i < j$, are calculated, we can form the first signature of the candidate set via the iteration

$$\begin{array}{l} \mathbf{s}_k^{(1)}(L-l) = sgn\{T_{L-l,L-l+1}\mathbf{s}_k^{(1)}(L-l+1) + \ldots + T_{L-l,\,L}\mathbf{s}_k^{(1)}(L)\}, \\ l = 1, 2, \ldots, L-1,\ \ \mathbf{s}_k^{(1)}(L) = 1. \end{array} \tag{21}$$

Then, the other candidate set signatures $\mathbf{s}_k^{(n)},\ n = 2, 3, \ldots, L-1$, are calculated as follows:

$$\begin{array}{l} \mathbf{s}_k^{(n)}(j) = \mathbf{s}_k^{(1)}(j),\ j = L-n+2, \ldots, L,\ \ \mathbf{s}_k^{(n)}(L-n+1) = -\mathbf{s}_k^{(1)}(L-n+1), \\ \mathbf{s}_k^{(n)}(L-l) = sgn\{T_{L-l,L-l+1}\mathbf{s}_k^{(n)}(L-l+1) + \ldots + T_{L-l,\,L}\mathbf{s}_k^{(n)}(L)\}, \\ l = n, \ldots, L-1. \end{array} \tag{22}$$

The total computational cost of the algorithm as implemented above is the cost of the Cholesky decomposition, plus calculation of $T_{i,j},\ i < j$, plus the cost of iterations (21) and (22). That is,

$$\text{Computational complexity} = \frac{L^3}{6} + \frac{L(L+1)(L-1)}{6} + \frac{L(L-1)}{2} + \frac{L(L-1)(2L-1)}{6} \equiv O(L^3). \tag{23}$$

For quaternary signatures the cost of (22) increases by a factor of 3, but the overall complexity remains $O(L^3)$. In either case, binary or quaternary, the trade-off in keeping the computational complexity at $O(L^3)$ (instead of $O(L^4)$) is the space requirement of $O(L^2)$ for the matrix $\mathbf{T}$. We conclude that the proposed signature optimization procedure has little overhead in comparison with [15]. In fact, at a higher level of system abstraction both schemes are bounded only by the cost of inverting $\tilde{\mathbf{R}}_k,\ \ O\left((L+N-1)^3\right)$.

D. Simulation studies

In this section, we compare the performance of the proposed signature optimization algorithm (binary and quaternary) against the following benchmarks: (i) The maximum-eigenvalue eigenvector of $\mathbf{H}_k^H \tilde{\mathbf{R}}_k^{-1} \mathbf{H}_k$, denoted by max-EV, which is the theoretical maximum SINR signature solution over the $\mathbb{C}^L$ field (cf. (7)); (ii) the binary and (iii) quaternary minimum Euclidean distance quantized versions of max-EV; and (iv) the algorithm in [15] where binary conditional maximization of a modified version of (11) was considered[1].

In Fig. 1, we consider the uplink multipath DS-CDMA signal model of Section II with spreading gain $L = 16$ and we assume the presence of $K = 8$ users. Each user signal experiences $N = 3$ paths with coefficents (zero-mean complex Gaussian random variables) of equal power. Then, following the notation of

[1] In [15], ad hoc posterior bit flipping tests after conditional maximization were executed that improved the final reported SINR performance. This is not considered/accounted for herein.

Section II, the *total average received SNR* for user k, $k = 0, 1, \ldots, 7$, over all paths is

$$\mathrm{SNR}_k \triangleq \frac{E_k \sum_{n=0}^{2} E\left\{|\alpha_{k,n}|^2\right\}}{\sigma^2} = \frac{E_k E\left\{||\boldsymbol{\alpha}_k||^2\right\}}{\sigma^2}. \tag{24}$$

We set $\mathrm{SNR}_{0-2} = 8\mathrm{dB}$, $\mathrm{SNR}_{3-5} = 9\mathrm{dB}$, $\mathrm{SNR}_{6,7} = 10\mathrm{dB}$. We initialize the signature set $\mathbf{s}_0, \mathbf{s}_1, \ldots, \mathbf{s}_7$ arbitrarily and execute each signature set design algorithm sequentially user-after-user in what we call a *multiuser adaptation cycle*. Several multiuser adaptation cycles are carried out. A fixed Walsh-Hadamard signature assignment is also included in the study to challenge, potentially, the notion of signature adaptivity. In Fig. 1, we plot the pre-detection SINR of a representative user per adaptation cycle averaged over $1,000$ random channel realizations and initial signature assignments. All algorithms are seen to converge in about three cycles. The proposed procedure offers superior performance for both binary and quaternary alphabets. The (non-adaptive) Walsh-Hadamard signature assignment, as expected arguably, exhibits rather poor performance. It is interesting to observe that under the proposed optimization scheme, upgrading the signature domain from binary to quaternary provides close to 0.8dB gain, while upgrading the domain from quaternary to the full complex field provides only 0.52dB additional gain.

In Fig. 2, we repeat the same study for a system with processing gain $L = 31$ and $K = 16$ users with SNR values $\mathrm{SNR}_{0-3} = 8\mathrm{dB}$, $\mathrm{SNR}_{4-7} = 9\mathrm{dB}$, $\mathrm{SNR}_{8-11} = 10\mathrm{dB}$, $\mathrm{SNR}_{12-15} = 11\mathrm{dB}$. A (non-adaptive) Gold signature assignment is included in the comparisons which, arguably contrary to common belief, fails disappointingly to withstand the asynchronous multipath environment. In terms of the adaptive signature design schemes, the conclusions are similar to the ones drawn from Fig. 1.

In Fig. 3, we repeat the study of Fig. 2 under finite sample support estimation of the signal autocorrelation matrix and plot the average pre-detection SINR against data record size after the third multiuser adaptation cycle. The dominance of the proposed signature design scheme (that does not rely on eigenvector estimates) is now even more prominent. In fact, both Cholesky-based algorithms (the proposed binary/quaternary and the binary conditional maximization procedure of [15]) experience lower performance degradation than the eigen-decomposition-based schemes.

Finally, to illustrate the performance of the signature design algorithms under single-user adaptation, in Fig. 4 we plot the bit-error-rate (BER) of a representative user versus SNR when the signal autocorrelation matrix is estimated from $3(L + N - 1)$ samples and all interferers have fixed, non-adapted Gold signature assignments. The comparative findings are no different than those obtained in Figs. 1-3 under the SINR metric and multiuser adaptation.

E. Conclusions

We considered the problem of adaptive signature optimization for CDMA communications in asynchronous mode of operation and/or multipath signal

propagation environments. Contrary to past and current research literature, we pursued finite-alphabet signature designs, binary and quaternary, in particular.

Finite-alphabet optimization of signatures is NP-hard. The proposed suboptimal algorithm described and studied in this report has computational complexity $O(L^3)$ and storage complexity $O(L^2)$ where L is the signature length under consideration. The algorithm can be viewed as a truly practical means for either single-user signature optimization or multi-user signature set optimization since no exchange of information between users is required.

Performance-wise, it is satisfying -and somewhat surprising arguably- to see that the quaternary adaptive designs are less than 1dB away in attained SINR from the theoretical complex-field-optimal signatures. Being a Cholesky-based procedure, the algorithm has favorable small-sample-support behavior; $3L$ or $4L$ data vectors suffice for effective adaptation, which is well within the coherence time of common commercial wireless channels.

References

[1] S. Ulukus and R. D. Yates, "Iterative construction of optimum signature sequence sets in synchronous CDMA systems," *IEEE Trans. Inform. Theory*, vol. 47, pp. 1989-1998, July 2001.

[2] C. Rose, S. Ulukus, and R. D. Yates, "Wireless systems and interference avoidance," *IEEE Trans. Wireless Commun.*, vol. 1, pp. 415-428, July 2002.

[3] P. Anigstein and V. Anantharam, "Ensuring convergence of the MMSE iteration for interference avoidance to the global optimum," *IEEE Trans. Inform. Theory*, vol. 49, pp. 873-885, Apr. 2003.

[4] P. Cotae, "Spreading sequence design for multiple cell synchronous DS-CDMA systems under total weighted squared correlation criterion," *EURASIP Journal Wireless Comm. and Networking*, vol. 2004, no. 1, pp. 4-11, Aug. 2004.

[5] O. Popescu and C. Rose, "Sum capacity and TSC bounds in collaborative multibase wireless systems," *IEEE Trans. Inform. Theory*, vol. 50, pp. 2433-2440, Oct. 2004.

[6] P. Viswanath, V. Anantharam, and D. N. C. Tse, "Optimal sequences, power control, and user capacity of synchronous CDMA systems with linear MMSE multiuser receivers," *IEEE Trans. Inform. Theory*, vol. 45, Sept. 1999, pp. 1968-1983.

[7] G. S. Rajappan and M. L. Honig, "Spreading code adaptation for DS-CDMA with multipath," in *Proc. IEEE MILCOM*, vol. 2, Los Angeles, CA, Oct. 2000, pp. 1164-1168.

[8] G. S. Rajappan and M. L. Honig, "Signature sequence adaptation for DS-CDMA with multipath," *IEEE J. Select. Areas Commun.*, vol. 20, pp. 384-395, Feb. 2002.

[9] J. I. Concha and S. Ulukus, "Optimization of CDMA signature sequences in multipath channels," in *Proc. IEEE Vehic. Tech. Conf.*, vol. 3, Rhodes, Greece, May 2001, pp. 1978-1982.

[10] G. N. Karystinos and D. A. Pados, "New bounds on the total squared correlation and optimum design of DS-CDMA binary signature sets," *IEEE Trans. Commun.*, vol. 51, pp. 48-51, Jan. 2003.

[11] C. Ding, M. Golin, and T. Klϕve, "Meeting the Welch and Karystinos-Pados bounds on DS-CDMA binary signature sets," *Des., Codes Cryptogr.*, vol. 30, pp. 73-84, Aug. 2003.

[12] P. Ipatov, "On the Karystinos-Pados bounds and optimal binary DS-CDMA signature ensembles," *IEEE Commun. Letters*, vol. 8, pp. 81-83, Feb. 2004.

[13] G. N. Karystinos and D. A. Pados, "The maximum squared correlation, sum capacity, and total asymptotic efficiency of minimum total-squared-correlation binary signature sets," *IEEE Trans. Inform. Theory*, vol. 51, pp. 348-355, Jan. 2005.

[14] F. Vanhaverbeke and M. Moeneclaey, "Sum capacity of equal-power users in overloaded channels," *IEEE Trans. Inform. Theory*, vol. 53, pp. 228-233, Feb. 2005.

[15] G. N. Karystinos and D. A. Pados, "Adaptive assignment of binary user spreading codes in DS-CDMA systems," in *Proc. of SPIE*, vol. 4395, Orlando, FL, Apr. 2001, pp. 137-144.

[16] T. H. Cormen, C. E. Leiserson, R. L. Rivest and C. Stein, *Introduction to Algorithms*. Cambridge, MA: MIT Press, 2001, 2nd ed.

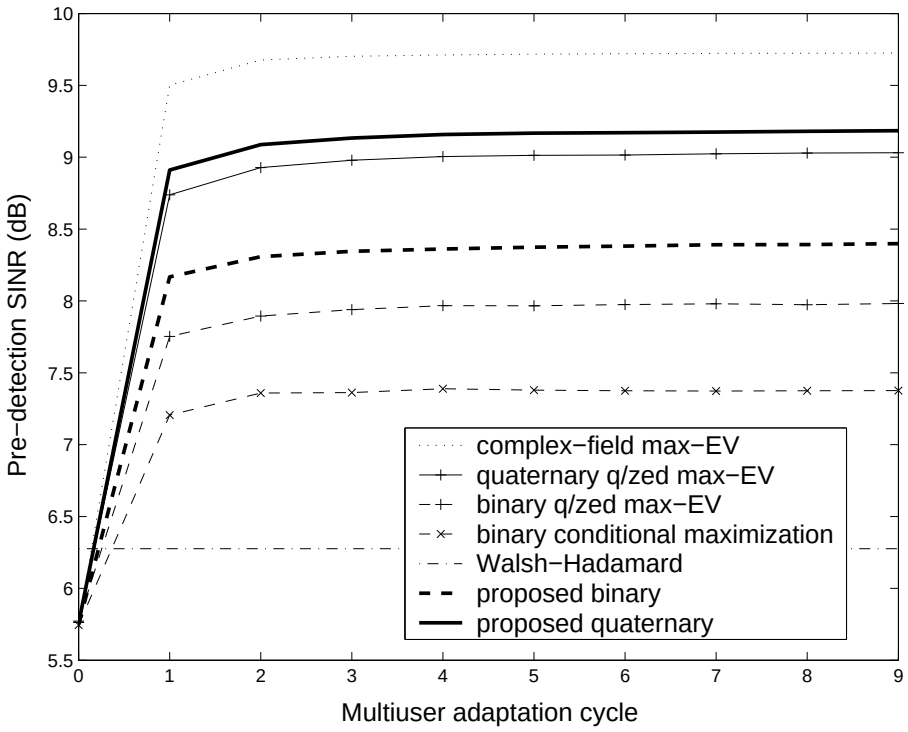

Fig. 1: Average pre-detection SINR for a representative user versus multiuser adaptation cycle ($L = 16,\ K = 8$).

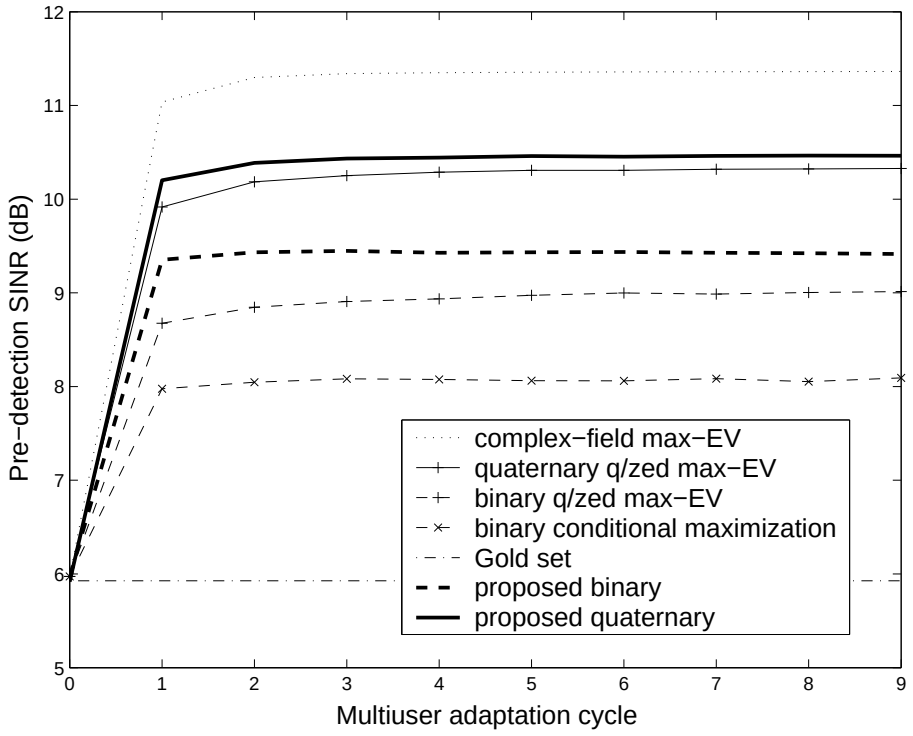

Fig. 2: Average pre-detection SINR for a representative user versus multiuser adaptation cycle ($L = 31,\ K = 16$).

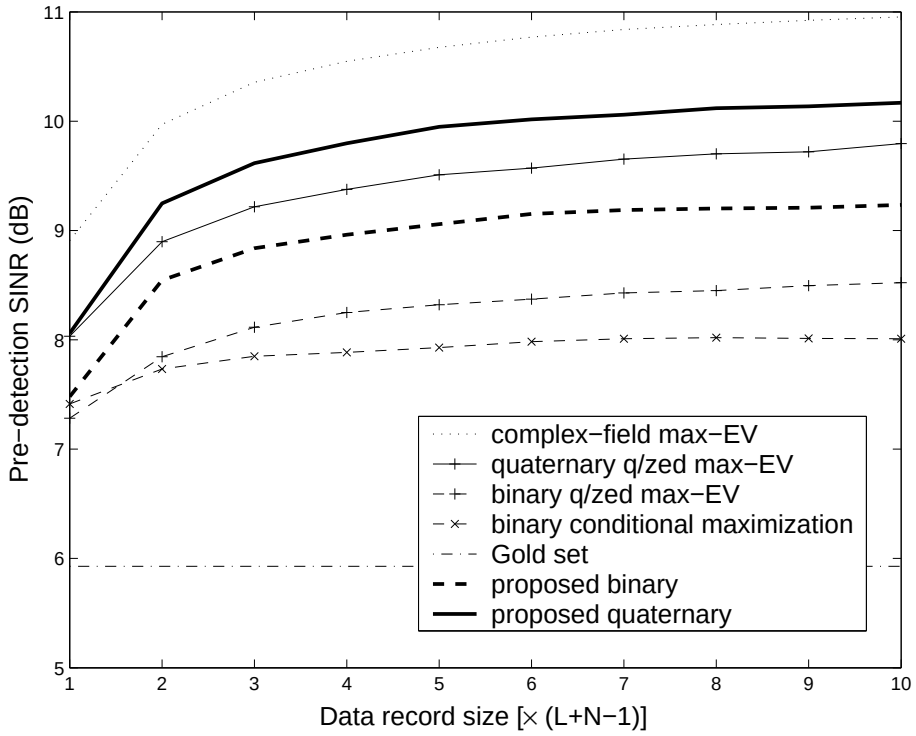

Fig. 3: Average pre-detection SINR for a representative user versus sample support ($L = 31$, $K = 16$, three multiuser adaptation cycles).

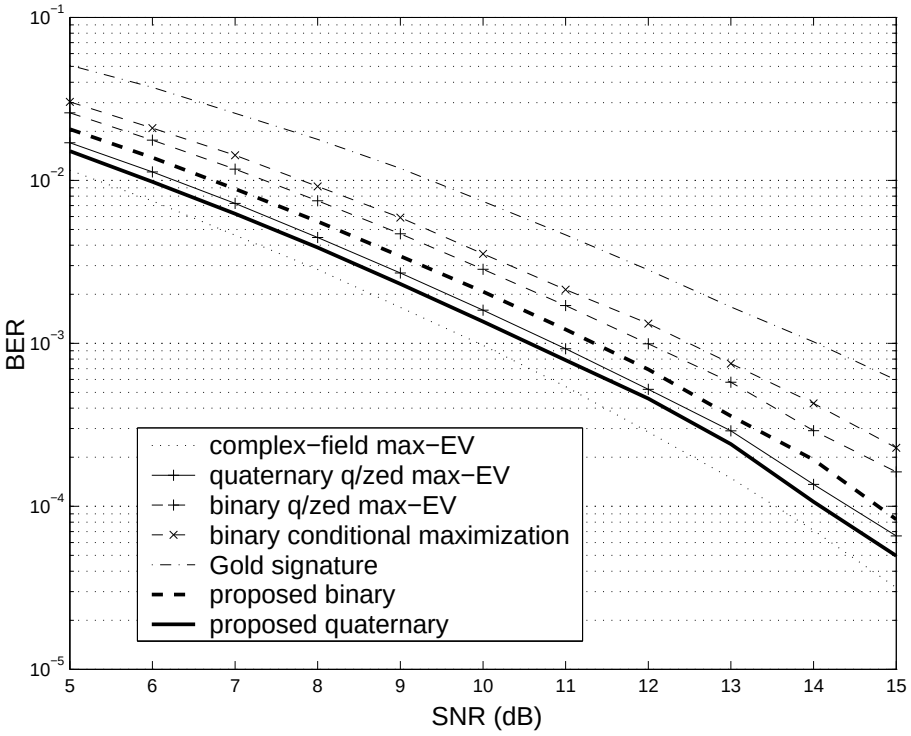

Fig. 4: BER versus SNR under single-user adaptation ($L = 31$, $K = 16$, fixed Gold MAI signatures, $3(L + N - 1)$ sample support).

III. New Bounds on the Periodic Total Squared Correlation of Binary Signature Sets and Optimal Designs

This work has been presented at IEEE MILCOM 2005, Atlantic City, NJ.

In code-division multiplexing applications, for example direct-sequence code-division multiple-access (DS-CDMA) cellular communications systems, each of the K participating signals/users is equipped with a unique identifying signature vector $\mathbf{s}_k \in \mathbb{C}^L,\ ||\mathbf{s}_k|| = 1,\ k = 1, 2, \ldots, K$. All signatures put together in the form of a matrix define what we call the signature set

$$\mathcal{S} \stackrel{\triangle}{=} [\mathbf{s}_1\ \mathbf{s}_2 \ldots \mathbf{s}_K] \in \mathbb{C}^{L \times K}. \tag{25}$$

In synchronous code-division multiplexing transmissions over well behaved Nyquist channels, we are interested in using a signature set with the smallest possible total squared correlation (TSC) value [2]-[7]

$$\mathrm{TSC}(\mathcal{S}) \stackrel{\triangle}{=} \sum_{i=1}^{K} \sum_{j=1}^{K} \left| \mathbf{s}_i^H \mathbf{s}_j \right|^2 \tag{26}$$

where H denotes the Hermitian operator. For complex/real-valued signature sets $\mathcal{S} \in \mathbb{C}^{L \times K}$ or $\mathbb{R}^{L \times K}$, if $K \geq L$, $\mathrm{TSC}(\mathcal{S}) \geq \frac{K^2}{L}$ [1] (of course, $\mathrm{TSC}(\mathcal{S}) \geq K$ if $K < L$). Overloaded ($K \geq L$) sets with TSC equal to $\frac{K^2}{L}$ have been known as Welch-bound-equality (WBE) sets. Algorithms and studies for the design of complex or real WBE signature sets can be found in [3]-[7]. In digital transmission systems, however, it is necessary to have finite-alphabet signature sets. Recently, new bounds were derived on the TSC of *binary antipodal* signature sets together with optimal designs for arbitrary signature lengths and set sizes [2]-[4]. The sum capacity, total asymptotic efficiency, and maximum squared correlation of minimum-TSC optimal binary sets were evaluated in [5]. The sum capacity of several other signature set designs under potentially a binary or quaternary alphabet was examined in [6]. All developments that follow in this present report refer to binary signature sets.

When asynchronous code-division multiplexing is attempted and/or the channel exhibits multipath behavior, apart from the total squared correlation between signatures we are also concerned about the individual periodic (cyclic) auto-correlation and the periodic (cyclic) cross-correlation values [8]. For notational simplicity, let $\mathbf{s}_{k|l}$ denote the *cyclic right-shifted* version of $\mathbf{s}_k \in \{\pm 1\}^L,\ k = 1, 2, \ldots, K$, by l bit positions, $l = 0, 1, 2, \ldots$ (hence, $\mathbf{s}_{k|0} = \mathbf{s}_{k|L} = \ldots = \mathbf{s}_k$). First, we define the cyclic extension matrix $\mathcal{S}_c \in \{\pm 1\}^{L \times KL}$ of the signature set $\mathcal{S} \in \{\pm 1\}^{L \times K}$

$$\mathcal{S}_c \triangleq \left[\mathbf{s}_{1|0}\ \mathbf{s}_{2|0}\dots\mathbf{s}_{K|0}\quad \mathbf{s}_{1|1}\ \mathbf{s}_{2|1}\dots\mathbf{s}_{K|1}\quad \dots\dots\quad \mathbf{s}_{1|L-1}\ \mathbf{s}_{2|L-1}\dots\mathbf{s}_{K|L-1}\right]. \tag{27}$$

Then, we define the periodic total squared correlation (PTSC) of the signature set $\mathcal{S}$ as the total squared correlation (TSC) of the matrix $\mathcal{S}_c$

$$\mathrm{PTSC}(\mathcal{S}) \triangleq \mathrm{TSC}(\mathcal{S}_c). \tag{28}$$

Since,

$$\mathbf{s}_{i|l_1}^T\mathbf{s}_{j|l_2} = \mathbf{s}_{i|0}^T\mathbf{s}_{j|l_2-l_1} = \mathbf{s}_{j|0}^T\mathbf{s}_{i|L-(l_2-l_1)},\ l_1 \le l_2,\ l_1,l_2 = 0,1,2,\dots,L-1,\ i,j = 1,2,\dots,K, \tag{29}$$

where T denotes the transpose operator, we can calculate

$$\mathrm{PTSC}(\mathcal{S}) = \begin{cases} KL^3 + 2L\sum_{k=1}^{K}\sum_{l=1}^{\frac{L-1}{2}}\left|\mathbf{s}_k^T\mathbf{s}_{k|l}\right|^2 + \\ \qquad 2L\sum_{i=1}^{K}\sum_{j=1,i<j}^{K}\sum_{l=0}^{L-1}\left|\mathbf{s}_i^T\mathbf{s}_{j|l}\right|^2,\ L \equiv 1 \pmod 2 \\ KL^3 + L\sum_{k=1}^{K}\left[2\sum_{l=1}^{\frac{L}{2}-1}\left|\mathbf{s}_k^T\mathbf{s}_{k|l}\right|^2 + \left|\mathbf{s}_k^T\mathbf{s}_{k|\frac{L}{2}}\right|^2\right] + \\ \qquad 2L\sum_{i=1}^{K}\sum_{j=1,i<j}^{K}\sum_{l=0}^{L-1}\left|\mathbf{s}_i^T\mathbf{s}_{j|l}\right|^2,\ L \equiv 0 \pmod 2. \end{cases} \tag{30}$$

The first two terms of the PTSC expressions (for odd or even L) contain all periodic auto-correlation contributions. The third, triple summation term contains all periodic cross-correlation contributions. Minimizing PTSC addresses the problem of minimizing periodic auto- and cross-correlations jointly. In the present work, we derive new lower bounds on the PTSC of binary signature sets for all possible values of K (number of signatures) and L (signature length). Then, we derive optimal designs for several (K, L) pair cases. The designs are based on Hadamard matrix transformations (an approach followed in [2] and [14], for example) and serve as proof-by-construction for the tightness of the pertinent PTSC bounds.

A. New Bounds on the PTSC of Binary Antipodal Signature Sets

Consider the cyclic extension matrix $\mathcal{S}_c \in \{\pm 1\}^{L\times KL}$ in (137) and denote its ith row by

$$\mathbf{d}_i \triangleq \left[\mathbf{s}_{1|0}(i)\dots\mathbf{s}_{K|0}(i)\quad \mathbf{s}_{1|1}(i)\dots\mathbf{s}_{K|1}(i)\quad \dots\dots\quad \mathbf{s}_{1|L-1}(i)\dots\mathbf{s}_{K|L-1}(i)\right]^T, i = 1,2,\dots,L, \tag{31}$$

where $\mathbf{s}_{k|l}(i),\ k = 1,2,\dots,K,\ l = 0,2,\dots,L-1$, refers to the ith element of vector $\mathbf{s}_{k|l}$. Then, by (28) and the "row-column equivalence" for the TSC metric of matrices [7],

$$\mathrm{PTSC}(\mathcal{S}) \quad = \quad K^2L^3 + \sum_{i=1}^{L}\sum_{j=1,j\neq i}^{L}\left|\mathbf{d}_i^T\mathbf{d}_j\right|^2. \tag{32}$$

Our goal is to obtain a bound on the term $\sum_{i=1}^{L}\sum_{j=1,j\neq i}^{L}\left|\mathbf{d}_i^T\mathbf{d}_j\right|^2$ for all (K,L) cases. For this purpose, we will make use of the following theorem.

Theorem 1 (*On the Properties of Cyclic Extension Matrices*) Let $\mathcal{S}_c = [\mathbf{d}_1\ \mathbf{d}_2 \dots \mathbf{d}_L]^T$, $\mathbf{d}_i \in \{\pm 1\}^{KL}$, $i = 1, 2, \dots, L$, be the cyclic extension matrix of $\mathcal{S} = [\mathbf{s}_1\ \mathbf{s}_2 \dots \mathbf{s}_K]$, $\mathbf{s}_k \in \{\pm 1\}^L$, $k = 1, 2, \dots, K$.
(i) Then,

$$\mathbf{d}_i^T \mathbf{d}_j = \sum_{k=1}^{K} \mathbf{s}_k^T \mathbf{s}_{k|j-i},\ i, j = 1, 2, \dots, L, \tag{33}$$

and

$$\sum_{i=1}^{L} \sum_{j=1, j\neq i}^{L} \left|\mathbf{d}_i^T \mathbf{d}_j\right|^2 = \begin{cases} 2L \sum_{j=2}^{\frac{L-1}{2}+1} \left|\mathbf{d}_1^T \mathbf{d}_j\right|^2, & L \equiv 1 \pmod 2 \\ L\left[2\sum_{j=2}^{\frac{L}{2}} \left|\mathbf{d}_1^T \mathbf{d}_j\right|^2 + \left|\mathbf{d}_1^T \mathbf{d}_{\frac{L}{2}+1}\right|^2\right], & L \equiv 0 \pmod 2. \end{cases} \tag{34}$$

(ii) If $KL \not\equiv 0 \pmod 4$, $\left|\mathbf{d}_1^T \mathbf{d}_j\right| \neq 0$ for all $j = 2, 3, \dots, L$. Specifically, if $KL \equiv 1 \pmod 2$, $\left|\mathbf{d}_1^T \mathbf{d}_j\right| \equiv 1 \pmod 2$ for all $j = 2, 3, \dots, L$; if $KL \equiv 2 \pmod 4$, $\left|\mathbf{d}_1^T \mathbf{d}_j\right| \equiv 2 \pmod 4$ for all $j = 2, 3, \dots, L$. □

From (32) and Theorem 1, Part (i), the PTSC of a binary signature set $\mathcal{S}$ equals

$$\mathrm{PTSC}(\mathcal{S}) = \begin{cases} K^2L^3 + 2L \sum_{j=2}^{\frac{L-1}{2}+1} \left|\mathbf{d}_1^T \mathbf{d}_j\right|^2, & L \equiv 1 \pmod 2 \\ K^2L^3 + L\left[2\sum_{j=2}^{\frac{L}{2}} \left|\mathbf{d}_1^T \mathbf{d}_j\right|^2 + \left|\mathbf{d}_1^T \mathbf{d}_{\frac{L}{2}+1}\right|^2\right], & L \equiv 0 \pmod 2 \end{cases} \tag{35}$$

and —interestingly— depends only on the sum of the periodic auto-correlations of the signatures for each shift ($\mathbf{d}_1^T \mathbf{d}_j = \sum_{k=1}^{K} \mathbf{s}_k^T \mathbf{s}_{k|j-1},\ j = 2, 3, \dots, L$). By (35) and Theorem 1, Part (ii),

$$\mathrm{PTSC}(\mathcal{S}) \geq \begin{cases} K^2L^3 + 2L\left(\frac{L-1}{2}\right), & L \equiv 1 \pmod 2,\ K \equiv 1 \pmod 2 \\ K^2L^3 + 8L\left(\frac{L-1}{2}\right), & L \equiv 1 \pmod 2,\ K \equiv 2 \pmod 4 \\ K^2L^3 + 8L\left(\frac{L}{2} - 1\right) + 4L, & L \equiv 2 \pmod 4,\ K \equiv 1 \pmod 2. \end{cases} \tag{36}$$

Simplifying/compressing (36) and adding the entry $KL \equiv 0 \pmod 4$, we conclude

$$\mathrm{PTSC}(\mathcal{S}) \geq \begin{cases} K^2L^3, & KL \equiv 0 \pmod 4 \\ K^2L^3 + 4L(L-1), & KL \equiv 2 \pmod 4 \\ K^2L^3 + L(L-1), & KL \equiv 1 \pmod 2. \end{cases} \tag{37}$$

Expression (37) defines our new bounds on the periodic total squared correlation of binary antipodal signature sets. In the following section, we develop signature set designs that meet these bounds with equality.

B. Design of Minimum PTSC Binary Antipodal Signature Sets

In view of the formulation introduced in Section I, minimum PTSC design of a signature set $\mathcal{S}$ is equivalent to minimum TSC design of an extension matrix $\mathcal{S}_c$.

In the following, $\mathbf{H}_N$ refers to a normalized Hadamard matrix[2] of size N with columns $\mathbf{h}_i,\ i = 1, 2, \ldots, N$. Vec$[\mathbf{A}]$ denotes the standard column-by-column vectorization operation on matrix $\mathbf{A}$ and diag$\{\mathbf{b}\}$ is the square diagonal matrix with the elements of vector $\mathbf{b}$ on its diagonal. Finally, we find it useful to introduce the *column replication* operator $\wedge p,\ p = 1, 2, \ldots$. If $A = [\mathbf{a}_1\ \mathbf{a}_2 \ldots \mathbf{a}_J]$, then $A^{\wedge p} \triangleq [\underbrace{\mathbf{a}_1\ \mathbf{a}_1 \ldots \mathbf{a}_1}_{p}\ \underbrace{\mathbf{a}_2\ \mathbf{a}_2 \ldots \mathbf{a}_2}_{p} \ldots \underbrace{\mathbf{a}_J\ \mathbf{a}_J \ldots \mathbf{a}_J}_{p}]$.

Below, we provide PTSC-optimal signature set designs under several K, L cases for both underloaded ($K \leq L$) and overloaded ($K > L$) systems.

Case 1: ***Underloaded Systems*** **($K \leq L$)**

Case 1: $K \equiv 0 \pmod 2,\ L = 2^n,\ n = 1, 2, \ldots$

Calculate $N = 4\left\lfloor \frac{K}{4} \right\rfloor$ (K is rounded down to the nearest multiple of four). Decompose N into $N = N_1 + N_2 + \ldots + N_J$ where $N_1 > N_2 > \ldots > N_J$ are powers of 2. Obtain a Hadamard matrix $\mathbf{H}_{N_1}$ and create the initial template matrix

$$\mathbf{\Theta}_{L \times N_1} = [\underbrace{\mathbf{H}_{N_1}\ \mathbf{H}_{N_1} \ldots \mathbf{H}_{N_1}}_{\frac{L}{N_1}}]^T. \tag{38}$$

Define the diagonal "correction" matrices

$$\mathbf{C}_i = \text{diag}\left\{ \text{Vec}\left[\left(\text{Vec}\left[\mathbf{H}_{N_1}\right]^{T^{\wedge N_1^{i-1}}} \right)^{T^{\wedge \frac{L}{N_1^{i+1}}}} \right] \right\},\ i = 1, 2, \ldots, \lfloor log_{N_1} L - 1 \rfloor, \tag{39}$$

and the final diagonal correction matrix

$$\mathbf{X} = \text{diag}\left\{ \text{Vec}\left[\text{Vec}\left[\mathbf{h}_1\ \mathbf{h}_2 \ldots \mathbf{h}_{\frac{L}{N_1^{\lfloor log_{N_1} L \rfloor}}} \right]^{\wedge N_1^{\lfloor log_{N_1} L \rfloor - 1}} \right] \right\}. \tag{40}$$

Calculate

$$\mathcal{S}_1^T = \mathbf{\Theta}^T \left(\prod_{i=1}^{\lfloor log_{N_1} L - 1 \rfloor} \mathbf{C}_i \right) \mathbf{X}. \tag{41}$$

Repeat (38)-(41) for $\{N_j\}_{j=2}^J$ to create $\{\mathcal{S}_j\}_{j=2}^J$. Each $\mathcal{S}_j,\ j = 1, 2, \ldots J$, is an $L \times N_j$ PTSC-optimal set. Concatenate to form

$$\mathcal{S}_{L \times N} = [\mathcal{S}_1\ \mathcal{S}_2 \ldots \mathcal{S}_J]. \tag{42}$$

[2]We recall that a Hadamard matrix $\mathbf{H}_N$ is an $N \times N$ matrix with elements $+1$ or -1 and orthogonal columns, $\mathbf{H}_N^T \mathbf{H}_N = N\mathbf{I}_N$ where $\mathbf{I}_N$ is the size-N identity matrix. A necessary condition for a Hadamard matrix to exist is that its size is a multiple of four, except for the trivial cases of size one or two.

If $K \equiv 0 \pmod 4$, then $\mathcal{S}$ in (42) is an $L \times K$ PTSC-optimal signature set. If $K \equiv 2 \pmod 4$, design PTSC-optimal sets $\mathcal{S}'_{L\times(K-2)}$ and $\mathcal{S}''_{L\times 2}$ as above and concatenate[3]; $\left[\mathcal{S}' \ \mathcal{S}''\right]$ is an $L \times K$ PTSC-optimal signature set. □

Case 2a: $K \equiv 0 \pmod 8$ and $K \geq 8\left\lceil \frac{\sqrt{4L}}{8} \right\rceil$, $L \not\equiv 2 \pmod 4$ and $L \neq 2^n$, $n = 1, 2, \ldots$

2b: $K \equiv 0 \pmod 8$ and $8\left\lceil \frac{\sqrt{4L}}{8} \right\rceil \leq K < 4\left\lceil \frac{L}{8} \right\rceil$, $L \equiv 2 \pmod 4$

Calculate $N = \frac{K}{2}$, $q = \left\lfloor \frac{L}{N} \right\rfloor$, and $r = L - N\left\lfloor \frac{L}{N} \right\rfloor$. Obtain a Hadamard matrix $\mathbf{H}_N$ and create the initial template matrix

$$\mathbf{\Theta}_{L\times N} = [\underbrace{\mathbf{H}_N \ \mathbf{H}_N \ldots \mathbf{H}_N}_{q} \ \mathbf{h}_1 \ \mathbf{h}_2 \ldots \mathbf{h}_r]^T. \tag{43}$$

If $r \neq 0$, define the diagonal correction matrices

$$\mathbf{C}_i = \text{diag}\left\{ \text{Vec}\left[\mathbf{h}_1 \ \mathbf{h}_2 \ldots \mathbf{h}_q \ \left[\underbrace{(-1)^{i+1} \ (-1)^{i+1} \ldots (-1)^{i+1}}_{r} \right]^T \right] \right\}, \ i = 1, 2. \tag{44}$$

If $r = 0$, define the diagonal correction matrices as follows:

$$\mathbf{C}_i = \text{diag}\left\{ \text{Vec}\left[\left[(-1)^{i+1}\mathbf{h}_1 \right] \ \mathbf{h}_2 \ldots \mathbf{h}_q \right] \right\}, \ i = 1, 2. \tag{45}$$

Calculate $\mathcal{S}_i^T = \mathbf{\Theta}^T\mathbf{C}_i$, $i = 1, 2$, and concatenate to form the PTSC-optimal set

$$\mathcal{S}_{L\times K} = [\mathcal{S}_1 \ \mathcal{S}_2]. \tag{46}$$

□

Case 3a: $K \equiv 0 \pmod 4$ and $4\left\lceil \frac{\sqrt{L}}{4} \right\rceil \leq K < 8\left\lceil \frac{\sqrt{4L}}{8} \right\rceil$, $L \equiv 0 \pmod K$

3b: $K \equiv 4 \pmod 8$ and $K > 8\left\lceil \frac{\sqrt{4L}}{8} \right\rceil$, $L \equiv 0 \pmod K$

Calculate $q = \frac{L}{K}$. Obtain a Hadamard matrix $\mathbf{H}_K$ and create the initial template matrix

$$\mathbf{\Theta}_{L\times K} = [\underbrace{\mathbf{H}_K \ \mathbf{H}_K \ldots \mathbf{H}_K}_{q}]^T. \tag{47}$$

Define the diagonal correction matrix

$$\mathbf{C} = \text{diag}\left\{ \text{Vec}\left[\mathbf{h}_1 \ \mathbf{h}_2 \ldots \mathbf{h}_q \right] \right\} \tag{48}$$

and calculate the PTSC-optimal set

$$\mathcal{S}^T = \mathbf{\Theta}^T\mathbf{C}. \tag{49}$$

---

[3]Notice that repetitive concatenation of the $\mathcal{S}''_{L\times 2}$ PTSC-optimal set would yield, mathematically, PTSC-optimal sets for any $L \times K$-even dimensions; it would do so, however, via signature repetition which is unacceptable application-wise.

□

Case 4: $K \equiv 0 \pmod 4$ and $K \geq 4\left\lceil \frac{L}{8} \right\rceil,\ L \equiv 2 \pmod 4$

Calculate $r = L - K$. Obtain a Hadamard matrix $\mathbf{H}_K$ and create the initial template matrix

$$\mathbf{\Theta}_{L\times K} = [\mathbf{H}_K\ \mathbf{h}_1\ \mathbf{h}_2 \dots \mathbf{h}_r]^T. \tag{50}$$

Define the diagonal correction matrix

$$\mathbf{C} = \text{diag}\left\{ \text{Vec}\left[\left[\underbrace{1\ 1 \dots 1}_{K} \right]^T \quad \left[\underbrace{1\ -1\ 1\ -1 \dots 1\ -1}_{r} \right]^T \right] \right\}. \tag{51}$$

Calculate the PTSC-optimal set

$$\mathcal{S}^T = \mathbf{\Theta}^T \mathbf{C}. \tag{52}$$

□

Some of our designs that follow utilize known *cyclic Hadamard sequences* $\mathbf{g}_M \in \{\pm 1\}^M$ of length $M \equiv 3 \pmod 4$ that have ideal two-level periodic autocorrelation,

$$\mathbf{g}_M^T \mathbf{g}_{M|m} = \begin{cases} M, & m = 0 \\ -1, & m = 1,\ 2, \dots, M-1, \end{cases} \tag{53}$$

and have been used in the past to construct cyclic Hadamard matrices [16]-[18]. In particular, if

$$\begin{aligned} \mathcal{M} \quad \triangleq \quad & \{M : \textit{(i)}\ M \text{ prime congruent to 3 (mod 4) or} \\ & \textit{(ii)}\ M \text{ congruent to 3 (mod 4) and product of ``twin primes'' } p \text{ and } p+2 \text{ or} \\ & \textit{(iii)}\ M = 2^n - 1,\ n = 2,\ 3, \dots \}, \end{aligned} \tag{54}$$

then there exists at least one systematic method [16]-[18] to construct such a sequence $\mathbf{g}_M$ when $M \in \mathcal{M}$. We continue with the presentation of the design cases.

Case 5: $K \equiv 2 \pmod 8$ and $K \geq 8\left\lceil \frac{\sqrt{4L}}{8} \right\rceil + 2,\ L \in \mathcal{M}$

Obtain the signature set $\mathcal{S}'_{L\times(K-2)}$ from (43)-(46) and form the PTSC-optimal set

$$\mathcal{S}_{L\times K} = \left[\mathcal{S}'\ \mathbf{g}_L\ \mathbf{g}_{L|1} \right]. \tag{55}$$

□

Case 6: $K \equiv 1 \pmod 8,\ K \geq 8\left\lceil \frac{\sqrt{4L}}{8} \right\rceil + 1$ and $K \neq L-2,\ L \in \mathcal{M}$

Obtain the signature set $\mathcal{S}'_{L\times(K-1)}$ from (43)-(46) and form the PTSC-optimal set

$$\mathcal{S}_{L\times K} = \left[\mathcal{S}'\ \mathbf{g}_L \right]. \tag{56}$$

□

Case 7: $K = L,\ L \in \mathcal{M}$

Set $N = K + 1$, obtain a Hadamard matrix $\mathbf{H}_N$ and remove its first row and column. Call the resulting size-K matrix $\mathbf{H}_N^{'}$. "Correct" with the diagonal matrix

$$\mathbf{C} = \mathrm{diag}\left\{\mathbf{g}_L\right\} \tag{57}$$

to obtain the PTSC-optimal set

$$\mathcal{S}^T = \mathbf{H}_N^{'}\mathbf{C}. \tag{58}$$

□

Case 8: $K \in \{L-4, L-2\},\ L \in \mathcal{M}$

Design directly the PTSC-optimal set

$$\mathcal{S}_{L\times K} = \left[\left[\underbrace{1\ 1\ \ldots 1}_{L-1}\ -1\right]^T\ \mathbf{g}_L\ \mathbf{g}_{L|1}\cdots\mathbf{g}_{L|K-2}\right]. \tag{59}$$

□

Next, we proceed with the presentation of our optimal designs for overloaded systems.

Case 2: ***Overloaded Systems*** *($K > L$)*

Case 1: $K \equiv 0 \pmod 4$

Obtain a Hadamard matrix $\mathbf{H}_K$ and trivially design the PTSC-optimal set

$$\mathcal{S}_{L\times K} = \left[\mathbf{h}_1\ \mathbf{h}_2 \ldots \mathbf{h}_L\right]^T. \tag{60}$$

Hence, interestingly, overloaded direct Hadamard designs are optimal under both the PTSC and TSC [2] metrics. □

Case 2: $K \equiv 2 \pmod 4,\ L \in \mathcal{M}$

Set $N = K - 2$, obtain a Hadamard matrix $\mathbf{H}_N$ and keep only the first L columns. Call the resulting matrix $\mathbf{H}_N^{'}$. Then,

$$\mathcal{S}_{L\times K} = \left[\mathbf{H}_N^{'T}\ \mathbf{g}_L\ \mathbf{g}_{L|1}\right] \tag{61}$$

is PTSC-optimal. □

Case 3: $K \equiv 1 \pmod 4,\ L \in \mathcal{M}$

Set $N = K - 1$, obtain a Hadamard matrix $\mathbf{H}_N$ and keep only the first L columns. Call the resulting matrix $\mathbf{H}_N^{'}$. Then,

$$\mathcal{S}_{L\times K} = \left[\mathbf{H}_N^{'T}\ \mathbf{g}_L\right] \tag{62}$$

is PTSC-optimal. □

Case 4: $K \equiv 3 \pmod 4,\ L \in \mathcal{M}$

Set $N = K + 1$, obtain a Hadamard matrix $\mathbf{H}_N$ and remove the first row and $N - L$ columns. Call the resulting matrix $\mathbf{H}_N^{'}$. "Correct" with the diagonal matrix

$$\mathbf{C} = \mathrm{diag}\left\{\mathbf{g}_L\right\} \tag{63}$$

to obtain the PTSC-optimal set

$$\mathcal{S}^T = \mathbf{H}_N^{'}\mathbf{C}. \tag{64}$$

□

In the following section, we discuss these design findings and present some examples.

C. Discussion and Examples

The optimal design cases presented in the previous section constitute proof-by-construction of the tightness of the corresponding PTSC bounds developed in Section II. To acquire a quantitative feeling of the coverage of the presented designs, if we restrict the domain of K, L to $\{1, 2, \ldots, 256\}$ (at present, it does not appear of practical interest to consider code-division applications outside this parameter range), we can calculate that Underloaded Cases 1 through 8 and Overloaded Cases 1 through 4 together represent 26.61% of all possible combination pairs $(K, L) \in \{1, 2, \ldots, 256\}^2$. Certainly, tightness of the bounds and optimal PTSC designs under the remaining cases is an important open research problem.

Direct comparison of our PTSC optimal designs with the TSC bounds and optimal sets in [2] shows that Underloaded Case 1 when K is a power of 2, Underloaded Case 3 and Overloaded Cases 1, 3, and 4 are doubly, both PTSC and TSC, optimal. Furthermore, we can now establish that the familiar Gold sets [15], which have been widely used for their periodic correlation properties [8], are not PTSC optimal (ironically, Gold sets were shown to be TSC optimal in [2]). To that respect, we recall [8], [15] that Gold sets are defined for $K \leq L + 2,\ L = 2^n - 1,\ n \geq 3$ and $n \not\equiv 0 \pmod 4$, and for every $i \neq j,\ i, j = 1, \ldots, K$, the periodic signature cross-correlations $\left|\mathbf{s}_i^T \mathbf{s}_{j|l}\right|,\ l = 0, \ldots, L-1$, have value $-1,\ -2^{\left\lfloor \frac{n+2}{2} \right\rfloor} - 1$, or $2^{\left\lfloor \frac{n+2}{2} \right\rfloor} - 1$ with frequency of occurrence ("correlation spectrum" [8]) $2^n - 2^{n-\alpha} - 1,\ 2^{n-\alpha-1} - 2^{\frac{n-\alpha-2}{2}}$ and $2^{n-\alpha-1} + 2^{\frac{n-\alpha-2}{2}}$, respectively, where $\alpha = 1$ if $n \equiv 1 \pmod 2$ and $\alpha = 2$ if $n \equiv 2 \pmod 4$. Consider such a Gold set $\mathcal{G}_{L\times K} = [\mathbf{s}_1\ \mathbf{s}_2 \ldots \mathbf{s}_K]$ where $\mathbf{s}_1,\ \mathbf{s}_2$ are the two *preferred m-sequences* [21] and call its cyclic extension matrix $\mathcal{G}_c$. By (28) and (30),

$$PTSC(\mathcal{G}) = TSC(\mathcal{G}_c) = KL^3 + 2L\sum_{k=1}^{K}\sum_{l=1}^{\frac{L-1}{2}}\left|\mathbf{s}_k^T\mathbf{s}_{k|l}\right|^2 + 2L\sum_{i=1}^{K}\sum_{j=1,\ i<j}^{K}\sum_{l=0}^{L-1}\left|\mathbf{s}_i^T\mathbf{s}_{j|l}\right|^2 \tag{65}$$

and utilizing the cross-correlation spectrum information

$$\begin{aligned}\sum_{l=0}^{L-1}\left|\mathbf{s}_i^T\mathbf{s}_{j|l}\right|^2 &= \Big[(2^n-2^{n-\alpha}-1)\,(-1)^2+\left(2^{n-\alpha-1}-2^{\frac{n-\alpha-2}{2}}\right)\\ &\quad \left(-2^{\lfloor\frac{n+2}{2}\rfloor}-1\right)^2+\left(2^{n-\alpha-1}+2^{\frac{n-\alpha-2}{2}}\right)\left(2^{\lfloor\frac{n+2}{2}\rfloor}-1\right)^2\Big]\\ &= (2^n-1)^2+2^n-2.\end{aligned} \tag{66}$$

Regarding the auto-correlation contributions, if $k=1,\ 2$,

$$2\sum_{l=1}^{\frac{L-1}{2}}\left|\mathbf{s}_k^T\mathbf{s}_{k|l}\right|^2=2^n-2; \tag{67}$$

if $k>2$,

$$2\sum_{l=1}^{\frac{L-1}{2}}\left|\mathbf{s}_k^T\mathbf{s}_{k|l}\right|^2>(-1)^2+\left(-2^{\lfloor\frac{n+2}{2}\rfloor}-1\right)^2+\left(2^{\lfloor\frac{n+2}{2}\rfloor}-1\right)^2\geq 2^{n+2}+3. \tag{68}$$

For $K\leq 2$, combining (65), (66), and (67) we calculate

$$\begin{aligned}PTSC(\mathcal{G}) &= KL^3+KL\,(2^n-2)+LK(K-1)\left[(2^n-1)^2+2^n-2\right]\\ &= K^2L^3+KL(L-1)+LK(K-1)(L-1).\end{aligned} \tag{69}$$

For $K>2$, combining (65), (66), and (68) we obtain

$$\begin{aligned}PTSC(\mathcal{G}) &> KL^3+2L(2^n-2)+(K-2)L\left(2^{n+2}+3\right)\\ &\quad +LK(K-1)\left[(2^n-1)^2+2^n-2\right]\\ &= K^2L^3+2L(L-1)+(K-2)L(4L+7)+LK(K-1)(L-1)\\ &> K^2L^3+K^2L(L-1).\end{aligned} \tag{70}$$

Expression (69) for $K=2$ and expression (70) for $K>2$ are strictly greater than the lower bounds of Section II which are achievable for some Gold-compatible values (K,L) as seen in Section III. Fig. 5 shows as an example a $(16,31)$ Gold set which has $PTSC=8213760$ together with our optimal $(16,31)$ design (under Underloaded Case 2a) with minimum $PTSC=K^2L^3=7626496$.

Other signature sets well known for their periodic correlation properties are the small and large-set Kasami designs [8], [16]. We recall that small-set Kasami designs are defined for lengths $L=2^n-1,\ n\equiv 0\ (\mathrm{mod}\ 2)$, and have size $K\leq 2^{\frac{n}{2}}$. The attained periodic cross-correlation values are $-1,\ -2^{\frac{n}{2}}-1,\ 2^{\frac{n}{2}}-1$, but their frequency of occurrence is not known in closed form as a function of n. Fig. 6 presents a $(2,15)$ small-set Kasami design with calculated $PTSC=15300$ together with our optimal $(2,15)$ design (under Underloaded Case 5) with minimum $PTSC=K^2L^3+4L(L-1)=14340$. We directly conclude that, in general, small-set Kasami designs are not PTSC optimal.

Large-set Kasami designs [8], [16] are defined for $L=2^n-1$ and even n. If $n\equiv 2\ (\mathrm{mod}\ 4),\ K\leq 2^{\frac{n}{2}}(2^n+1)$; if $n\equiv 0\ (\mathrm{mod}\ 4),\ K\leq 2^{\frac{n}{2}}(2^n+1)-1$. Fig. 7(a) shows an $(8,15)$ large-set Kasami design that has $PTSC=227040$. Fig.

7(b) shows our PTSC-optimal set $\mathcal{S}^{opt}_{15\times 8}$ designed under Underloaded Case 2a with minimum PTSC value 216000. Hence, in general, large-set Kasami are not optimal either.

We conclude this section with an example of an overloaded PTSC-optimal design $\mathcal{S}^{opt}_{31\times 42}$ given in Fig. 8. The set is designed under our Overloaded Case 2 procedure and has minimum PTSC value 52555044.

D. Conclusions

We derived bounds on the periodic (cyclic) total squared correlation (PTSC) of binary signature sets for any signature length L and set size K and provided optimal constructions for a variety of K, L values that establish the tightness of the corresponding bounds. The constructions include underloaded ($K \leq L$) and overloaded ($K > L$) design cases and cover, as an example, 26.61% of all possible combinations of K, L in $\{1, 2, \ldots, 256\}$.

Side results of the presented research include derivation of a lower bound on the PTSC of Gold sets which is seen to be strictly larger than the general derived bounds. PTSC-optimal constructions described herein for Gold-compatible (K, L) pairs, as well as small and large-set Kasami, establish that neither the Gold nor the Kasami sets are PTSC-optimal in general. In view of these findings, the developed PTSC-optimal sets take precedence whenever the periodic correlation properties of signatures is of concern in code-division multiplexing applications.

References

[1] M. Rupf and J. L. Massey, "Optimum sequence multisets for synchronous code-division-multiple-access channels," *IEEE Trans. Inform. Theory*, vol. 40, pp. 1261-1266, July 1994.

[2] R. L. Welch, "Lower bounds on the maximum cross correlation of signals," *IEEE Trans. Inform. Theory*, vol. IT-20, pp. 397-399, May 1974.

[3] P. Vishwanath, V. Anantharaman, and D. N. C. Tse, "Optimal sequences, power control, and user capacity of synchronous CDMA systems with linear MMSE multiuser receivers," *IEEE Trans. Inform. Theory*, vol. 45, pp. 1968-1983, Sep. 1999.

[4] S. Ulukus and R. D. Yates, "Iterative construction of optimum signatures sequences sets in synchronous CDMA systems," *IEEE Trans. Inform. Theory*, vol. 47, pp. 1989-1998, July 2001.

[5] C. Rose, S. Ulukus, and R. D. Yates, "Wireless systems and interference avoidance," *IEEE Trans. Wireless Commun.*, vol. 1, pp. 415-428, Mar. 2002.

[6] P. Cotae, "Spreading sequence design for multiple cell synchronous DS-CDMA systems under total weighted squared correlation criterion," *EURASIP Journal Wireless Comm. and Networking*, vol. 2004, no. 1, pp. 4-11, Aug. 2004.

[7] O. Popescu and C. Rose, "Sum capacity and TSC bounds in collaborative multibase wireless systems," *IEEE Trans. Inform. Theory*, vol. 50, pp. 2433-2440, Oct. 2004.

[8] G. N. Karystinos and D. A. Pados, "New bounds on the total squared correlation and optimum design of DS-CDMA binary signature sets," *IEEE Trans. Commun.*, vol. 51, pp. 48-51, Jan. 2003.

[9] C. Ding, M. Golin, and T. Klϕve, "Meeting the Welch and Karystinos-Pados bounds on DS-CDMA binary signature sets," *Des., Codes Cryptogr.*, vol. 30, pp. 73-84, Aug. 2003.

[10] P. Ipatov, "On the Karystinos-Pados bounds and optimal binary DS-CDMA signature ensembles," *IEEE Commun. Letters*, vol. 8, pp. 81-83, Feb. 2004.

[11] G. N. Karystinos and D. A. Pados, "The maximum squared correlation, sum capacity, and total asymptotic efficiency of minimum total-squared-correlation binary signature sets," *IEEE Trans. Inform. Theory*, vol. 51, pp. 348-355, Jan. 2005.

[12] F. Vanhaverbeke and M. Moeneclaey, "Sum capacity of equal-power users in overloaded channels," *IEEE Trans. Inform. Theory*, vol. 53, pp. 228-233, Feb. 2005.

[13] D. V. Sarwate and M. B. Pursley, "Crosscorrelation properties of pseudorandom and related sequences," *Proceedings of the IEEE*, vol. 68, pp. 593-619, May 1980.

[14] B. J. Wysocki and T. A. Wysocki, "Modified Walsh-Hadamard sequences for DS CDMA wireless systems," *Intern. Journal Adaptive Control and Signal Proc.*, vol. 16, pp. 589-602, Sept. 2002.

[15] J. L. Massey and T. Mittelholzer, "Welch's bound and sequence sets for code-division multiple-access systems," *Sequences II, Methods in Communication, Security, and Computer Sciences*, R. Capocelli, A. De Santis, and U. Vaccaro, Eds. New York: Springer-Verlag, 1993.

[16] H.-Y. Song and S. W. Golomb, "On the existence of cyclic Hadamard difference sets," *IEEE Trans. Inform. Theory*, vol. 4, pp. 1266-1268, July 1994.

[17] S. W. Golomb and H.-Y. Song, "A conjecture on the existence of cyclic Hadamard difference sets," *Journal Statist. Planning and Inference*, vol. 62, pp. 39-41, 1997.

[18] L. D. Baumert, *Cyclic Difference Sets (Lecture Notes in Mathematics Vol. 182).* New York: Springer-Verlag, 1971.

[19] ——, *Shift Register Sequences*. San Francisco, CA: Holden-Day, 1967; Laguna Hills, CA: Aegean Park Press, 1982 (revised ed.).

[20] R. G. Stanton and D. A. Sprott, "A family of difference sets," *Canadian J. Math.*, vol. 10, pp. 73-77, 1958.

[21] N. Zierler, "Linear recurring sequences," *J. Soc. Ind. Appl. Math.*, vol. 7, pp. 31-48, Mar. 1959.

[22] R. Gold, "Optimal binary sequences for spread spectrum multiplexing," *IEEE Trans. Inform. Theory*, vol. IT-13, pp. 619-621, Oct. 1967.

[23] T. Kasami, "Weight distribution formula for some class of cyclic codes," Coordinated Science Laboratory, University of Illinois, Urbana, Tech. Rep. R-285 (AD632574), 1966.

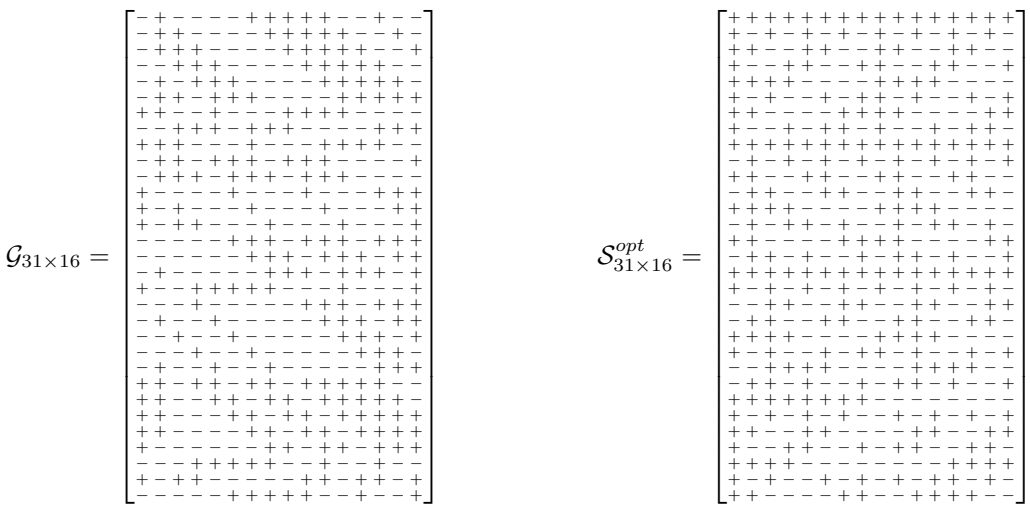

Fig. 5. (a) $\mathcal{G}_{31\times16}$ Gold set with $PTSC = 8213760$. (b) Optimal signature set $\mathcal{S}^{opt}_{31\times16}$ designed under Underloaded Case 2a with $PTSC = (16)^2(31)^3 = 7626496$.

$$\mathcal{K}_{15\times 2}^{ss} = \begin{bmatrix} - & - \\ - & + \\ - & + \\ + & + \\ - & + \\ - & + \\ + & + \\ + & - \\ - & + \\ + & + \\ - & + \\ + & - \\ + & + \\ + & - \\ + & - \end{bmatrix} \qquad \mathcal{S}_{15\times 2}^{opt} = \begin{bmatrix} - & + \\ + & + \\ + & + \\ + & - \\ - & + \\ + & + \\ + & - \\ - & - \\ - & + \\ + & - \\ - & + \\ + & - \\ - & - \\ - & - \\ - & - \end{bmatrix}$$

(a) (b)

Fig. 6. (a) $\mathcal{K}_{15\times 2}^{ss}$ small-set Kasami with $PTSC = 15300$. (b) Optimal signature set $\mathcal{S}_{15\times 2}^{opt}$ designed under Underloaded Case 5 with $PTSC = (2)^2(15)^3 + 4(15)(14) = 14340$.

$$\mathcal{K}^{ls}_{15\times 8} = \begin{bmatrix} + & - & - & + & + & - & - & + \\ + & + & - & + & - & - & + & - \\ - & + & - & - & + & - & + & + \\ - & - & - & + & + & - & - & + \\ + & + & - & + & - & + & - & + \\ - & - & + & + & - & - & + & + \\ - & - & - & + & + & + & + & - \\ - & - & + & - & + & + & - & + \\ - & + & - & - & + & + & - & - \\ - & - & - & + & + & - & - & + \\ + & - & + & - & + & - & + & - \\ + & - & + & + & - & + & - & - \\ - & - & - & + & + & + & + & - \\ - & - & + & - & + & - & + & - \\ + & - & + & + & - & - & + & + \end{bmatrix} \qquad \mathcal{S}^{opt}_{15\times 8} = \begin{bmatrix} + & + & + & + & + & + & + & + \\ + & - & + & - & + & - & + & - \\ + & + & - & - & + & + & - & - \\ + & - & - & + & + & - & - & + \\ + & + & + & + & + & + & + & + \\ - & + & - & + & - & + & - & + \\ + & + & - & - & + & + & - & - \\ - & + & + & - & - & + & + & - \\ + & + & + & + & + & + & + & + \\ + & - & + & - & + & - & + & - \\ - & - & + & + & - & - & + & + \\ - & + & + & - & - & + & + & - \\ + & + & + & + & - & - & - & - \\ + & - & + & - & - & + & - & + \\ + & + & - & - & - & - & + & + \end{bmatrix}$$

(a) (b)

Fig. 7. (a) $\mathcal{K}^{ls}_{15\times 8}$ large-set Kasami with $PTSC = 227040$. (b) Optimal $\mathcal{S}^{opt}_{15\times 8}$ designed under Underloaded Case 2a with $PTSC = (8)^2(15)^3 = 216000$.

$$\mathcal{S}^{opt}_{31\times 42} = \begin{bmatrix}
+ & - & - \\
+ & - & - & + & + & - & - & - & - & + & - & + & - & + & + & + & + & - & - & + & + & - & - & + & + & - & + & - & - & - & - & + & - & + & - & + & + & + & + & - & - & + & + & - \\
+ & - & + & + & - & - & - & - & + & - & + & - & + & + & + & + & - & - & + & - & + & - & - & + & + & - & + & + & - & - & - & - & + & - & + & - & + & + & + & + & - & - & + & - & + \\
+ & + & + & - & - & - & - & + & - & + & - & + & + & + & + & - & - & + & - & - & + & + & + & - & - & + & + & - & - & - & - & + & - & + & - & + & + & + & + & - & - & + & - & - & + \\
+ & + & - & - & - & - & + & - & + & - & + & + & + & + & - & - & + & - & - & + & + & + & - & - & - & - & + & - & + & - & + & + & + & + & - & - & + & - & - & + & + & + \\
+ & - & - & - & - & + & - & + & - & + & + & + & + & - & - & + & - & - & + & + & - & - & - & + & + & + & - & + & - & + & + & + & + & - & - & + & - & - & + & + & - & - & + \\
+ & - & - & + & - & + & - & + & + & + & - & - & + & - & - & + & + & - & + & - & - & - & + & - & + & - & + & + & + & + & - & - & + & - & - & + & + & - & - & + & + \\
+ & - & - & - & + & - & + & - & + & + & + & - & - & + & - & - & + & + & - & + & - & - & - & + & - & + & - & + & + & + & + & - & - & + & - & - & + & + & - & - & + & - \\
+ & - & + & - & + & - & + & + & + & + & - & - & + & - & - & + & + & - & - & - & + & - & + & - & + & + & + & + & - & - & + & - & - & + & + & - & - & - & + & - & - & + \\
+ & + & - & + & - & + & + & + & + & - & - & + & - & - & + & + & - & - & - & + & + & - & + & - & + & + & + & + & - & + & - & - & + & + & - & - & - & + & - & - & + & + \\
+ & - & + & - & + & + & + & + & - & - & + & - & - & + & + & - & - & - & + & + & - & + & - & + & + & + & + & - & - & + & - & - & + & + & - & - & - & + & - & - & + & + \\
+ & + & - & + & + & + & + & - & - & + & - & - & + & + & - & - & - & - & + & - & + & + & - & + & + & + & + & - & - & + & - & - & + & + & - & - & - & + & - & - & + & + \\
+ & - & + & + & + & + & - & - & + & - & - & + & + & - & - & - & - & + & - & + & - & + & + & + & + & - & - & + & - & - & + & + & - & - & - & + & - & + & - & - & - & + \\
+ & + & + & + & + & - & - & + & - & - & + & + & - & - & - & - & + & - & + & - & + & + & + & + & - & - & + & - & - & + & + & - & - & - & - & + & - & + & - & - & - & - \\
+ & + & + & + & - & - & + & - & - & + & + & - & - & - & - & + & - & + & - & + & + & + & + & - & - & + & - & - & + & + & - & - & - & + & - & + & - & + & + & - & - \\
+ & + & + & - & - & + & - & - & + & + & - & - & - & - & + & - & + & - & + & + & + & + & - & - & + & - & - & + & + & - & - & - & + & - & + & - & + & + & + & + & - & - \\
+ & + & - & - & + & - & - & + & + & - & - & - & - & + & - & + & - & + & + & + & + & - & - & + & - & - & + & + & - & - & - & + & - & + & - & - & + & + & + & + & + \\
+ & - & - & + & - & - & + & + & - & - & - & - & + & - & + & - & + & + & + & + & - & - & + & - & - & + & + & - & - & - & + & - & + & - & + & + & + & + & - & + & + \\
+ & - & + & - & - & + & + & - & - & - & + & - & + & - & + & + & + & - & + & - & + & - & - & + & + & - & - & - & + & - & + & - & + & + & + & + & - & + & + \\
+ & + & - & - & + & + & - & - & - & - & + & - & + & - & + & + & + & + & - & - & + & - & - & + & + & - & - & - & + & - & + & - & + & + & + & + & - & - & - \\
+ & + & + & + & + & + & + & + & + & + & + & + & + & + & + & + & + & + & - & - & - & - & - & - & - & - & - & - & - & - & - & - & - & - & + & + \\
+ & - & - & + & + & - & - & - & - & + & - & + & + & + & + & - & - & + & - & - & + & - & + & + & + & - & + & - & + & - & - & - & - & + & + & - & - & + \\
+ & - & + & + & - & - & - & - & + & - & + & - & + & + & + & - & - & + & - & - & + & - & - & + & + & + & - & + & - & + & - & - & - & - & + & - & + & - & + \\
+ & + & + & - & - & - & - & + & - & + & - & + & + & + & + & - & - & + & - & - & - & - & + & + & + & - & + & + & - & + & + & - & - & - & + & + & - & + & - & - \\
+ & + & - & - & - & - & + & - & + & - & + & + & + & + & - & - & + & - & - & + & - & - & + & + & + & - & + & - & + & - & - & - & - & + & + & - & + & + & - & - \\
+ & - & - & - & - & + & - & + & - & + & + & + & - & - & + & - & - & + & + & - & + & + & + & - & + & - & + & - & - & - & - & + & + & - & + & - & + & - & - \\
+ & - & - & - & + & - & + & - & + & + & + & - & - & + & - & - & + & + & - & + & + & + & - & + & - & + & - & - & - & - & + & + & - & + & + & - & - & + & + & - \\
+ & - & - & + & - & + & - & + & + & + & + & - & - & + & - & - & + & + & - & - & - & + & + & - & + & - & + & - & - & - & + & + & - & + & - & + & + & - & + & - \\
+ & - & + & - & + & - & + & + & + & + & - & - & + & - & - & + & + & - & - & - & + & - & + & - & + & - & - & - & + & + & - & + & + & - & - & + & + & - & - & + \\
+ & + & - & + & - & + & + & + & + & - & - & + & - & - & + & + & - & - & - & - & - & + & - & + & - & - & - & + & + & - & + & + & + & + & - & - \\
+ & - & + & - & + & + & + & + & - & - & + & - & - & + & + & - & - & - & - & + & - & + & - & + & - & - & - & + & + & - & + & + & + & + & - & - & + \\
\end{bmatrix}$$

Fig. 8. Optimal signature set $\mathcal{S}^{opt}_{31\times 42}$ designed under Overloaded Case 2 with minimum $PTSC = (42)^2(31)^3 + 4(31)(30) = 52555044$.

IV. Rank-2-optimal Adaptive Design of Binary Spreading Codes

This work has been published in the IEEE Transactions on Information Theory, Sept. 2007.

The performance of direct-sequence code-division-multiple-access (DS-CDMA) systems is determined by the set of user spreading codes in conjunction with channel and receiver design specifics. In recent literature, several methods have been presented for the design of real/complex-valued [1]-[14] or binary [8], [15]-[24] sets of DS-CDMA spreading codes under various optimization criteria. Among them, in [1]-[6], [14]-[22] the spreading code set is treated as a single matrix parameter to be optimized while the works in [7]-[12], [23], [24] present iterative algorithms that update the codes of the set individually in a round-robin fashion.

In particular, sets of spreading codes that minimize the total squared correlation (TSC) were designed in [1], [2], while distributed algorithms that iteratively decrease TSC by updating one-by-one the individual codes of the set were developed in [7]-[10]. Band-limited sets that maximize the user capacity of synchronous DS-CDMA systems were constructed in [3]. Optimal sets for asynchronous DS-CDMA systems were designed in [4]-[6], while the iterative method of [9], [10] was modified to suit asynchronous systems in [11] and multipath channels in [12]. Collaborative multibase designs were studied in [13]. In all the above developments, each user spreading code was allowed to take any value in the real vector space subject to a (unit-)norm constraint.

In [17], we concentrated on binary sets of spreading codes and derived new lower bounds on the TSC. Optimal binary sets that meet the TSC bound with equality were also designed in [17], as well as in [18],[19], while their sum capacity, total asymptotic efficiency, and maximum squared correlation were evaluated in [20]. In addition, a searching algorithm for minimum-TSC spreading code sets with low cross-correlation spectrum was presented in [21]. Interestingly, if we consider binary sets of spreading codes for transmission over a synchronous DS-CDMA channel with unequal channel gains for different users, then the minimum-TSC sets of [17]-[19] also minimize the corresponding total weighted squared correlation (TWSC) [14] as long as the system is underloaded and the spreading code length (processing gain) is odd or a multiple of four.

For overloaded systems, however, with unequal user gains, the minimum-TWSC optimality of minimum-TSC binary sets is lost; the design of optimal binary sets for such systems is still an open problem. In an attempt to design appropriate binary spreading codes for overloaded synchronous transmissions with unequal received power values as well as asynchronous transmissions over -potentially- multipath channels, suboptimal distributed algorithms were presented in [8], [23], [24]. In these works, the user codes are updated one-by-one, similar to the approach followed in [7]-[12] for real-valued spreading codes, simplifying the set design problem to the adaptive design of one spreading code in the presence of colored interference.

In this report, we revisit the work of [8], [23], [24] and consider again the adaptive design of binary spreading codes that -in the presence of colored interference- maximize the signal-to-interference-plus-noise ratio (SINR) at the output of the maximum-SINR (MSINR) filter. The optimal code is a function of the disturbance (interference plus noise) autocovariance matrix and its evaluation over the binary field is NP-hard [24]. Instead, in this present work we propose to eigendecompose and approximate the inverse disturbance autocovariance matrix by its *two* maximum-energy components alone. Then, we show how to optimize the binary spreading code under the *rank-2* approximation of the inverse disturbance autocovariance matrix with lower than quadratic complexity. We demonstrate the significant SINR performance superiority of the proposed rank-2-optimal adaptive design in comparison to direct hard-limiting of the maximum eigenvector of the inverse disturbance autocovariance matrix (or the minimum eigenvector of the interference autocovariance matrix) [8], [24], which we see to be equivalent to rank-1-optimal adaptive binary spreading code design. Moreover, simulation studies indicate that the proposed rank-2-optimal spreading code can be the exact full-rank-optimal solution with significantly higher probability than the rank-1-optimal code (for example, when the returned rank-1-optimal code is globally optimal with probability 0.4, the rank-2-optimal code is globally optimal with probability 0.85). In fact, simple iterative Hamming-distance-1 steepest descent search [22], [24] initialized at the proposed rank-2-optimal spreading code raises the probability of convergence to the full-rank-optimal solution to as high as 0.95. Certainly, the proposed adaptive binary code design can serve as an appropriate initialization point for other, potentially more sophisticated, iterative binary search procedures.

A. Signal Model and Problem Statement

Consider the vector signal model

$$\mathbf{r} = b\sqrt{P}\mathbf{s} + \mathbf{y} \tag{71}$$

where $b \in \{\pm 1\}$ is a uniformly distributed bit random variable, $\mathbf{s} \in \mathbb{R}^L$ a deterministic vector waveform (spreading code) with $\|\mathbf{s}\| = 1$ such that all collected energy is absorbed/represented by the scalar $P > 0$, and $\mathbf{y} \in \mathbb{R}^L$ is a zero-mean random disturbance vector with positive definite autocovariance matrix $\mathbf{R} = E\left\{\mathbf{y}\mathbf{y}^T\right\}$ ($E\{\cdot\}$ denotes statistical expectation and T is the transpose operator).

The general signal model of (71) covers, for example, synchronous DS-CDMA transmissions where a user of interest with spreading code $\mathbf{s}$ transmits over an additive noise channel in the presence of K interfering users. In that case, the overall additive disturbance term takes the form $\mathbf{y} = \sum_{k=1}^{K} b_k\sqrt{P_k}\mathbf{s}_k + \mathbf{n}$ where $b_k \in \{\pm 1\}$, $P_k > 0$, and $\mathbf{s}_k \in \mathbb{R}^L$ are the uniformly distributed user bit, received energy per bit, and normalized deterministic spreading code of the kth interferer, $k = 1, 2, \ldots, K$, and $\mathbf{n}$ represents additive zero-mean channel noise. Similarly, (71) can model asynchronous DS-CDMA transmissions when

the receiver is synchronized with the signal of interest or can be extended to cover multipath transmissions if $\mathbf{s}$ is replaced by the effective (channel processed) user signature.

For an arbitrary spreading code $\mathbf{s}$, the linear filter/receiver $\mathbf{w}$ that exhibits maximum SINR at its output has the form

$$\mathbf{w}(\mathbf{s}) = c\mathbf{R}^{-1}\mathbf{s},\ c > 0, \tag{72}$$

and the (maximum) output SINR value is

$$\mathrm{SINR}(\mathbf{s}) = \frac{E\left\{\left(\mathbf{w}^T(\mathbf{s})\, b\sqrt{P}\mathbf{s}\right)^2\right\}}{E\left\{\left(\mathbf{w}^T(\mathbf{s})\,\mathbf{z}\right)^2\right\}} = P\mathbf{s}^T\mathbf{R}^{-1}\mathbf{s}. \tag{73}$$

We recall that, if the additive disturbance vector $\mathbf{y}$ is Gaussian, then $\mathrm{sgn}\left[\mathbf{w}^T(\mathbf{s})\,\mathbf{r}\right]$ is the minimum bit-error-rate (BER) detector with error probability given by $\mathrm{BER}(\mathbf{s}) = Q\left(\sqrt{P\mathbf{s}^T\mathbf{R}^{-1}\mathbf{s}}\right)$ where $Q(a) = \int_a^\infty \frac{1}{\sqrt{2\pi}} e^{-\frac{t^2}{2}} dt$.

Our objective is to design the spreading code $\mathbf{s}$ so that the corresponding $\mathrm{SINR}(\mathbf{s})$ value is maximized (and $\mathrm{BER}(\mathbf{s})$ is minimized under the Gaussian additive disturbance assumption). Since the disturbance autocovariance matrix $\mathbf{R}$ is positive definite,

$$\mathbf{R} = \sum_{i=1}^{L} \lambda_i \mathbf{q}_i \mathbf{q}_i^T,\ \lambda_1 \geq \lambda_2 \geq \ldots \geq \lambda_L > 0,\ \|\mathbf{q}_i\| = 1,\ i = 1, 2, \ldots, L, \tag{74}$$

represents its eigendecomposition where λ_i and $\mathbf{q}_i$ are the ith eigenvalue and normalized eigenvector, respectively, of $\mathbf{R}$. Then, the *real-valued* spreading code $\mathbf{s}$ that maximizes $\mathrm{SINR}(\mathbf{s})$ is given by [10]-[12], [24]

$$\mathbf{s}_{\mathbb{R}-\mathrm{OPT}} \stackrel{\triangle}{=} \arg \max_{\mathbf{s}\in\mathbb{R}^L, \|\mathbf{s}\|=1} \left\{P\mathbf{s}^T\mathbf{R}^{-1}\mathbf{s}\right\} = \mathbf{q}_L. \tag{75}$$

Therefore, the optimal real-valued code $\mathbf{s}_{\mathbb{R}-\mathrm{OPT}}$ can be obtained with complexity that is dominated by the complexity of the eigendecomposition of the $L \times L$ matrix $\mathbf{R}$.

In this present work, we are interested in maximizing $\mathrm{SINR}(\mathbf{s})$ subject to the constraint that $\mathbf{s}$ is *binary*. The problem of obtaining the optimal binary spreading code,

$$\mathbf{s}_{\mathrm{OPT}} \stackrel{\triangle}{=} \arg \max_{\mathbf{s}\in\left\{\pm\frac{1}{\sqrt{L}}\right\}^L} \left\{P\mathbf{s}^T\mathbf{R}^{-1}\mathbf{s}\right\}, \tag{76}$$

is NP-hard [23], [24] and can be solved through exhaustive search over all possible L-bit combinations. In the next section, we seek a computationally efficient alternative for the design of a spreading code $\mathbf{s} \in \left\{\pm\frac{1}{\sqrt{L}}\right\}^L$.

B. Rank-2-optimal Design of Binary Spreading Codes

Given the eigendecomposition of $\mathbf{R}$ in (74),

$$\mathbf{R}^{-1} = \sum_{i=1}^{L} \frac{1}{\lambda_i} \mathbf{q}_i \mathbf{q}_i^T, \; \frac{1}{\lambda_L} \geq \frac{1}{\lambda_{L-1}} \geq \ldots \geq \frac{1}{\lambda_1} > 0, \; \|\mathbf{q}_i\| = 1, \; i = 1, 2, \ldots, L, \tag{77}$$

and the binary spreading code optimization problem in (76) can be rewritten as

$$\mathbf{s}_{\mathrm{OPT}} = \arg \max_{\mathbf{s} \in \left\{ \pm \frac{1}{\sqrt{L}} \right\}^L} \left\{ \sum_{i=1}^{L} \frac{1}{\lambda_i} \left(\mathbf{s}^T \mathbf{q}_i \right)^2 \right\} \tag{78}$$

where $0 \leq \left(\mathbf{s}^T \mathbf{q}_i \right)^2 \leq 1$, $i = 1, 2, \ldots, L$. Therefore, the optimal binary vector $\mathbf{s}_{\mathrm{OPT}}$ maximizes the sum of its weighted projections on the eigenvectors $\mathbf{q}_i$ with weights $1/\lambda_i$, $i = 1, \ldots, L$.

If we simplify the optimization problem by keeping only the strongest term $\frac{1}{\lambda_L} \left(\mathbf{s}^T \mathbf{q}_L \right)^2$ in (78) (which is equivalent to using the approximation $\mathbf{R}^{-1} \simeq \frac{1}{\lambda_L} \mathbf{q}_L \mathbf{q}_L^T$ in (76)), we obtain the *rank-1-optimal* spreading code

$$\mathbf{s}_1 \stackrel{\triangle}{=} \arg \max_{\mathbf{s} \in \left\{ \pm \frac{1}{\sqrt{L}} \right\}^L} \left\{ \left(\mathbf{s}^T \mathbf{q}_L \right)^2 \right\} = \pm \mathrm{sgn} \left(\mathbf{q}_L \right) \tag{79}$$

where $\mathrm{sgn}(\cdot)$ denotes the sign operator. Hence, we showed that the rank-1-optimal binary code is simply the minimum-eigenvalue eigenvector of $\mathbf{R}$ passed through a sign hard-limiter. From another point of view, if we follow the common approach of: (i) first relaxing the binary constraint by allowing $\mathbf{s} \in \mathbb{R}^L$, $\|\mathbf{s}\| = 1$, (ii) then solving the relaxed problem to obtain $\mathbf{s}_{\mathbb{R}-\mathrm{OPT}} = \mathbf{q}_L$, and finally mapping $\mathbf{s}_{\mathbb{R}-\mathrm{OPT}} = \mathbf{q}_L$ to the binary field by taking the sign of its components, then we again obtain the rank-1-optimal binary spreading code $\mathrm{sgn} \left(\mathbf{s}_{\mathbb{R}-\mathrm{OPT}} \right) = \mathrm{sgn} \left(\mathbf{q}_L \right) = \mathbf{s}_1$. Therefore, the relaxation approach in [8], [24] is equivalent to rank-1 approximation of $\mathbf{R}^{-1}$.

To obtain a binary spreading code with higher SINR than $\mathrm{SINR} \left(\mathbf{s}_1 \right)$, in this present work we propose to keep the two strongest terms $\frac{1}{\lambda_L} \left(\mathbf{s}^T \mathbf{q}_L \right)^2 + \frac{1}{\lambda_{L-1}} \left(\mathbf{s}^T \mathbf{q}_{L-1} \right)^2$ in (78) or -equivalently- use rank-2 approximation of $\mathbf{R}^{-1} \simeq \frac{1}{\lambda_L} \mathbf{q}_L \mathbf{q}_L^T + \frac{1}{\lambda_{L-1}} \mathbf{q}_{L-1} \mathbf{q}_{L-1}^T$. Then, our optimization problem becomes

$$\mathbf{s}_2 = \arg \max_{\mathbf{s} \in \left\{ \pm \frac{1}{\sqrt{L}} \right\}^L} \left\{ \frac{1}{\lambda_L} \left(\mathbf{s}^T \mathbf{q}_L \right)^2 + \frac{1}{\lambda_{L-1}} \left(\mathbf{s}^T \mathbf{q}_{L-1} \right)^2 \right\}. \tag{80}$$

Below, we show that the rank-2-optimal binary vector $\mathbf{s}_2$ in (80) can always be obtained with less than quadratic complexity (less than the complexity required for the eigendecomposition of $\mathbf{R}$).

We begin by defining the complex vector

$$\mathbf{z} \stackrel{\triangle}{=} \frac{1}{\sqrt{\lambda_L}} \mathbf{q}_L + j \frac{1}{\sqrt{\lambda_{L-1}}} \mathbf{q}_{L-1}. \tag{81}$$

Then, the problem in (80) is converted to

$$\mathbf{s}_2 = \arg \max_{\mathbf{s} \in \left\{ \pm \frac{1}{\sqrt{L}} \right\}^L} \left\{ \left| \mathbf{s}^T \mathbf{z} \right|^2 \right\} = \arg \max_{\mathbf{s} \in \left\{ \pm \frac{1}{\sqrt{L}} \right\}^L} \left\{ \left| \mathbf{s}^T \mathbf{z} \right| \right\}. \tag{82}$$

In an effort to solve (82) in less than quadratic complexity, we consider the auxiliary-variable techniq ue that has been used in a communications theory context before in [25] and then again in [26]. Let $\mathbf{s} = [s_1 \;\; s_2 \;\; \ldots \;\; s_L]^T$ and $\mathbf{z} = [z_1 \;\; z_2 \;\; \ldots \;\; z_L]^T$ where

$$z_i = |z_i| \, e^{j\phi_i}, \qquad -\frac{\pi}{2} \leq \phi_i < \frac{3\pi}{2}, \qquad i = 1, 2, \ldots, L. \tag{83}$$

We introduce an auxiliary variable $\phi \in [-\pi, \pi)$ and rewrite the quantity to be maximized as

$$\left| \mathbf{s}^T \mathbf{z} \right| = \max_{\phi \in [-\pi, \pi)} \left\{ \mathrm{Re} \left\{ \mathbf{s}^T \mathbf{z} e^{-j\phi} \right\} \right\} = \max_{\phi \in [-\pi, \pi)} \left\{ \sum_{i=1}^{L} s_i \, |z_i| \cos\left(\phi - \phi_i\right) \right\} \tag{84}$$

where $\mathrm{Re}\{\cdot\}$ extracts the real part of a complex number. Then,

$$\begin{aligned} \max_{\mathbf{s} \in \left\{ \pm \frac{1}{\sqrt{L}} \right\}^L} \left\{ \left| \mathbf{s}^T \mathbf{z} \right| \right\} &= \max_{\mathbf{s} \in \left\{ \pm \frac{1}{\sqrt{L}} \right\}^L} \max_{\phi \in [-\pi, \pi)} \left\{ \sum_{i=1}^{L} s_i \, |z_i| \cos\left(\phi - \phi_i\right) \right\} \\ &= \max_{\phi \in [-\pi, \pi)} \left\{ \sum_{i=1}^{L} |z_i| \max_{s_i \in \left\{ \pm \frac{1}{\sqrt{L}} \right\}} \left\{ s_i \cos\left(\phi - \phi_i\right) \right\} \right\} \qquad (85) \\ &= \max_{\phi \in [-\pi, \pi)} \left\{ \sum_{i=1}^{L} |z_i| \, \frac{1}{\sqrt{L}} \left| \cos\left(\phi - \phi_i\right) \right| \right\}, \qquad (86) \end{aligned}$$

since for any $\phi \in [-\pi, \pi)$ the optimal s_i value in (85) is $s_i(\phi) = \frac{1}{\sqrt{L}} \mathrm{sgn}\left(\cos\left(\phi - \phi_i\right)\right)$, $i = 1, 2, \ldots, L$. The final quantity $\sum_{i=1}^{L} |z_i| \, \frac{1}{\sqrt{L}} \left| \cos\left(\phi - \phi_i\right) \right|$ in (86) is maximized for a particular value $\phi_{\mathrm{OPT}} \in [-\pi, \pi)$ and $\mathbf{s}(\phi_{\mathrm{OPT}}) = [s_1(\phi_{\mathrm{OPT}}) \;\; s_2(\phi_{\mathrm{OPT}}) \;\; \ldots \;\; s_L(\phi_{\mathrm{OPT}})]^T$ is the rank-2-optimal binary vector we are searching for in (12), i.e. $\mathbf{s}_2 = \mathbf{s}(\phi_{\mathrm{OPT}})$. We will now show that we can always construct a set of L spreading codes $\mathcal{U} = \{\mathbf{u}_1, \mathbf{u}_2, \ldots, \mathbf{u}_L\}$, $\mathbf{u}_i \in \left\{ \pm \frac{1}{\sqrt{L}} \right\}^L$, and guarantee that $\mathbf{s}(\phi_{\mathrm{OPT}}) \in \mathcal{U}$. Therefore, the maximization in (12) can be carried out over a set of L candidates only without loss of optimality.

Partition $\mathbb{Z}_L = \{1, 2, \ldots, L\}$ into

$$I_1 = \left\{ i: \;\; \phi_i \in \left[-\frac{\pi}{2}, \frac{\pi}{2} \right) \right\} \qquad \text{and} \qquad I_= \left\{ i: \;\; \phi_i \in \left[\frac{\pi}{2}, \frac{3\pi}{2} \right) \right\} = \mathbb{Z}_L - I_1 \tag{87}$$

and define the set of angles

$$\hat{\phi}_i \triangleq \begin{cases} \phi_i, & i \in I_1 \\ \phi_i - \pi, & i \in I_2 \end{cases}, \qquad i = 1, 2, \ldots, L, \tag{88}$$

such that $-\frac{\pi}{2} \leq \hat{\phi}_i < \frac{\pi}{2}$, $i = 1, 2, \ldots, L$. Define, for notational simplicity, the vector operation $\hat{\mathbf{s}}(\phi) \stackrel{\triangle}{=} [\hat{s}_1(\phi) \;\; \hat{s}_2(\phi) \;\; \ldots \;\; \hat{s}_L(\phi)]^T$ with $\hat{s}_i(\phi) \stackrel{\triangle}{=} \operatorname{sgn}\left(\cos\left(\phi - \hat{\phi}_i\right)\right)$, $i = 1, 2, \ldots, L$, $\phi \in [-\pi, \pi)$. Then,

$$s_i(\phi) = \begin{cases} \frac{\hat{s}_i(\phi)}{\sqrt{L}}, & i \in I_1 \\ -\frac{\hat{s}_i(\phi)}{\sqrt{L}}, & i \in I_2 \end{cases}, \qquad i = 1, 2, \ldots, L. \tag{89}$$

Consider a mapping e from $\mathbb{Z}_L$ to $\mathbb{Z}_L$ that sorts $\hat{\phi}_1, \hat{\phi}_2, \ldots, \hat{\phi}_L$: $-\frac{\pi}{2} \leq \hat{\phi}_{e(1)} \leq \hat{\phi}_{e(2)} \leq \ldots \leq \hat{\phi}_{e(L)} < \frac{\pi}{2}$. In (85), (86), maximization with respect to ϕ can be carried out over any subinterval of length π. We choose $\hat{\phi}_{e(1)} - \frac{\pi}{2}$ and $\hat{\phi}_{e(1)} + \frac{\pi}{2}$ as the limits of such a subinterval and rewrite the original optimization problem of (85) as

$$\max_{\mathbf{s} \in \left\{\pm\frac{1}{\sqrt{L}}\right\}^L} \left\{\left|\mathbf{s}^T \mathbf{z}\right|\right\} = \max_{\phi \in \left[\hat{\phi}_{e(1)} - \frac{\pi}{2}, \hat{\phi}_{e(1)} + \frac{\pi}{2}\right)} \left\{ \sum_{i=1}^{L} |z_i| \max_{s_i \in \left\{\pm\frac{1}{\sqrt{L}}\right\}} \{s_i \cos(\phi - \phi_i)\} \right\}. \tag{90}$$

By examining the subintervals $\left[\hat{\phi}_{e(1)} - \frac{\pi}{2}, \hat{\phi}_{e(2)} - \frac{\pi}{2}\right)$, $\left[\hat{\phi}_{e(2)} - \frac{\pi}{2}, \hat{\phi}_{e(3)} - \frac{\pi}{2}\right)$, $\ldots$, $\left[\hat{\phi}_{e(L-1)} - \frac{\pi}{2}, \hat{\phi}_{e(L)} - \frac{\pi}{2}\right)$, $\left[\hat{\phi}_{e(L)} - \frac{\pi}{2}, \hat{\phi}_{e(1)} + \frac{\pi}{2}\right)$, we conclude that

$$\left[\hat{s}_{e(1)}(\phi) \;\; \hat{s}_{e(2)}(\phi) \;\; \ldots \;\; \hat{s}_{e(L)}(\phi)\right] =$$

$$\begin{cases} [+1 \; -1 \; -1 \; \ldots -1 \; -1], & \hat{\phi}_{e(1)} - \frac{\pi}{2} \leq \phi < \hat{\phi}_{e(2)} - \frac{\pi}{2} \\ [+1 \; +1 \; -1 \; \ldots -1 \; -1], & \hat{\phi}_{e(2)} - \frac{\pi}{2} \leq \phi < \hat{\phi}_{e(3)} - \frac{\pi}{2} \\ \qquad\qquad \vdots & \\ [+1 \; +1 \; +1 \; \ldots +1 \; -1], & \hat{\phi}_{e(L-1)} - \frac{\pi}{2} \leq \phi < \hat{\phi}_{e(L)} - \frac{\pi}{2} \\ [+1 \; +1 \; +1 \; \ldots +1 \; +1], & \hat{\phi}_{e(L)} - \frac{\pi}{2} \leq \phi < \hat{\phi}_{e(1)} + \frac{\pi}{2}. \end{cases} \tag{91}$$

We collect the L binary vectors that appear in the L cases above, $\tilde{\mathbf{u}}_i \stackrel{\triangle}{=} [\underbrace{+1 \; \ldots \; +1}_{i} \; \underbrace{-1 \; \ldots \; -1}_{L-i}]^T$, $i = 1, 2, \ldots, L$, and create the matrix

$$\tilde{\mathbf{U}} \stackrel{\triangle}{=} [\tilde{\mathbf{u}}_1 \;\; \tilde{\mathbf{u}}_2 \;\; \ldots \;\; \tilde{\mathbf{u}}_L] \tag{92}$$

whose ith row we denote by $\tilde{\mathbf{d}}_i^T$, $i = 1, 2, \ldots, L$. Then, we reorganize $\tilde{\mathbf{U}}$ to $\hat{\mathbf{U}} = [\hat{\mathbf{u}}_1 \;\; \hat{\mathbf{u}}_2 \;\; \ldots \;\; \hat{\mathbf{u}}_L] \stackrel{\triangle}{=} \left[\hat{\mathbf{d}}_1 \;\; \hat{\mathbf{d}}_2 \;\; \ldots \;\; \hat{\mathbf{d}}_L\right]^T$ by defining the binary vectors

$$\hat{\mathbf{d}}_i \stackrel{\triangle}{=} \tilde{\mathbf{d}}_{e^{-1}(i)}, \qquad i = 1, 2, \ldots, L, \tag{93}$$

where $e^{-1} : \mathbb{Z}_L \to \mathbb{Z}_L$ is the inverse sorting mapping (note that $\hat{\mathbf{s}}(\phi) \in \{\hat{\mathbf{u}}_1, \hat{\mathbf{u}}_2, \ldots, \hat{\mathbf{u}}_L\}$ for any $\phi \in \left[\hat{\phi}_{e(1)} - \frac{\pi}{2}, \hat{\phi}_{e(1)} + \frac{\pi}{2}\right)$). Finally, we define

$$\mathbf{d}_i \stackrel{\triangle}{=} \begin{cases} \frac{1}{\sqrt{L}} \hat{\mathbf{d}}_i, & i \in I_1 \\ -\frac{1}{\sqrt{L}} \hat{\mathbf{d}}_i, & i \in I_2 \end{cases}, \qquad i = 1, 2, \ldots, L, \tag{94}$$

and construct

$$\mathbf{U} = [\mathbf{u}_1 \;\; \mathbf{u}_2 \;\; \ldots \;\; \mathbf{u}_L] \stackrel{\triangle}{=} [\mathbf{d}_1 \;\; \mathbf{d}_2 \;\; \ldots \;\; \mathbf{d}_L]^T . \tag{95}$$

The set $\mathcal{U} \stackrel{\triangle}{=} \{\mathbf{u}_1, \mathbf{u}_2, \ldots, \mathbf{u}_L\}$ contains $\mathbf{s}$ for any $\phi \in \left[\hat{\phi}_{e(1)} - \frac{\pi}{2}, \hat{\phi}_{e(1)} + \frac{\pi}{2}\right)$. But $\phi_{\mathrm{OPT}} \in \left[\hat{\phi}_{e(1)} - \frac{\pi}{2}, \hat{\phi}_{e(1)} + \frac{\pi}{2}\right)$, which implies $\mathbf{s}(\phi_{\mathrm{OPT}}) = \mathbf{s}_2 \in \mathcal{U}$. Hence, (82) becomes

$$\mathbf{s}_2 = \arg\max_{\mathbf{s}\in\mathcal{U}} \left\{ \left| \mathbf{s}^T \mathbf{z} \right| \right\}. \tag{96}$$

We conclude that the maximization task in (82) has been converted to an equivalent linear-complexity maximization problem in (96). The complexity of the construction of $\mathcal{U}$ is dominated by the complexity of the sorting function e which is of order $O(L \log_2 L)$. Therefore, we have described a method to obtain the rank-2-optimal binary vector $\mathbf{s}_2$ in (80) with complexity that is dominated by the complexity of the eigendecomposition of the $L \times L$ matrix $\mathbf{R}$ alone.

As a brief summary, the sequence of the proposed calculations is as follows. The autocovariance matrix $\mathbf{R}$ is eigendecomposed as in (74) followed by the computation of the $\mathbf{z}$ vector by Eq. (81). The sets I_1 and I_2 are constructed through (87); the angles $\hat{\phi}_1, \hat{\phi}_2, \ldots, \hat{\phi}_L$ are calculated by (88) and sorted to $\hat{\phi}_{e(1)} \leq \hat{\phi}_{e(2)} \leq \ldots \leq \hat{\phi}_{e(L)}$. Next, $\tilde{\mathbf{U}}$ is constructed as in (92) and reorganized to $\hat{\mathbf{U}}$ via (93); then, $\mathbf{U}$ is found by (95). The columns of $\mathbf{U}$, $\mathbf{u}_1, \mathbf{u}_2, \ldots, \mathbf{u}_L$, are used to calculate the quantities $\left|\mathbf{u}_1^T \mathbf{z}\right|, \left|\mathbf{u}_2^T \mathbf{z}\right|, \ldots, \left|\mathbf{u}_L^T \mathbf{z}\right|$ that are compared to each other to identify the maximum value among them, say $\left|\mathbf{u}_j^T \mathbf{z}\right|$ for some $j \in \{1, 2, \ldots, L\}$. The latter determines the rank-2-optimal binary spreading code $\mathbf{s}_2 = \mathbf{u}_j$.

C. Simulation Studies

We consider a DS-CDMA system where the user of interest transmits over an additive zero-mean white Gaussian noise channel with variance σ^2 in the presence of K synchronous interferers. The system processing gain (spreading code length) is $L = 16$. The received signal-to-noise ratio (SNR) of the user of interest, $\mathrm{SNR} \stackrel{\triangle}{=} \frac{P}{\sigma^2}$, is set to 10dB, while the received SNRs of the K interferers, $\mathrm{SNR}_k \stackrel{\triangle}{=} \frac{P_k}{\sigma^2}$, $k = 1, 2, \ldots, K$, are uniformly spaced between 8dB and 11dB. The interfering spreading codes are randomly generated.

In our studies, we compare the SINR performance of: *(i)* the *optimal* binary spreading code $\mathbf{s}_{\mathrm{OPT}}$ of (76) obtained through exhaustive search over all possible L-bit combinations; *(ii)* the *rank-1-optimal* binary spreading code $\mathbf{s}_1$ of (79) obtained by applying the sign operator on the minimum-eigenvalue eigenvector of the interference-plus-noise autocovariance matrix [8], [24]; and *(iii)* the proposed *rank-2-optimal* binary spreading code $\mathbf{s}_2$ of (80) obtained by the procedure developed in Section III. For comparison purposes, we evaluate the SINR loss, $\mathrm{SINR}(\mathbf{s}_{\mathrm{OPT}}) - \mathrm{SINR}(\mathbf{s})$, of $\mathbf{s} = \mathbf{s}_1$ or $\mathbf{s}_2$ with respect to the SINR of the optimal binary spreading code $\mathbf{s}_{\mathrm{OPT}}$. The results that we present are averages over $1,000$ randomly generated interference signature-set realizations.

In Fig. 9, we plot the SINR loss of the rank-1-optimal and rank-2-optimal binary spreading codes as a function of the number of interferers K. Since we are particularly interested in overloaded systems, we vary K from 16 to 40 interferers. We observe that the proposed rank-2-optimal spreading code exhibits less than 0.04dB performance loss which is significantly lower than the performance loss of the rank-1-optimal code (interestingly, both loss values decrease as K increases).

In Fig. 10, we plot the probability of global, full-rank, optimality $\Pr\{\mathbf{s} = \mathbf{s}_{\rm OPT}\}$ for the rank-1-optimal and rank-2-optimal binary spreading codes as a function of the number of interferers K. We observe that $.23 \leq \Pr\{\mathbf{s}_1 = \mathbf{s}_{\rm OPT}\} \leq .43$, while $.75 \leq \Pr\{\mathbf{s}_2 = \mathbf{s}_{\rm OPT}\} \leq .86$ as K is varied from 16 to 40 interferers. Therefore, with the proposed optimization of the binary spreading code under the rank-2 approximation of the inverse disturbance autocovariance matrix, we have practically doubled the probability that the designed spreading code is full-rank optimal with only $O(L \log_2 L)$ additional computational cost.

To the extend that neither the rank-1-optimal nor the rank-2-optimal binary spreading code design is globally optimal with probability one, the returned codes can potentially be used as the initialization point of an iterative steepest descent search [22], [24] that may converge to a (suboptimal in general) spreading code with higher SINR. In this spirit, we repeated the studies of Figs. 9 and 10 and fed the returned codes $\mathbf{s}_1$ and $\mathbf{s}_2$ to a Hamming-distance-1 steepest descent search to produce the improved spreading codes $\mathbf{s}_{1,\rm SD}$ and $\mathbf{s}_{2,\rm SD}$, correspondingly. In Fig. 11 we plot the SINR loss of $\mathbf{s}_{1,\rm SD}$ and $\mathbf{s}_{2,\rm SD}$; in Fig. 12 we plot the corresponding probabilities of full-rank optimality. The SINR superiority of the rank-2 approach is maintained. Interestingly, we observe that $\Pr\{\mathbf{s}_{2,\rm SD} = \mathbf{s}_{\rm OPT}\} \geq .9$ for any interference load. For example, when $K = 20$ the probability of global optimality is .95 for $\mathbf{s}_{2,\rm SD}$ (and .79 for $\mathbf{s}_{1,\rm SD}$). To examine the speed of convergence of the steepest descent search, in Fig. 13 we plot the evolution of the SINR value as a function of the number of iterations. The SINR of the globally optimal code $\mathbf{s}_{\rm OPT}$ is included as reference. We observe that when the search is initialized at the proposed rank-2-optimal code, convergence is achieved within three iterations only.

D. Conclusions

In the broad context of spread-spectrum communications (for example CDMA systems) or chip-based signal waveform design, we considered the problem of adaptively identifying the binary code that maximizes the signal-to-interference-plus-noise ratio (SINR) at the output of the maximum-SINR filter. The optimal code is a function of the disturbance autocovariance matrix and the optimization problem is NP-hard. Instead, we developed a new algorithm of less than quadratic complexity for the computation of the optimal code under rank-2 approximation of the inverse disturbance autocovariance matrix.

As an illustration of practical significance, we demonstrated the great SINR performance improvement of the proposed rank-2-optimal adaptive design for

overloaded CDMA systems with unequal user power over the rank-1-optimal adaptive design which -as we showed- is equivalent to direct hard-limiting of the minimum-eigenvalue eigenvector of the disturbance autocovariance matrix. In fact, the proposed rank-2-optimal design practically doubles the probability that the returned code is full-rank-optimal and when the rank-2-optimal design is used to initialize trivial Hamming-distance-1 steepest descent, the full-rank optimal code is reached with probability greater than 0.9 (within three iterations). Certainly, the proposed adaptive binary code design may serve well as the initialization point for other, potentially more sophisticated, iterative binary search procedures.

References

[1] P. Viswanath, V. Anantharam, and D. N. C. Tse, "Optimal sequences, power control, and user capacity of synchronous CDMA systems with linear MMSE multiuser receivers," *IEEE Trans. Inform. Theory*, vol. 45, pp. 1968-1983, Sept. 1999.

[2] P. Cotae, "An algorithm for obtaining Welch bound equality sequences for S-CDMA channels," *AEÜ. Int. J. Electron. Commun.*, vol. 55, pp. 95-99, Mar. 2001.

[3] T. Guess, "User-capacity-maximization in synchronous CDMA subject to RMS-bandlimited signature waveforms," *IEEE Trans. on Communications*, vol. 52, pp. 457-466, Mar. 2004.

[4] S. Stanczak and H. Boche, "Optimal signature sequences for asynchronous CDMA systems with fixed signal delays," in *Proc. 5th International Symposium on Wireless Personal Multimedia Communications*, Honolulu, HI, Oct. 2002, vol. 3, pp. 1147-1151.

[5] H. Boche and S. Stanczak, "Iterative algorithm for finding optimal resource allocation in symbol asynchronous CDMA channels with different SINR requirements," in *Proc. 36th Asilomar Conference on Signals, Systems and Computers*, Pacific Grove, CA, Nov. 2002, vol. 2, pp. 1909-1913.

[6] J. Luo, S. Ulukus and A. Ephremides, "Optimal sequences and sum capacity of symbol asynchronous CDMA systems," *IEEE Trans. Inform. Theory*, vol. 51, pp. 2760-2769, Aug. 2005.

[7] P. B. Rapajic and B. S. Vucetic, "Linear adaptive transmitter-receiver structures for asynchronous CDMA systems," *European Trans. Telecomm.*, vol. 6, pp. 21-28, Jan.-Feb. 1995.

[8] T. F. Wong and T. M. Lok, "Transmitter adaptation in multicode DS-CDMA systems," *IEEE J. Select. Areas Commun.*, vol. 19, pp. 69-82, Jan. 2001.

[9] S. Ulukus and R. D. Yates, "Iterative construction of optimum signature sets in synchronous CDMA systems," *IEEE Trans. Inform. Theory*, vol. 47, pp. 1989-1998, July 2001.

[10] C. Rose, S. Ulukus, and R. D. Yates, "Wireless systems and interference avoidance," *IEEE Trans. Wireless Communications*, vol. 1, pp. 415-428, July 2002.

[11] S. Ulukus and R. D. Yates, "User capacity of asynchronous CDMA systems with matched filter receivers and optimum signature sequences," *IEEE Trans. Inform. Theory*, vol. 50, pp. 903-909, May 2004.

[12] J. L. Concha and S. Ulukus, "Optimization of CDMA signature sequences in multipath channels," in *Proc. IEEE VTC-S 2001*, Rhodes, Greece, May 2001, vol. 3, pp. 1978-1982.

[13] O. Popescu and C. Rose, "Sum capacity and TSC bounds in collaborative multibase wireless systems," *IEEE Trans. Inform. Theory*, vol. 50, pp. 2433-2438, Oct. 2004.

[14] P. Cotae, "On minimizing total weighted square correlation of CDMA systems," in *Proc. IEEE ISIT 2003*, Yokohama, Japan, July 2003, p. 389.

[15] J. L. Massey and T. Mittelholzer, "Welch's bound and sequence sets for code-division multiple-access systems," in Sequences II, Methods in Communication, Security, and Computer Sciences, R. Capocelli, A. De Santis, and U. Vaccaro, Eds. New York: Springer-Verlag, 1993, pp. 63-78.

[16] M. Rupf and J. L. Massey, "Optimum sequence multisets for synchronous code-division multiple-access channels," *IEEE Trans. Inform. Theory*, vol. 40, pp. 1261-1266, July 1994.

[17] G. N. Karystinos and D. A. Pados, "New bounds on the total squared correlation and optimum design of DS-CDMA binary signature sets," *IEEE Trans. Commun.*, vol. 51, pp. 48 -51, Jan. 2003.

[18] C. Ding, M. Golin, and T. Klove, "Meeting the Welch and Karystinos-Pados bounds on DS-CDMA binary signature sets," *Designs, Codes and Cryptography*, vol. 30, pp. 73-84, Aug. 2003.

[19] V. P. Ipatov, "On the Karystinos-Pados bounds and optimal binary DS-CDMA signature ensembles," *IEEE Comm. Letters*, vol. 8, pp. 81-83, Feb. 2004.

[20] G. N. Karystinos and D. A. Pados, "The maximum squared correlation, total asymptotic efficiency, and sum capacity of minimum total-squared-correlation binary signature sets," *IEEE Trans. Inform. Theory*, vol. 51, pp. 348-355, Jan. 2005.

[21] P. D. Papadimitriou and C. N. Georghiades, "Code-search for optimal TSC binary sequences with low crosscorrelation spectrum," in *Proc. IEEE MILCOM 2003*, Boston, MA, Oct. 2003, vol. 2, pp. 1071-1076.

[22] F. Vanhaverbeke and M. Moeneclaey, "Binary signature sets for increased user capacity on the downlink of CDMA Systems," *IEEE Trans. Wireless Communications*, to appear.

[23] G. N. Karystinos and D. A. Pados, "Adaptive assignment of binary user spreading codes in DS-CDMA systems," in *Proc. SPIE's 15th Annual Intern. Symp., Digital Wireless Comm. Conf.*, Orlando, FL, Apr. 2001, vol. 4395, pp. 137-144.

[24] C. W. Sung and H. Y. Kwan, "Heuristic algorithms for binary sequence assignment in DS-CDMA systems," in *Proc. IEEE Intern. Symp. Personal, Indoor and Mobile Radio Commun.*, Sept. 2002, vol. 5, pp. 2327-2331.

[25] K. M. Mackenthun, Jr., "A fast algorithm for multiple-symbol differential detection of MPSK," *IEEE Trans. Commun.*, vol. 42, pp. 1471-1474, Feb./Mar./Apr. 1994.

[26] W. Sweldens, "Fast block noncoherent decoding," *IEEE Comm. Letters*, vol. 5, pp. 132-134, Apr. 2001.

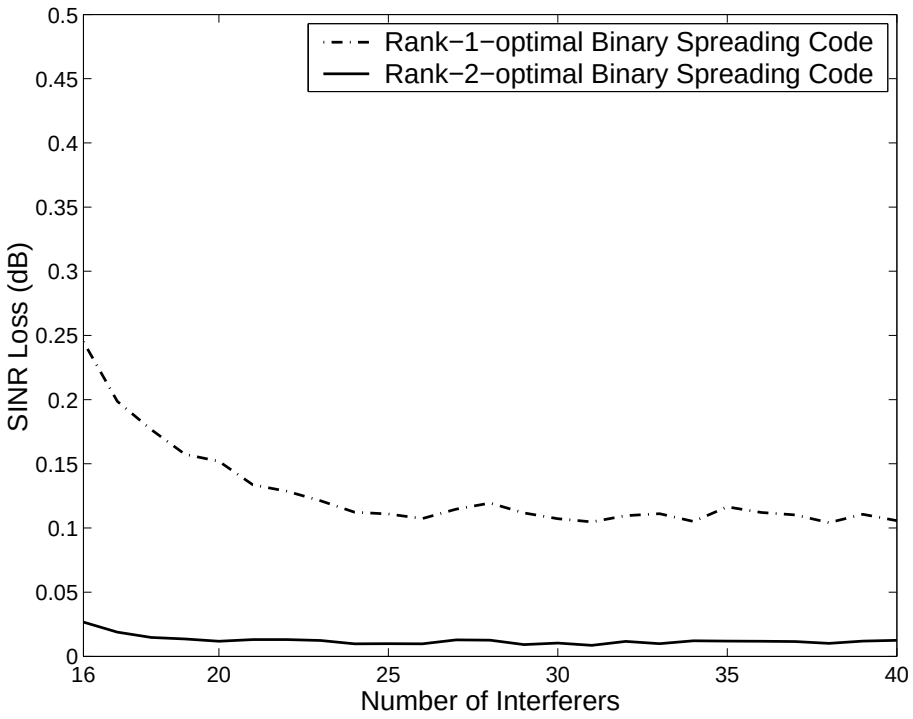

Fig. 9: SINR loss of rank-1-optimal and rank-2-optimal binary spreading code designs versus number of interferers (signature length $L = 16$).

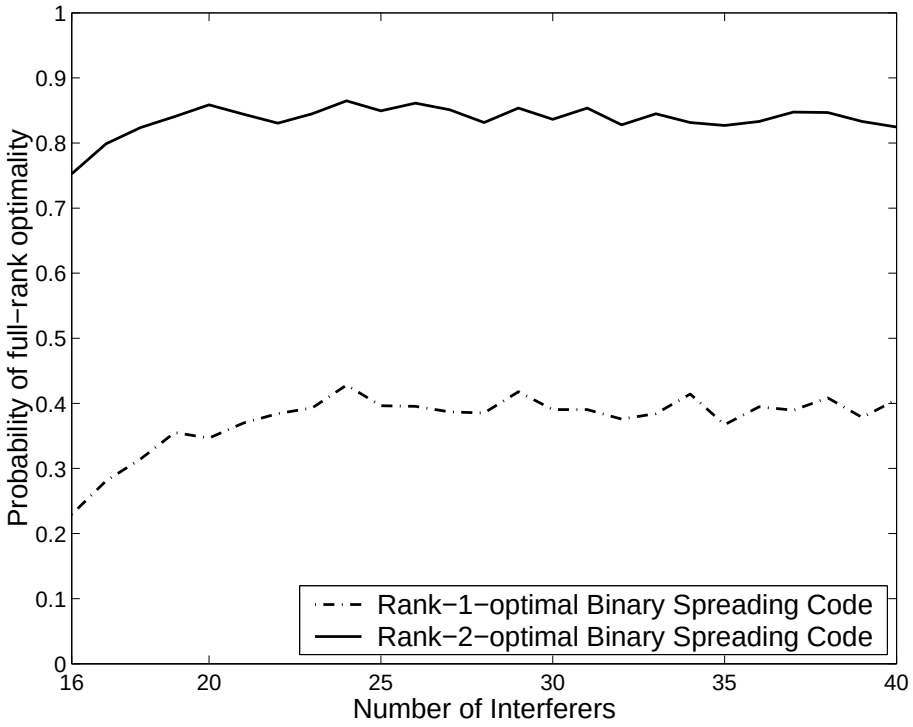

Fig. 10: Probability of full-rank optimality of rank-1-optimal and rank-2-optimal binary spreading code designs versus number of interferers.

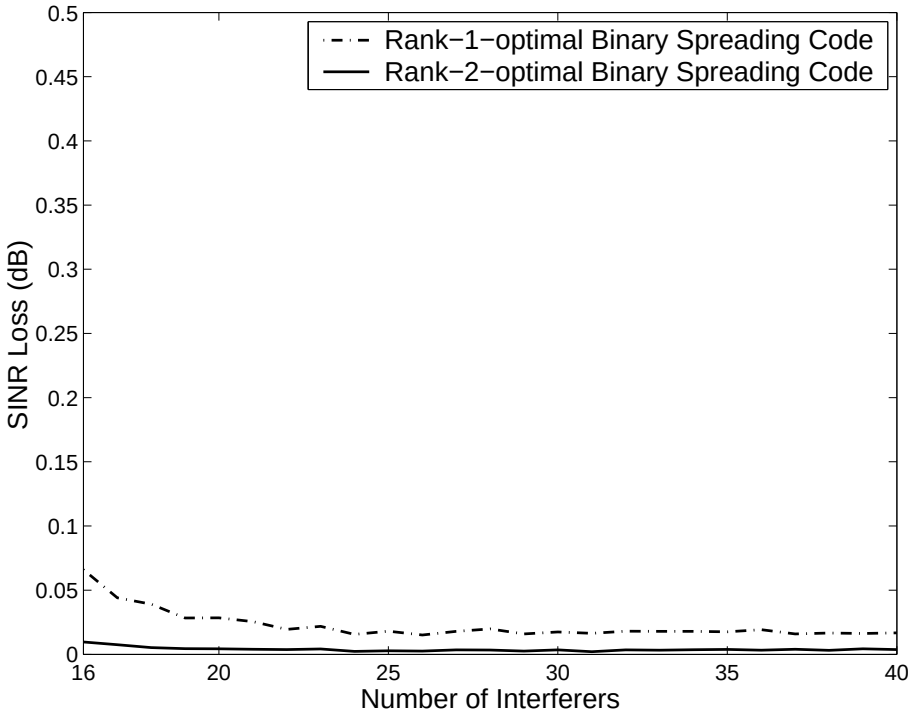

Fig. 11: SINR loss of steepest descent upon convergence with rank-1-optimal and rank-2-optimal initialization.

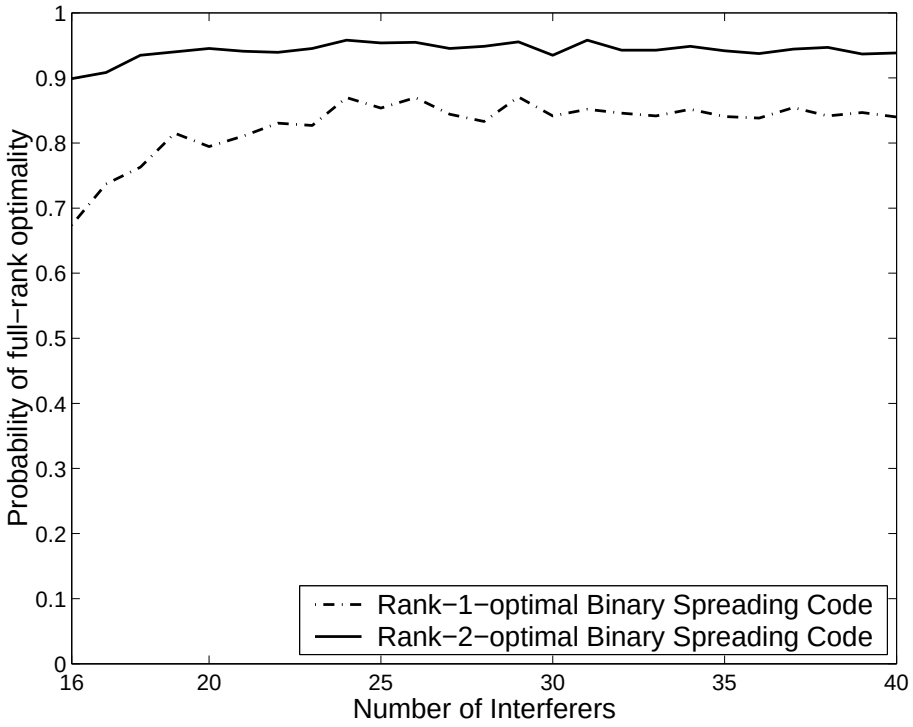

Fig. 12: Probability of full-rank optimality of steepest descent search upon convergence with rank-1-optimal and rank-2-optimal initialization.

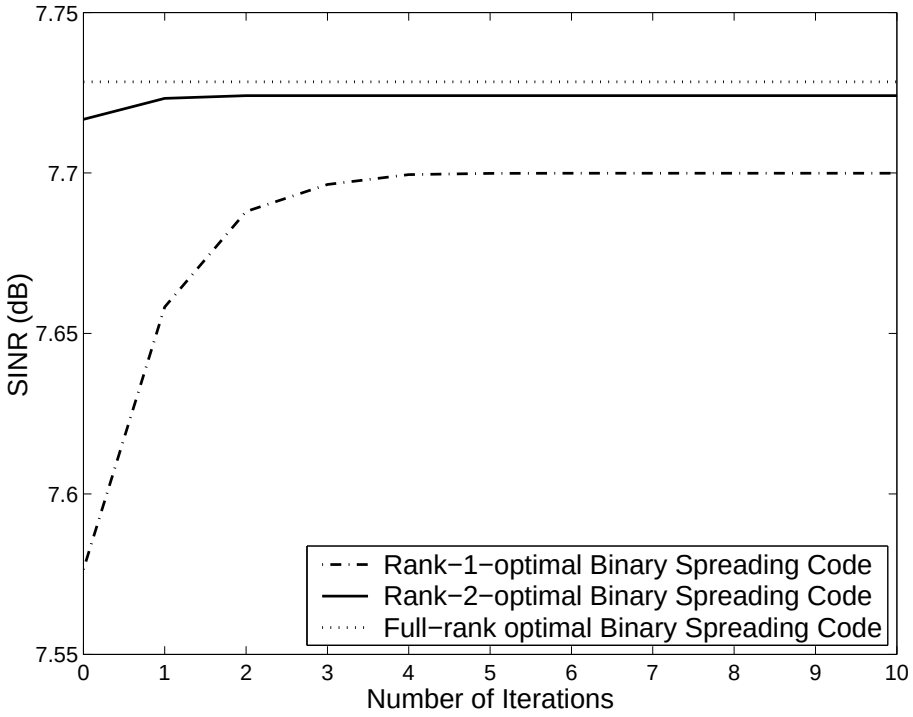

Fig. 13: SINR of steepest descent with rank-1-optimal and rank-2-optimal initialization versus number of iterations.

V. Scalable TSC-optimal Overloading of Binary Signature Sets

The work has been presented at IEEE GLOBECOM 2006.

In code-division multiplexing applications, for example direct-sequence code-division multiple-access (DS-CDMA) cellular communications systems, each of the K participating signals/users is equipped with a unique identifying signature vector $\mathbf{s}_k \in \mathbb{C}^L,\ ||\mathbf{s}_k|| = 1,\ k = 1, 2, \ldots, K$. All signatures put together in the form of a matrix define what we call the signature set

$$\mathcal{S} \stackrel{\triangle}{=} [\mathbf{s}_1\ \mathbf{s}_2 \ldots \mathbf{s}_K] \in \mathbb{C}^{L \times K}. \tag{97}$$

In synchronous code-division multiplexing transmissions over well behaved Nyquist channels, we are interested in using a signature set with the smallest possible total squared correlation (TSC) value [1]-[6]

$$\mathrm{TSC}(\mathcal{S}) \stackrel{\triangle}{=} \sum_{i=1}^{K} \sum_{j=1}^{K} \left| \mathbf{s}_i^H \mathbf{s}_j \right|^2 \tag{98}$$

where H denotes the Hermitian operator. For complex/real-valued signature sets $\mathcal{S} \in \mathbb{C}^{L \times K}$ or $\mathbb{R}^{L \times K}$, if $K \geq L$, $\mathrm{TSC}(\mathcal{S}) \geq \frac{K^2}{L}$ [1] (of course, $\mathrm{TSC}(\mathcal{S}) \geq K$ if $K < L$). Overloaded ($K \geq L$) sets with TSC equal to $\frac{K^2}{L}$ have been known as Welch-bound-equality (WBE) sets. Algorithms and studies for the design of complex or real WBE signature sets can be found in [3]-[10]. While not an issue for underloaded systems, it is well understood that as new users enter/exit an overloaded system the existing signature set has to be *re-designed* or *re-cast* to maintain TSC optimality (WBE sets do not stay optimal if signatures are added/removed). As a solution to the scalability problem in the complex/real vector domain, two subclasses of WBE sets are proposed in [11] that provide satisfactory TSC/signal-to-interference-plus-noise ratio (SINR) performance as the number of users changes dynamically.

In digital transmission systems it is necessary to have finite-alphabet signature sets. Recently, new bounds were derived on the TSC of *binary antipodal* signature sets together with optimal designs for arbitrary signature lengths and set sizes [2]-[4]. Studying the designs provided therein we observe that, similar to the complex/real-field case, as long as the system is underloaded users can be accommodated in and out without having to change the existing signature set to maintain TSC optimality. In the overloaded regime, when additional users enter/exit the system the existing signature set has to be re-designed/re-cast. In this paper, we present a complete solution to the scalability problem for binary sets with overloading up to 100%.

Consider a $(K = L + n, L),\ n \in \{-1, 0, 1, 2\}$, TSC-optimal fixed initial matrix $\mathcal{S}_I \stackrel{\triangle}{=} [\mathbf{s}_1\ \mathbf{s}_2 \ldots \mathbf{s}_{L+n}]$,
$\mathbf{s}_k \in \left\{ \pm \frac{1}{\sqrt{L}} \right\}^L,\ k = 1, 2, \ldots, L + n,\ n \in \{-1, 0, 1, 2\}$, given by [2]-[4]. To this

set, we will append N, $1 \leq N \leq L+2$, carefully designed unique signatures $\{\mathbf{s}_{L+n+k}\}_{k=1}^{N}$, $n \in \{-1, 0, 1, 2\}$, that define the *extended* signature matrix

$$\mathcal{S}_E \stackrel{\triangle}{=} [\mathbf{s}_{L+n+1} \ldots \mathbf{s}_{L+n+N}] \in \left\{\pm\frac{1}{\sqrt{L}}\right\}^{L\times N}. \tag{99}$$

The complete $(K = L+n+N, L)$ signature matrix $\mathcal{S}$ can then be expressed as

$$\mathcal{S} \stackrel{\triangle}{=} [\mathcal{S}_I \ \mathcal{S}_E] \in \left\{\pm\frac{1}{\sqrt{L}}\right\}^{L\times(L+n+N)}. \tag{100}$$

From (98) and (100),

$$\mathrm{TSC}(\mathcal{S}) = \mathrm{TSC}(\mathcal{S}_I) + \mathrm{TSC}(\mathcal{S}_E) + \mathrm{F}(\mathcal{S}_I, \mathcal{S}_E) \tag{101}$$

where $\mathrm{F}(\mathcal{S}_I, \mathcal{S}_E)$ is the sum of the absolute squared cross-correlations between every signature in set $\mathcal{S}_I$ and every signature in set $\mathcal{S}_E$,

$$\mathrm{F}(\mathcal{S}_I, \mathcal{S}_E) = 2\sum_{\substack{i\in\{1,2,\ldots,L+n\}\\ j\in\{L+n+1,\ldots,L+n+N\}}} |\mathbf{s}_i^T \mathbf{s}_j|^2 \tag{102}$$

(T denotes the transpose operator). To provide scalable signature set designs and control the TSC value, in this paper we consider the problem of minimizing the TSC of $\mathcal{S} = [\mathcal{S}_I \ \mathcal{S}_E]$ subject to $\mathcal{S}_I$ being fixed and TSC-optimal. In past related literature, $\mathcal{S}_I$ and $\mathcal{S}_E$ were designed to be orthogonal binary Hadamard sets (which requires the signature length L to be a multiple of four) scrambled independently by complex random PN-sequences [15]. The mutual interference, quantified as a loss in SINR, between the two sets of signatures was suppressed through iterative detection. In [11] it was shown that for a fixed and optimal $\mathcal{S}_I$, $\mathrm{TSC}(\mathcal{S}) \geq L + 3N$ for all $\mathcal{S} \in \mathbb{C}^{L\times(L+N)}$, $1 \leq N \leq L$. Here, we derive new tighter bounds on the conditional TSC of binary sets for all overloaded-by-N cases where $1 \leq N \leq L+2$. The work can be easily extended to cover higher overloading (from a practical perspective, however, overloading by more than 100% may not be of much interest at present). In addition, we provide optimal constructions that meet the new conditional TSC bounds with equality (hence, establish their tightness). Included numerical comparison studies show that the proposed sets minimally exceed the global TSC bound of [2] and, in fact, in certain cases meet the bound with equality and become globally TSC optimal.

A. New Bounds on the Conditional TSC of Overloaded Binary Sets

Our goal is to derive lower bounds on (101) subject to $\mathcal{S}_I$ being fixed and optimal over all $\mathcal{S}_E \in \left\{\left\{\pm\frac{1}{\sqrt{L}}\right\}^{L\times N} - \mathcal{S}_I\right\}$ where $1 \leq N \leq L+2$. We derive the (conditional TSC) bounds on a case-by-case basis.

Case 1: $L \equiv 0 \pmod 4$, $1 \leq N \leq L$.
Let $\mathcal{S}_I$ be an optimal (L, L) initial matrix with $\mathrm{TSC}(\mathcal{S}_I) = L$ as observed from Table I[4]. From [2], the set $\mathcal{S}^{'} = [\mathcal{S}_I \ \mathbf{s}]$ is optimal for any $\mathbf{s} \in \{\pm\frac{1}{\sqrt{L}}\}^L$ and

$$\mathrm{TSC}(\mathcal{S}^{'}) - \mathrm{TSC}(\mathcal{S}_I) - \|\mathbf{s}\|^2 = \left(\frac{(L+1)^2}{L} + \frac{L-1}{L}\right) - L - 1 = 2; \tag{103}$$

hence, for any arbitrary extension matrix $\mathcal{S}_E \in \left\{\pm\frac{1}{\sqrt{L}}\right\}^{L\times N}$, $\mathrm{F}(\mathcal{S}_I, \mathcal{S}_E) = 2N$. From Table I, $\mathrm{TSC}(\mathcal{S}_E) \geq N$ and we calculate

$$TSC(\mathcal{S}) \geq L + 3N. \tag{104}$$

Case 2: $L \equiv 2 \pmod 4$, $1 \leq N \leq L + 2$.
Let $\mathcal{S}_I$ be an optimal $(L+2, L)$ initial matrix with $\mathrm{TSC}(\mathcal{S}_I) = \frac{(L+2)^2}{L}$ as calculated from Table I. From [2], the set $\mathcal{S}^{'} = [\mathcal{S}_I \ \mathbf{s}]$ is optimal for any $\mathbf{s} \in \{\pm\frac{1}{\sqrt{L}}\}^L$ and

$$\mathrm{TSC}(\mathcal{S}^{'}) - \mathrm{TSC}(\mathcal{S}_I) - \|\mathbf{s}\|^2 = \left(\frac{(L+3)^2}{L} + \frac{L-1}{L}\right) - \frac{(L+2)^2}{L} - 1 = 2 + \frac{4}{L}; \tag{105}$$

hence, for any arbitrary extension matrix $\mathcal{S}_E \in \left\{\pm\frac{1}{\sqrt{L}}\right\}^{L\times N}$, $\mathrm{F}(\mathcal{S}_I, \mathcal{S}_E) = 2N\left(\frac{L+2}{L}\right)$. From Table I,

$$\mathrm{TSC}(\mathcal{S}_E) \quad \geq \quad \begin{cases} N + \frac{2(N-1)^2}{L^2}, & N \equiv 1 \pmod 2 \\ N + \frac{2N(N-1)}{L^2}, & N \equiv 0 \pmod 2 \end{cases} \tag{106}$$

and we calculate

$$\mathrm{TSC}(\mathcal{S}) \quad \geq \quad \begin{cases} \frac{(L+2)^2}{L} + N + \frac{2(N-1)^2}{L^2} + \frac{2N(L+2)}{L}, & N \equiv 1 \pmod 2 \\ \frac{(L+2)^2}{L} + N + \frac{2N(N-1)}{L^2} + \frac{2N(L+2)}{L}, & N \equiv 0 \pmod 2. \end{cases} \tag{107}$$

Case 3: $L \equiv 3 \pmod 4$, $1 \leq N \leq L + 1$.
Let $\mathcal{S}_I$ be an optimal $(L+1, L)$ initial matrix. By Table I, $\mathrm{TSC}(\mathcal{S}_I) = \frac{(L+1)^2}{L}$. By [2], $\mathcal{S}^{'} = [\mathcal{S}_I \ \mathbf{s}]$ is optimal for any $\mathbf{s} \in \{\pm\frac{1}{\sqrt{L}}\}^L$ and

$$\mathrm{TSC}(\mathcal{S}^{'}) - \mathrm{TSC}(\mathcal{S}_I) - \|\mathbf{s}\|^2 = \left(\frac{(L+2)^2}{L} + \frac{L-1}{L}\right) - \frac{(L+1)^2}{L} - 1 = 2 + \frac{2}{L}; \tag{108}$$

[4]Table I of [2] is reproduced for convenience in Table I herein.

hence, for any arbitrary extension matrix $\mathcal{S}_E \in \left\{\pm\frac{1}{\sqrt{L}}\right\}^{L\times N}$, $\mathrm{F}(\mathcal{S}_I, \mathcal{S}_E) = 2N\left(\frac{L+1}{L}\right)$. From Table I,

$$\mathrm{TSC}(\mathcal{S}_E) \geq N + \frac{N(N-1)}{L^2} \tag{109}$$

and we calculate

$$\mathrm{TSC}(\mathcal{S}) \geq \frac{(L+1)^2}{L} + N + \frac{N(N-1)}{L^2} + \frac{2N(L+1)}{L}. \tag{110}$$

Case 4: $L \equiv 1 \pmod 4$, $1 \leq N \leq L-2$.
Let $\mathcal{S}_I$ be an optimal $(L-1, L)$ initial matrix[5]. By Table I, $\mathrm{TSC}(\mathcal{S}_I) = L - 1 + \frac{(L-1)(L-2)}{L^2}$. $\mathcal{S}_I$ can be obtained[6] from an optimal $(L-1, L-1)$ set $\mathcal{S}^{''}$, i.e. $\mathcal{S}_I$ contains an optimal (hence, orthogonal [2]) submatrix $\mathcal{S}^{''}$ of size $(L-1, L-1)$. This property is utilized in the following Lemma and Theorem, which, in turn, are used to derive the bound.

Lemma 1: Let $\mathcal{S}^{''} = \left[\mathbf{s}_1^{''}\ \mathbf{s}_2^{''} \ldots \mathbf{s}_{L-1}^{''}\right] \in \left\{\pm\frac{1}{\sqrt{L}}\right\}^{(L-1)\times(L-1)}$, $L \equiv 1 \pmod 4$, be the optimal (orthogonal) submatrix of $\mathcal{S}_I$. Then, for any $\mathbf{x} \in \left\{\pm\frac{1}{\sqrt{L}}\right\}^{L-1}$, $\sum_{i=1}^{L-1} \mathbf{x}^T\mathbf{s}_i^{''} \in (\frac{L-1}{L}, -\frac{L-1}{L})$.
Proof: The vectors $\mathbf{s}_1^{''}, \ldots, \mathbf{s}_{L-1}^{''}$ form an orthogonal basis for $\mathbb{R}^{L-1}$. Then, for any $\mathbf{x} \in \left\{\pm\frac{1}{\sqrt{L}}\right\}^{L-1}$,

$$\mathbf{x} = a_1\mathbf{s}_1^{''} + a_2\mathbf{s}_2^{''} + \ldots + a_{L-1}\mathbf{s}_{L-1}^{''} \tag{111}$$

where $a_i \in \mathbb{R}$ and at least one $a_i \neq 0$, $i = 1, 2, \ldots, L-1$. Using (111),

$$\sum_{i=1}^{L-1} \mathbf{x}^T\mathbf{s}_i^{''} = \frac{L-1}{L}\left(a_1 + a_2 + \ldots + a_{L-1}\right). \tag{112}$$

Let $s_i^{''}(1)$, $i = 1, \ldots, L-1$ denote the first element of $\mathbf{s}_i^{''}$ and $x(1)$ the first element of $\mathbf{x}$. Without loss of generality, over the binary antipodal signature field $s_i^{''}(1) = \frac{1}{\sqrt{L}}$, $i = 1, 2, \ldots, L-1$. Since, $x(1) \in \{\pm\frac{1}{\sqrt{L}}\}$, $\sum_{i=1}^{L-1} a_i = \pm 1$ and the result follows. ∎

Theorem 1: Let $\mathcal{S}_I$ be an optimal $(L-1, L)$, $L \equiv 1 \pmod 4$, initial matrix. Create the (L, L) set $\mathcal{S}^{'} = \left[\mathcal{S}_I\ [\pm\frac{1}{\sqrt{L}}\ \mathbf{x}^T]^T\right]$ for an arbitrary $\mathbf{x} \in \{\pm\frac{1}{\sqrt{L}}\}^{L-1}$. Then,

$$\underset{\mathbf{x}\in\{\pm\frac{1}{\sqrt{L}}\}^{L-1}}{argmin} \left[\mathrm{TSC}(S^{'}) - \mathrm{TSC}(S_I)\right] = 1 + 2\frac{(L-2)(L-1)}{L^2}.$$

[5]No systematic construction of (L, L), $L \equiv 1 \pmod 4$, TSC-optimal sets is known [2]-[4].
[6]To the best of the authors' knowledge, no other method is known to systematically obtain an $(L-1, L)$ TSC-optimal set.

Proof: Design an $(L, L-1)$ optimal set $\mathcal{S}^{'''} = \left[\mathcal{S}^{''}\mathbf{x}\right]$ where $\mathbf{x} \in \{\pm\frac{1}{\sqrt{L}}\}^{L-1}$ and $\mathcal{S}^{''} = \left[\mathbf{s}_1^{''}\ \mathbf{s}_2^{''} \ldots \mathbf{s}_{L-1}^{''}\right]$, $\mathbf{s}_i^{''} \in \{\frac{1}{\sqrt{L}}\}^{L-1}$, is an optimal (orthogonal) $(L-1, L-1)$ set. From [2],

$$\mathrm{TSC}(\mathcal{S}^{'''}) - \mathrm{TSC}(\mathcal{S}^{''}) = \frac{(L-1)^2}{L^2} + 2\sum_{i=1}^{L-1}\left(\mathbf{x}^T\mathbf{s}_i^{''}\right)^2 = 3\frac{(L-1)^2}{L^2}. \tag{113}$$

Hence,

$$\sum_{i=1}^{L-1}\left(\mathbf{x}^T\mathbf{s}_i^{''}\right)^2 = \frac{(L-1)^2}{L^2}. \tag{114}$$

Now append any row vector $\left\{\pm\frac{1}{\sqrt{L}}\right\}^{1\times L}$ to the top of $\mathcal{S}^{'''}$ to form $\mathcal{S}^{'}$. Then, using (114),

$$\begin{aligned}\mathrm{TSC}(\mathcal{S}^{'}) - \mathrm{TSC}(\mathcal{S}_I) &= 1 + 2\textstyle\sum_{i=1}^{L-1}\left(\mathbf{x}^T\mathbf{s}_i^{''} \pm \frac{1}{L}\right)^2 \\ &= 1 + 2\left[\frac{(L-1)^2}{L^2} + \frac{L-1}{L^2} \pm \frac{2}{L}\textstyle\sum_{i=1}^{L-1}\mathbf{x}^T\mathbf{s}_i^{''}\right].\end{aligned} \tag{115}$$

From Lemma 1, $\sum_{i=1}^{L-1}\mathbf{x}^T\mathbf{s}_i^{''} = \pm\frac{L-1}{L}$. Therefore,

$$\underset{\mathbf{x}\in\{\pm\frac{1}{\sqrt{L}}\}^{L-1}}{argmin}\left[\mathrm{TSC}(S^{'}) - \mathrm{TSC}(S_I)\right] = 1 + 2\left[\frac{(L-1)^2}{L^2} - \frac{(L-1)}{L^2}\right] \tag{116}$$

∎

From Theorem 1, for any arbitrary extension matrix $\mathcal{S}_E \in \left\{\pm\frac{1}{\sqrt{L}}\right\}^{L\times N}$, $\mathrm{F}(\mathcal{S}_I, \mathcal{S}_E) \geq \frac{2N}{L^2}(L-2)(L-1)$. From Table I,

$$\mathrm{TSC}(\mathcal{S}_E) \geq N + \frac{N(N-1)}{L^2} \tag{117}$$

and we calculate

$$\mathrm{TSC}(\mathcal{S}) \geq L-1+\frac{(L-1)(L-2)}{L^2}+N+\frac{N(N-1)}{L^2}+\frac{2N}{L^2}(L-2)(L-1). \tag{118}$$

Table II summarizes our findings in (104), (107), (110), and (118).

B. Scalable Conditionally TSC-optimal Binary Sets

Following our formulation and notation in (100), (101), conditionally TSC-optimal design of an overloaded signature set $\mathcal{S}$ is equivalent to designing an extension matrix $\mathcal{S}_E$ such that $\mathrm{TSC}(\mathcal{S}_E)$ and $\mathrm{F}(\mathcal{S}_I, \mathcal{S}_E)$ are jointly minimized.

In the following, $\mathbf{H}_P$ with columns $\mathbf{h}_i,\ i = 1, \ldots, P$, represents a Hadamard matrix[7] of size P. Below, we provide scalable conditionally TSC-optimal signature set designs for all lengths L and overloading of (about) 100%.

Case 1: $L \equiv 0 \pmod 4$, $1 \leq N \leq L$.
Let $\mathcal{S}_I = \frac{1}{\sqrt{L}}\mathbf{H}_L$ be the (L, L) optimal [2] initial matrix. Obtain (an equivalent Hadamard matrix) $\mathbf{M}_L$ by multiplying any row of $\frac{1}{\sqrt{L}}\mathbf{H}_L$ by -1 and select any N columns from $\mathbf{M}_L$ to form the extension matrix $\mathcal{S}_E = [\mathbf{m}_1\ \mathbf{m}_2 \ldots \mathbf{m}_N]$. It can be shown that

$$\mathrm{TSC}(\mathcal{S}) = L + 3N \tag{119}$$

which is equal to the bound in (104). Hence, $\mathcal{S}$ is conditionally optimal.

It is interesting to note that the designs of Vanhaverbeke, Moeneclaey, and Sari in [15] fall under this case, meet the bound, and are conditionally optimal.

Case 2: $L \equiv 2 \pmod 4$, $1 \leq N \leq L + 2$.
Obtain $\mathbf{H}_{L+2}$ and omit the first two rows to create the $(L + 2, L)$ optimal [3] initial matrix $\mathcal{S}_I = \frac{1}{\sqrt{L}}\mathbf{H}'_{L+2}$. Obtain $\mathbf{M}_{L+2}$ by multiplying any of the last $L - 2$ rows of $\frac{1}{\sqrt{L}}\mathbf{H}_{L+2}$ by -1. Omit the first two rows of $\mathbf{M}_{L+2}$, select any $\lfloor \frac{N}{2} \rfloor$ columns that begin with $[\frac{1}{\sqrt{L}}\ \ \frac{1}{\sqrt{L}}]^T$ and any $\lceil \frac{N}{2} \rceil$ columns that begin with $[\frac{1}{\sqrt{L}}\ \ \frac{-1}{\sqrt{L}}]^T$ to create the extension set $\mathcal{S}_E = \mathbf{M}'_{L+2}$. It can be shown that

$$\mathrm{TSC}(\mathcal{S}) = \begin{cases} \frac{(L+2)^2}{L} + N + \frac{2(N-1)^2}{L^2} + \frac{2N(L+2)}{L}, & N \equiv 1 \pmod 2 \\ \frac{(L+2)^2}{L} + N + \frac{2N(N-2)}{L^2} + \frac{2N(L+2)}{L}, & N \equiv 0 \pmod 2 \end{cases} \tag{120}$$

which is equal to our bounds in (107). Hence, $\mathcal{S}$ is conditionally optimal.
Case 3: $L \equiv 3 \pmod 4$, $1 \leq N \leq L + 1$.
Obtain $\mathbf{H}_{L+1}$ and omit the first row to create the $(L + 1, L)$ optimal [2] initial matrix $\mathcal{S}_I = \frac{1}{\sqrt{L}}\mathbf{H}'_{L+1}$. Obtain $\mathbf{M}_{L+1}$ by multiplying any of the last $L - 1$ rows of $\frac{1}{\sqrt{L}}\mathbf{H}_{L+1}$ by -1. Omit the first row of $\mathbf{M}_{L+1}$ and select any N columns to create the extension matrix $\mathcal{S}_E = \mathbf{M}'_{L+1}$. It can be shown that

$$\mathrm{TSC}(\mathcal{S}) = \frac{(L+1)^2}{L} + N + \frac{N(N-1)}{L^2} + \frac{2N(L+1)}{L} \tag{121}$$

which is equal to our bound in (110). Hence, $\mathcal{S}$ is conditionally optimal.
Case 4: $L \equiv 1 \pmod 4$, $1 \leq N \leq L - 2$.
Obtain $\frac{1}{\sqrt{L}}\mathbf{H}_{L-1}$ and multiply the kth column, $k \in \{1, 2, \ldots, L-1\}$, by -1

[7] We recall that a Hadamard matrix $\mathbf{H}_N$ is an $N \times N$ matrix with elements $+1$ or -1 and orthogonal columns, $\mathbf{H}_N^T\mathbf{H}_N = N\mathbf{I}_N$ where $\mathbf{I}_N$ is the size-N identity matrix. A necessary condition for a Hadamard matrix to exist is that its size is a multiple of four, except for the trivial cases of size one or two. Without loss of generality, the first row and the first column of $\mathbf{H}_N$ contain only $+1$.

to create $\mathbf{H}_{L-1}^{'}=\left[\mathbf{h}_1^{'}\ \mathbf{h}_2^{'}\ldots\ \mathbf{h}_{L-1}^{'}\right]$. Append the row vector $[\underbrace{\frac{1}{\sqrt{L}}\ \frac{1}{\sqrt{L}}\ldots\frac{1}{\sqrt{L}}}_{L-1}]$ as the first row to $\mathbf{H}_{L-1}^{'}$ to create the initial matrix $\mathcal{S}_I=\mathbf{H}_{L-1}^{''}$, which is an $(L-1,L)$ optimal set [2]. Multiply the first row of $\mathbf{H}_{L-1}^{'}$ by -1 and exclude the kth column to create $\mathbf{M}_{L-2}^{'}=\left[\mathbf{m}_1^{'}\ \mathbf{m}_2^{'}\ldots\ \mathbf{m}_{L-2}^{'}\right]$. Finally, append the row vector $[\underbrace{\frac{-1}{\sqrt{L}}\ \frac{-1}{\sqrt{L}}\ldots\frac{-1}{\sqrt{L}}}_{L-2}]$ as the first row to $\mathbf{M}_{L-2}^{'}$ and keep any N columns to create the extension matrix $\mathcal{S}_E=\mathbf{M}_{L-2}^{''}=\left[\mathbf{m}_1^{''}\ \mathbf{m}_2^{''}\ldots\ \mathbf{m}_N^{''}\right]$. We calculate

$$\mathrm{TSC}(\mathcal{S})=L-1+\frac{(L-1)(L-2)}{L^2}+N+\frac{N(N-1)}{L^2}+\frac{2N}{L^2}(L-1)(L-2) \tag{122}$$

which is equal to our bound in (118). Hence, $\mathcal{S}$ is conditionally optimal. The derivation of (122) is provided in Appendix A.

To conclude the presentation and establish that all set designs $\mathcal{S}$ provided herein contain unique signatures, we need only to observe that for any matrix $\mathbf{M}_P=[\mathbf{m}_1\ \mathbf{m}_2\ldots,\mathbf{m}_P]$, $\mathbf{m}_i\in\left\{\pm\frac{1}{\sqrt{P}}\right\}^P$, $i=1,\ldots,P$, obtained by multiplying any row of $\mathbf{H}_P=[\mathbf{h}_1\ \mathbf{h}_2\ldots,\mathbf{h}_P]$, $\mathbf{h}_i\in\left\{\pm\frac{1}{\sqrt{P}}\right\}^P$, $i=1,\ldots,P$, by -1, if $d(\mathbf{h}_i,\mathbf{m}_j)$ denote the Hamming distance between $\mathbf{h}_i,\mathbf{m}_j$, $i,j=1,2,\ldots,P$. Then,

$$\left|\mathbf{h}_i^T\mathbf{m}_j\right|=\left|1-\frac{2d(\mathbf{h}_i,\mathbf{m}_j)}{P}\right|. \tag{123}$$

By construction of $\mathbf{M}_P$, if $i=j$, $d(\mathbf{h}_i,\mathbf{m}_j)=1$ and if $i\neq j$, $d(\mathbf{h}_i,\mathbf{m}_j)=\frac{P}{2}\pm1$. From (123)

$$\left|\mathbf{h}_i^T\mathbf{m}_j\right|=\begin{cases}1-\frac{2}{P}, & i=j\\ \frac{2}{P}, & i\neq j\end{cases}. \tag{124}$$

Hence, every column of $\mathbf{M}_P$ is different from every column of $\mathbf{H}_P$.

Regarding the scalability characteristics of the presented designs for medium-access-control (MAC), as users enter the system we may assign signatures at will first from $\mathcal{S}_I$ and then from $\mathcal{S}_E$ without having to change the existing/deployed signature set. In the event of a user leaving the system from the extended set $\mathcal{S}_E$ no action is needed to maintain conditional TSC optimality. If a user leaves from the initial set $\mathcal{S}_I$ and $\mathcal{S}_E$ is non-empty then its signature should be reassigned to an $\mathcal{S}_E$ user (or simply to the next incoming user) to regain conditional optimality.

C. Numerical Evaluation and Comparisons

In this section we evaluate numerically the TSC quality of the proposed overloaded signature sets. Fig. 14 shows as an example a $[19,16]$ conditionally

TSC-optimal set (obtained under Case 1). The natural benchmark is the unconditionally minimum attainable TSC value in [2]. Fig. 15 plots the TSC value of our Case 1, $L = 16$ design against the bound for all $1 \leq N \leq 16$. Figs. 16, 17, and 18 carry out similar comparative studies for $L = 14$ (Case 2), $L = 15$ (Case 3), and $L = 17$ (Case 4) designs, respectively.

A broader comment on the TSC quality of the proposed conditionally optimal sets for varying lengths L is offered by the following proposition.

Proposition 1: The TSC of the designs described in Section III is always within $\frac{L}{4} + \frac{1}{2}$ from the bounds in [2].

Proof: Let $\mathcal{S}$ be a Section III design and let minTSC denote the corresponding TSC lower bound in [2]. We can show that (see Appendix B)

$$\text{TSC}(S) - \text{minTSC} \leq \begin{cases} \frac{L}{4}, & L \equiv 0(\text{mod } 4), \\ & \text{with equality at } N = \frac{L}{2} \\ \frac{L}{4} - \frac{1}{L} - \frac{2}{L^2} + \frac{1}{2}, & L \equiv 2(\text{mod } 4), \\ & \text{with equality at } N = \frac{L+2}{2} \\ \frac{L}{4} - \frac{1}{4L} - \frac{1}{4L^2} + \frac{1}{4}, & L \equiv 3(\text{mod } 4), \\ & \text{with equality at } N = \frac{L+1}{2} \\ \frac{L}{4} - \frac{1}{4L} - \frac{1}{4L^2} + \frac{1}{4}, & L \equiv 1(\text{mod } 4). \end{cases} \tag{125}$$

Somewhat finer bounds depending on the form of the total number of signatures K are derived in Appendix B and given in Table III. ∎

D. Conclusions

We first derived lower bounds on the conditional total squared correlation of overloaded binary signature sets grown on full-load TSC-optimal sets for any signature length L and set size $K = L+N+n$, $1 \leq N \leq L+2$, $n \in \{-1, 0, 1, 2\}$. Then, we presented conditionally optimal designs for all such (K, L) set sizes (which establish the tightness of the corresponding bounds).

We analyzed the TSC performance of the conditionally optimal $(L + N, L)$ signature sets against the TSC of optimal $(L + N, L)$ sets and found that we are always within $\frac{L}{4} + \frac{1}{2}$ or better. Direct comparison of the conditionally TSC-optimal designs with the TSC bounds and optimal sets in [2] shows that: Case 1 when $N = \{1, 2, L - 2, L - 1, L\}$, Case 2 when $N = \{1, 2, L, L + 1, L + 2\}$, Case 3 when $N = \{1, 2, L - 1, L, L + 1\}$, and Case 4 when $N = \{L - 3, L - 2\}$ are unconditionally TSC-optimal (that is overloads near 0% or 100% are handled TSC optimally). Numerically, maximum TSC performance degradation is observed when the sets are about 50% overloaded. The observed degradation value is, arguably, a reasonable price to pay for the gained scalability.

References

[1] R. L. Welch, "Lower bounds on the maximum cross correlation of signals," *IEEE Trans. Inform. Theory*, vol. IT-20, pp. 397-399, May 1974.

[2] M. Rupf and J. L. Massey, "Optimum sequence multisets for synchronous code-division-multiple-access channels," *IEEE Trans. Inform. Theory*, vol. 40, pp. 1261-1266, July 1994.

[3] P. Vishwanath, V. Anantharaman, and D. N. C. Tse, "Optimal sequences, power control, and user capacity of synchronous CDMA systems with linear MMSE multiuser receivers," *IEEE Trans. Inform. Theory*, vol. 45, pp. 1968-1983, Sept. 1999.

[4] S. Ulukus and R. D. Yates, "Iterative construction of optimum signatures sequences sets in synchronous CDMA systems," *IEEE Trans. Inform. Theory*, vol. 47, pp. 1989-1998, July 2001.

[5] C. Rose, S. Ulukus, and R. D. Yates, "Wireless systems and interference avoidance," *IEEE Trans. Wireless Commun.*, vol. 1, pp. 415-428, Mar. 2002.

[6] P. Cotae, "Spreading sequence design for multiple cell synchronous DS-CDMA systems under total weighted squared correlation criterion," *EURASIP Journal Wireless Comm. and Networking*, vol. 2004, no. 1, pp. 4-11, Aug. 2004.

[7] O. Popescu and C. Rose, "Sum capacity and TSC bounds in collaborative multibase wireless systems," *IEEE Trans. Inform. Theory*, vol. 50, pp. 2433-2440, Oct. 2004.

[8] J. Luo, S. Ulukus, and A. Ephremides, "Optimal sequences and sum capacity of symbol asynchronous CDMA systems," *IEEE Trans. Inform. Theory*, vol. 51, pp. 2760-2769, Aug. 2005.

[9] P. Cotae, "On the optimal sequences and total weighted square correlation of synchronous CDMA systems in multipath channels," *IEEE Trans. Vehic. Tech.*, vol. 56, pp. 2063-2072, July 2007.

[10] G. S. Rajappan and M. L. Honig, "Signature sequence adaptation for DS-CDMA with multipath," *IEEE J. Select. Areas Commun.*, vol. 20, pp. 384-395, Feb. 2002.

[11] T. Strohmer, R. W. Heath Jr., and A. J. Paulraj, "On the design of optimal spreading sequences for CDMA systems," in *Proc. IEEE Asilomar Conf. on Signals, Syst., and Comp.*, vol. 2, Pacific Grove, CA, Nov. 2002, pp. 1434-1438.

[12] G. N. Karystinos and D. A. Pados, "New bounds on the total squared correlation and optimum design of DS-CDMA binary signature sets," *IEEE Trans. Commun.*, vol. 51, pp. 48-51, Jan. 2003.

[13] C. Ding, M. Golin, and T. Kløve, "Meeting the Welch and Karystinos-Pados bounds on DS-CDMA binary signature sets," *Des., Codes Cryptogr.*, vol. 30, pp. 73-84, Aug. 2003.

[14] P. Ipatov, "On the Karystinos-Pados bounds and optimal binary DS-CDMA signature ensembles," *IEEE Commun. Letters*, vol. 8, pp. 81-83, Feb. 2004.

[15] F. Vanhaverbeke, M. Moeneclaey, and H. Sari, "DS/CDMA with two sets of orthogonal spreading sequences and iterative detection," *IEEE Commun. Letters*, vol. 4, pp. 289-291, Sept. 2000.

E. Appendix A: Derivation of TSC for scalable $L \equiv 1 \pmod 4$ designs

Consider $\mathcal{S}^{'} = \left[\mathcal{S}_I \ \mathbf{m}_i^{''}\right]$, $i = 1, 2, \ldots, N$, where $\mathbf{m}_i^{''} = \left[\frac{-1}{\sqrt{L}} \ \mathbf{m}_i^{'T}\right]^T$. Then,

$$\begin{aligned} \mathrm{TSC}(\mathcal{S}^{'}) - \mathrm{TSC}(\mathcal{S}_I) &= 1 + 2\sum_{j=1}^{L-1} \left|\mathbf{m}^{'T}_i \mathbf{h}^{'}_j - \tfrac{1}{L}\right|^2 \\ &= 1 + 2\left[\sum_{j=1}^{L-1} \left|\mathbf{m}^{'T}_i \mathbf{h}^{'}_j\right|^2 + \sum_{j=1}^{L-1} \tfrac{1}{L^2} - \tfrac{2}{L}\sum_{i=1}^{L-1} \mathbf{m}^{'T}_i \mathbf{h}^{'}_j\right] \\ &= 1 + 2\left[\tfrac{(L-1)^2}{L^2} + \tfrac{L-1}{L^2} - \tfrac{2}{L}\sum_{j=1}^{L-1} \mathbf{m}^{'T}_i \mathbf{h}^{'}_j\right] \end{aligned} \tag{126}$$

where the last equality is from (114). From Lemma 1, $\sum_{j=1}^{L-1} \mathbf{m}^{'T}_i \mathbf{h}^{'}_j = \pm\frac{L-1}{L}$. We now show that for our construction $\sum_{j=1}^{L-1} \mathbf{m}^{'T}_i \mathbf{h}^{'}_j = \frac{L-1}{L}$ for all $i = 1, \ldots, N$. Expanding and simplifying,

$$\sum_{j=1}^{L-1} \mathbf{m}^{'T}_i \mathbf{h}^{'}_j = \frac{L-3}{L} + \sum_{j=1, j\neq i}^{L-1} \mathbf{m}^{'T}_i \mathbf{h}^{'}_j \tag{127}$$

($\mathbf{m}^{'T}_i \mathbf{h}^{'}_i = \frac{L-3}{L}$ since $d(\mathbf{m}^{'}_i, \mathbf{h}^{'}_i) = 1$). Also note that $\forall j \neq i$ $\mathbf{m}^{'T}_i \mathbf{h}^{'}_j = \pm\frac{2}{L}$ because $d(\mathbf{m}^{'}_i, \mathbf{h}^{'}_j) = \frac{L-1}{2} \pm 1$. Assume $\sum_{j=1}^{L-1} \mathbf{m}^{'T}_i \mathbf{h}^{'}_j = \frac{-(L-1)}{L}$ for which a necessary and sufficient condition is $\sum_{j=1, j\neq i}^{L-1} \mathbf{m}^{'T}_i \mathbf{h}^{'}_j = \frac{-2(L-2)}{L}$ or $\mathbf{m}^{'T}_i \mathbf{h}^{'}_j = \frac{-2}{L}$ $\forall j \neq i$. By design, since we multiplied the kth column of $\mathbf{H}^{'}_{L-1}$ by -1, when $j = k$, $\mathbf{m}^{'T}_i \mathbf{h}^{'}_j = \frac{2}{L}$; hence, $\sum_{j=1, j\neq i}^{L-1} \mathbf{m}^{'T}_i \mathbf{h}^{'}_j \neq \frac{-2(L-2)}{L}$. Therefore, from Lemma 1, $\sum_{j=1}^{L-1} \mathbf{m}^{'T}_i \mathbf{h}^{'}_j = \frac{L-1}{L}$. Substituting (127) in (126) we have $\mathrm{TSC}(\mathcal{S}^{'}) - \mathrm{TSC}(\mathcal{S}_I) = 1 + 2\frac{(L-2)(L-1)}{L^2}$ for our choice of extension matrix $\mathcal{S}_E$ which is the minimum possible by Theorem 1. Then,

$$\mathrm{F}(\mathcal{S}_I, \mathcal{S}_E) = \frac{2N}{L^2}(L-2)(L-1) \tag{128}$$

and since, from Table I,

$$\mathrm{TSC}(\mathcal{S}_E) = N + \frac{N(N-1)}{L^2} \tag{129}$$

we obtain (122).

F. Appendix B: Derivation of (125)

Case 1: $L \equiv 0 \pmod 4$, $1 \leq N \leq L$.
Consider an $(L+N, L)$ conditionally optimal TSC set $\mathcal{S}$. Calculate and define the following $\mathrm{TSC}(\mathcal{S}) - \mathrm{minTSC}$ difference functions where minTSC is the

unconditional TSC bound of an $(L+N, L)$ set:

$$\begin{array}{lcll} \Delta_1(N) & \triangleq & L+3N-\frac{(L+N)^2}{L}, & N\equiv 0 \pmod 4 \\ \Delta_2(N) & \triangleq & L+3N-\frac{(L+N)^2}{L}-\frac{2(L-2)}{L}, & N\equiv 2 \pmod 4 \\ \Delta_3(N) & \triangleq & L+3N-\frac{(L+N)^2}{L}-\frac{L-1}{L}, & N\equiv 1 \pmod 2. \end{array} \tag{130}$$

To find the integer value of $N \in \{1, 2, ..., L\}$ that maximizes the functions above, we first extend their domain to all real $N \in [1, L]$ and denote the extended functions by $\Delta_1^{'}(N)$, $\Delta_2^{'}(N)$, and $\Delta_3^{'}(N)$, respectively. Differentiating each of these functions with respect to N over the continuous field yields maximum at $N = \frac{L}{2}$ for all three cases. Since $\Delta_2^{'}(\frac{L}{2}) < \Delta_3^{'}(\frac{L}{2}) < \Delta_1^{'}(\frac{L}{2}) = \Delta_1(\frac{L}{2})$, we set $\Delta_1(\frac{L}{2}) = \frac{L}{4}$ as the upper bound. This bound is tight only for $N \equiv 0 \pmod 4$. For $N \equiv 2 \pmod 4$ and $N \equiv 1 \pmod 2$, $\Delta_2^{'}(\frac{L}{2})$ and $\Delta_3^{'}(\frac{L}{2})$ form tighter upper bounds, correspondingly. These bounds are presented in Table III.

Case 2: $L \equiv 2 \pmod 4$, $1 \le N \le L+2$.
Consider an $(L+N, L)$ conditionally optimal TSC set $\mathcal{S}$. Calculate and define the difference functions $\mathrm{TSC}(\mathcal{S}) - \mathrm{minTSC}$

$$\begin{array}{lcll} \Delta_1(N) & \triangleq & frac(L+2)^2 L+N+\frac{2N(N-2)}{L^2}+\frac{2N(L+2)}{L}-\frac{(L+N+2)^2}{L}, & N\equiv 0 \pmod 4 \\ \Delta_2(N) & \triangleq & \frac{(L+2)^2}{L}+N+\frac{2N(N-2)}{L^2}+\frac{2N(L+2)}{L}-\frac{(L+N+2)^2}{L}-\frac{2(L-2)}{L}, & N\equiv 2 \pmod 4 \\ \Delta_3(N) & \triangleq & \frac{(L+2)^2}{L}+N+\frac{2(N-1)^2}{L^2}+\frac{2N(N-2)}{L}-\frac{(L+N+2)^2}{L}-\frac{L-1}{L}, & N\equiv 1 \pmod 2. \end{array} \tag{131}$$

Then, extending the domain of the three functions to real $N \in [1, L+2]$ and maximizing over N, we find that the maximum of all domain-extended functions $\Delta_i^{'}(N)$, $i = 1, 2, 3$, is at $N = \frac{L+2}{2}$. Since $\Delta_2^{'}(\frac{L+2}{2}) < \Delta_3^{'}(\frac{L+2}{2}) < \Delta_1^{'}(\frac{L+2}{2}) = \Delta_1(\frac{L+2}{2})$, we set $\Delta_1(\frac{L+2}{2}) = \frac{L}{4} - \frac{1}{L} - \frac{2}{L^2} + \frac{1}{2}$ as the upper bound. This bound is tight only for $N \equiv 0 \pmod 4$. For $N \equiv 2 \pmod 4$ and $N \equiv 1 \pmod 2$, $\Delta_2^{'}(\frac{L+2}{2})$ and $\Delta_3^{'}(\frac{L+2}{2})$, correspondingly, form tighter upper bounds presented in Table III.

Case 3: $L \equiv 3 \pmod 4$, $1 \le N \le L+1$.
We calculate the differences $\mathrm{TSC}(\mathcal{S}) - \mathrm{minTSC}$ as follows

$$\begin{array}{lcll} \Delta_1(N) & \triangleq & \frac{(L+1)^2}{L}+N+\frac{N(N-1)}{L^2}+\frac{2N(L+1)}{L}-\frac{(L+N+1)^2}{L}, & N\equiv 0 \pmod 4 \\ \Delta_2(N) & \triangleq & \frac{(L+1)^2}{L}+N+\frac{N(N-1)}{L^2}+\frac{2N(L+1)}{L}-\frac{(L+N+1)^2}{L}-\frac{2(L-1)^2}{L^2}, & N\equiv 2 \pmod 4 \\ \Delta_3(N) & \triangleq & \frac{(L+1)^2}{L}+N+\frac{N(N-1)}{L^2}+\frac{2N(L+1)}{L}-\frac{(L+N+1)^2}{L}-\frac{L-1}{L}, & N\equiv 1 \pmod 2. \end{array} \tag{132}$$

Then, extending the domain of the three functions to $N \in [1, L+1]$ and maximizing over N, we find that the maximum of all domain-extended functions $\Delta_i^{'}(N)$, $i = 1, 2, 3$, is at $N = \frac{L+1}{2}$. Since $\Delta_2^{'}(\frac{L+1}{2}) < \Delta_3^{'}(\frac{L+1}{2}) < \Delta_1^{'}(\frac{L+1}{2}) = \Delta_1(\frac{L+1}{2})$, we set $\Delta_1(\frac{L+1}{2}) = \frac{L}{4} - \frac{1}{4L} - \frac{1}{4L^2} + \frac{1}{4}$ as the upper bound. This bound is tight only for $N \equiv 0 \pmod 4$. For $N \equiv 2 \pmod 4$ and $N \equiv 1 \pmod 2$, $\Delta_2^{'}(\frac{L+1}{2})$ and $\Delta_3^{'}(\frac{L+1}{2})$, correspondingly, form tighter upper bounds presented in Table III.

Case 4: $L \equiv 1 \pmod 4$, $1 \leq N \leq L-2$.
As in the previous cases, we calculate $\mathrm{TSC}(\mathcal{S}) - \mathrm{minTSC}$ to be

$$\begin{aligned}
\Delta_1(N) &\triangleq L - 1 + \tfrac{(L-1)(L-2)}{L^2} + N + \tfrac{N(N-1)}{L^2} + \tfrac{2N(L^2-3L+2)}{L^2} - \tfrac{(L-1+N)^2}{L}, \\
&\qquad N \equiv 0 \pmod 4 \\
\Delta_2(N) &\triangleq L - 1 + \tfrac{(L-1)(L-2)}{L^2} + N + \tfrac{N(N-1)}{L^2} + \tfrac{2N(L^2-3L+2)}{L^2} - \tfrac{(L-1+N)^2}{L} \\
&\qquad - \tfrac{2(L-1)^2}{L^2}, \ N \equiv 2 \pmod 4 \\
\Delta_3(N) &\triangleq L - 1 + \tfrac{(L-1)(L-2)}{L^2} + N + \tfrac{N(N-1)}{L^2} + \tfrac{2N(L^2-3L+2)}{L^2} - \tfrac{(L-1+N)^2}{L} \\
&\qquad - \tfrac{L-1}{L}, \ N \equiv 1 \pmod 2.
\end{aligned} \tag{133}$$

Letting $N \in [1, L-2]$ and differentiating, we find that the maximum of all domain-extended functions $\Delta_i^{'}(N)$, $i = 1, 2, 3$, is at $N = \frac{L-3}{2}$. Note that this value of N lies only in the integer domain of $\Delta_3(N)$. Since $\Delta_2^{'}(\frac{L-3}{2}) < \Delta_3^{'}(\frac{L-3}{2}) < \Delta_1^{'}(\frac{L-3}{2})$, we set $\Delta_1^{'}(\frac{L-3}{2}) = \frac{L}{4} - \frac{1}{4L} - \frac{1}{4L^2} + \frac{1}{4}$ as the upper bound. Unlike previous derivations, this bound is not tight for $N \equiv 0 \pmod 4$. For $N \equiv 2 \pmod 4$ and $N \equiv 1 \pmod 2$, $\Delta_2^{'}(\frac{L-3}{2})$ and $\Delta_3^{'}(\frac{L-3}{2})$, correspondingly, form tighter upper bounds presented in Table III.

TABLE I FROM [2]

UNDERLOADED SIGNATURE SET $(K \leq L)$

Processing Gain	Number of Users	Lower Bound on TSC
$L \equiv 0 \pmod 4$	Any K	K
$L \equiv 2 \pmod 4$	$K \equiv 0 \pmod 2$	$K + 2\frac{K(K-2)}{L^2}$
	$K \equiv 1 \pmod 2$	$K + 2\left(\frac{K-1}{L}\right)^2$
$L \equiv 1 \pmod 2$	Any K	$K + \frac{K(K-1)}{L^2}$

OVERLOADED SIGNATURE SET $(K \geq L)$

Number of Users	Processing Gain	Lower Bound on TSC
$K \equiv 0 \pmod 4$	Any L	$\frac{K^2}{L}$
$K \equiv 2 \pmod 4$	$L \equiv 0 \pmod 2$	$\frac{K^2}{L} + 2\frac{L-2}{L}$
	$L \equiv 1 \pmod 2$	$\frac{K^2}{L} + 2\left(\frac{L-1}{L}\right)^2$
$K \equiv 1 \pmod 2$	Any L	$\frac{K^2}{L} + \frac{L-1}{L}$

TABLE II
OVERLOADING OF TSC-OPTIMAL SETS

Signature Length	BaseTSC− optimalSet	Add − on Signatures	Lower Bound on TSC
$L \equiv 0 \pmod 4$	(L, L)	$1 \leq N \leq L$	$L + 3N$
$L \equiv 2 \pmod 4$	$(L+2, L)$	$1 \leq N \leq L+2$	$\frac{(L+2)^2}{L} + N + \frac{2(N-1)^2}{L^2} + \frac{2N(L+2)}{L}$, $N \equiv 1 \pmod 2$; $\frac{(L+2)^2}{L} + N + \frac{2N(N-1)}{L^2} + \frac{2N(L+2)}{L}$, $N \equiv 0 \pmod 2$
$L \equiv 3 \pmod 4$	$(L+1, L)$	$1 \leq N \leq L+1$	$\frac{(L+1)^2}{L} + N + \frac{N(N-1)}{L^2} + \frac{2N(L+1)}{L}$
$L \equiv 1 \pmod 4$	$(L-1, L)$	$1 \leq N \leq L-2$	$L - 1 + \frac{(L-1)(L-2)}{L^2} + N + \frac{N(N-1)}{L^2} + \frac{2N}{L^2}(L-2)(L-1)$

TABLE III
UPPER BOUNDS ON TSC($\mathcal{S}$) − minTSC
(tight for ($K \equiv 0 \pmod 4, L \equiv 0, 2, 3 \pmod 4$) and ($K \equiv 1 \pmod 2, L \equiv 1 \pmod 4$))

	$K \equiv 0 \pmod 4$	$K \equiv 2 \pmod 4$	$K \equiv 1 \pmod 2$
$L \equiv 0 \pmod 4$	$\frac{L}{4}$	$\frac{L}{4} - 2\frac{L-2}{L}$	$\frac{L}{4} - \frac{L-1}{L}$
$L \equiv 2 \pmod 4$	$\frac{L}{4} - \frac{1}{L} - \frac{2}{L^2} + \frac{1}{2}$	$\frac{L}{4} - \frac{1}{L} - \frac{2}{L^2}$ $+\frac{1}{2} - 2\frac{L-2}{L}$	$\frac{L}{4} - \frac{1}{L} - \frac{2}{L^2}$ $+\frac{1}{2} - \frac{L-1}{L}$
$L \equiv 3 \pmod 4$	$\frac{L}{4} - \frac{1}{4L} - \frac{1}{4L^2} + \frac{1}{4}$	$\frac{L}{4} - \frac{1}{4L} - \frac{1}{4L^2}$ $+\frac{1}{4} - 2\left(\frac{L-1}{L}\right)^2$	$\frac{L}{4} - \frac{1}{4L} - \frac{1}{4L^2}$ $+\frac{1}{4} - \frac{L-1}{L}$
$L \equiv 1 \pmod 4$	$\frac{L}{4} - \frac{1}{4L} - \frac{1}{4L^2} + \frac{1}{4}$	$\frac{L}{4} - \frac{1}{4L} - \frac{1}{4L^2}$ $+\frac{1}{4} - 2\left(\frac{L-1}{L}\right)^2$	$\frac{L}{4} - \frac{1}{4L} - \frac{1}{4L^2}$ $+\frac{1}{4} - \frac{L-1}{L}$

$$\mathcal{S} = \begin{bmatrix}
+ & + & + & + & + & + & + & + & + & + & + & + & + & + & + & + & + & + \\
+ & - & + & - & + & - & + & - & + & - & + & - & + & - & + & - & + & - \\
+ & + & - & - & + & + & - & - & + & + & - & - & + & + & - & - & - & + \\
+ & - & - & + & + & - & - & + & + & - & - & + & + & - & - & + & + & - \\
+ & + & + & + & - & - & - & - & + & + & + & + & - & - & - & - & + & + \\
+ & - & + & - & - & + & - & + & + & - & + & - & - & + & - & + & + & - \\
+ & + & - & - & - & - & + & + & + & + & - & - & - & - & + & + & - & + \\
+ & - & - & + & - & + & + & - & + & - & - & + & - & + & + & - & + & - \\
+ & + & + & + & + & + & + & + & - & - & - & - & - & - & - & + & + & + \\
+ & - & + & - & + & - & + & - & - & + & - & + & - & + & + & - & - & + \\
+ & + & - & - & + & + & - & - & - & - & + & + & - & - & + & + & - & - \\
+ & - & - & + & + & - & - & + & - & + & + & - & - & + & + & - & + & - \\
+ & + & + & + & - & - & - & - & - & - & - & + & + & + & + & + & + & + \\
+ & - & + & - & - & + & - & + & - & + & - & + & - & + & - & + & - & - \\
+ & + & - & - & - & - & + & + & - & - & + & + & + & - & - & - & + & - \\
+ & - & - & + & - & + & + & - & - & + & + & - & + & - & - & + & + & - \\
\end{bmatrix}$$

Fig. 14: $(19, 16)$ conditionally TSC-optimal signature set.

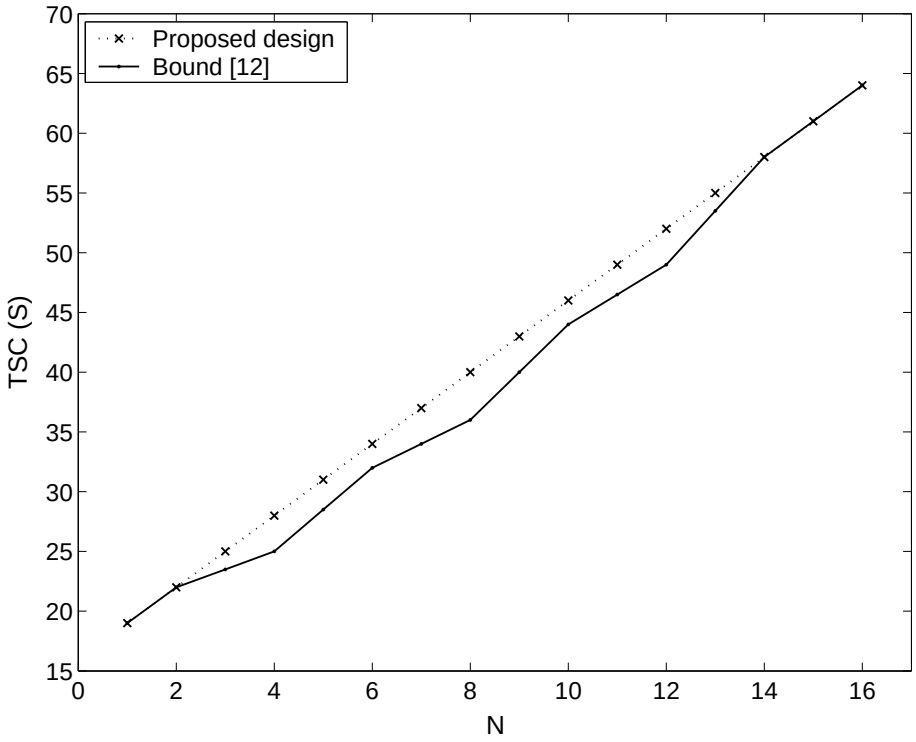

Fig. 15: TSC of proposed conditionally optimized signature set (under Case 1) against bound ($L = 16, 1 \leq N \leq 16$).

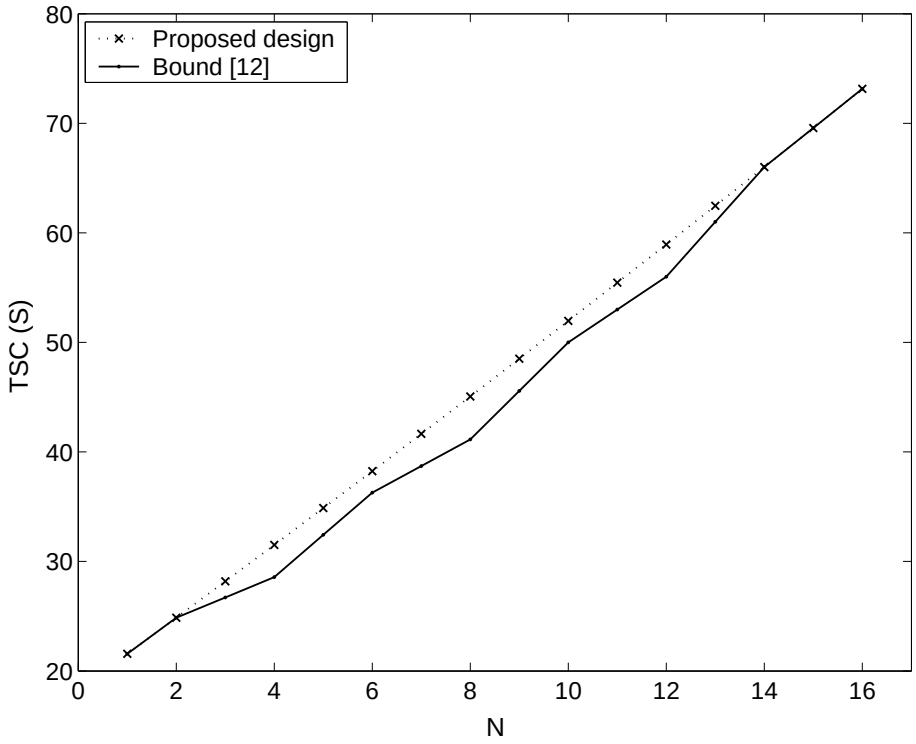

Fig. 16: TSC of proposed conditionally optimized signature set (under Case 2) against bound ($L = 14, 1 \leq N \leq 16$).

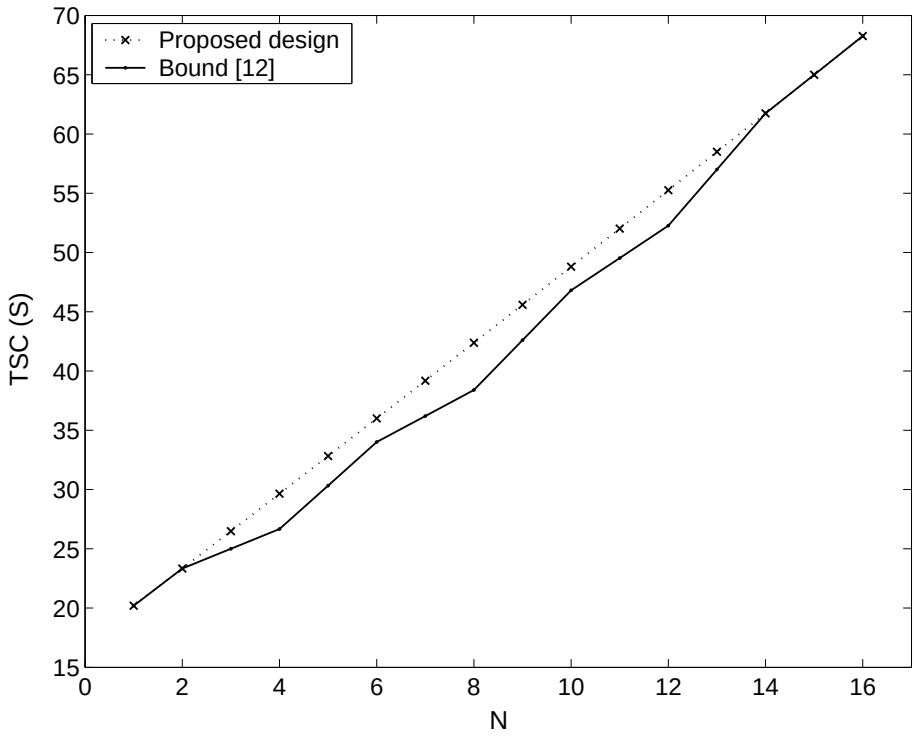

Fig. 17: TSC of proposed conditionally optimized signature set (under Case 3) against bound ($L = 15, 1 \leq N \leq 16$).

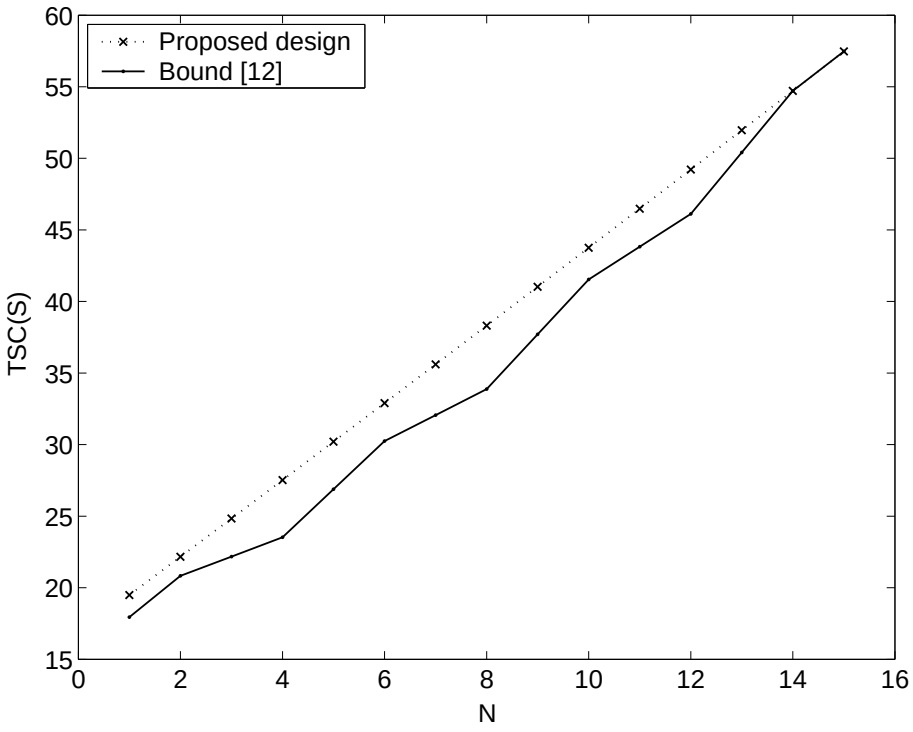

Fig. 18: TSC of proposed conditionally optimized signature set (under Case 4) against bound ($L = 17, 1 \leq N \leq 15$).

VI. New Bounds on the Aperiodic Total Squared Correlation of Binary Signature Sets and Optimal Designs

This work has been presented at IEEE ICC 2007, Scotland, UK.

In code-division multiple access (CDMA) systems, each of the K participating users is assigned a distinct spreading sequence or signature $\mathbf{s}_k \in \mathbb{C}^L$, $||\mathbf{s}_k|| = 1$, $k = 1, 2, \ldots K$. Organizing the K signatures as the columns of a matrix, we define the *signature matrix*

$$\mathcal{S} \stackrel{\triangle}{=} [\mathbf{s}_1 \ \mathbf{s}_2 \ldots \mathbf{s}_K] \in \mathbb{C}^{L \times K}. \tag{134}$$

In synchronous CDMA communications over ideal Nyquist channels, we are interested in using signature sets with minimum total squared correlation (TSC)

$$\mathrm{TSC}(\mathcal{S}) \stackrel{\triangle}{=} \sum_{i=1}^{K} \sum_{j=1}^{K} \left| \mathbf{s}_i^H \mathbf{s}_j \right|^2 \tag{135}$$

where H denotes the Hermitian operator. For overloaded ($K \geq L$) complex/real-valued signature sets $\mathcal{S} \in \mathbb{C}^{L \times K}$ or $\mathbb{R}^{L \times K}$, $\mathrm{TSC}(\mathcal{S}) \geq \frac{K^2}{L}$ [1] (of course, $\mathrm{TSC}(\mathcal{S}) \geq K$ if $K < L$). Overloaded ($K \geq L$) sets with TSC equal to $\frac{K^2}{L}$ have been known as Welch-bound-equality (WBE) sets. A few algorithms and studies for the design of complex or real WBE signature sets can be found in recent literature.

In digital transmission systems, however, it is necessary to have finite-alphabet signature sets. Recently, new bounds were derived on the TSC of *binary antipodal* signature sets together with optimal designs for arbitrary signature lengths and set sizes [2]-[4]. The sum capacity, total asymptotic efficiency, and maximum squared correlation of minimum-TSC optimal binary sets were evaluated in [5]. The sum capacity of several other signature set designs under potentially a binary or quaternary alphabet was examined in [6]. In this paper, we deal strictly with binary antipodal signatures represented as (unnormalized) column vectors in $\{\pm 1\}^L$.

When asynchronous code-division multiplexing is attempted and/or the channel exhibits multipath behavior, apart from the total squared correlation between signatures we are also concerned about the individual periodic and aperiodic correlation values between the signatures. For notational simplicity, we define $\mathbf{a}_{k|l}^T \in \{0, \pm 1\}^{1 \times (2L-1)}$ by

$$\mathbf{a}_{k|l}^T \stackrel{\triangle}{=} [\underbrace{0 \ldots 0}_{l} \ \ \mathbf{s}_k(1) \ \mathbf{s}_k(2) \ldots \mathbf{s}_k(L) \ \ \underbrace{0 \ldots 0}_{L-1-l}], l = 0, 1, \ldots, 2L-2, \tag{136}$$

to represent the *zero-padded-by-(L-1) cycli-shifted-by-l* version of $\mathbf{s}_k^T \in \{\pm 1\}^{1 \times L}$, $k = 1, 2, \ldots, K$ (T denotes the transpose operator and $\mathbf{s}_k(i), i = 1, 2, \ldots, L$, $k = 1, 2, \ldots, K$, refers to the ith element of vector $\mathbf{s}_k$). Next, we define the

zero-padded cyclic extension matrix $\mathcal{S}_{zpc} \in \{0, \pm 1\}^{(2L-1)\times K(2L-1)}$ of the signature set $\mathcal{S} \in \{\pm 1\}^{L\times K}$ as

$$\mathcal{S}_{zpc} \stackrel{\triangle}{=} [\mathbf{a}_{1|0}\ \mathbf{a}_{2|0} \ldots \mathbf{a}_{K|0} \quad \mathbf{a}_{1|1}\ \mathbf{a}_{2|1} \ldots \mathbf{a}_{K|1}\ \ldots\ldots \\ \mathbf{a}_{1|2L-2}\ \mathbf{a}_{2|2L-2} \ldots \mathbf{a}_{K|2L-2}] \tag{137}$$

and the aperiodic total squared correlation (ATSC)[8] of the signature set $\mathcal{S}$ as the total squared correlation (TSC) of the matrix $\mathcal{S}_{zpc}$

$$\mathrm{ATSC}(\mathcal{S}) \stackrel{\triangle}{=} \mathrm{TSC}(\mathcal{S}_{zpc}). \tag{138}$$

Then,

$$\mathrm{ATSC}(\mathcal{S}) = \sum_{k=1}^{K} \sum_{l=0}^{2L-2} \left|\mathbf{a}_{k|0}^T \mathbf{a}_{k|l}\right|^2 + (2L-1) \sum_{i=1}^{K} \sum_{j=1, i\neq j}^{K} \sum_{l=0}^{2L-2} \left|\mathbf{a}_{i|0}^T \mathbf{a}_{j|l}\right|^2. \tag{139}$$

The first term in (139) contains all aperiodic auto-correlation contributions; the second term contains all aperiodic cross-correlation contributions. For complex/real-valued signature sets $\mathcal{S} \in \mathbb{C}^{L\times K}$ or $\mathbb{R}^{L\times K}$, $\mathrm{ATSC}(\mathcal{S}) \geq K^2L^2(2L-1)$ directly by the TSC bound in [1] and our formulation (4),(5). Hence, these constructions establish tightness of the above ATSC bound over the binary domain for those specific cases.

In our work, we first derived new lower bounds on the ATSC of binary signature sets for all possible values of K (number of signatures) and L (signature length). Then, we presented optimal designs for several (K, L) pairs. The designs are based on Hadamard matrix transformations and serve as proof-by-construction for the tightness of the corresponding ATSC bounds. The new bounds and designs have already been publiced and presented in the 2007 IEEE International Conference on Communications (ICC).

A. Discussion and Examples

The optimal design cases that we produced constitute proof-by-construction of the tightness of our corresponding ATSC bounds. Under the $KL \equiv 0 \pmod 4$ design case, we relied significantly on ACS literature; new advancements have been made under the $KL \equiv 2 \pmod 4$ and $KL \equiv 1 \pmod 2$ design cases. To acquire a quantitative feeling of the coverage of the presented designs, if we restrict the domain of K, L to $\{1, 2, \ldots, 256\}$ (at present, it does not appear of practical interest to consider code-division applications outside this parameter range), we can calculate that Underloaded Cases 1 through 6 and Overloaded Cases 1 through 4 together represent 27.91% of all possible combination pairs $(K, L) \in \{1, 2, \ldots, 256\}^2$. Maximum coverage in the number of users is available

[8] Another signature set correlation metric of interest is the periodic total squared correlation (PTSC) which is lower bounded by K^2L^3 for complex/real-valued signature sets $\mathcal{S} \in \mathbb{C}^{L\times K}$ or $\mathbb{R}^{L\times K}$ [1],[10],[9]. Recently, new lower bounds on the PTSC of binary antipodal signature sets were derived, together with optimal designs for many signature lengths and set sizes, in [9],[10].

in overloaded systems when $L \in \mathcal{M}_{1,MF}$, i.e. optimal signature sets are available for all values of $K > L$.

Certainly, tightness of the bounds and optimal ATSC designs under the remaining cases is an important open research problem. Two results need to be highlighted in this regard; the non-existence of Barker sequences for $60 < L < 10^{22}$ [14] and the non-existence of $(2, L)$ ACS sets if all prime divisors of L are not congruent to 1 (mod 4).

Since the ATSC of each signature set that we constructed equals the corresponding lower bound, by our own Theorem Number 2 all designs are jointly ATSC- and PTSC-optimal.[9] In addition, direct comparison of our ATSC-optimal designs with the TSC bounds and optimal sets in [2] shows that Underloaded Cases 1 and 2 when K is a power of 2, Underloaded Case 3(i), and Overloaded Cases 1 through 4 are triple, ATSC-, PTSC- and TSC-optimal. This remarkable conclusion captures and demonstrates the inherent robustness of these binary designs.

We will now establish that the familiar Gold and "small" or "large" Kasami sets [15], [16], which have been widely used for their correlation properties [8], are not ATSC optimal in general. It suffices to find at least one (K, L) signature set in the Gold/Kasami-compatible range that has lower (preferably minimum) ATSC than the corresponding Gold/Kasami set in order to prove sub-optimality of the latter. Fig. 19(a) provides an example of a Gold set $\mathcal{G}_{31\times 24}$ with $ATSC = 43474212$; Fig. 19(b) provides an optimal signature set $\mathcal{S}^{opt}_{31\times 24}$ designed under our Underloaded Case 3(ii) with minimum $ATSC = 33765696$. In Fig. 20(a) we show a $(2, 15)$ signature set with lower (but not minimum) $ATSC = 33292$ than a $(2, 15)$ small-set Kasami design, shown in Fig. 20(b), with $ATSC = 34220$. We follow with Fig. 21 which provides a large-set Kasami design $\mathcal{K}^{ls}_{15\times 8}$ with $ATSC = 441264$ and an optimal signature set $\mathcal{S}^{opt}_{15\times 8}$ designed under our Underloaded Case 3(ii) with minimum $ATSC = 417600$.

We conclude with an example of an overloaded ATSC-optimal design $\mathcal{S}^{opt}_{14\times 25}$ given in Fig. 22. The set is designed under our Overloaded Case 2 and has minimum ATSC value $ATSC = 3308526$.

B. Conclusions

We derived lower bounds on the aperiodic total squared correlation of binary antipodal signature sets for any set size (K, L). We provided optimal designs for a range of (K, L) pairs that establish the tightness of the corresponding lower bounds. The constructions include underloaded ($K \leq L$) and overloaded ($K > L$) design cases and cover, as an example, 27.91% of all possible combinations of K, L in $\{1, 2, \ldots, 256\}$.

Side results of this work include establishing that maximal-merit-factor sequences (and, hence, Barker sequences) are ATSC-optimal and that neither Gold nor small- or large-set Kasami sequences are ATSC-optimal in general.

[9] The Barker sequence $\mathbf{g}_4$ applicable to Underloaded Case 5 and Overloaded Cases 3 and 4 is double, ATSC- and PTSC-optimal.

In view of these findings, the developed ATSC-optimal sets take precedence in code-division multiplexing applications.

References

[1] R. L. Welch, "Lower bounds on the maximum cross correlation of signals," *IEEE Trans. Inform. Theory*, vol. IT-20, pp. 397-399, May 1974.

[2] G. N. Karystinos and D. A. Pados, "New bounds on the total squared correlation and optimum design of DS-CDMA binary signature sets," *IEEE Trans. Commun.*, vol. 51, pp. 48-51, Jan. 2003.

[3] C. Ding, M. Golin, and T. Klϕve, "Meeting the Welch and Karystinos-Pados bounds on DS-CDMA binary signature sets," *Des., Codes Cryptogr.*, vol. 30, pp. 73-84, Aug. 2003.

[4] P. Ipatov, "On the Karystinos-Pados bounds and optimal binary DS-CDMA signature ensembles," *IEEE Commun. Letters*, vol. 8, pp. 81-83, Feb. 2004.

[5] G. N. Karystinos and D. A. Pados, "The maximum squared correlation, sum capacity, and total asymptotic efficiency of minimum total-squared-correlation binary signature sets," *IEEE Trans. Inform. Theory*, vol. 51, pp. 348-355, Jan. 2005.

[6] F. Vanhaverbeke and M. Moeneclaey, "Sum capacity of equal-power users in overloaded channels," *IEEE Trans. Inform. Theory*, vol. 53, pp. 228-233, Feb. 2005.

[7] J. L. Massey and T. Mittelholzer, "Welch's bound and sequence sets for code-division multiple-access systems," *Sequences II, Methods in Communication, Security, and Computer Sciences*, R. Capocelli, A. De Santis, and U. Vaccaro, Eds. New York: Springer-Verlag, 1993.

[8] D. V. Sarwate and M. B. Pursley, "Crosscorrelation properties of pseudorandom and related sequences," *Proc. of IEEE*, vol. 68, pp. 593-619, May 1980.

[9] H. Ganapathy and D. A. Pados , "Optimal binary signatures sets under cyclic shifts," in *Proc. IEEE MILCOM*, Atlantic City, NJ, Oct. 2005, vol. 2, pp. 890-896.

[10] H. Ganapathy and D. A. Pados , "New bounds the periodic total squared correlation of binary signature sets and optimal designs," *IEEE Trans. Commun.*, submitted.

[11] M. Golay, "Complementary Series," *IEEE Trans. Inform. Theory*, vol. IT-7, pp. 82-87, Apr. 1961.

[12] R. J. Turyn, "Hadamard matrices, Baumert-Hall units, four symbol sequences, pulse compression and surface wave encodings," *J. Combin. Theory A*, vol. 16, pp. 313-333, 1974.

[13] S. W. Golomb and R. A. Scholtz, "Generalized Barker Sequences," *IEEE Trans. Inform. Theory*, vol. IT-13, pp. 619-621, Oct. 1967.

[14] K. H. Leung, S. L. Ma, and B. Schmidt, "Nonexistence of abelian difference sets: Landers conjecture for prime power orders," *Trans. Amer. Math. Soc.*, vol. 356, pp. 4343-4358, 2004.

[15] R. Gold, "Optimal binary sequences for spread spectrum multiplexing," *IEEE Trans. Inform. Theory*, vol. IT-13, pp. 619-621, Oct. 1967.

[16] T. Kasami, "Weight distribution formula for some class of cyclic codes," Coordinated Science Laboratory, University of Illinois, Urbana, Tech. Rep. R-285 (AD632574), 1966.

$$\mathcal{G}_{31\times 24} = \begin{bmatrix}
- & + & - & - & - & - & + & + & + & + & + & - & - & + & - & - & + & - & - & - & - & - & + & + \\
- & + & + & - & - & - & - & + & + & + & + & + & - & - & + & - & - & + & - & - & - & - & - & + \\
- & + & + & + & - & - & - & - & + & + & + & + & + & - & - & + & - & - & + & - & - & - & - & - \\
- & - & + & + & + & - & - & - & - & + & + & + & + & + & - & - & + & - & - & + & - & - & - & - \\
- & + & - & + & + & + & - & - & - & - & + & + & + & + & + & - & - & + & - & - & + & - & - & - \\
- & + & + & - & + & + & + & - & - & - & - & + & + & + & + & + & - & - & + & - & - & + & - & - \\
+ & + & - & - & + & - & - & - & + & + & + & + & - & - & - & - & - & + & + & - & + & + & - & + \\
- & - & + & + & + & - & + & + & - & - & - & - & + & + & + & + & + & - & - & + & - & - & + & - \\
+ & + & + & - & - & - & + & - & - & - & + & + & + & - & - & - & - & - & + & + & - & + & + & + \\
- & + & + & - & + & + & + & - & + & + & + & - & - & - & - & + & + & + & + & - & - & + & - & - \\
- & + & + & + & - & + & + & + & - & + & + & + & - & - & - & - & + & + & + & + & + & - & - & + \\
+ & - & - & - & - & + & - & - & - & + & - & - & - & + & + & + & - & - & - & - & - & + & + & + \\
+ & - & + & - & - & - & + & - & - & - & + & - & - & - & + & + & + & + & - & - & - & - & - & + \\
- & - & - & - & - & + & + & + & + & - & + & + & + & - & + & + & + & - & - & - & + & + & + & + \\
- & - & - & - & - & - & + & + & + & - & + & + & + & - & + & + & + & - & - & - & - & + & + & + \\
+ & - & - & + & + & + & + & - & - & - & + & - & - & - & + & - & - & - & + & + & + & + & + & + \\
- & - & - & + & - & - & - & - & - & + & + & + & - & + & + & + & - & + & + & + & - & - & - & - \\
- & + & - & - & + & - & - & - & + & + & + & - & + & + & + & - & + & + & + & - & - & - & - & - \\
- & - & + & - & - & + & - & - & - & - & + & + & + & - & + & + & + & - & + & + & + & - & - & - \\
- & - & - & + & - & - & + & - & - & - & - & + & + & + & - & + & + & + & - & + & + & + & - & - \\
- & + & - & - & + & - & - & + & - & - & - & - & - & + & + & + & - & + & + & + & - & + & + & + \\
+ & + & - & + & + & - & + & + & - & + & + & + & + & + & - & - & - & + & - & - & - & + & - & - \\
+ & + & - & - & + & + & - & + & + & - & + & + & + & + & + & - & - & - & + & - & - & - & + & - \\
+ & + & - & - & - & + & + & - & + & + & - & + & + & + & + & + & - & - & - & + & - & - & - & + \\
+ & + & - & - & - & - & + & + & - & + & - & + & + & + & + & + & - & - & - & + & - & - & - & - \\
+ & - & - & - & - & - & - & + & + & - & + & + & - & + & + & + & + & + & - & - & - & + & - & - \\
- & - & - & + & + & + & + & - & - & + & - & - & + & - & - & - & - & - & + & + & + & - & + & - \\
+ & - & + & + & - & - & - & - & + & + & - & + & + & - & + & + & + & + & + & - & - & - & + & + \\
- & - & - & - & - & + & + & + & + & - & - & + & - & - & + & - & - & - & - & + & + & + & - & + \\
\end{bmatrix}$$

(a)

$$\mathcal{S}^{opt}_{31\times 24} = \begin{bmatrix}
+ & + \\
+ & - & - & + & - & - & - & + & + & + & - & + & + & - & - & + & - & - & - & + & + & + & - & + \\
+ & + & - & - & + & - & - & - & + & + & + & - & + & + & - & - & + & - & - & - & + & + & + & - \\
+ & - & + & - & - & + & - & - & - & + & + & + & + & - & + & - & - & + & - & - & - & + & + & + \\
+ & + & - & + & - & - & + & - & - & - & + & + & + & + & - & + & - & - & + & - & - & - & + & + \\
+ & + & + & - & + & - & - & + & - & - & - & + & + & + & + & - & + & - & - & + & - & - & - & + \\
+ & + & + & + & - & + & - & - & + & - & - & - & + & + & + & + & - & + & - & - & + & - & - & - \\
+ & - & + & + & + & - & + & - & - & + & - & - & + & - & + & + & + & - & + & - & - & + & - & - \\
+ & - & - & + & + & + & - & + & - & - & + & - & - & + & - & + & + & + & - & + & - & - & + & - \\
+ & - & - & - & + & + & + & - & + & - & - & + & + & - & - & - & + & + & + & - & + & - & - & + \\
+ & + & - & - & + & - & + & + & - & + & - & - & + & + & - & - & - & + & + & + & - & + & - & - \\
+ & - & + & - & - & - & + & + & + & - & + & - & + & - & + & - & - & - & + & + & + & - & + & - \\
+ & + \\
- & + & + & - & + & + & + & - & - & - & + & - & - & + & + & - & + & + & + & - & - & - & + & - \\
+ & + & - & - & + & - & - & - & + & + & + & - & + & + & - & - & + & - & - & - & + & + & + & - \\
- & + & - & + & + & - & + & + & - & - & - & + & - & - & + & - & + & + & + & - & - & + & - & + \\
+ & + & - & - & + & + & + & - & - & - & + & - & + & + & + & - & + & + & + & - & - & - & + & - \\
+ & + & + & - & - & + & - & - & + & - & + & + & + & - & + & + & + & - & - & - & + & - & - & + \\
+ & + & + & + & - & + & + & - & - & + & - & + & + & + & - & + & + & + & - & - & - & + & - & - \\
- & + & - & - & - & + & - & + & + & - & + & + & - & + & - & - & - & + & - & + & + & - & + & + \\
- & + & + & - & - & - & + & - & + & - & + & - & + & + & - & - & - & + & - & + & + & - & + & + \\
- & + & + & + & - & - & + & - & + & + & - & - & + & + & + & - & - & - & + & - & + & + & - & - \\
+ & + & - & - & + & + & + & - & - & + & + & + & - & - & - & + & + & + & - & + & - & + & - & - \\
- & + & - & + & + & + & - & - & - & + & - & + & - & + & - & + & + & + & - & - & - & + & - & + \\
+ & + & + & + & + & + & + & + & + & + & + & + & + & - & - & - & - & - & - & - & - & - & - & - \\
+ & - & - & + & - & - & + & - & - & - & + & - & + & + & - & + & + & + & - & - & - & + & - & - \\
+ & + & - & - & + & - & - & - & + & + & + & - & - & - & + & + & - & + & + & + & - & - & - & + \\
+ & - & + & - & - & + & - & - & - & + & + & + & - & + & - & + & + & - & + & + & + & - & - & - \\
+ & + & - & + & - & - & + & - & - & - & + & + & - & - & + & - & + & + & - & + & + & + & - & - \\
+ & + & + & - & + & - & - & + & - & - & - & + & - & - & - & + & - & + & + & - & + & + & + & - \\
+ & + & + & + & - & + & - & - & + & - & - & - & - & - & - & - & + & - & + & + & - & + & + & + \\
\end{bmatrix}$$

(b)

Fig. 19. (a) $\mathcal{G}_{31\times 24}$ Gold set with $ATSC = 43474212$. (b) Optimal signature set $\mathcal{S}^{opt}_{31\times 24}$ designed under Underloaded Case 3(ii) with $ATSC = (24)^2(31)^2(2(31)-1) = 33765696$.

$$\mathcal{K}^{ss}_{15\times 2} = \begin{bmatrix} - & - \\ - & + \\ - & + \\ + & + \\ - & + \\ - & + \\ + & + \\ + & - \\ - & + \\ + & + \\ - & + \\ + & - \\ + & - \\ + & - \end{bmatrix} \qquad \mathcal{S}_{15\times 2} = \begin{bmatrix} - & + \\ + & + \\ + & + \\ + & - \\ - & + \\ + & + \\ + & - \\ - & - \\ - & + \\ + & - \\ - & + \\ + & - \\ - & - \\ - & - \end{bmatrix}$$

(a) (b)

Fig. 20. (a) $\mathcal{K}^{ss}_{15\times 2}$ small-set Kasami with $ATSC = 34220$. (b) Numerically generated $\mathcal{S}_{15\times 2}$ signature set with $ATSC = 33292$.

$$\mathcal{K}^{ls}_{15\times 8} = \begin{bmatrix} + & - & - & + & + & - & - & + \\ + & + & - & + & - & - & + & - \\ - & + & - & - & + & - & + & + \\ - & - & - & + & + & - & - & + \\ + & + & - & + & - & + & - & + \\ - & - & + & + & - & - & + & + \\ - & - & - & + & + & + & + & - \\ - & - & + & - & + & + & - & + \\ - & + & - & - & + & + & - & - \\ - & - & - & + & + & - & - & + \\ + & - & + & - & + & - & + & - \\ + & - & + & + & - & + & - & - \\ - & - & - & + & + & + & + & - \\ - & - & + & - & + & - & + & - \\ + & - & + & + & - & - & - & + \end{bmatrix} \qquad \mathcal{S}^{opt}_{15\times 8} = \begin{bmatrix} + & + & + & + & + & + & + & + \\ + & - & + & - & + & - & + & - \\ + & + & - & - & + & + & - & - \\ + & - & - & + & + & - & - & + \\ + & + & + & + & + & + & + & + \\ - & + & - & + & - & + & - & + \\ + & + & - & - & + & + & - & - \\ - & + & + & - & - & + & + & - \\ + & + & + & + & + & + & + & + \\ + & - & + & - & + & - & + & - \\ - & - & + & + & - & - & + & + \\ - & + & + & - & - & + & + & - \\ + & + & + & + & - & - & - & - \\ + & - & + & - & - & + & - & + \\ + & + & - & - & - & - & + & + \end{bmatrix}$$

(a) (b)

Fig. 21. (a) $\mathcal{K}^{ls}_{15\times 8}$ large-set Kasami with $ATSC = 441264$. (b) Optimal $\mathcal{S}^{opt}_{15\times 8}$ designed under Underloaded Case 3(ii) with $ATSC = (8)^2(15)^2(2(15)-1) = 417600$.

$$\mathcal{S}^{opt}_{14\times 25} = \begin{bmatrix} + & + \\ + & - & - & + & - & - & - & + & + & + & - & + & + & - & - & + & - & - & - & + & + & + & - & + & + \\ + & + & - & - & + & - & - & - & + & + & + & - & + & + & - & - & + & - & - & - & + & + & + & - & - \\ + & - & + & - & - & + & - & - & - & + & + & + & + & - & + & - & - & + & - & - & - & + & + & + & + \\ + & + & - & + & - & - & + & - & - & - & + & + & + & - & + & - & - & + & - & - & - & + & + & - & - \\ + & + & + & - & + & - & - & + & - & - & - & + & + & + & - & + & - & - & + & - & - & - & + & + & + \\ + & + & + & + & - & + & - & - & + & - & - & - & + & + & + & - & + & - & - & + & - & - & - & + & - \\ + & - & + & + & + & - & + & - & - & + & - & + & - & - & + & + & + & - & + & - & - & + & - & - & - \\ + & - & - & + & + & + & - & + & - & - & + & - & + & - & - & + & + & + & - & + & - & - & + & - & + \\ + & - & - & - & + & + & + & - & + & - & - & + & + & - & - & - & + & + & + & - & + & - & - & + & + \\ + & + & - & - & - & + & + & + & - & + & - & - & + & + & - & - & - & + & + & + & - & + & - & - & - \\ + & - & + & - & - & - & + & + & + & - & + & - & + & - & - & - & + & + & + & - & + & - & - & - & - \\ + & + & + & + & + & + & + & + & + & + & - & - & - & - & - & - & - & - & - & - & - & - & - & - & - \\ + & - & - & + & - & - & - & + & + & + & - & + & - & + & + & - & + & + & + & - & - & - & + & - & - \end{bmatrix}$$

Fig. 22. Optimal signature set $\mathcal{S}^{opt}_{14\times 25}$ designed under Overloaded Case 2 with minimum $ATSC = (25)^2(14)^2(2(14)-1) + (2(14)-1)(3(14)-4) = 3308526$.

VII. Upward Scaling of Minimum-TSC Binary Signature Sets

The work has been published in the IEEE Communications Letters, Nov. 2007.

In multiuser communication systems that follow the code-division multiplexing paradigm, multiple signals are transmitted simultaneously in time and frequency. Each signal -potentially associated with a distinct user- is assigned an individual signature (spreading code). A fundamental measure of the quality of the code-division communication link is the total squared correlation (TSC) [1] over the set of assigned signatures. For a K-signal system with signature length L, if the signature set is denoted by $S = \{\mathbf{s}_1, \mathbf{s}_2, \cdots, \mathbf{s}_K\}$, $\|\mathbf{s}_i\| = L$, $i = 1, 2, \cdots, K$, then the TSC of the signature set S is defined as the sum of the squared magnitudes of all inner products between signatures,

$$TSC(S) \stackrel{\triangle}{=} \sum_{i=1}^{K} \sum_{j=1}^{K} |\mathbf{s}_i^T \mathbf{s}_j|^2. \tag{140}$$

In the theoretical context of TSC optimized signature sets that are real (or complex) valued, one may consider the early work of Welch [1] followed by representative works in [2]-[13].

Findings in [1]-[13] constitute only pertinent performance bounds for digital communication systems with digital signatures. Recently, new bounds on the TSC of *binary* signature sets were presented [14] that led to minimum-TSC optimal binary signature set designs for almost all[10] signature lengths and set sizes [14]-[14]. The sum capacity, total asymptotic efficiency, and maximum squared correlation of the minimum-TSC binary sets were evaluated in [15]. The user capacity of minimum and non-minimum-TSC binary sets was identified and compared in [18]. A procedure to find minimum-TSC binary signature sets with low cross-correlation spectrum was presented in [19]. A binary code allocation scheme is examined in [20] and tested against the Karystinos-Pados (KP) bounds and sequence sets [14].

The technical problem that we consider in this letter is upward scaling of an overloaded ($K > L$) min-TSC binary set. Consider the min-TSC optimal constructions in [14]-[14] for any $K = L$ (fully loaded systems). Subsets of $K < L$ signatures maintain TSC optimality and signatures can be returned and reassigned without loss of optimality. This is not the case unfortunately, in general, given a min-TSC overloaded set (K, L) where $K > L$. Addition of a signature, for example, may require complete redesign/reassignment of the $(K + 1, L)$ set. In this letter, motivated by our prior work in [21], we develop a novel scheme that returns a binary signature for the new signal in the system that lies near the continuous-valued arcs of least TSC increase. The quality of the new binary signature design is tested directly against the KP TSC bound.

[10]The case $K = L \equiv 1 \pmod 4$ remains the only open problem at present in min-TSC optimal binary set design [14]-[14].

The rest of this paper is organized as follows. Section II presents our formulation of the optimization problem under consideration. The proposed algorithm is presented in Section III. Studies and comparisons with the TSC bound are included in Section IV.

A. Formulation

We consider a code division multiplexing system with code length L and $K \geq L$ signals (overloaded). The K signals utilize a minimum TSC optimal binary signature set S designed according to [14]-[14], $S = \{\mathbf{s}_1, \mathbf{s}_2, \cdots, \mathbf{s}_K\}$, $\mathbf{s}_i \in \{\pm 1\}^L$, $i = 1, \cdots, K$. When a new signal enters this system with signature $\mathbf{s}_{K+1} \in \{\pm 1\}^L$, the TSC of the $K+1$ signatures given the signatures of the K preexisting signals is

$$\begin{aligned} TSC_{K+1|K} &= \sum_{i=1}^{K+1} \sum_{j=1}^{K+1} |\mathbf{s}_i^T \mathbf{s}_j|^2 \\ &= \sum_{i=1}^{K} \sum_{j=1}^{K} |\mathbf{s}_i^T \mathbf{s}_j|^2 + |\mathbf{s}_{K+1}^T \mathbf{s}_{K+1}|^2 + 2 \sum_{i=1}^{K} |\mathbf{s}_{K+1}^T \mathbf{s}_i|^2 \\ &= TSC_K + L^2 + 2\mathbf{s}_{K+1}^T \sum_{i=1}^{K} \mathbf{s}_i \mathbf{s}_i^T \mathbf{s}_{K+1} \end{aligned} \tag{141}$$

where TSC_K denotes the TSC of the K preexisting signals in the system that utilize a minimum TSC binary signature set. If we denote the autocorrelation matrix of the preexisting K signatures by

$$\mathbf{R}_K = \sum_{i=1}^{K} \mathbf{s}_i \mathbf{s}_i^T, \tag{142}$$

(141) shows that conditional minimization of $TSC_{K+1|K}$ with respect to $\mathbf{s}_{K+1}$ for fixed (min-TSC-valued) TSC_K reduces to

$$\mathbf{s}_{K+1} = arg \min_{\mathbf{s}_i \in \{\pm 1\}^L} \mathbf{s}^T \mathbf{R}_K \mathbf{s}. \tag{143}$$

Exhaustive search over all 2^L vectors in $\{\pm 1\}^L$ to find the one that minimizes (143) is, of course, unacceptable computationally even for moderate values of L. Below, we propose a low cost search algorithm that creates a signature candidate list of size linear in L.

B. Proposed Algorithm

Let $f(\mathbf{s})$ denote the cost function in (143) that we try to minimize,

$$f(\mathbf{s}) \stackrel{\triangle}{=} \mathbf{s}^T \mathbf{R}_K \mathbf{s}. \tag{144}$$

We relax, for a moment, our requirement for binary antipodal signature (sequence) alphabet and assume, instead, that $\mathbf{s}$ is real-valued with the same norm, $\mathbf{s} \in \mathbb{R}^L$, $\mathbf{s}^T\mathbf{s} = L$. Then, the real-field optimization problem becomes

$$\mathbf{s}_{K+1,opt}^{(r)} = arg \min_{\mathbf{s}\in\mathbb{R}^L, \mathbf{s}^T\mathbf{s}=L} f(\mathbf{s}) \tag{145}$$

where the superscript (r) indicates that $\mathbf{s}_{K+1,opt}^{(r)}$ is real-valued. The optimization in (247) is carried over a hypersphere in $\mathbb{R}^L$ of radius L centered at the origin.

Let $\{\mathbf{q}_1, \mathbf{q}_2, \cdots, \mathbf{q}_L\}$ be the L eigenvectors of $\mathbf{R}_K$ with corresponding eigenvalues $\lambda_1 \leq \lambda_2 \leq \cdots \leq \lambda_L$. The real-valued sequence that minimizes the right-hand-side of (247) is well known and equal to the eigenvector that corresponds to the minimum eigenvalue of the matrix $\mathbf{R}_K$,

$$\mathbf{s}_{K+1,opt}^{(r)} = arg \min_{\mathbf{s}\in\mathbb{R}^L, \mathbf{s}^H\mathbf{s}=L} f(\mathbf{s}) = \mathbf{q}_1. \tag{146}$$

Consider now the following $L-1$ lines in $\mathbb{R}^L$,

$$\mathbf{q}_1 - \rho\mathbf{q}_i, \quad i = 2, \cdots, L, \quad \rho \in \mathbb{R}. \tag{147}$$

The lines in (249) lie on the plane that is tangent to the searching hypersphere, pass through the real minimizer $\mathbf{q}_1$, and define mutually orthogonal directions of least increase in the cost function $f(\mathbf{s})$, $\mathbf{s} \in \mathbb{R}^L$, from the optimum point $\mathbf{s}_{K+1,opt}^{(r)} = \mathbf{q}_1$. That is, algebraically, for fixed ρ and $i = 2, 3, \cdots, L$,

$$\mathbf{q}_i = arg \min_{\mathbf{v}\in\Omega_\mathbf{v}} \{f(\mathbf{q}_1) - f(\frac{\mathbf{q}_1 - \rho\mathbf{v}}{\sqrt{1+\rho^2}})\} \tag{148}$$

where $\Omega_\mathbf{v} = \{\mathbf{v} : \mathbf{v}^T\mathbf{q}_j = 0, j = 1, 2, \cdots, i-1, \mathbf{v}^T\mathbf{v} = 1\}$.

Projection of the above least-increase lines onto the searching hypersphere results in the slowest increase arcs given by

$$\frac{\mathbf{q}_1 - \rho\mathbf{q}_i}{\sqrt{1+\rho^2}}, \quad i = 2, \cdots, L, \quad \rho \in \mathbb{R}. \tag{149}$$

The slowest increase arcs in (250) trace the searching hypersphere, extend from $-\mathbf{q}_i$ to $\mathbf{q}_i$, $i = 2, \cdots, L$, and pass through the optimum point $\mathbf{s}_{K+1,opt}^{(r)}$. On each of these arcs, the function $f(\mathbf{s})$, $\mathbf{s} \in \mathbb{R}^L$, takes values in $[\lambda_1 L,\ \lambda_i L]$, $i = 2, \cdots, L$, respectively. Our objective is to identify the binary sequences that are closest in the l_2-sense to the above least-increase arcs [22]. It is important to note that for any given $i \in \{2, 3, \cdots, L\}$, the binary sequences that are closest in the l_2-sense to the arc $\frac{\mathbf{q}_1 - \rho\mathbf{q}_i}{\sqrt{1+\rho^2}}$, $\rho \in \mathbb{R}$, can be expressed as $sgn(\mathbf{q}_1 - \rho\mathbf{q}_i)$; the set of all binary signatures of the form $sgn(\mathbf{q}_1 - \rho\mathbf{q}_i)$, $\rho \in \mathbb{R}$, has cardinality at most $L+1$.

Our proposed binary signature search algorithm is described below.

Algorithm

For $i = 2, \cdots, P$ $(P \leq L)$ do:

Step 1
Calculate

$$\rho_n \stackrel{\triangle}{=} q_{1,n}/q_{i,n}, \quad n = 1, \cdots, L, \tag{150}$$

where $q_{i,n}$, $n = 1, \cdots, L$, is the nth element of the vector $\mathbf{q}_i$. The points in (150) define non-overlapping intervals in $\mathbb{R}$ such that, for any given i, signatures of the form $sgn(\mathbf{q}_1 - \rho\mathbf{q}_i)$ that correspond to values of ρ in adjacent intervals have opposite signs in exactly one coordinate. Let $\rho'_1 < \rho'_2 < \cdots < \rho'_L$ be a rearrangement of $\rho_1, \rho_2, \cdots, \rho_L$ in ascending order and let u be the index of the first positive element in the ordered sequence $\rho'_1, \rho'_2, \cdots, \rho'_L$, i.e. $\rho'_{u-1} < 0 < \rho'_u$, $u \in \{1, 2, \cdots, L\}$.

Step 2

Find the binary sequence that is closest to the arc $\frac{\mathbf{q}_1 - \rho\mathbf{q}_i}{\sqrt{1+\rho^2}}$ for each interval of ρ, i.e. for $\rho \in (-\infty, \rho'_1), (\rho'_1, \rho'_2), \cdots, (\rho'_{L-1}, \rho'_L), (\rho'_L, \infty)$. There are $L+1$ binary sequences in total denoted as $\mathbf{s}^{0,i}_{K+1}, \mathbf{s}^{1,i}_{K+1}, \cdots, \mathbf{s}^{L,i}_{K+1}$ that can be computed recursively,

$$\mathbf{s}^{0,i}_{K+1} = sgn[\mathbf{q}_1], \tag{151}$$

$$\mathbf{s}^{l+1,i}_{K+1} = \mathbf{s}^{l,i}_{K+1} - 2s^{0,i}_{K+1,u+l}\mathbf{e}_{u+l}, \;\; l = 0, 1, \cdots, L-u, \tag{152}$$

$$\mathbf{s}^{l,i}_{K+1} = \mathbf{s}^{l+1,i}_{K+1} - 2s^{0,i}_{K+1,u+l}\mathbf{e}_{u+l}, \;\; l = -1, -2, \cdots, 1-u, \tag{153}$$

where $s^{0,i}_{K+1,u+l}$ is the $(u+l)$th element of $\mathbf{s}^{0,i}_{K+1}$ and $\mathbf{e}_{u+l}$ is the $(u+l)$-unit vector in $\mathbb{R}^L$.

Step 3

Evaluate TSC_{K+1} for each binary signature $\mathbf{s}^{l,i}_{K+1}$ returned by Step 2, $l = 0, \cdots, L$, and choose the binary signature that gives minimum TSC. ■

The above procedure identifies and composes $L+1$ binary sequences for each one of a total $P-1$ $(P \leq L)$ slowest increase arcs[11]; we select the signature that gives minimum TSC among all $(P-1)L+1$ candidates. Our experimental studies indicate that $P = 2$ or 3 (i.e. one or two slowest increase arcs) is sufficient to closely approximate the performance level reached when all possible slowest increase arcs are considered $(P = L)$.

C. Experimental Studies

We consider a code-division multiplexing system with signature length $L = 16$. We assume that initially there are $K = 16$ users (fully-loaded system) that utilize a minimum TSC optimal binary signature set (orthogonal Walsh-Hadamard in this trivial case).

In Fig. 29, we plot the TSC of the code-division multiplexing system $(K+1, L = 16)$ for $K = 16$ up to 31 where each (K, L) signature set is optimally min-TSC designed by [14] and the $K+1$ signature is added by the procedure in the previous section. The quality of the resulting $(K+1, L)$ design is tested against the $(K+1, L)$ TSC bound of [14].

[11] The binary sequence $\mathbf{s}^{0,i}_{K+1} = sgn[\mathbf{q}_1]$ is common in all slowest increase arcs.

Fig. 30 repeats the study for the $(K+1, L=31)$ system set-up with $K=31$ up to 61. As with the studies of Fig. 1, the comparison with theoretical minimum TSC bounds is very favorable. Frequently, the resulting sequence set is absolutely TSC optimal.

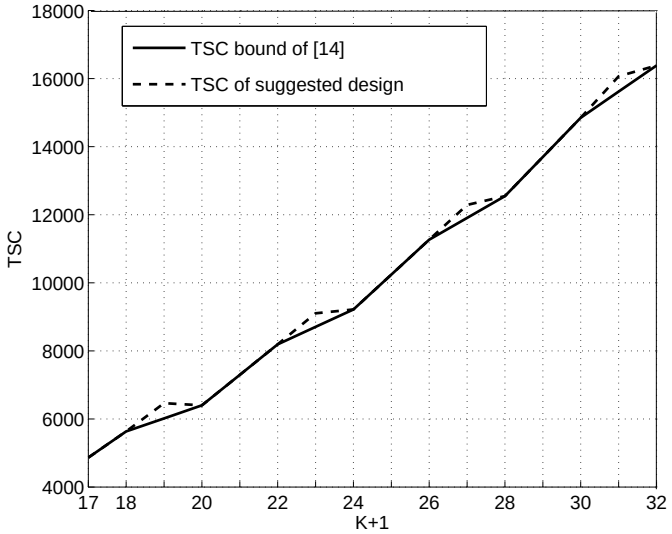

Fig. 25: TSC of $(K+1, L=16)$ signature set.

References

[1] L. R. Welch, "Lower bounds on the maximum cross correlation of signals," *IEEE Trans. Inform. Theory*, vol. IT-20, pp. 397-399, May 1974.

[2] M. Rupf and J. L. Massey, "Optimum sequence multisets for synchronous code-division multiple-access channels," *IEEE Trans. Inform. Theory*, vol. 40, pp. 1261-1266, July 1994.

[3] P. Viswanath, V. Anantharam, and D. N. C. Tse, "Optimal sequences, power control, and user capacity of synchronous CDMA systems with linear MMSE multiuser receivers," *IEEE Trans. Inform. Theory*, vol. 45, pp. 1968-1983, Sept. 1999.

[4] P. Cotae, "An algorithm for obtaining Welch bound equality sequences for S-CDMA channels," *AEÜ. Int. J. Electron. Commun.*, vol. 55, pp. 95-99, Mar. 2001.

[5] C. Rose, S. Ulukus, and R. D. Yates, "Wireless systems and interference avoidance," *IEEE Trans. Wireless Commun.*, vol. 1, pp. 415-428, July 2002.

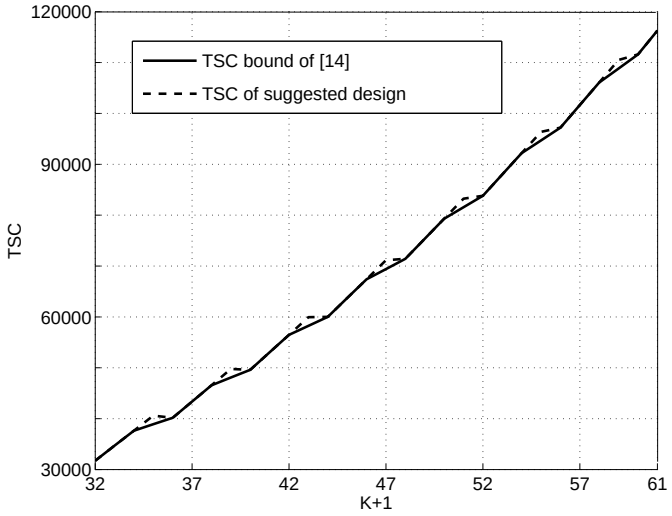

Fig. 26: TSC of $(K+1, L=31)$ signature set.

[6] P. Anigstein and V. Anantharam, "Ensuring convergence of the MMSE iteration for interference avoidance to the global optimum," *IEEE Trans. Inform. Theory*, vol. 49, pp. 873-885, Apr. 2003.

[7] H. Boche and S. Stanczak, "Iterative algorithm for finding optimal resource allocation in symbol asynchronous CDMA channels with different SINR requirements," in *Proc. 36th Asilomar Conf. on Signals, Syst. and Computers*, Pacific Grove, CA, Nov. 2002, vol. 2, pp. 1909-1913.

[8] J. Luo, S. Ulukus, and A. Ephremides, "Optimal sequences and sum capacity of symbol asynchronous CDMA systems," *IEEE Trans. Inform. Theory*, vol. 51, pp. 2760-2769, Aug. 2005.

[9] O. Popescu and C. Rose, "Sum capacity and TSC bounds in collaborative multibase wireless systems," *IEEE Trans. Inform. Theory*, vol. 50, pp. 2433-2438, Oct. 2004.

[10] T. Guess, "User-capacity-maximization in synchronous CDMA subject to RMS-bandlimited signature waveforms," *IEEE Trans. Commun.*, vol. 52, pp. 457-466, Mar. 2004.

[11] G. S. Rajappan and M. L. Honig, "Signature sequence adaptation for DS-CDMA with multipath," *IEEE J. Select. Areas Commun.*, vol. 20, pp. 384-395, Feb. 2002.

[12] P. Cotae, "Transmitter adaptation algorithm for multicellular synchronous CDMA systems with multipath," *IEEE J. Select. Areas Commun.*, vol. 24, pp. 94-103, Jan. 2006.

[13] P. Cotae, "On the optimal sequences and total weighted square correlation of synchronous CDMA systems in multipath channels," *IEEE Trans. Vehic. Tech.*, vol. 56, pp. 2063-2072, July 2007.

[14] G. N. Karystinos and D. A. Pados, "New bounds on the total squared correlation and optimum design of DS-CDMA binary signature sets," *IEEE Trans. Commun.*, vol. 51, pp. 48-51, Jan. 2003.

[15] C. Ding, M. Golin, and T. Klϕve, "Meeting the Welch and Karystinos-Pados bounds on DS-CDMA binary signature sets," *Designs, Codes and Cryptography*, vol. 30, pp. 73-84, Aug. 2003.

[16] V. P. Ipatov, "On the Karystinos-Pados bounds and optimal binary DS-CDMA signature ensembles," *IEEE Comm. Letters*, vol. 8, pp. 81-83, Feb. 2004.

[17] G. N. Karystinos and D. A. Pados, "The maximum squared correlation, total asymptotic efficiency, and sum capacity of minimum total-squared-correlation binary signature sets," *IEEE Trans. Inform. Theory*, vol. 51, pp. 348-355, Jan. 2005.

[18] F. Vanhaverbeke and M. Moeneclaey, "Binary signature sets for increased user capacity on the downlink of CDMA Systems," *IEEE Trans. Wireless Commun.*, vol. 5, pp. 1795-1804, July 2006.

[19] P. D. Papadimitriou and C. N. Georghiades, "Code-search for optimal TSC binary sequences with low crosscorrelation spectrum," in *Proc. IEEE MILCOM*, Boston, MA, Oct. 2003, vol. 2, pp. 1071-1076.

[20] H. Y. Kwan and T. M. Lok, "Binary-code-allocation scheme in DS-CDMA systems," *IEEE Trans. Vehic. Tech.*, vol. 56, pp. 134-145, Jan. 2007.

[21] L. Wei, S. N. Batalama, D. A. Pados and B. Suter, "Adaptive binary signature design for code division multiplexing," in *Proc. IEEE MILCOM*, Washington, D.C., Oct. 2006.

[22] P. Spasojevic and C. N. Georghiades, "The slowest descent method and its application to sequence estimation," *IEEE Trans. Commun.*, vol. 49, pp. 1592-1604, Sept. 2001.

VIII. Short-data-record Adaptive Detection

The work has been presented at the 2007 IEEE Radar Conference, Boston, MA.

In the context of an array radar application with M antenna elements (spatial channels) and N pulses per coherent processing interval (CPI), optimum signal detection in the presence of spatial and temporal Gaussian noise requires joint space-time matched filtering in the MN complex vector space. Since prior knowledge of the noise covariance matrix is not available, the maximum-likelihood sample average estimate is often used, developed from K noise only vector samples that correspond to distinct range cells. This is the so called secondary data set. Then, the inverse of the sample-matrix is considered as an estimate of the inverse covariance matrix. This approach is known as the Sample-Matrix-Inversion method (SMI) and in [1] it was shown to outperform the recursive least-mean-squares (LMS) adaptive implementation of the matched filter (MF) processor in terms of convergence rate and small-sample output SNR characteristics. Still, it was found that $K \geq 2MN$ independent and identically distributed (i.i.d.) training data samples are needed to maintain with probability 1/2 a loss lower than or equal to 3dB compared to the ideal MF. Simple variance normalization of the MF decision statistic led to a Constant False Alarm Rate (CFAR) test [2] for Neyman-Pearson detection. System optimization in the generalized likelihood ratio (GLR) sense was pursued in [3] and analyzed in [4]. The resulting test statistic offers embedded CFAR behavior, converges to the ideal MF solution at least in probability as the number of secondary data K grows, and it is shown in [2] to outperform the SMI approach for $K = 2MN$, except for high SNR regions.

It is important to note that the SMI and GLR tests are both asymptotically optimal to the extent that they converge in a probabilistic sense to the optimum ideal MF as the size of the secondary data set grows to infinity. However, for finite sample support no optimality can be claimed in either case and superior probability of detection performance for a fixed false alarm rate is theoretically possible by other filtering means. Moreover, both methods share the need to invert the sample covariance matrix of the noise process.

Arguably, in airborne surveillance systems the training data size requirements make the practicality of these approaches questionable even for moderate values of M and N. This is particularly true if we consider a highly non-stationary, non-homogeneous [5] operating environment, typically encountered in practice, that necessitates brief data collection. In this present work, we consider the auxiliary-vector (AV) iterative algorithm [7], [8] to develop an infinite sequence of decision statistics. The objective is linear space-time adaptive processing with sample support near (or below) the space-time product MN. The AV algorithm is a non-invasive procedure where no explicit matrix inversion/eigen-decomposition/diagonalization is attempted. Mathematically, it creates an infinite sequence of filters that begins from the target vector and converges to the ideal matched filter. The development of the iterative algorithm is founded solely on statistical signal processing principles.

The practical motivation behind the development of the AV algorithm is

adaptive signal processing where the input autocorrelation matrix is assumed unknown and it is sample-average estimated by a given data record. When the autocorrelation matrix is substituted by its estimate in the recursively generated sequence of filters, the corresponding filter estimators offer the means for effective control over the filter estimator bias versus (co-)variance trade-off [9]. Starting from the zero-variance, high-bias (for non-white inputs) target vector, we can go all the way up to the unbiased, yet high-variance for small data record sizes, AMF estimate and anywhere in between. As a result, adaptive filters from this developed class are seen to outperform in probability of detection (for any given false alarm) all known and tested adaptive detection means (including for example the multistage Wiener filter algorithm [10], [11] which is known [7] to be equivalent to an orthogonalized version of the AV algorithm with vector-optimum AV weights[12]). It is worth mentioning that the familiar trial-and-error tuning to problem and data-record-size specifics of the real-valued LMS gain or RLS inverse matrix initialization constant or SMI diagonal loading parameter that plagues field practitioners is now replaced by an automated data-based integer choice of one of the recursively generated filters [8]. Numerical and simulation results included in this work support the theoretical arguments and promote the new method as the processor of choice when only small secondary data training sets are available.

A. Signal Model and Background

We consider a narrowband uniform linear array radar with M antenna elements (subarrays or spatial channels). We assume that each element collects the complex (I/Q) return of a series of N coherent pulses for some given range cell $k = 1, \ldots, K_{max} = T_{PRI}/T$, where T_{PRI} is the pulse repetition interval and T is the pulse duration. We organize the received data in the form of a matrix $\mathbf{X}_{M\times N}$, where $X(m,n)$, $m = 1, \ldots, M$, $n = 1, \ldots, N$, denotes the m-element, n-pulse signal sample. The objective is to cope with system and surrounding disturbances and detect in $\mathbf{X}_{M\times N}$ the presence of a desired signal of unknown amplitude. Without loss of generality and for notational simplicity, we consider a "vectorized" form of $\mathbf{X}_{M\times N}$, where $\mathrm{Vec}(\mathbf{X}_{M\times N}) = \mathbf{x}_{MN\times 1}$ is constructed by sequencing all matrix columns in the form of a vector.

We begin by casting the detection problem in the context of binary hypothesis testing. We denote the disturbance only hypothesis by H_0 and the target plus disturbance hypothesis by H_1.

$$\begin{aligned} H_0 &: \mathbf{x} = \mathbf{j} + \mathbf{c} + \mathbf{n} \\ H_1 &: \mathbf{x} = \alpha\mathbf{v} + \mathbf{j} + \mathbf{c} + \mathbf{n}. \end{aligned} \tag{154}$$

In (154), $\mathbf{j}$ represents a mixture of L broadband directional interferers (jammers)

[12]The orthogonal version of the AV algorithm with conditionally optimal AV weights as presented in [12], [13] can still outperform the multistage Wiener filter [10], [11] under small sample support.

in the far field, where $\mathbf{j} = \mathrm{Vec}(\mathbf{J}_{M\times N})$ with

$$J(m,n) = \sum_{l=1}^{L} J_l(n)\, e^{j2\pi(m-1)\frac{\sin\theta_l d}{\lambda}}, \qquad n = 1,\ldots,N,\ m = 1,\ldots,M. \tag{155}$$

We assume that $J_l(n), l = 1,\ldots,L$, is complex white Gaussian distributed to account for channel fading at the pulse-repetition frequency as in the model of [14], [15]. The antenna element spacing is d and the radar carrier wavelength is λ. The direction of arrival (DOA) $\theta_l, l = 1,\ldots,L$, is assumed to be uniformly distributed in $[-\pi/2, \pi/2]$. We find it convenient to define the spatial frequency $f_l \stackrel{\triangle}{=} \frac{\sin\theta_l d}{\lambda}$, $l = 1,\ldots,L$, and assume that f_l is uniformly distributed in [-0.5,0.5] with proper selection of d and λ. In addition, $\mathbf{c}_{MN\times 1}$ in (154) accounts for colored Gaussian noise with covariance matrix $\mathbf{R}_c$ and corresponds to a radar clutter region. Spatially and temporally white disturbances are denoted by $\mathbf{n}$. The signal or "steering vector" of interest, $\mathbf{v}$, is present in $\mathbf{x}$ under hypothesis H_1 only. Without loss of generality we assume that $\mathbf{v}^H\mathbf{v} = 1$ (H denotes the Hermitian operator) such that all energy signal characteristics are absorbed in the unknown complex amplitude constant α. For completeness, if $\mathbf{v} = \mathrm{Vec}(\mathbf{V}_{M\times N})$ then

$$V(m,n) = \frac{1}{\sqrt{MN}}\, e^{j2\pi(m-1)\frac{\sin\theta_s d}{\lambda} + j2\pi(n-1)\frac{2\nu}{\lambda f_{\mathrm{PR}}}}, \qquad n = 1,\ldots,N,\ m = 1,\ldots,M. \tag{156}$$

In (156), $\theta_s \in [-\pi/2, \pi/2]$ is the angle of arrival of the signal (target) of interest, ν is the target radial velocity, and f_{PR} is the radar pulse repetition frequency. Once again, it is convenient to define the spatial target frequency $f_s \stackrel{\triangle}{=} \frac{\sin\theta_s d}{\lambda}$ and the "normalized Doppler" target frequency $f_D \stackrel{\triangle}{=} \frac{2\nu}{\lambda f_{\mathrm{PR}}}$. In this case we assume that $f_s, f_D \in [-0.5, 0.5]$.

Given a data vector $\mathbf{x}$ that corresponds to some range cell $k \in \{1,\ldots,K_{\max}\}$, the objective is to decide in favor of H_0 or H_1 in a way that maximizes the probability of detection $P_D = \Pr\{H_1 \text{ decided}|H_1 \text{ true}\}$ subject to a given false alarm constraint $P_{\mathrm{FA}} = \Pr\{H_1 \text{ decided}|H_0 \text{ true}\} \le \rho$. The optimum decision rule is well known [16], [17] and of the form

$$|\mathbf{w}^H\mathbf{x}| \underset{H_0}{\overset{H_1}{\gtrless}} \tau \tag{157}$$

where $\tau > 0$ is the threshold parameter to be determined according to the condition $P_{\mathrm{FA}} = \rho$ and $\mathbf{w}$ is the linear filter defined by

$$\mathbf{w} = b\mathbf{R}^{-1}\mathbf{v} \tag{158}$$

where b is an arbitrary positive scalar. In (158), $\mathbf{R} = E_{H_0}\{\mathbf{x}\mathbf{x}^H\}$ where $E_{H_i}\{\cdot\}$ denotes the statistical expectation operation under $H_i, i = 0, 1$. Then the variance under H_0 of the test statistic $\mathbf{w}^H\mathbf{x}$ is $\mathrm{Var}_{H_0}\{\mathbf{w}^H\mathbf{x}\} = \mathbf{v}^H\mathbf{R}^{-1}\mathbf{v}$ which

implies that the modified test statistic $\frac{\mathbf{v}^H\mathbf{R}^{-1}\mathbf{x}}{\sqrt{\mathbf{v}^H\mathbf{R}^{-1}\mathbf{v}}}$ is zero-mean unit-variance complex Gaussian distributed. As a consequence $\left|\frac{\mathbf{v}^H\mathbf{R}^{-1}\mathbf{x}}{\sqrt{\mathbf{v}^H\mathbf{R}^{-1}\mathbf{v}}}\right|^2$ is chi-square distributed with two degrees of freedom and leads to the familiar CFAR (constant false alarm rate) optimum decision rule

$$\frac{|\mathbf{v}^H\mathbf{R}^{-1}\mathbf{x}|^2}{\mathbf{v}^H\mathbf{R}^{-1}\mathbf{v}} \underset{H_0}{\overset{H_1}{\gtrless}} \lambda, \qquad (\lambda > 0). \tag{159}$$

Substitution in (159) of the sample-average covariance matrix estimate $\hat{\mathbf{R}}(K) = \frac{1}{K}\sum_{k=1}^{K}\mathbf{x}_k\mathbf{x}_k^H$ from K data samples from H_0 defines the so called CFAR adaptive matched filter (AMF) detector [2]. In contrast, we recall that the generalized likelihood ratio (GLR) test of [3] and [4] is

$$\frac{|\mathbf{v}^H[\hat{\mathbf{R}}(K)]^{-1}\mathbf{x}|^2}{\mathbf{v}^H[\hat{\mathbf{R}}(K)]^{-1}\mathbf{v}(1+\frac{1}{K}\mathbf{x}^H[\hat{\mathbf{R}}(K)]^{-1}\mathbf{x})} \underset{H_0}{\overset{H_1}{\gtrless}} \gamma, \qquad (\gamma > 0). \tag{160}$$

In the following section we revisit the auxiliary-vector (AV) algorithm [7], [8] to develop new decision statistics that maintain the principle of linear filtering for signal detection in Gaussian disturbance. Compared to AMF, GLR, multistage Wiener filter and other approaches we achieve superior adaptation performance, especially when we operate with small secondary data sets.

B. Auxiliary-Vector Detection

The AV algorithm generates an infinite sequence of filters $\{\mathbf{w}_n\}_{n=0}^{\infty}$ that is initialized at the steering vector of interest

$$\mathbf{w}_0 = \mathbf{v}. \tag{161}$$

At each step $k+1$ of the algorithm, $k = 0, 1, 2, \ldots$, we incorporate in $\mathbf{w}_k$ an "auxiliary" vector component $\mathbf{g}_{k+1}$ that is orthogonal to $\mathbf{v}$ (but not necessarily orthogonal to previously generated auxiliary vectors) and weighted by a scalar μ_{k+1} and we form the next filter in the sequence

$$\mathbf{w}_{k+1} = \mathbf{w}_k - \mu_{k+1}\mathbf{g}_{k+1}. \tag{162}$$

The auxiliary vector $\mathbf{g}_{k+1}$ is chosen to maximize, under fixed norm, the magnitude of the cross-correlation between its output $\mathbf{g}_{k+1}^H\mathbf{x}$ and the previous filter output $\mathbf{w}_k^H\mathbf{x}$ and is given by

$$\mathbf{g}_{k+1} = \mathbf{R}\mathbf{w}_k - (\mathbf{v}^H\mathbf{R}\mathbf{w}_k)\mathbf{v}. \tag{163}$$

The scalar μ_{k+1} is selected such that it minimizes the output variance of the filter $\mathbf{w}_{k+1}$ or equivalently minimizes the MS error between $\mathbf{w}_k^H\mathbf{x}$ and $\mu_{k+1}^*\mathbf{g}_{k+1}^H\mathbf{x}$. The MS-optimum μ_{k+1} is

$$\mu_{k+1} = \frac{\mathbf{g}_{k+1}^H\mathbf{R}\mathbf{w}_k}{\mathbf{g}_{k+1}^H\mathbf{R}\mathbf{g}_{k+1}}. \tag{164}$$

The AV filter recursion is completely defined by (161)-(164). Theoretical analysis of the AV algorithm was pursued in [7]. The results are summarized below in the form of a theorem.

Theorem 1 *Let* $\mathbf{R}$ *be a Hermitian positive definite matrix. Consider the iterative algorithm of eqs. (161)-(164).*
(i) *Successive auxiliary vectors generated through (162)-(164) are orthogonal:* $\mathbf{g}_i^H \mathbf{g}_{i+1} = 0$, $i = 1, 2, 3, \ldots$, *(but in general* $\mathbf{g}_i^H \mathbf{g}_j \neq 0$ *for* $|i - j| \neq 1$*).*
(ii) *The generated sequence of auxiliary-vector weights* $\{\mu_n\}$, $n = 1, 2, \ldots$, *is real-valued, positive, and bounded:* $0 < \frac{1}{\lambda_{\max}} \leq \mu_n \leq \frac{1}{\lambda_{\min}}$, $n = 1, 2, \ldots$, *where* $\lambda_{\max}$ *and* $\lambda_{\min}$ *are the maximum and minimum, correspondingly, eigenvalues of* $\mathbf{R}$*.*
(iii) *The sequence of auxiliary vectors* $\{\mathbf{g}_n\}$, $n = 1, 2, \ldots$, *converges to the* $\mathbf{0}$ *vector:* $\lim_{n \to \infty} \mathbf{g}_n = \mathbf{0}$.
(iv) *The sequence of auxiliary-vector filters* $\{\mathbf{w}_n\}$, $n = 1, 2, \ldots$, *converges to the optimum filter:* $\lim_{n \to \infty} \mathbf{w}_n = \frac{\mathbf{R}^{-1}\mathbf{v}}{\mathbf{v}^H \mathbf{R}^{-1} \mathbf{v}}$. □

If $\mathbf{R}$ is unknown and sample-average estimated from a data record of K samples, then Theorem 1 shows that

$$\hat{\mathbf{w}}_n(K) \underset{n \to \infty}{\longrightarrow} \hat{\mathbf{w}}_\infty(K) = \frac{\left[\hat{\mathbf{R}}(K)\right]^{-1} \mathbf{v}}{\mathbf{v}^H \left[\hat{\mathbf{R}}(K)\right]^{-1} \mathbf{v}} \tag{165}$$

where $\hat{\mathbf{w}}_\infty(K)$ is the widely used filter estimator known as the sample-matrix-inversion (SMI) filter [1]. The output sequence begins from $\hat{\mathbf{w}}_0(K) = \mathbf{v}$, which is a *0*-variance, fixed-valued, estimator that may be severely biased ($\hat{\mathbf{w}}_0(K) = \mathbf{v} \neq \frac{\mathbf{R}^{-1}\mathbf{v}}{\mathbf{v}^H \mathbf{R}^{-1} \mathbf{v}}$) unless $\mathbf{R} = \sigma^2 \mathbf{I}$ for some $\sigma > 0$. In the latter trivial case, $\hat{\mathbf{w}}_0(K)$ is already the perfect filter. Otherwise, the next filter estimator in the sequence, $\hat{\mathbf{w}}_1(K)$, has significantly reduced bias due to the optimization procedure employed at the expense of non-zero estimator (co-)variance. As we move up in the sequence of filter estimators $\hat{\mathbf{w}}_n(K)$, $n = 0, 1, 2, \ldots$, the bias decreases rapidly to zero while the variance rises slowly to the SMI ($\hat{\mathbf{w}}_\infty(K)$) levels (cf. (165)).

For the proposed AV sequence of filters $\mathbf{w}_n$ and any number of auxiliary vectors $n = 0, 1, 2, \ldots$, the decision statistics $\frac{\mathbf{w}_n^H \mathbf{x}}{\sqrt{\mathbf{w}_n^H \mathbf{R} \mathbf{w}_n}}$ are *0*-mean, unit-variance complex Gaussian. Then,

$$\frac{|\, \mathbf{w}_n^H \mathbf{x} \,|^2}{\mathbf{w}_n^H \mathbf{R} \mathbf{w}_n} \underset{H_0}{\overset{H_1}{\gtrless}} \lambda \tag{166}$$

defines a CFAR test in parallel to the optimum matched-filter test in (159). In adaptive implementations of $\mathbf{w}_n$ where the covariance matrix $\mathbf{R}$ is estimated from a data record of K samples, the adaptive auxiliary-vector test becomes

$$\frac{|\, \hat{\mathbf{w}}_n(K)^H \mathbf{x} \,|^2}{\hat{\mathbf{w}}_n(K)^H \hat{\mathbf{R}} \hat{\mathbf{w}}_n(K)} \underset{H_0}{\overset{H_1}{\gtrless}} \hat{\lambda}(K). \tag{167}$$

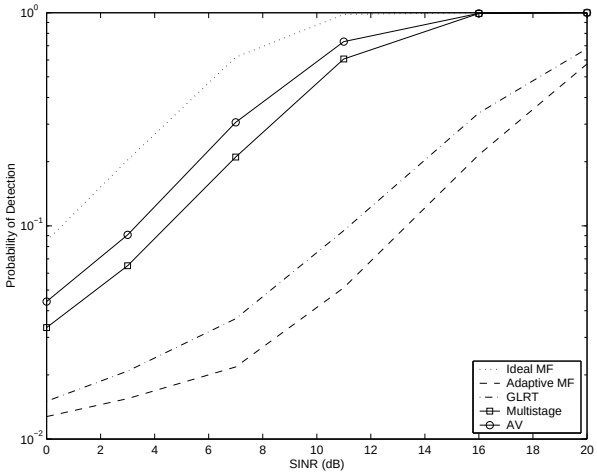

Fig. 23: P_D vs SINR (one-lag temporal clutter correlation 0.4).

The test is asymptotically CFAR (as $K \to \infty$, $\hat{\lambda}(K) \to \lambda$ in (159) for the optimum normalized matched-filter test for any given false alarm rate $P_{\rm FA}$). For finite training sets it qualifies as Cell-Averaging CFAR (CA-CFAR), as seen by the test denominator.

As a brief summary, the sequence of calculations for the design of the joint S-T auxiliary-vector filter estimator is as follows. The data record of K joint S-T input data vectors $\mathbf{x}_1, \mathbf{x}_2, \ldots, \mathbf{x}_K$ is utilized to obtain the estimate $\hat{\mathbf{R}}(K)$ of $\mathbf{R}$. Then, the sequence of AV filter estimators $\hat{\mathbf{w}}_0(K), \hat{\mathbf{w}}_1(K), \hat{\mathbf{w}}_2(K), \ldots$ is generated by the recursive algorithm of (161)-(164) with the *true* autocorrelation matrix $\mathbf{R}$ substituted by the *estimate* $\hat{\mathbf{R}}(K)$. A specific AV filter estimator $\hat{\mathbf{w}}_{n_0}(K)$ from the sequence can be selected by the cross-validation criterion of Qiao and Batalama [8] and used for detection according to (167).

C. Numerical and Simulation Studies

In this section we support and illustrate the preceding theoretical developments through two representative case-studies based on the hypothesis testing problem in (154). In all cases we assume presence of a mixture of 3 (three) broadband interferers with Jammer-to-Noise-Ratio JNR $= \frac{E\{|\mathbf{j}_l|^2\}}{\sigma^2} \approx 35dB$, $l = 1, 2, 3$. The jammers follow the model in (155) and the spatial frequency f_l, $l = 1, 2, 3$, is randomly drawn from the uniform $[-0.5, 0.5]$ distribution. The "peak" clutter (colored Gaussian noise) to noise ratio is fixed at CNR $= \frac{\sigma_c^2}{\sigma^2} = 40dB$. The false alarm rate is set at $P_{\rm FA} = .01$ and for simulation purposes threshold and probability of detection estimates P_D are based on $10,000$ samples from H_0 and H_1 respectively. All presented results are averages over 100 independent Monte-Carlo runs for arbitrarily chosen target vectors and jammers. P_D values

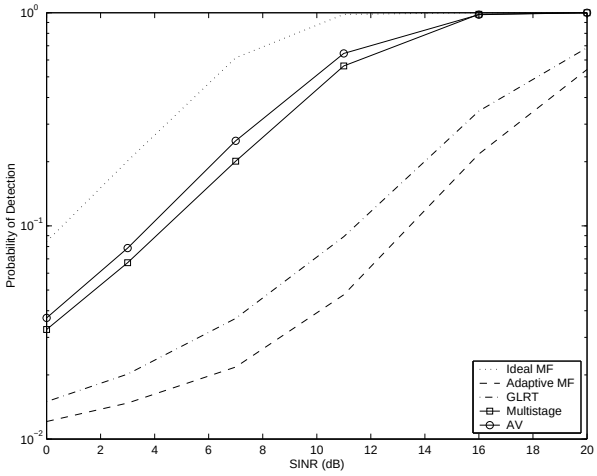

Fig. 24: P_D vs SINR (one-lag temporal clutter correlation 0.6).

are plotted as a function of the total SINR defined by

$$\text{SINR} \stackrel{\triangle}{=} |\ \alpha\ |^2\ \mathbf{v}^H \mathbf{R}^{-1} \mathbf{v}. \tag{168}$$

We assume a radar array system with $M = 5$ antenna elements (channels) and $N = 12$ pulses per coherent processing interval (CPI). the GLR test, and the adaptive AV filter $\mathbf{w}_n$ in (13), all for secondary data sets of size $K = MN = 60$. All studies include the ideal matched filter as a reference point, and the adaptive matched filter, GLR test, multistage Wiener filter, and AV filter, all for secondary data sets of size $K = MN = 60$.

Figures 27 and 28 present probability of detection versus SINR results for two different clutter scenarios generated as in [18] with normalized one-lag temporal clutter correlation 0.4 and 0.6, respectively. We note that relatively low temporal clutter correlation (low pulse-repetition frequency f_{PR} and/or high clutter velocity) results to benign eigenvalue distributions. We observe that in both cases the proposed AV filter $\mathbf{w}_n$ in (161)-(164) outperforms the multistage Wiener filter and offers significant performance gains over the adaptive matched filter and the GLR test.

References

[1] I. S. Reed, J. D. Mallet, and L. E. Brennan, "Rapid convergence rate in adaptive arrays," *IEEE Trans. Aerospace and Electr. Syst.*, vol. 10, pp. 853-863, Nov. 1974.

[2] F. C. Robey, D. R. Fuhrmann, E. J. Kelly, and R. Nitzberg, "A CFAR adaptive matched filter detector," *IEEE Trans. Aerosp. and Electr. Syst.*, vol. 28, pp. 208-216, June 1992.

[3] E. J. Kelly, "An adaptive detection algorithm," *IEEE Trans. Aerosp. and Electr. Syst.*, vol. 22, pp. 115-127, Mar. 1986.

[4] E. J. Kelly, "Performance of an adaptive detection algorithm; Rejection of unwanted signals," *IEEE Trans. Aerosp. and Electr. Syst.*, vol. 25, pp. 122-133, Mar. 1989.

[5] W. L. Melvin and M. C. Wicks, "Improving practical space-time adaptive radar," in *Proc. of 1997 IEEE National Radar Conf.*, pp. 48-53, Syracuse, NY, May 1997.

[6] H. Wang and L. Cai, "On adaptive spatial-temporal processing for airborne surveillance radar systems," *IEEE Trans. Aerosp. and Electr. Syst.*, vol. 30, pp. 660-670, July 1994.

[7] D. A. Pados and G. N. Karystinos, "An iterative algorithm for the computation of the MVDR filter," *IEEE Trans. Signal Proc.*, vol. 49, pp. 290-300, Feb. 2001.

[8] H. Qiao and S. N. Batalama, "Data record-based criteria for the selection of an auxiliary vector estimator of the MMSE/MVDR filter," *IEEE Trans. Commun.*, vol. 51, pp. 1700-1708, Oct. 2003.

[9] N. E. Nahi, *Estimation Theory and Applications*. Huntington, NY: R. E. Krieger Publishing Co., 1976.

[10] J. S. Goldstein, I. S. Reed, P. A. Zulch, and W. L. Melvin, "A multistage STAP CFAR detection technique," in *Proc. IEEE Radar Conf.*, Dallas, TX, May 1998, pp. 111-116.

[11] J. S. Goldstein, I. S. Reed, and L. L. Scharf, "A multistage representation of the Wiener filter based on orthogonal projections," *IEEE Trans. Inform. Theory*, vol. 44, pp. 2943-2959, Nov. 1998.

[12] D. A. Pados, T. Tsao, J. Michels, and M. Wicks, "Joint domain space-time adaptive processing with small training data sets," in *Proc. IEEE Radar Conf.*, Dallas, TX, May 1998, pp. 99-104.

[13] D. A. Pados and S. N. Batalama, " Joint space-time auxiliary-vector filtering for DS/CDMA systems with antenna arrays," *IEEE Trans. Commun.*, vol. 47, pp. 1406-1415, Sept. 1999.

[14] J. R. Roman and D. W. Davis, "Multichannel system identification and detection theory using output data techniques: Volume II," USAF Rome Laboratory, Report No. SSC-TR-96-02, Oct. 1996.

[15] J. Ward, "Space-time adaptive processing for airborne radar," MIT Lincoln Laboratory, Technical Report No. TR-1015, Dec. 1994.

[16] H. L. Van Trees, *Detection, Estimation and Modulation Theory, Part I* , New York, NY: Wiley, 1968.

[17] L. E. Brennan and I. S. Reed, "Theory of adaptive radar," *IEEE Trans. Aerosp. and Electr. Syst.*, vol. 9, pp. 237-252, Mar. 1973.

[18] J. H. Michels, T. Tsao, B. Himed, and M. Rangaswamy, "Space-time adaptive processing (STAP) in airborne radar applications," in *Proc. IASTED Intern. Conf. on Sign. Proc. and Comm.*, Canary Islands, Spain, Feb. 1998.

IX. Subspace Direction Finding with an Auxiliary-Vector Basis

This work has been presented at the 2005 SPIE Defense and Security Symposium, Orlando, FL, and has been published at the IEEE Transactions on Signal Processing, Feb. 2007.

Solutions for the classical direction-of-arrival (DOA) estimation problem can be broadly categorized into maximum-likelihood-type (ML) algorithms [1], which are based on techniques for the maximization of the probability density function of the received signal, and subspace algorithms, which are based on the decomposition of the autocovariance matrix of the received signal. Among the most successful and popular subspace algorithms are the MUSIC [2] and ESPRIT [3] procedures. In general, ML-type algorithms have superior performance compared to subspace-based techniques when the signal-to-noise (SNR) ratio is small or the number of snapshots is small. Also, the performance of subspace-based estimators degrades substantially in the case of correlated signal sources as compared to ML schemes.

In this work, we attempt to exploit the structure of the received data autocovariance matrix in a new way. When K distinct signals in space impinge on M antenna elements ($K < M$), the input autocovariance matrix consists of a rank K signal subspace and a rank $M-K$ noise subspace. Using the concept of maximum cross-correlation auxiliary vectors (AV's) [4], we create an *extended* non-eigenvector signal subspace basis of rank $K+1$ (eigen decomposition is not carried out at all). The *extended* signal subspace encompasses the *true* signal subspace of rank K and the scanning vector dimension itself. Then, the proposed DOA estimation algorithm simply looks for the collapse of the rank of the extended signal subspace from $K+1$ to K when the scanning vector falls in the signal subspace. Extensive simulation studies demonstrate that significant resolution performance improvements may be gained over MUSIC, ESPRIT, and ML schemes for both uncorrelated and correlated sources.

A. Signal model

Consider a uniform linear array (ULA) with M elements and let θ represent the DOA of an impinging source whose array response vector is given by

$$\mathbf{s}_\theta = [1, e^{-j\frac{\omega}{c}d\,sin\theta}, \ldots, e^{-j(M-1)\frac{\omega}{c}d\,sin\theta}]^H \tag{169}$$

where ω is the carrier frequency, c is the signal propagation speed, d is the inter-element spacing, and H denotes the Hermitian operator. When K narrowband signals ($K < M$) on the same carrier impinge on the array with distinct angles of arrival $\theta_1, \theta_2, \ldots, \theta_K$, the received signal snapshot at time i, $\mathbf{r}_i \in \mathbb{C}^M$, is of the form

$$\mathbf{r}_i = \mathbf{A}\mathbf{x}_i + \mathbf{n}_i, \quad i = 1, \ldots, N, \tag{170}$$

where $\mathbf{A}_{M\times K} \stackrel{\triangle}{=} [\mathbf{s}_{\theta_1}, \ldots, \mathbf{s}_{\theta_K}]$, $\mathbf{x}_i \in \mathbb{C}^K$ is the zero mean composite source signal vector, and $\mathbf{n}_i \in \mathbb{C}^M$ represents Gaussian noise with mean zero and autocorrelation matrix $E\{\mathbf{n}\mathbf{n}^H\} = \sigma^2\mathbf{I}$ ($E\{\cdot\}$ denotes statistical expectation). To

avoid mathematical -and presentation- ambiguities, the array response vectors $\mathbf{s}_{\theta_1}, \ldots, \mathbf{s}_{\theta_K}$ are considered to be linearly independent, i.e. the inter-element spacing is no greater than half the carrier wavelength. The autocovariance matrix of the array input is

$$\mathbf{R} \stackrel{\triangle}{=} E\{\mathbf{r}\mathbf{r}^H\} = \mathbf{A}\mathbf{R}_s\mathbf{A}^H + \sigma^2\mathbf{I} \tag{171}$$

where

$$\mathbf{R}_s \stackrel{\triangle}{=} E\{\mathbf{x}\mathbf{x}^H\}. \tag{172}$$

The source signal autocovariance matrix $\mathbf{R}_s$ is diagonal when the sources are uncorrelated and is non-diagonal and non-singular for partially correlated sources. Complete knowledge of $\mathbf{R}$ cannot be assumed usually; instead, we may use as necessary the sample-average estimated array input autocovariance matrix given by

$$\hat{\mathbf{R}} = \frac{1}{N}\sum_{i=1}^{N}\mathbf{r}_i\mathbf{r}_i^H \tag{173}$$

where N is the available observation data record size.

B. Auxiliary-vector extended signal subspace basis

In this section, we consider the signal model presented above and develop a novel non-eigenvector basis that spans the signal subspace extended in dimension by the DOA scanner vector $\mathbf{s}_\theta$, $\theta \in (-90^o, 90^o)$. Essential theoretical background for this derivation is provided by the adaptive filtering work in [4]. Details follow.

In contrast to the work in [4], here we define the initial vector in our basis calculations $\mathbf{v}_0(\theta)$ as follows:

$$\mathbf{v}_0(\theta) \stackrel{\triangle}{=} \frac{\mathbf{R}\mathbf{s}_\theta}{\|\mathbf{R}\mathbf{s}_\theta\|}. \tag{174}$$

When the sources are uncorrelated and it happens to be $\theta = \theta_j$ for some $j \in \{1, \ldots, K\}$,

$$\mathbf{R}\mathbf{s}_{\theta_j} = \left(E\left\{\mathbf{x}^2[j]\right\}M + \sigma^2\right)\mathbf{s}_{\theta_j} + \sum_{k=1,\, k\neq j}^{K} E\left\{\mathbf{x}^2[k]\right\}\mathbf{s}_{\theta_k}^H\mathbf{s}_{\theta_j}\,\mathbf{s}_{\theta_k}. \tag{175}$$

From (175) we can see that $\mathbf{v}_0(\theta_j)$ is a linear combination of the K array response vectors and lies in the *true* signal subspace of dimension K. However, when $\theta \neq \theta_j$, $j = 1, \ldots, K$,

$$\mathbf{R}\mathbf{s}_\theta = \sum_{k=1}^{K} E\left\{\mathbf{x}^2[k]\right\}\mathbf{s}_{\theta_k}^H\mathbf{s}_\theta\,\mathbf{s}_{\theta_k} + \sigma^2\mathbf{s}_\theta \tag{176}$$

and $\mathbf{v}_0(\theta)$ is a linear combination of the $K+1$ array response vectors and lies in the *extended* signal subspace of dimension $K+1$ which encompasses the *true* signal subspace.

Having defined $\mathbf{v}_0(\theta)$ (the first vector in our basis to be formed), we now seek

a vector $\mathbf{g}_1(\theta)$ ("auxiliary vector" as we call it) that maximizes the magnitude of the statistical cross-correlation between the $\mathbf{v}_0(\theta)$ processed received data, $\mathbf{v}_0^H(\theta)\mathbf{r}$, and the $\mathbf{g}_1(\theta)$ processed data, $\mathbf{g}_1^H(\theta)\mathbf{r}$, subject to the orthonormality constraint $\mathbf{g}_1^H(\theta)\mathbf{v}_0(\theta) = 0$ and $\mathbf{g}_1^H(\theta)\mathbf{g}_1(\theta) = 1$:

$$\begin{aligned}\mathbf{g}_1(\theta) &\triangleq \underset{\substack{\mathbf{g}_1(\theta)\\ \mathbf{g}_1^H(\theta)\mathbf{v}_0(\theta)=0,\|\mathbf{g}_1(\theta)\|=1}}{argmax} \left\{\left|E\left\{\mathbf{v}_0^H(\theta)\mathbf{r}\mathbf{r}^H\mathbf{g}_1(\theta)\right\}\right|\right\} \\ &= \underset{\substack{\mathbf{g}_1(\theta)\\ \mathbf{g}_1^H(\theta)\mathbf{v}_0(\theta)=0,\|\mathbf{g}_1(\theta)\|=1}}{argmax} \left\{\left|\mathbf{v}_0^H(\theta)\mathbf{R}\mathbf{g}_1(\theta)\right|\right\}. \end{aligned} \tag{177}$$

This constraint optimization problem was first posed and solved in [5] yielding

$$\mathbf{g}_1(\theta) = \frac{(\mathbf{I} - \mathbf{v}_0(\theta)\mathbf{v}_0^H(\theta))\mathbf{R}\mathbf{v}_0(\theta)}{\|(\mathbf{I} - \mathbf{v}_0(\theta)\mathbf{v}_0^H(\theta))\mathbf{R}\mathbf{v}_0(\theta)\|}. \tag{178}$$

The vector $\mathbf{g}_1(\theta)$ has unit norm, is orthogonal to $\mathbf{v}_0(\theta)$, and is a linear combination of the K source array response vectors when $\theta = \theta_j, \quad j = 1, \ldots, K$, or $K+1$ array response vectors including $\mathbf{s}_\theta$, when $\theta \neq \theta_j$.

To fill in the proposed basis, we define the intermediate vector

$$\mathbf{w}_1(\theta) \triangleq \mathbf{v}_0(\theta) - \mu_1(\theta)\mathbf{g}_1(\theta) \tag{179}$$

where the scalar $\mu_1(\theta)$ is the value that minimizes the output variance of the $\mathbf{w}_1(\theta)$ processed data, $E\left\{\left|\mathbf{w}_1^H(\theta)\mathbf{r}\right|^2\right\}$ [6], and equals

$$\mu_1(\theta) = \frac{\mathbf{g}_1^H(\theta)\mathbf{R}\mathbf{v}_0(\theta)}{\mathbf{g}_1^H(\theta)\mathbf{R}\mathbf{g}_1(\theta)}. \tag{180}$$

Then, recursively, for $n = 2, \ldots, K-1$ we optimize the basis as follows:[13]

$$\mathbf{g}_n(\theta) = \frac{\left(\mathbf{I} - \mathbf{v}_0(\theta)\mathbf{v}_0^H(\theta) - \sum_{i=1}^{n-1}\mathbf{g}_i(\theta)\mathbf{g}_i^H(\theta)\right)\mathbf{R}\mathbf{w}_{n-1}(\theta)}{\left\|(\mathbf{I} - \mathbf{v}_0(\theta)\mathbf{v}_0^H(\theta) - \sum_{i=1}^{n-1}\mathbf{g}_i(\theta)\mathbf{g}_i^H(\theta))\mathbf{R}\mathbf{w}_{n-1}(\theta)\right\|}, \tag{181}$$

$$\mu_n(\theta) = \frac{\mathbf{g}_n^H(\theta)\mathbf{R}\mathbf{w}_{n-1}(\theta)}{\mathbf{g}_n^H(\theta)\mathbf{R}\mathbf{g}_n(\theta)}, \tag{182}$$

$$\mathbf{w}_n(\theta) = \mathbf{w}_{n-1}(\theta) - \mu_n(\theta)\mathbf{g}_n(\theta). \tag{183}$$

The final auxiliary vector $\mathbf{g}_K(\theta)$ that completes the construction of the basis is not normalized:

$$\mathbf{g}_K(\theta) = \left(\mathbf{I} - \mathbf{v}_0(\theta)\mathbf{v}_0^H(\theta) - \sum_{i=1}^{K-1}\mathbf{g}_i(\theta)\mathbf{g}_i^H(\theta)\right)\mathbf{R}\mathbf{w}_{K-1}(\theta). \tag{184}$$

[13] At each step, $\mathbf{g}_n(\theta)$ maximizes the cross-correlation magnitude between the $\mathbf{w}_{n-1}(\theta)$ processed data, $\mathbf{w}_{n-1}^H(\theta)\mathbf{r}$, and the $\mathbf{g}_n(\theta)$ processed data, $\mathbf{g}_n^H(\theta)\mathbf{r}$. Then, $\mu_n(\theta)$ minimizes the variance $E\left\{\left|\mathbf{w}_n^H(\theta)\mathbf{r}\right|^2\right\}$.

When $\theta = \theta_j,\ j = 1, \ldots, K$, $\mathbf{g}_K(\theta) = \mathbf{0}$ and

$$span\{\mathbf{v}_0(\theta_j), \mathbf{g}_1(\theta_j), \ldots, \mathbf{g}_{K-1}(\theta_j)\} = span\{\mathbf{s}_{\theta_1}, \ldots, \mathbf{s}_{\theta_K}\}. \tag{185}$$

In this case, the vectors $\{\mathbf{v}_0(\theta_j), \mathbf{g}_1(\theta_j), \ldots, \mathbf{g}_{K-1}(\theta_j)\}$ form an *orthonormal* basis for the *true* signal subspace. When $\theta \neq \theta_j,\ j = 1, \ldots, K$, however,

$$span\{\mathbf{v}_0(\theta), \mathbf{g}_1(\theta), \ldots, \mathbf{g}_K(\theta)\} = span\{\mathbf{s}_\theta, \mathbf{s}_{\theta_1}, \ldots, \mathbf{s}_{\theta_K}\} \tag{186}$$

and including $\mathbf{g}_k(\theta)$ we have formed an *orthogonal* basis for the *extended* signal subspace.

Calculation of the auxiliary vectors $\mathbf{g}_1(\theta), \mathbf{g}_2(\theta), \ldots, \mathbf{g}_K(\theta)$ as presented above in (178)-(184) requires calculation of the intermediate vectors $\mathbf{w}_n(\theta)$ and scalars $\mu_n(\theta),\ n = 1, 2, \ldots, K-1$. Proposition 1 below shows that direct second-order recursive calculation of $\mathbf{g}_2(\theta), \ldots, \mathbf{g}_{K-1}(\theta)$ is possible (see also [7]-[9]), while calculation of the final unnormalized auxiliary vector $\mathbf{g}_K(\theta)$ needs in addition a (first-order) recursion on $\mu_n(\theta)$. [14]

Proposition 1: The auxiliary vectors $\mathbf{g}_2(\theta), \mathbf{g}_3(\theta), \ldots, \mathbf{g}_{K-1}(\theta)$ can be calculated as follows:

$$\mathbf{g}_n(\theta) = \frac{\left(\mathbf{I} - \sum_{i=n-2}^{n-1} \mathbf{g}_i(\theta)\mathbf{g}_i^H(\theta)\right)\mathbf{R}\mathbf{g}_{n-1}(\theta)}{\left\|\left(\mathbf{I} - \sum_{i=n-2}^{n-1} \mathbf{g}_i(\theta)\mathbf{g}_i^H(\theta)\right)\mathbf{R}\mathbf{g}_{n-1}(\theta)\right\|},\ \ n = 2, 3, \ldots, K-1, \tag{187}$$

where $\mathbf{g}_1(\theta)$ is given by (178) and $\mathbf{g}_0(\theta) = \mathbf{v}_0(\theta)$.

The final (unnormalized) auxiliary vector $\mathbf{g}_K(\theta)$ equals

$$\mathbf{g}_K(\theta) = -\mu_{K-1}(\theta)\left(\mathbf{I} - \sum_{i=K-2}^{K-1} \mathbf{g}_i(\theta)\mathbf{g}_i^H(\theta)\right)\mathbf{R}\mathbf{g}_{K-1}(\theta) \tag{188}$$

where

$$\mu_n(\theta) = -\mu_{n-1}(\theta)\frac{\mathbf{g}_n^H(\theta)\mathbf{R}\mathbf{g}_{n-1}(\theta)}{\mathbf{g}_n^H(\theta)\mathbf{R}\mathbf{g}_n(\theta)},\ \ n = 2, 3, \ldots, K-1, \tag{189}$$

and $\mu_1(\theta)$ is given by (180). ∎

C. DOA estimation

Having defined the auxiliary-vector basis $\{\mathbf{v}_0(\theta), \mathbf{g}_1(\theta), \ldots, \mathbf{g}_K(\theta)\}$, we are now ready to describe the proposed DOA estimation procedure. Let Δ be the prearranged angle search step in degrees and, without loss of generality, say that $180^o/\Delta^o$ is an integer. Define $\theta^{(n)} = n\Delta^o,\ n = 1, 2, \ldots, 180^o/\Delta^o$, and

$$\mathbf{S}(\theta^{(n)}) = \left[\mathbf{v}_0(\theta^{(n)}), \mathbf{g}_1(\theta^{(n)}), \ldots, \mathbf{g}_K(\theta^{(n)})\right]. \tag{190}$$

[14] Alternatively, the proposed basis $\{\mathbf{v}_0(\theta), \mathbf{g}_1(\theta), \ldots, \mathbf{g}_K(\theta)\}$ can be calculated by: (i) Gram-Schmidt orthonormalization of the Krylov-type basis [10]-[12] $\{\mathbf{R}\mathbf{s}_\theta, \mathbf{R}^2\mathbf{s}_\theta, \ldots, \mathbf{R}^{K+1}\mathbf{s}_\theta\}$ that is modified to begin with the first-order vector $\mathbf{R}\mathbf{s}_\theta$ or (ii) through the first $K+1$ stages of the multistage Wiener filter representation [8], [13] when the initialization of the first stage is changed to $\mathbf{R}\mathbf{s}_\theta$. In either case, the last vector in the basis is to be left unnormalized.

The proposed spectrum for DOA estimation[15] is

$$P_{AV}(\theta^{(n)}) \stackrel{\triangle}{=} \frac{1}{\|\mathbf{g}_K^H(\theta^{(n)})\mathbf{S}(\theta^{(n-1)})\|^2}, \ n = 2, 3, \ldots, 180^o/\Delta^o. \tag{191}$$

To analyze the behavior of $P_{AV}(\theta^{(n)})$ and its suitability for DOA estimation, we consider first the case where the input autocovariance matrix $\mathbf{R}$, as it participates in $\mathbf{g}_K(\theta^{(n)})$ and $\mathbf{S}(\theta^{(n-1)})$, is perfectly known. When $\theta^{(n)} = \theta_j, \ j = 1, \ldots, K$, $\mathbf{g}_K(\theta^{(n)}) = \mathbf{0}$. As $\theta^{(n)} \to \theta_j, \ j = 1, \ldots, K$, $P_{AV}(\theta^{(n)}) \to \infty$ and a peak in the spectrum is to be observed. When, on the other hand, $\theta^{(n)} \neq \theta_j, \ j = 1, \ldots, K$, $\mathbf{g}_K(\theta^{(n)})$ is a linear combination of the K source signal array response vectors and $\mathbf{s}_{\theta^{(n)}}$. The columns of $\mathbf{S}(\theta^{(n-1)})$ span the source signal subspace extended by the $\mathbf{s}_{\theta^{(n-1)}}$ dimension. Hence, a part of $\mathbf{g}_K(\theta^{(n)})$ lies in the subspace of $\mathbf{S}(\theta^{(n-1)})$ and $\mathbf{g}_K^H(\theta^{(n)})\mathbf{S}(\theta^{(n-1)}) \neq \mathbf{0}$. Having $\theta^{(n-1)} = \theta_j, \ \ j = 1, \ldots, K$, does not affect these findings.

In practical scenarios where $\mathbf{R}$ is not known and is instead estimated from finitely many collected data (by (173) for example), the above arguments become approximate in an estimation theoretic sense. When $\theta^{(n)} = \theta_j, \ j = 1, \ldots, K$, $\hat{\mathbf{g}}_K(\theta^{(n)}) \neq \mathbf{0}$ with probability one. We expect, however, that $\left\|\hat{\mathbf{g}}_K(\theta^{(n)})\right\|$ becomes increasingly small as the data record size increases. At the same time, $\hat{\mathbf{g}}_K(\theta^{(n)}) \perp \{\hat{\mathbf{v}}_0(\theta^{(n)}), \ldots, \hat{\mathbf{g}}_{K-1}(\theta^{(n)})\}$ by design and $\hat{\mathbf{g}}_K(\theta^{(n)})$ lies outside the *approximate* signal subspace. Hence, $\left\|\hat{\mathbf{g}}_K^H(\theta^{(n)})\hat{\mathbf{S}}(\theta^{(n-1)})\right\| \simeq 0$ and we expect to see peaks in $P_{AV}(\theta^{(n)})$ as $\theta^{(n)} \to \theta_j, \ j = 1, \ldots, K$.

The computational complexity of the algorithm outlined above is $O(M^2K)$ per test angle or $O(\frac{180}{\Delta}M^2K)$ in total (notice that no direct matrix inversion operation is required). As a reference comparison, MUSIC and ESPRIT cost one full eigenvector decomposition of $O(M^3)$.

D. Simulation studies

For illustration purposes we consider a uniform linear antenna array of ten elements ($M = 10$) and two narrowband uncorrelated binary phase-shift-keying (BPSK) signals ($K = 2$) received in additive white Gaussian noise. The inter-element spacing of the array is set exactly equal to half the center wavelength of the signals ($d = \frac{\pi c}{\omega}$).

First, we fix the signal angles of arrival at -1^o and 1^o and the SNR's at 7dB. In Fig. 27, we examine the proposed AV basis spectrum when the observation data record size is $N = 60$ as compared with MUSIC and the conventional matched-filter (MF) spectrum. The AV spectrum resolves the two sources; MF and MUSIC both fail.

In Fig. 28, we ease somewhat the problem to 3^o of separation and add to the comparisons ESPRIT and the widely successful and popular grid-ML estimator of [14, 15] that intends to approximate the true ML solution [16, 17] by searching

[15]The proposed use, herein, of the modified orthogonal AV algorithm for DOA estimation via (191) is in sharp contrast to the use in [13] of the standard multistage Wiener filter representation algorithm of [8] for conventional reduced-rank ML-type DOA estimation.

over a set of $\binom{N}{K}$ selected grid points. Fig. 28(a) presents a probability of resolution[16] versus SNR study when $N = 50$. In Fig. 28(b), the SNR values are fixed at 0dB and the probability of resolution is plotted against sample support. The AV basis scheme significantly outperforms grid-ML at somewhat lower computational cost.[17] MF, as one might expect, fails to resolve at all SNR values in Fig. 28(a). MUSIC fails as well when SNR=0dB for all data record sizes in Fig. 28(b).

Next, we repeat the study of Fig. 28 for a scenario that involves random Gaussian correlated sources s_1, s_2 generated as follows:

$$s_1 \sim \mathcal{N}(0, \sigma_s^2) \quad \text{and } s_2 = ps_1 + \sqrt{1-p^2}\, s_3 \tag{192}$$

where $s_3 \sim \mathcal{N}(0, \sigma_s^2)$ and p is the correlation coefficient. Alongside standard MUSIC and ESPRIT, we consider MUSIC and ESPRIT upon spatial smoothing [18]. Interestingly, Fig. 29 demonstrates that for correlation values as high as $p = 0.7$, the AV-basis estimator continues to outperform grid-ML in probability of resolution (as well as MUSIC and ESPRIT with or without spatial smoothing). Fig. 29(a) plots the probability of resolution as a function of the signals' SNR= $\frac{\sigma_s^2}{\sigma^2}$ for fixed data record size $N = 50$. Fig. 29(b) plots the probability of resolution as a function of N when SNR=5dB. At correlation value $p = 0.9$, the AV and grid-ML probability of resolution curves are seen to intersect (Fig. 30). At small sample support, AV estimation continues to significantly outperform grid-ML (Fig. 30(b)).

E. Conclusion

We derived a new basis for the extended signal subspace that does not involve eigenvectors and includes the search vector dimension. Borrowing terminology from related recent literature, we called the elements of the basis auxiliary vectors (AV's). In this report, we used the new AV basis for direction-of-arrival estimation with remarkable success relative to (grid-)ML-type estimation for uncorrelated or even highly correlated sources (the latter being especially true under small sample support operation). Intuitively, one may attribute the success to the specific basis in use together with the joint effect of rank collapsing on the norm of the last AV and its projection onto the previously calculated scanner-extended signal subspace.

[16] Two sources with DOA θ_1 and θ_2 are said to be resolved if the respective estimates $\hat{\theta}_1$ and $\hat{\theta}_2$ are such that both $|\hat{\theta}_1 - \theta_1|$ and $|\hat{\theta}_2 - \theta_2|$ are less than $|\theta_1 - \theta_2|/2$ [14].

[17] The AV estimator is run with $\Delta = 0.5^o$ for a computational cost of the order of $O(360M^2K)$. Grid-ML has complexity $O\left(\binom{N}{K} M^2K\right)$. Here (Fig. 28), $N = 50$, $K = 2$, and $\binom{N}{K} = 1225$.

References

[1] F. C. Schweppe, "Sensor array data processing for multiple-signal sources," *IEEE Trans. Inform. Theory*, vol. IT-14, pp. 294-305, March 1968.

[2] R. O. Schmidt, "Multiple emitter location and signal parameter estimation," *IEEE Trans. Antennas and Propagation*, vol. AP-34, pp. 276-280, March 1986.

[3] R. H. Roy and T. Kailath, "ESPRIT-estimation of signal parameters via rotational invariance techniques," *IEEE Trans. Acoust., Speech, and Signal Proc.*, vol. ASSP-37, pp. 984-995, July 1989.

[4] D. A. Pados and S. N. Batalama, "Joint space-time auxiliary-vector filtering for DS/CDMA systems with antenna arrays," *IEEE Trans. Commun.*, vol. 47, pp. 1406-1415, Sept. 1999.

[5] A. Kansal, S. N. Batalama, and D. A. Pados, "Adaptive maximum SINR RAKE filtering for DS-CDMA multipath fading channels," *IEEE J. Select. Areas Commun.*, vol. 16, pp. 1765-1773, Dec. 1998.

[6] D. A. Pados and S. N. Batalama, "Low-complexity blind detection of DS/CDMA signals: auxiliary-vector receivers," *IEEE Trans. Commun.*, vol. 45, pp. 1586-1594, Dec. 1997.

[7] W. Chen, U. Mitra, and P. Schniter, "On the equivalence of three reduced rank linear estimators with applications to DS-CDMA," *IEEE Trans. Inform. Theory*, vol. 48, pp. 2609-2614, Sept. 2002.

[8] J. S. Goldstein, I. S. Reed, and L. L. Scharf, "A multistage representation of the Wiener filter based on orthogonal projections," *IEEE Trans. Inform. Theory*, vol. 44, pp. 2943-2959, Nov. 1998.

[9] B. Xu, C. Yang, and S. Mao, "Further insights on the equivalence of AVF and MSWF," in *Proc. IEEE Intern. Conf. Acoust., Speech, and Signal Proc.*, vol. 2, Montreal, Canada, May 2004, pp. 857-860.

[10] W. Xiao and M. L. Honig, "Large system transient analysis of adaptive least squares filtering," *IEEE Trans. Inform. Theory*, vol. 51, pp. 2447-2474, July 2005.

[11] S. Buryukh and K. Abed-meraim, "Reduced-rank adaptive filtering using krylov subspace," *EURASIP Journal on Applied Signal Proc.*, vol. 2002, no. 12, pp. 1387-1400, Dec. 2002.

[12] M. K. Schneider and A. S. Willsky, "Krylov subspace estimation," *SIAM J. Sci. Comput.*, vol. 22, no. 5, pp. 1840-1864, 2001.

[13] L. Huang, S. Wu, D. Feng, and L. Zhang, "Low complexity method for signal subspace fitting," *IEE Electronics Letters*, vol. 40, pp. 847-848, July 2004.

[14] P. Stoica and A. B. Gershman, "Maximum-likelihood DOA estimation by data-supported grid search," *IEEE Signal Proc. Letters*, vol. 6, pp. 273-275, Oct. 1999.

[15] A. B. Gershman and P. Stoica, "Data-supported optimization for maximum likelihood DOA estimation," in *Proc. IEEE Sensor Array and Multichannel Signal Proc. Workshop*, Cambridge, MA, March 2000, pp. 337-341.

[16] I. Ziskind and M. Wax, "Maximum likelihood localization of multiple sources by alternating projection," *IEEE Trans. Acoust., Speech, and Signal Proc.*, vol. ASSP-36, pp. 1553-1560, Oct. 1988.

[17] P. Stoica and K. C. Sharman, "Maximum likelihood methods for direction-of-arrival estimation," *IEEE Trans. Acoust., Speech, and Signal Proc.*, vol. ASSP-38, pp. 1132-1143, July 1990.

[18] T. Shan, M. Wax, and T. Kailath, "On spatial smoothing for direction-of-arrival estimation of coherent signals," *IEEE Trans. Acoust., Speech, and Signal Proc.*, vol. ASSP-33, pp. 806-811, Aug. 1985.

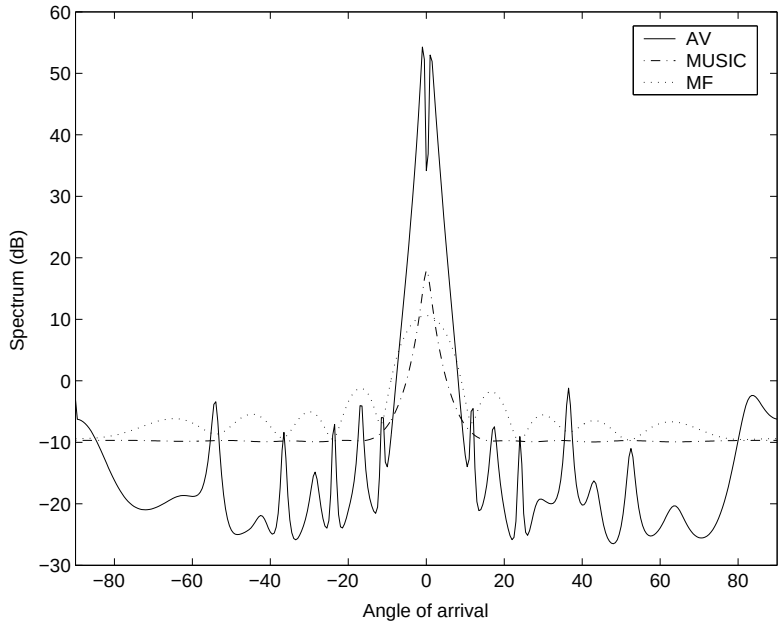

Fig. 27: AV, MUSIC, and MF spectra ($\theta_1 = -1^o, \theta_2 = 1^o$, SNR_1=SNR_2=7dB, $N = 50$).

(a)

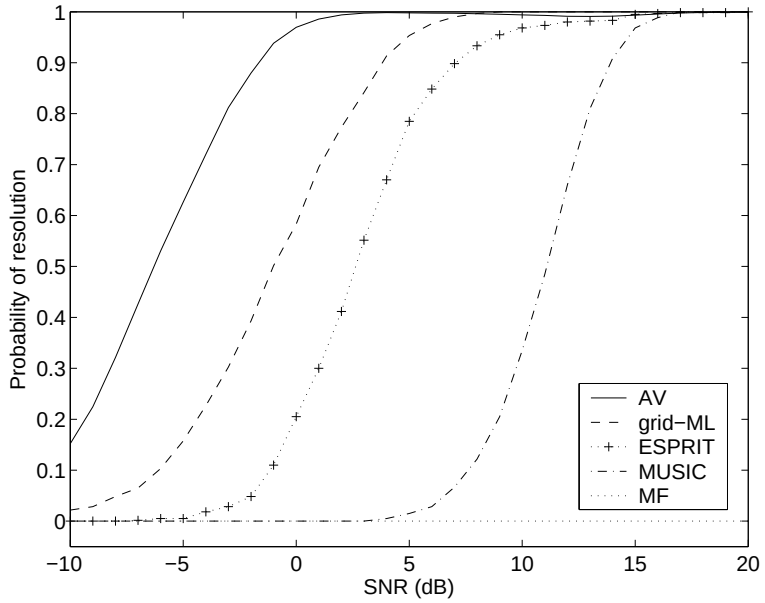

(b)

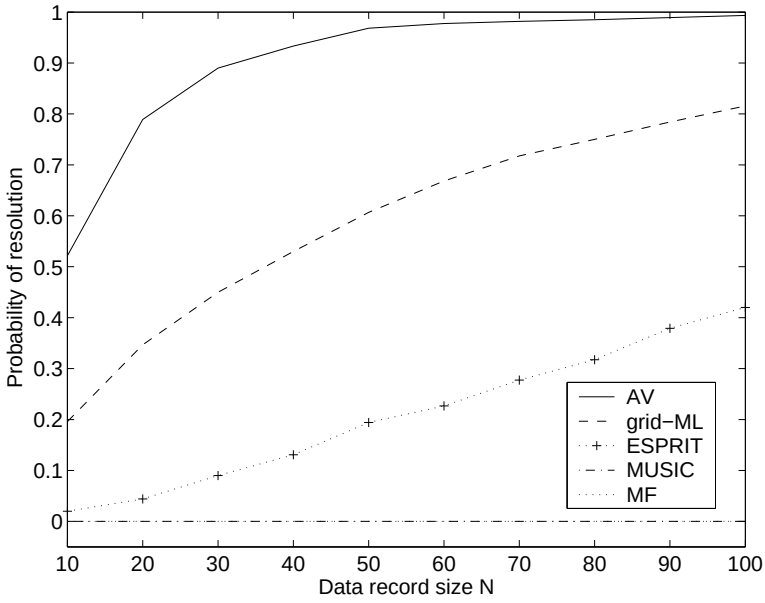

Fig. 28: (a) Probability of resolution versus SNR (separation 3^o, $N = 50$). (b) Probability of resolution versus sample support (separation 3^o, SNR_1=SNR_2=0dB).

(a)

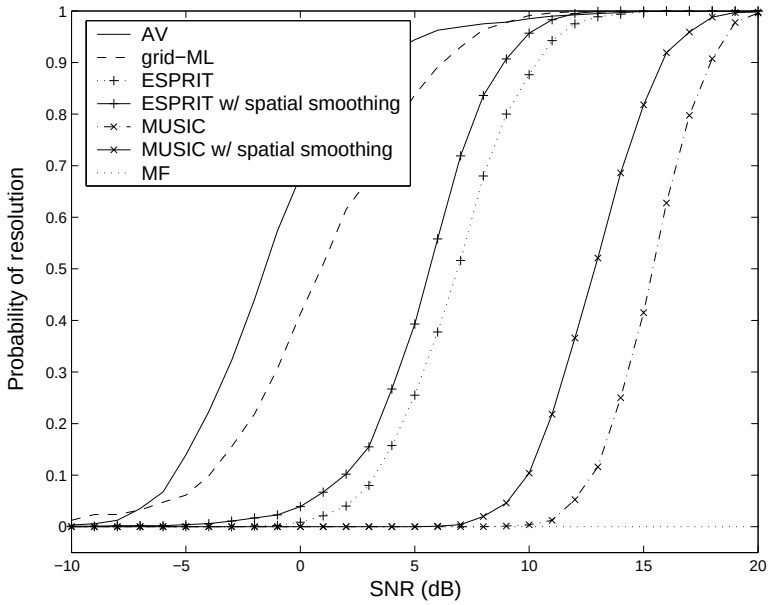

(b)

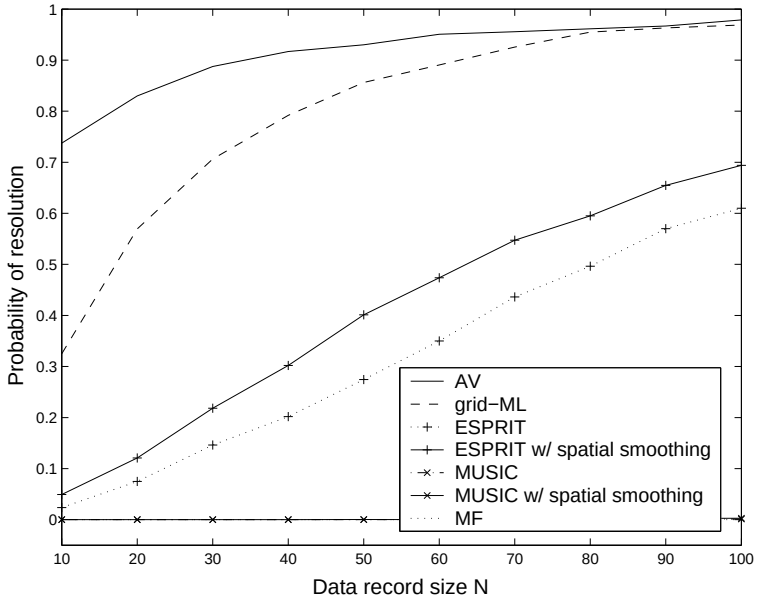

Fig. 29: (a) Probability of resolution versus SNR (separation 3^o, $N = 50$, correlation 70%). (b) Probability of resolution versus sample support (separation 3^o, SNR_1=SNR_2=5dB, correlation 70%).

(a)

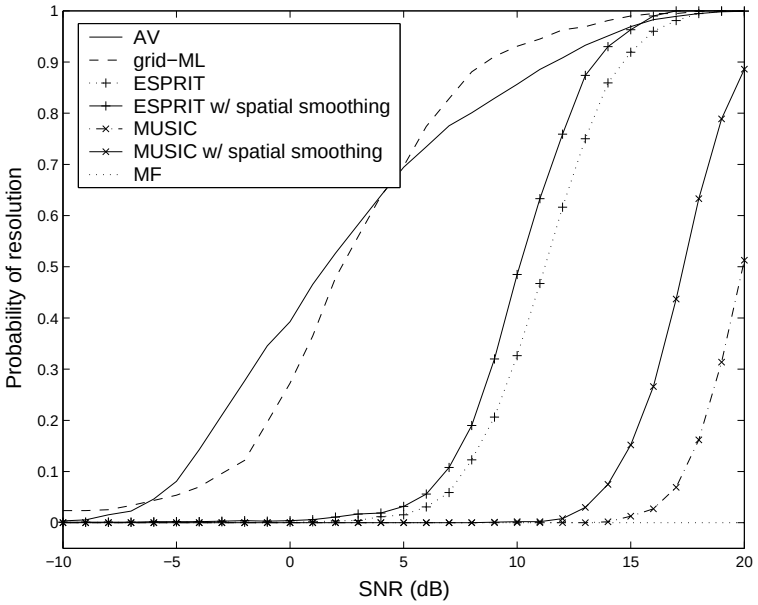

(b)

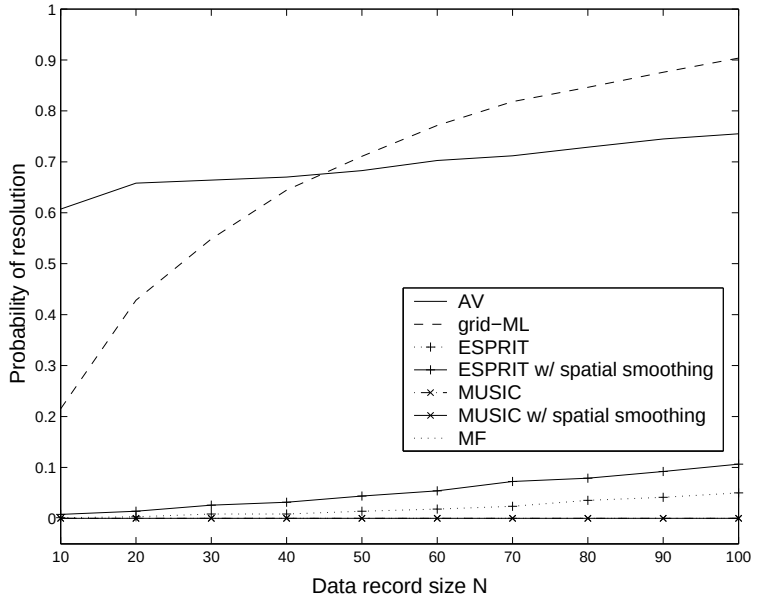

Fig. 30: (a) Probability of resolution versus SNR (separation 3^o, $N = 50$, correlation 90%). (b) Probability of resolution versus sample support (separation 3^o, SNR_1=SNR_2=5dB, correlation 90%).

X. An 8×8 Quasi-Orthogonal STBC Form for Transmissions over Eight or Four Antennas

This work has been presented at IEEE ICASSP 2007, Honolulu, Hawaii.

Orthogonal space-time block codes (O-STBC) [1] achieve full transmit diversity and allow single-symbol (two real symbols) maximum likelihood (ML) decoding. The drawback of O-STBCs is that full-rate codewords do not exist for more than two transmit antennas. For the case of four transmit antennas, the rate limitation of O-STBCs was overcome by quasi-orthogonal (QO) STBCs at the expense of diversity loss [2]-[4]. Full-rate full-diversity quasi-orthogonal codewords for 4-transmit-antennas were then presented in [5], [6] by retaining the code structure of [2], [3] and modifying the constellation of some of the symbols. ML decoding of the QO-STBCs in [5], [6] requires joint detection of two symbols (four real symbols). Interleaving real and imaginary parts of different symbols enables single-symbol decoding of full-rank, full-diversity QO-STBCs for the 4-transmit-antenna case [7], [8], at the expense of some performance loss in comparison with joint two-symbol dectection [5].

The codewords in [1]-[8] partition the symbols into orthogonal sets and ML detection requires only joint decoding of the symbols in each orthogonal set individually. Since the complexity of the ML decoder increases exponentially with the number of symbols in each orthogonal set, a trade-off between rate/diversity and decoding requirements is taking shape, especially for large number of transmit antennas. In [9], QO-STBCs for 8 transmit antennas that attain full diversity and full rate were presented that require, however, joint detection of four symbols (eight real symbols). Reduction in complexity was achieved for the 8-antenna case through the process of interleaving the real and imaginary parts of different symbols [10], [11]; the codewords can be partitioned into four orthogonal sets and hence require joint two-symbol decoding only.

In this paper we present a new two-symbol-decodable, full rate, full diversity order, 8×8 QO-STBC form that can be applied across either 4-transmit or 8-transmit-antenna systems. The proposed QO-STBC employs constellation rotation (CR) and symbol-interleaving similar to [10], [11], however, the 8×8 codeword can be divided into two 4×4 codewords without the omission of any symbols. We initially concentrate our efforts on the codeword for the 8-transmit-antenna system and evaluate conditions on the rotation angles necessary for the codeword to achieve full diversity order. Since several rotation angle pairs may exist that maximize the diversity order, we investigate different criteria for rotation angle selection to further improve error-rate performance. Common choice for rotation angle optimization of QO-STBCs is the maximization of the diversity product which in turn leads to minimization of the pairwise-error-probability (PEP)-upper-bound at (asymptotically) high signal-to-noise ratios (SNR) [12]. However, for space-time codes with large diversity order and/or large number of transmit antennas, diversity product maximization may not provide satisfactory PEP-bound minimization and error-rate performance over operable SNRs [13]. Contrary to the popular choice of diversity

product maximization, we pursue other means of optimizing the rotation angles to improve system performance. Within the class of two-symbol decodable, full rate 8×8 QO-STBCs we examine four different rotation angle optimization criteria: (i) We find a new expression for the rotation angles that maximize the diversity product of the suggested codeword. (ii) We show that sum-eigenvalue maximization as proposed in [13] is irrelevant/non-applicable to the 8-transmit-antenna QO-STBCs. (iii) We suggest, instead, and solve minimum-eigenvalue maximization. (iv) Finally, we use directly the PEP-upper-bound to obtain new true PEP-upper-bound optimal rotation angles.

The rest of the paper deals with codeword design and rotation angle optimization for the 4-transmit-antenna system. For the 4-transmit-antenna system we allow the channel coefficients of the first 4×4 codeword block to be correlated with the channel coefficients of the next 4×4 codeword block. We show that as long as the correlation is less than 100%, a diversity order of 8 is achieved using only 4 antennas. Using the PEP-upper-bound results for fast fading time-correlated channels in [14], we re-evaluate the PEP-upper-bound to incorporate the channel correlation. We then optimize the rotation angles using the four criteria discussed above for the 8-transmit-antenna case. We find that the rotation angles that maximize the diversity product for the uncorrelated 8-transmit-antenna system also maximize the diversity product for the correlated 4-transmit-antenna system. Arguably, this may be somewhat surprising because it did not seem possible in the past to make diversity product rotation angle optimization independent of the correlation coefficient [14]. For the other three criteria, we show that sum-eigenvalue maximization as proposed in [13] is again irrelevant/non-applicable to the 4-transmit-antenna case, while the remaining two criteria (minimum-eigenvalue minimization and PEP-upper-bound minimization) yield complicated rather intractable optimization equations as they become dependent on the correlation coefficient.

A. Code Structure and Transceiver Model

Let N_t be the number of transmit antennas, N_r the number of receive antennas, and T the number of time slots over which the code is transmitted. We denote the number of transmitted symbols by K. The eight symbols a_k, $k = 1, \ldots, K(=8)$, to be transmitted are formed by mapping the incoming bits onto known constellations, e.g. quadrature-amplitude-modulated (QAM), while their corresponding constellation rotated version $\bar{a}_k$, $k = 1, \ldots, K(=8)$, is created by

$$\begin{array}{ll} \bar{a}_m & = (a_{mR} + i a_{mI}) e^{i\phi}, \;\; m = 1, 2, 5, 6, \\ \bar{a}_n & = (a_{nR} + i a_{nI}) e^{i\theta}, \;\; n = 3, 4, 7, 8, \end{array} \tag{193}$$

where a_{kR} and a_{kI} denote the real and imaginary part of the symbol a_k, respectively, and ϕ, θ, are the rotation angles to be optimized. The symbols $\bar{a}_k$ are

interleaved to form x_k, $k = 1, \ldots, K(= 8)$,

$$\begin{array}{ll} x_1 = \bar{a}_{1R} + i\bar{a}_{5I}, & x_2 = \bar{a}_{2R} + i\bar{a}_{6I}, \\ x_3 = \bar{a}_{3R} + i\bar{a}_{7I}, & x_4 = \bar{a}_{4R} + i\bar{a}_{8I}, \\ x_5 = \bar{a}_{5R} + i\bar{a}_{1I}, & x_6 = \bar{a}_{6R} + i\bar{a}_{2I}, \\ x_7 = \bar{a}_{7R} + i\bar{a}_{3I}, & x_8 = \bar{a}_{8R} + i\bar{a}_{4I}. \end{array} \tag{194}$$

We now form/define $\mathbf{X}_1$ and $\mathbf{X}_2$ as shown below

$$\mathbf{X_1} = \begin{bmatrix} x_1 & x_2 & x_3 & x_4 \\ -x_2^* & x_1^* & -x_4^* & x_3^* \\ x_3 & x_4 & x_1 & x_2 \\ -x_4^* & x_3^* & -x_2^* & x_1^* \end{bmatrix}, \mathbf{X_2} = \begin{bmatrix} x_5 & x_6 & x_7 & x_8 \\ -x_6^* & x_5^* & -x_8^* & x_7^* \\ x_7 & x_8 & x_5 & x_6 \\ -x_8^* & x_7^* & -x_6^* & x_5^* \end{bmatrix}. \tag{195}$$

Consider now availability of either $N_t = 8$ or $N_t = 4$ transmit antennas. Below, we describe our transceiver model for each case.

Case 1: Eight transmit antennas

The transmitted codeword $\mathbf{X}$ is of the form

$$\mathbf{X} = \begin{bmatrix} \mathbf{X}_1 & \mathbf{0_{4\times 4}} \\ \mathbf{0_{4\times 4}} & \mathbf{X}_2 \end{bmatrix} \tag{196}$$

and the $N_t(= 8) \times N_r$ received signal matrix $\mathbf{Y}$ is given by

$$\mathbf{Y} = \rho\sqrt{\frac{A}{N_t}}\mathbf{X}\mathbf{H} + \mathbf{N} \tag{197}$$

where A is the received signal energy at each receive antenna, $\mathbf{H}$ is the $8 \times N_r$ channel matrix and $\mathbf{N}$ is the $8 \times N_r$ noise matrix. The elements of $\mathbf{H}$ and $\mathbf{N}$ are modeled as independent and identically distributed complex Gaussian random variables of zero mean and unit variance without loss of generality; $\rho = \sqrt{2}$ satisfies the energy constraint $E\{\|\mathbf{X}\|_F^2\} = TN_t$ ($E\{\cdot\}$ is the expectation operator and $\|\cdot\|_F^2$ denotes Frobenius norm of a matrix). From an implementation point of view, reduction of the large peak-to-average-power ratio (PAPR) created by the zeros during transmission of (196) is achieved by multiplying $\mathbf{X}$ by an 8×8 normalized Hadamard matrix before transmission. This effect is reversed at the receiver by multiplying the received signal matrix by the transpose of the Hadamard matrix. The net transceiver model still takes up the form in (196) and (197) by virtue of the orthogonality of the Hadamard matrix.

Case 2: Four transmit antennas

Assume now that we have available only $N_t = 4$ antennas. We transmit $\mathbf{X}_1$ in the first four time slots and $\mathbf{X}_2$ in the next four time slots. The $4 \times N_r$ received signal matrices $\mathbf{Y}_1$ and $\mathbf{Y}_2$ are given by

$$\mathbf{Y}_1 = \rho\sqrt{\frac{A}{N_t}}\mathbf{X}_1\mathbf{H}_1 + \mathbf{N}_1, \;\; \mathbf{Y}_2 = \rho\sqrt{\frac{A}{N_t}}\mathbf{X}_2\mathbf{H}_2 + \mathbf{N}_2. \tag{198}$$

Similar to the 8-transmit-antenna case, the elements of the $4 \times N_r$ matrices, $\mathbf{H}_1$, $\mathbf{H}_2$, $\mathbf{N}_1$ and $\mathbf{N}_2$ are modeled as identically distributed complex Gaussian random variables (with zero mean and unit variance). $\rho = 1$ satisfies the energy constraint $E\{\|\mathbf{X}_1\|_F^2\} = E\{\|\mathbf{X}_2\|_F^2\} = TN_t$. Individually within a matrix, the entries are taken to be independent from each other; $\mathbf{N}_1$ as a whole is independent of $\mathbf{N}_2$, $\mathbf{H}_1$ and $\mathbf{H}_2$ are independent from $\mathbf{N}_1$ and $\mathbf{N}_2$, but $\mathbf{H}_1$ and $\mathbf{H}_2$ are characterized as potentially correlated with each other via a correlation coefficient p. To express the correlation between the elements of the two channel matrices we define the extended channel matrix $\mathbf{H}_e \triangleq \left[\mathbf{H}_1^T \ \mathbf{H}_2^T\right]^T$ and obtain

$$E\{\mathbf{h}_{ej}\mathbf{h}_{el}^H\} = \begin{cases} \begin{bmatrix} \mathbf{I}_4 & p\mathbf{I}_4 \\ p\mathbf{I}_4 & \mathbf{I}_4 \end{bmatrix}, & j = l, \\ \mathbf{0}_8, & otherwise, \end{cases} \qquad j,\, l = 1, \ldots, N_r, \tag{199}$$

where $\mathbf{h}_{ej}$, $j = 1, \ldots, N_r$, are the columns of $\mathbf{H}_e$ and p is the correlation coefficient. In similar fashion to $\mathbf{H}_e$, the extended noise matrix may be defined as $\mathbf{N}_e \triangleq \left[\mathbf{N}_1^T \ \mathbf{N}_2^T\right]^T$ with

$$E\{\mathbf{n}_{ej}\mathbf{n}_{el}^H\} = \begin{cases} \begin{bmatrix} \mathbf{I}_4 & \mathbf{0}_4 \\ \mathbf{0}_4 & \mathbf{I}_4 \end{bmatrix}, & j = l, \\ \mathbf{0}_8, & otherwise, \end{cases} \qquad j,\, l = 1, \ldots, N_r, \tag{200}$$

where $\mathbf{n}_{ej}$, $j = 1, \ldots, N_r$, are the columns of $\mathbf{N}_e$. Combining $\mathbf{Y}_1$ and $\mathbf{Y}_2$ in (198) into a single equation we have

$$\mathbf{Y}_e = \rho\sqrt{\frac{A}{Nt}}\mathbf{X}\mathbf{H}_e + \mathbf{N}_e \tag{201}$$

where $\mathbf{Y}_e = [\mathbf{Y}_1^T \ \mathbf{Y}_2^T]^T$ and $\mathbf{X}$ is defined in (196). It is important to note that (198) represents a system with time-correlated channel coefficients while (201) represents a system in which the channel coefficients are correlated across space (channel coefficients of the four actual antennas correlated with the channel coefficients of the four *virtual* antennas). This distinction is important when obtaining the PEP-upper-bound for the 4-transmit-antenna system later in the presentation.

We now proceed with the description of the ML detector for both cases. Let $\mathcal{A}$ represent the symbol constellation and $\mathcal{Z}$ denote the set of $|\mathcal{A}|^K$ symbol vector points ($|\cdot|$ denoting cardinality of a set) in the complex K-dimensional space. If $f(\cdot)$ represents the one-to-one mapping of the symbol vector $\mathbf{a} \in \mathcal{A}^K$ into $\mathbf{X}$, for the 8-antenna case the ML estimate of the symbol vector assuming perfect channel state information at the receiver is

$$\begin{aligned} \mathbf{a}_{ML} &= \underset{\hat{\mathbf{a}} \in \mathcal{A}^K,\, \hat{\mathbf{X}} = f(\hat{\mathbf{a}})}{argmin} \|\mathbf{Y} - \rho\sqrt{\tfrac{A}{N_t}}\hat{\mathbf{X}}\mathbf{H}\|_F^2 \\ &= \underset{\hat{\mathbf{a}} \in \mathcal{A}^K,\, \hat{\mathbf{X}} = f(\hat{\mathbf{a}})}{argmin} \sum_{j=1}^{N_r} \left\{ \tfrac{A\rho^2}{N_t}\mathbf{h}_j^H\hat{\mathbf{X}}^H\hat{\mathbf{X}}\mathbf{h}_j - 2\rho\sqrt{\tfrac{A}{N_t}}Re\left\{\mathbf{y}_j^H\hat{\mathbf{X}}\mathbf{h}_j\right\}\right\} \end{aligned} \tag{202}$$

(H is the conjugate transpose operator and $Re\{\cdot\}$ denotes real part) where $\mathbf{y}_j$, $\mathbf{h}_j$, $j = 1, \ldots, N_r$, are the columns of $\mathbf{Y}$ and $\mathbf{H}$ respectively. Expanding $\hat{\mathbf{X}}^H\hat{\mathbf{X}}$ we have

$$\hat{\mathbf{X}}^H\hat{\mathbf{X}} = \begin{bmatrix} a\mathbf{I}_2 & b\mathbf{I}_2 & & \\ b\mathbf{I}_2 & a\mathbf{I}_2 & \mathbf{0} & \\ & & c\mathbf{I}_2 & d\mathbf{I}_2 \\ \mathbf{0} & & d\mathbf{I}_2 & c\mathbf{I}_2 \end{bmatrix} \tag{203}$$

where

$$\begin{array}{rcl} a & \triangleq & \sum_{k=1}^{K} |\hat{x}_k|^2, \\ b & \triangleq & \sum_{k=1}^{K/2} 2Re\{\hat{x}_k^*\hat{x}_{k+K/2}\}, \\ c & \triangleq & \sum_{k=K+1}^{2K} |\hat{x}_k|^2, \\ d & \triangleq & \sum_{k=K+1}^{K+K/2} 2Re\{\hat{x}_k^*\hat{x}_{k+K/2}\}, \quad K = 4. \end{array} \tag{204}$$

Substituting (193) and (194) in (204) we obtain

$$\begin{array}{rcl} a & = & \hat{\hat{a}}_{1R}^2 + \hat{\hat{a}}_{2R}^2 + \hat{\hat{a}}_{3R}^2 + \hat{\hat{a}}_{4R}^2 + \hat{\hat{a}}_{5I}^2 + \hat{\hat{a}}_{6I}^2 + \hat{\hat{a}}_{7I}^2 + \hat{\hat{a}}_{8I}^2, \\ b & = & 2\hat{\hat{a}}_{1R}\hat{\hat{a}}_{3R} + 2\hat{\hat{a}}_{2R}\hat{\hat{a}}_{4R} + 2\hat{\hat{a}}_{5I}\hat{\hat{a}}_{7I} + 2\hat{\hat{a}}_{6I}\hat{\hat{a}}_{8I}, \\ c & = & \hat{\hat{a}}_{5R}^2 + \hat{\hat{a}}_{6R}^2 + \hat{\hat{a}}_{7R}^2 + \hat{\hat{a}}_{8R}^2 + \hat{\hat{a}}_{1I}^2 + \hat{\hat{a}}_{2I}^2 + \hat{\hat{a}}_{3I}^2 + \hat{\hat{a}}_{4I}^2, \\ d & = & 2\hat{\hat{a}}_{5R}\hat{\hat{a}}_{7R} + 2\hat{\hat{a}}_{6R}\hat{\hat{a}}_{8R} + 2\hat{\hat{a}}_{1I}\hat{\hat{a}}_{3I} + 2\hat{\hat{a}}_{2I}\hat{\hat{a}}_{4I}. \end{array} \tag{205}$$

From (205) we observe that inter-symbol-interference occurs among the following symbol pairs $(\hat{\hat{a}}_1,\ \hat{\hat{a}}_3)$, $(\hat{\hat{a}}_2,\ \hat{\hat{a}}_4)$, $(\hat{\hat{a}}_5,\ \hat{\hat{a}}_7)$, and $(\hat{\hat{a}}_6,\ \hat{\hat{a}}_8)$. In (202), since multiplying $\hat{\mathbf{X}}^H\hat{\mathbf{X}}$ by $\mathbf{h}_j^H$ and $\mathbf{h}_j$ does not create any additional cross-terms between the symbols $\hat{\hat{a}}_k$, ML-decoding of the symbol vector $\mathbf{a}$ can be reduced to jointly decoding the symbol pairs $\left\{(\hat{\hat{a}}_1, \hat{\hat{a}}_3), (\hat{\hat{a}}_2, \hat{\hat{a}}_4), (\hat{\hat{a}}_5, \hat{\hat{a}}_7), (\hat{\hat{a}}_6, \hat{\hat{a}}_8)\right\}$ independently. Since $\hat{\hat{a}}_k$ is obtained by rotating the constellation of $\hat{a}_k$, $k = 1, \ldots, 8$, decoding the symbols pairs $\{(\hat{a}_1, \hat{a}_3), (\hat{a}_2, \hat{a}_4), (\hat{a}_5, \hat{a}_7), (\hat{a}_6, \hat{a}_8)\}$ independently is ML-optimum. For the 4-transmit-antenna case we replace $\mathbf{H}$ by $\mathbf{H}_e$ and $\mathbf{Y}$ by $\mathbf{Y}_e$ in (202) to obtain a similar result.

As a concluding remark, we can show that our suggested code structure in (196) for the 8-transmit-antenna case is equivalent to the one in [10]. However, we do favor the code in (196) for two reasons: (i) Its simplicity in code construction enables our theoretical analysis on rotation angle optimization and, (ii) unlike the codewords in [10], [11], the codeword in (196) may be applied to a 4-transmit-antenna system across eight time-slots without omitting any symbols. Having shown already that the code supports ML-optimal two-symbol decoding, we now evaluate its diversity order and seek the rotation angles that improve error-rate performance.

B. Diversity Order Calculation: Eight Transmit Antennas

The probability of receiving the codeword $\widetilde{\mathbf{X}}$ when $\mathbf{X} \neq \widetilde{\mathbf{X}}$ is transmitted is upper bounded by [12]

$$Pr(\mathbf{X} \to \widetilde{\mathbf{X}}) \leq \frac{1}{2}\left(\prod_{i=1}^{R}\left\{\frac{1}{1 + \frac{\rho^2 A\lambda_i}{4N_t}}\right\}\right)^{N_r} \tag{206}$$

where R is the rank of $(\mathbf{X}-\widetilde{\mathbf{X}})$ and $\lambda_i,\ i=1,\ldots,R$, are the eigenvalues of $(\mathbf{X}-\widetilde{\mathbf{X}})^H(\mathbf{X}-\widetilde{\mathbf{X}})$. The minimum value of R obtained over all codeword pairs is called the diversity order of the system [12] and dictates the slope of the error-rate curves at asymptotically high SNR values. To obtain the diversity order of the codeword in (196) we require the eigenvalues λ_i of $(\mathbf{X}-\widetilde{\mathbf{X}})^H(\mathbf{X}-\widetilde{\mathbf{X}})$. Set $\Delta\mathbf{X} \stackrel{\triangle}{=} \mathbf{X}-\widetilde{\mathbf{X}}$ and $\Delta\mathbf{x}_k \stackrel{\triangle}{=} \mathbf{x}_k-\widetilde{\mathbf{x}}_k,\ k=1,\ldots,8$; then,

$$\Delta\mathbf{X}^H\Delta\mathbf{X} = \begin{bmatrix} \Delta a\mathbf{I}_2 & \Delta b\mathbf{I}_2 & & \\ \Delta b\mathbf{I}_2 & \Delta a\mathbf{I}_2 & \mathbf{0} & \\ & & \Delta c\mathbf{I}_2 & \Delta d\mathbf{I}_2 \\ \mathbf{0} & & \Delta d\mathbf{I}_2 & \Delta c\mathbf{I}_2 \end{bmatrix} \tag{207}$$

where

$$\begin{array}{rcl} \Delta a & \stackrel{\triangle}{=} & \sum_{k=1}^{K}|\Delta x_k|^2, \\ \Delta b & \stackrel{\triangle}{=} & \sum_{k=1}^{K/2} 2Re\{\Delta x_k^*\Delta x_{k+K/2}\}, \\ \Delta c & \stackrel{\triangle}{=} & \sum_{k=K+1}^{2K}|\Delta x_k|^2, \\ \Delta d & \stackrel{\triangle}{=} & \sum_{k=K+1}^{K+K/2} 2Re\{\Delta x_k^*\Delta x_{k+K/2}\},\ \ K=4. \end{array} \tag{208}$$

The block diagonal nature of $\Delta\mathbf{X}^H\Delta\mathbf{X}$ in (207) allows us to calculate its eigenvalues as $\{(\Delta a-\Delta b),\ (\Delta a+\Delta b),\ (\Delta c-\Delta d),\ (\Delta c+\Delta d)\}$ which exist with multiplicity of two. Expanding and simplifying, the eigenvalues are as shown below:

$$\begin{array}{l} \{\ (\Delta\bar{a}_{1R}-\Delta\bar{a}_{3R})^2+(\Delta\bar{a}_{2R}-\Delta\bar{a}_{4R})^2+(\Delta\bar{a}_{5I}-\Delta\bar{a}_{7I})^2+(\Delta\bar{a}_{6I}-\Delta\bar{a}_{8I})^2, \\ (\Delta\bar{a}_{1R}+\Delta\bar{a}_{3R})^2+(\Delta\bar{a}_{2R}+\Delta\bar{a}_{4R})^2+(\Delta\bar{a}_{5I}+\Delta\bar{a}_{7I})^2+(\Delta\bar{a}_{6I}+\Delta\bar{a}_{8I})^2, \\ (\Delta\bar{a}_{5R}-\Delta\bar{a}_{7R})^2+(\Delta\bar{a}_{6R}-\Delta\bar{a}_{8R})^2+(\Delta\bar{a}_{1I}-\Delta\bar{a}_{3I})^2+(\Delta\bar{a}_{2I}-\Delta\bar{a}_{4I})^2, \\ (\Delta\bar{a}_{5R}+\Delta\bar{a}_{7R})^2+(\Delta\bar{a}_{6R}+\Delta\bar{a}_{8R})^2+(\Delta\bar{a}_{1I}+\Delta\bar{a}_{3I})^2+(\Delta\bar{a}_{2I}+\Delta\bar{a}_{4I})^2\ \}. \end{array} \tag{209}$$

As each eigenvalue is a summation of squares, the set of minimum eigenvalues over all possible codewords pairs is

$$\left\{(\Delta\bar{a}_{1R}-\Delta\bar{a}_{3R})^2,(\Delta\bar{a}_{1R}+\Delta\bar{a}_{3R})^2,(\Delta\bar{a}_{1I}-\Delta\bar{a}_{3I})^2,(\Delta\bar{a}_{1I}+\Delta\bar{a}_{3I})^2\right\} \tag{210}$$

and represents the worst case scenario for the upper bound in (206). As long as all eigenvalues in (210) are non-zero, the codeword $\mathbf{X}$ achieves the maximum diversity order of 8. We now attempt to identify conditions on the rotation angles that have to be satisfied to allow the codeword $\mathbf{X}$ to achieve full diversity order.

It is easily observed that all the eigenvalues in (210) are non-zero if and only if the product of the eigenvalues in (210) is non-zero, which in turn is the square root of the minimum value of the determinant of the $\Delta\mathbf{X}^H\Delta\mathbf{X}$. We have,

$$\begin{array}{l} \min\ det(\Delta\mathbf{X}^H\Delta\mathbf{X}) \\ \quad = \left[(\Delta\bar{a}_{1R}-\Delta\bar{a}_{3R})^2(\Delta\bar{a}_{1R}+\Delta\bar{a}_{3R})^2(\Delta\bar{a}_{1I}-\Delta\bar{a}_{3I})^2(\Delta\bar{a}_{1I}+\Delta\bar{a}_{3I})^2\right]^2 \\ \quad = \left[(\Delta\bar{a}_{1R}^2-\Delta\bar{a}_{3R}^2)(\Delta\bar{a}_{1I}^2-\Delta\bar{a}_{3I}^2)\right]^4 \\ \quad = \left[\begin{array}{l} \left[(\Delta a_{1R}cos(\phi)-\Delta a_{1I}sin(\phi))^2-(\Delta a_{3R}cos(\theta)-\Delta a_{3I}sin(\theta))^2\right] \\ \times\left[(\Delta a_{1R}sin(\phi)+\Delta a_{1I}cos(\phi))^2-(\Delta a_{3R}sin(\theta)+\Delta a_{3I}cos(\theta))^2\right] \end{array}\right]^4. \end{array} \tag{211}$$

For fixed ϕ, θ, we categorize (211) into five cases depending on the values of Δa_{1R}, Δa_{3R}, Δa_{1I}, Δa_{3I}. Note that we cannot have $\Delta a_{1R} = \Delta a_{3R} = \Delta a_{1I} = \Delta a_{3I} = 0$.

Case 1: Only one non-zero value

$$\min det(\Delta \mathbf{X}^H \Delta \mathbf{X}) = [(\Delta a_{1R} cos(\phi))^2 (\Delta a_{1R} sin(\phi))^2]^4. \tag{212}$$

If any of $cos(\phi)$, $sin(\phi)$, $cos(\theta)$, $sin(\theta)$ is zero, full diversity order is not achieved.

Case 2: Two non-zero values both from same symbol

$$\begin{aligned}\min det(\Delta \mathbf{X}^H \Delta \mathbf{X}) = [\big((\Delta a_{1R} cos(\phi) - \Delta a_{1I} sin(\phi))^2\big) \\ \big((\Delta a_{1R} sin(\phi) + \Delta a_{1I} cos(\phi))^2\big)]^4.\end{aligned} \tag{213}$$

Let $\mathcal{A}$ denote the constellation of the symbols a_k, $k = 1, \ldots, K,$, $\mathcal{A}_\phi$ and $\mathcal{A}_\theta$ denote the constellations of symbols formed by rotating $\mathcal{A}$ by ϕ and θ, respectively. If any two symbols chosen from $\mathcal{A}_\phi$ or $\mathcal{A}_\theta$ have the same real part or the same imaginary part, full diversity order cannot be achieved.

Case 3: Two non-zero values both either real or imaginary

$$\begin{aligned}\min det(\Delta \mathbf{X}^H \Delta \mathbf{X}) = \big(\big[(\Delta a_{1R} cos(\phi))^2 - (\Delta a_{3R} cos(\theta))^2\big] \\ \big[(\Delta a_{1R} sin(\phi))^2 - (\Delta a_{3R} sin(\theta))^2\big]\big)^4.\end{aligned} \tag{214}$$

If $\theta = \phi$, full diversity order cannot be achieved.

Case 4: Two non-zero values, one from real part of one symbol and other from imaginary part of other symbol

$$\begin{aligned}\min det(\Delta \mathbf{X}^H \Delta \mathbf{X}) = \big(\big[(\Delta a_{1R} cos(\phi))^2 - (\Delta a_{3I} sin(\theta))^2\big] \\ \big[(\Delta a_{1R} sin(\phi))^2 - (\Delta a_{3I} cos(\theta))^2\big]\big)^4.\end{aligned} \tag{215}$$

If $\theta = \phi \pm \pi/2$, full diversity order cannot be achieved.

Case 5: All values are non-zero

If the square distance between the real parts of any two symbols from $\mathcal{A}_\phi$ is equal to the square distance between the real parts of any two symbols from $\mathcal{A}_\theta$ or the square distance between the imaginary parts of any two symbols from $\mathcal{A}_\phi$ is equal to the square distance between the imaginary parts of any two symbols from $\mathcal{A}_\theta$, full diversity order is not achieved.

For a given constellation, several pairs of ϕ, θ may exist that satisfy the exclusion conditions listed above. In the next section, we investigate four different criteria for rotation angle optimization.

C. Rotation Angle Optimization: Eight Transmit Antennas

We now consider four different criteria to optimize the rotation angles and for each criterion, we show how ϕ, θ can be obtained for the codeword in (196) using (210). For ease in reference, our findings (values of ϕ, θ for each criterion) are summarized in Table IV.

Case 1: Diversity product maximization

At high SNR values assuming full transmit diversity order and $N_r = 1$, (206) can be *approximated* by

$$Pr(\mathbf{X} \to \widetilde{\mathbf{X}}) \leq \frac{1}{2} \left(\prod_{i=1}^{N_t} \lambda_i \right)^{-1} \left(-\frac{A}{4N_t} \right)^{-N_t}. \tag{216}$$

Worst-case minimization of the bound in (216) is equivalent to maximization of the minimum product of the eigenvalues (determinant of $\Delta\mathbf{X}^H\Delta\mathbf{X}$) over all possible codeword pairs, which in turn is commonly represented by the diversity product ζ,

$$\zeta = \frac{1}{2\sqrt{N_t}} min_{\mathbf{X} \neq \tilde{\mathbf{X}}} \left| det\left[\Delta\mathbf{X}\Delta\mathbf{X}^H\right] \right|^{1/(2T)}. \tag{217}$$

Diversity product maximization was used as the rotation angle design criterion in [10], [11]. For the codeword in (196), the minimum determinant of $\Delta\mathbf{X}^H\Delta\mathbf{X}$ over all codeword pairs is

$$\begin{aligned} &\min det(\Delta\mathbf{X}^H\Delta\mathbf{X}) = \\ &\quad \left[(\Delta a_{1R} cos(\phi) - \Delta a_{1I} sin(\phi))^2 - (\Delta a_{3R} cos(\theta) - \Delta a_{3I} sin(\theta))^2\right]^4 \\ &\quad \times \left[(\Delta a_{1R} sin(\phi) + \Delta a_{1I} cos(\phi))^2 - (\Delta a_{3R} sin(\theta) + \Delta a_{3I} cos(\theta))^2\right]^4 \end{aligned} \tag{218}$$

and ϕ, θ should be chosen to maximize (218). We evaluate and conclude (see Table IV) that the codeword in (196) (and the proposed codewords in [10], [11]) achieve diversity product of 0.1747 with 4-QAM constellation and 0.1071 with the non-rectangular 8-QAM constellation for the 8-transmit-antenna case.

Case 2: Minimum sum-of-eigenvalues maximization

In [13], it was proposed that for high diversity order systems (number of transmit antennas greater than four) the minimum trace of $\Delta\mathbf{X}^H\Delta\mathbf{X}$ is to be maximized over all codeword pairs. From our expression (209), we observe that

$$\begin{aligned} \min\left(Tr(\Delta\mathbf{X}^H\Delta\mathbf{X})\right) &= 2\left[(\Delta\bar{a}_{1R} - \Delta\bar{a}_{3R})^2 + (\Delta\bar{a}_{1R} + \Delta\bar{a}_{3R})^2\right. \\ &\quad \left. +(\Delta\bar{a}_{1I} - \Delta\bar{a}_{3I})^2 + (\Delta\bar{a}_{1I} + \Delta\bar{a}_{3I})^2\right] \\ &= 4[\Delta\bar{a}_{1R}^2 + \Delta\bar{a}_{3R}^2 + \Delta\bar{a}_{1I}^2 + \Delta\bar{a}_{3I}^2] \\ &= 4[\Delta a_{1R}^2 + \Delta a_{3R}^2 + \Delta a_{1I}^2 + \Delta a_{3I}^2] \end{aligned} \tag{219}$$

which is independent of ϕ, θ.

Hence, for the proposed codeword and that of [10], [11], the sum-of-eigenvalues criterion in [13] is not relevant.

Case 3: Minimum eigenvalue maximization

If $r < N_t$ eigenvalues of $\Delta\mathbf{X}^H\Delta\mathbf{X}$ are significantly less than 1, then even for large SNR values, $1 + \frac{A\lambda_i}{4N_t} \simeq 1$ and (206) is *approximated* by

$$Pr(\mathbf{X} \to \widetilde{\mathbf{X}}) \leq \frac{1}{2}\left(\prod_{i=1}^{N_t-r}\lambda_i\right)^{-1}\left(-\frac{A}{4N_t}\right)^{-(N_t-r)}. \tag{220}$$

The system seems to lose diversity; for the codeword in (196) and the proposed codewords in [10], [11] the occurrence of the eigenvalues in pairs causes loss of diversity in steps of two. In such circumstances, it appears reasonable to consider rotation angle choices that maximize the minimum possible eigenvalue over all pairs of codewords. For our code structure in (196), the rotation angles that maximize the minimum eigenvalue are

$$\begin{aligned}(\phi,\theta) = \underset{\phi,\theta}{argmax}\ \min\big\{&(\Delta\bar{a}_{1R} - \Delta\bar{a}_{3R})^2, (\Delta\bar{a}_{1R} + \Delta\bar{a}_{3R})^2,\\ &(\Delta\bar{a}_{1I} - \Delta\bar{a}_{3I})^2, (\Delta\bar{a}_{1I} + \Delta\bar{a}_{3I})^2\big\}.\end{aligned} \tag{221}$$

The solution is listed in Table IV.

Case 4: PEP-bound Minimization

We now show that for all STBCs that employ CR and have no more than two unique eigenvalues of $\Delta\mathbf{X}^H\Delta\mathbf{X}$ over all possible codeword pairs, maximization of the diversity product is equivalent to minimization of the upper bound on PEP for all SNRs. Minimization of the bound in (206) is equivalent to maximizing $\prod_{i=1}^{R}\left\{1 + \frac{A\lambda_i}{4N_t}\right\}$. If λ_1 and λ_2 represent the 2 unique eigenvalues of $\Delta\mathbf{X}^H\Delta\mathbf{X}$, then

$$\begin{aligned} argmax\ \prod_{i=1}^{R}\left(1 + \tfrac{A\lambda_i}{4N_t}\right) &= argmax\ \left[\left(1 + \tfrac{A\lambda_1}{4N_t}\right)\left(1 + \tfrac{A\lambda_2}{4N_t}\right)\right]^q \\ &= argmax\ \left[1 + \tfrac{A}{4N_t}(\lambda_1+\lambda_2) + \tfrac{A^2}{16N_t^2}(\lambda_1\lambda_2)\right]^q \end{aligned} \tag{222}$$

where q denotes the multiplicity of the eigenvalues. Since

$$q(\lambda_1 + \lambda_2) = tr(\Delta\mathbf{X}^H\Delta\mathbf{X}) = \|\Delta\mathbf{X}\|_F^2$$

is independent of rotation angles[18] we need to maximize only the product of the eigenvalues to minimize the bound in (206). In the case of a single unique eigenvalue (as in O-STBCs for example), the STBC is independent of the rotation angle.

[18] Constellation rotation or interleaving does not change the transmitted energy of the STBC codeword.

While the case of two unique eigenvalues applies to the 4×4 QO-STBCs proposed in [5], [7], [8] and their choice of rotation angle is PEP-bound optimal, for the 8×8 codewords four unique eigenvalues exist and maximizing the eigenvalue (diversity) product over all possible codeword pairs does not necessarily minimize the maximum bound in (206).

We now directly find the rotation angles that minimize the maximum (worst case) PEP-upper-bound. Substitution of (210) in (206) gives us the worst case scenario for all codeword pairs. We need to optimize ϕ, θ such that

$$\begin{gathered}(\phi,\theta) = \underset{\phi,\theta}{argmax}\ \prod_{i=1}^{4}\left[\left(1+\frac{A\lambda_i}{4N_t}\right)\right]^2, \\ \lambda_i = \left\{(\Delta\bar{a}_{1R}-\Delta\bar{a}_{3R})^2,(\Delta\bar{a}_{1R}+\Delta\bar{a}_{3R})^2,(\Delta\bar{a}_{1I}-\Delta\bar{a}_{3I})^2,(\Delta\bar{a}_{1I}+\Delta\bar{a}_{3I})^2\right\}, \\ i=1,2,3,4.\end{gathered} \tag{223}$$

Suitable values for A can be chosen such that $A\lambda_i > 1$ for all $i = 1, 2, 3, 4$. The solution is listed in Table IV.

In the next section, we aim to extend the results that we have obtained for the 8-transmit-antenna case to the correlated 4-transmit-antenna system.

D. Diversity Order Calculation and Rotation Angle Optimization: Four Transmit Antennas

Due to the correlation that exists between elements of $\mathbf{H}_1$ and $\mathbf{H}_2$, the PEP-upper-bound in (206) requires reevaluation. The new PEP-upper-bound can be obtained either by considering the time-correlated channel model in (198) or the space-correlated channel model in (201). We begin with the time-correlated model in (198).

Defining $\mathbf{X}_t \triangleq [\mathbf{X}_1^T\ \mathbf{X}_2^T]^T$ and $\Delta\mathbf{X}_t \triangleq \mathbf{X}_t - \widetilde{\mathbf{X}}_t$ where $\mathbf{X}_t \neq \widetilde{\mathbf{X}}_t$, the PEP for a time-correlated fast fading channel (channel coefficients changing every time slot) is upper-bounded by [14]

$$Pr(\mathbf{X}_t \rightarrow \widetilde{\mathbf{X}}_t) \leq \begin{pmatrix} 2r_tN_r-1 \\ r_tN_r \end{pmatrix} \left(\prod_{i=1}^{r_t}\Lambda_{ti}\right)^{-N_r} \left(\frac{A}{N_t}\right)^{-r_tN_r} \tag{224}$$

where r_t is the rank of the matrix $(\Delta\mathbf{X}_t\Delta\mathbf{X}_t^H)\circ\mathbf{R}_t$ ($\circ$ is the Hadamard product operator), Λ_{ti}, $i = 1, \ldots, r_t$, are the non-zero eigenvalues of $(\Delta\mathbf{X}_t\Delta\mathbf{X}_t^H)\circ\mathbf{R}_t$, and $\mathbf{R}_t$ is the time-correlated channel matrix to be evaluated. Conforming with the signal model in [14], with $T = 4$ and $N_r = 1$ the received signal vector $\mathbf{y}_{e1} \triangleq [\mathbf{y}_1^T\ \mathbf{y}_2^T]^T$ ($\mathbf{y}_1$ and $\mathbf{y}_2$ are the first columns of $\mathbf{Y}_1$, $\mathbf{Y}_2$ in (198)) is

$$\mathbf{y}_{e1} = \sqrt{\frac{A}{Nt}}[\mathbf{D}_1,\ldots,\mathbf{D}_{N_t}]\mathbf{h}_t + \mathbf{n}_t \tag{225}$$

where $\mathbf{D}_i = diag\{\mathbf{x}_{ti}\}$ are the $2T \times 2T$ matrices created by the columns of $\mathbf{X}_t$, $\mathbf{x}_{ti}$, $i = 1, 2, \cdots, N_t$. The $2T \times 1$ noise vector $\mathbf{n}_t$ satisfies $E\{\mathbf{n}_t\mathbf{n}_t^H\} = \mathbf{I}_{2T}$.

The $2TN_t \times 1$ channel vector is $\mathbf{h}_t = [\mathbf{h}_{t1}^T, \ldots, \mathbf{h}_{tN_t}^T]^T$ where $\mathbf{h}_{ti}$ is the vector corresponding to the ith, $i = 1, \ldots, N_t$, transmit antenna. If $h_{e_{i,j}}$, $i = 1, \ldots, 2N_t$, $j = 1, \ldots, N_r$, represent the elements of $\mathbf{H}_e = [\mathbf{H}_1^T \mathbf{H}_2^T]^T$, then $\mathbf{h}_{ti} = \begin{bmatrix} h_{e_{i,1}} & h_{e_{i,1}} & h_{e_{i,1}} & h_{e_{i,1}} & h_{e_{i+N_t,1}} & h_{e_{i+N_t,1}} & h_{e_{i+N_t,1}} & h_{e_{i+N_t,1}} \end{bmatrix}^T$. The time-correlated channel matrix $\mathbf{R}_t$ can now be defined as

$$\mathbf{R}_t \triangleq E\{\mathbf{h}_{ti}\mathbf{h}_{ti}^H\} = \begin{bmatrix} \mathbf{1}_4 & p\mathbf{1}_4 \\ p\mathbf{1}_4 & \mathbf{1}_4 \end{bmatrix}, \; i = 1, \ldots, N_t, \tag{226}$$

where $\mathbf{1}_4$ is a 4×4 all-one matrix. Having evaluated $\mathbf{R}_t$, we calculate

$$\begin{aligned} (\Delta\mathbf{X}_t\Delta\mathbf{X}_t^H) \circ \mathbf{R}_t &= \begin{bmatrix} \Delta\mathbf{X}_1\Delta\mathbf{X}_1^H & p\Delta\mathbf{X}_1\Delta\mathbf{X}_2^H \\ p\Delta\mathbf{X}_2\Delta\mathbf{X}_1^H & \Delta\mathbf{X}_2\Delta\mathbf{X}_2^H \end{bmatrix} \\ &= \begin{bmatrix} \Delta\mathbf{X}_1 & \mathbf{0}_4 \\ \mathbf{0}_4 & \Delta\mathbf{X}_2 \end{bmatrix} \begin{bmatrix} \mathbf{I}_4 & p\mathbf{I}_4 \\ p\mathbf{I}_4 & \mathbf{I}_4 \end{bmatrix} \begin{bmatrix} \Delta\mathbf{X}_1^H & \mathbf{0}_4 \\ \mathbf{0}_4 & \Delta\mathbf{X}_2^H \end{bmatrix} \\ &= \Delta\mathbf{X}\mathbf{R}_s\Delta\mathbf{X}^H \end{aligned} \tag{227}$$

with $\mathbf{R}_s \triangleq E\{\mathbf{h}_{ej}\mathbf{h}_{el}^H\} = \begin{bmatrix} \mathbf{1}_4 & p\mathbf{1}_4 \\ p\mathbf{1}_4 & \mathbf{1}_4 \end{bmatrix}$ for $j = l$ from (199). Since $eig(\mathbf{R}_s\Delta\mathbf{X}^H\Delta\mathbf{X}) = eig(\Delta\mathbf{X}\mathbf{R}_s\Delta\mathbf{X}^H)$ [15], expanding $\mathbf{R}_s\Delta\mathbf{X}^H\Delta\mathbf{X}$ we have

$$\mathbf{R}_s\Delta\mathbf{X}^H\Delta\mathbf{X} = \begin{bmatrix} \Delta a\mathbf{I}_2 & \Delta b\mathbf{I}_2 & p\Delta c\mathbf{I}_2 & p\Delta d\mathbf{I}_2 \\ \Delta b\mathbf{I}_2 & \Delta a\mathbf{I}_2 & p\Delta d\mathbf{I}_2 & p\Delta c\mathbf{I}_2 \\ p\Delta a\mathbf{I}_2 & p\Delta b\mathbf{I}_2 & \Delta c\mathbf{I}_2 & \Delta d\mathbf{I}_2 \\ p\Delta b\mathbf{I}_2 & p\Delta a\mathbf{I}_2 & \Delta d\mathbf{I}_2 & \Delta c\mathbf{I}_2 \end{bmatrix}. \tag{228}$$

This concludes the analysis work for the PEP-upper-bound for the time-correlated model in (224).

When we consider the space-correlated model in (201) we obtain the PEP-upper-bound as

$$Pr(\mathbf{X} \to \widetilde{\mathbf{X}}) \leq \frac{1}{2} \left(\prod_{i=1}^{r_t} \left\{ \frac{1}{1 + \frac{A\Lambda_{ti}}{4N_t}} \right\} \right)^{N_r} \tag{229}$$

where r_t and Λ_{ti} have the same definition as before. For clarity and brevity in presentation, the derivation of (229) is shifted to the Appendix. Even though the obtained expressions in (224) and (229) differ, they both are primarily functions of Λ_{ti} which need to be evaluated for rotation angle optimization. Due to the loss of the block diagonal structure (cf. (228)), individual eigenvalues of $\mathbf{R}_s\Delta\mathbf{X}^H\Delta\mathbf{X}$ do not yield simplified expressions as was the case for the 8-transmit-antenna system. However, the product and sum of the eigenvalues can still be evaluated.

Case 1: Diversity product maximization

We have

$$\prod_{i=1}^{N_t} \Lambda_{ti} = det(\mathbf{R}_s\Delta\mathbf{X}^H\Delta\mathbf{X}) = det(\mathbf{R}_s)det(\Delta\mathbf{X}^H\Delta\mathbf{X}) \tag{230}$$

and the diversity product for the 4-transmit-antenna case is given by

$$\begin{aligned}\zeta &= \frac{1}{2\sqrt{N_t}} min_{\mathbf{X}\neq\widetilde{\mathbf{X}}} \left| det\left[\Delta\mathbf{X}\Delta\mathbf{X}^H\right] det[\mathbf{R}_s]\right|^{1/(2T)} \\ &= \frac{(1-p^2)^{2/T}}{2\sqrt{N_t}} min_{\mathbf{X}\neq\widetilde{\mathbf{X}}} \left| det\left[\Delta\mathbf{X}\Delta\mathbf{X}^H\right]\right|^{1/(2T)}. \end{aligned} \quad (231)$$

We conclude that the rotation angles ϕ, θ that maximize the diversity product for the uncorrrelated 8-transmit-antenna case also maximize the diversity product for the correlated 4-transmit-antenna case (for any correlation coefficient value) and provide maximum diversity order of 8[19]. This might seem, arguably, surprising in the context of the findings in [14] where for fast fading time-correlated channels optimal diversity-product rotation angles are a function of the correlation coefficient p. We can also observe that when $p = 1$, the diversity product in (231) becomes zero and the maximum achievable rank of $\mathbf{R}_s\Delta\mathbf{X}^H\Delta\mathbf{X}$ is 4 ($\Delta a = \Delta c$ and $\Delta b = \Delta d$) which seems intuitively satisfying as $\mathbf{X}_2$ experiences the same fading as $\mathbf{X}_1$. Hence, fluctuation in the channel conditions are actually beneficial to the proposed transmission scheme.

Case 2: Minimum sum-of-eigenvalues maximization

Substituting from (205),

$$\sum_{i=1}^{N_t} \Lambda_{ti} = Tr(\mathbf{R}_s\Delta\mathbf{X}^H\Delta\mathbf{X}) = 2(\Delta a{+}\Delta c) = 2\sum_{i=i}^{8} \Delta\bar{a}_{iR}^2{+}\Delta\bar{a}_{iI}^2 = 2\sum_{i=i}^{8} \Delta a_{iR}^2{+}\Delta a_{iI}^2 \quad (232)$$

which is independent of the rotation angles ϕ, θ. Hence, once again, maximization of the minimum sum of eigenvalues (criterion suggested in [13]) is irrelevant to this system. Obtaining ϕ, θ for the other two criteria (minimum eigenvalue maximization and direct PEP-bound minimization) proposed in Section IV requires knowledge of each individual eigenvalue of $\mathbf{R}_s\Delta\mathbf{X}^H\Delta\mathbf{X}$. Even though the eigenvalues can be evaluated, they yield complicated expressions that are functions of p.

As a concluding remark, most important aspect of the proposed transmission scheme for the 4-transmit-antenna case is that it allows for transmit diversity order of 8 with no additional physical hardware at the transmitter (4 antennas only) and requires only joint two-symbol decoding at the receiver. In the bellowing section, we evaluate the error-rate performance of the codeword $\mathbf{X}$ along with the various criteria for rotation angle optimization proposed in Section IV.

E. Simulation Studies

We divide the presentation of our simulations studies into the 4 and 8-transmit-antenna case. In all studies we set $N_r = 1$.

[19] However, due to the correlation between the corresponding elements of $\mathbf{H}_1$ and $\mathbf{H_2}$, the codeword $\mathbf{X}$ experiences a loss in diversity product by a factor of $(1-p^2)^{2/T}$.

Case 1: Four Transmit Antennas

To evaluate the performance of the 8×8 QO-STBC transmitted by 4 antennas only, we compare its error-rate performance against the 4×4 QO-STBC codeword in [5]. Note that to our best knowledge, for a system with 4 transmit antennas the code in [5] has the best error-rate performance of all QO-STBCs that jointly decode two symbols or less. Since our proposed codeword has diversity order of 8 and rate 1 over 8 time slots, we may compare against two different 4×4 QO-STBC transmission schemes. In one scenario, we transmit the 4×4 QO-STBC codeword over the first four time slots and then repeat the same codeword over the next four time slots to maintain diversity order of 8 with, however, code rate 1/2 (4 symbols over 8 time slots). In the second scenario, we transmit a 4×4 QO-STBC codeword over the first four time slots and then transmit a new 4×4 QO-STBC codeword over the next four time slots to maintain code rate of 1 (8 symbols over 8 time slots) with, however, diversity order 4.

The elements of the channel matrices, $h_{1_{i,j}}$ in $\mathbf{H}_1$ and $h_{2_{i,j}}$ in $\mathbf{H}_2$, are correlated and generated as follows:

$$h_{1_{i,j}} \sim \mathcal{CN}(0,1) \quad \text{and } h_{2_{i,j}} = p h_{1_{i,j}} + \sqrt{1-p^2}\, z_{i,j},\ i = 1, \ldots, N_t,\ j = 1, \quad (233)$$

where $z_{i,j} \sim \mathcal{CN}(0,1)$ and p is the correlation coefficient ($\mathcal{CN}$ stands for complex Gaussian random variable). In Fig. 1, we plot the block-error-rate as a function of the received signal-to-noise-ratio (SNR) for (i) our 4-antenna codeword transmission scheme in (195), (ii) transmission rate 1/2, diversity order 8 transmission of the 4×4 QO-STBC of [5], and (iii) transmission rate 1, diversity order 4, 4×4 QO-STBC. We consider three channel fading correlation scenarios, $p = 0$, $p = 0.5$, and $p = 0.8$. For rate 1 codewords, we select the symbols from a 4-QAM constellation, while for rate 1/2 codewords the symbols are chosen from a 16-QAM constellation to maintain equal spectral efficiency for all transmission schemes. Under diversity product minimization, the rotation angles for our proposed codeword are $\{\phi, \theta\} = \{37.9, 21.4\}$, while for the 4×4 QO-STBC codeword, the rotation angle is $\pi/4$ as calculated in [5]. Since the 4×4 QO-STBC has only two unique eigenvalues, the angle of $\pi/4$ is also PEP-bound optimal (not the case, however, for the proposed 4-transmit-antenna transmission scheme).

From Fig. 31, we observe a substantial gain in performance achieved by transmitting the proposed 8×8 codeword over four antennas when compared with the two other 4×4 QO-STBC schemes. The best achievable performance from the 4×4 QO-STBC codeword of [5] is the direct rate 1, diversity order 4 transmission, which the proposed transmission scheme outperforms handily even in the extreme scenario of 80% channel correlation. In fact, to that respect it may be worth noting that our matrices $\mathbf{X}_1$ and $\mathbf{X}_2$ may not need to be transmitted directly one after the other in time. Separating the transmissions of the two codeword blocks over several time-slot blocks (block interleaving) may help reduce the effective coefficient value of p when allowed.

Case 2: Eight Transmit Antennas

We now evaluate the performance of 8×8 QO-STBC in (196) under 8-element antenna transmission and minimum eigenvalue CR optimization by (221), diversity product CR optimization by (218), and the proposed direct maximum PEP-bound CR optimization by (223). In Fig. 32, we plot the block-error-rate versus SNR when the symbols are chosen from a 4-QAM constellation. For direct PEP-bound optimization of ϕ, θ, we solve for A to obtain a received SNR of 20dB. We observe that the rotation angles that maximize the diversity product and the rotation angles that minimize the maximum PEP bound provide the best results, with the latter having indeed better performance. The exact angle values are shown in Table IV (along with the resulting diversity product and minimum eigenvalue).

In Fig. 33, we repeat the studies of Fig. 2 for symbols chosen from an 8-QAM non-rectangular constellation [5]. To obtain the PEP-bound optimal ϕ, θ, values we solve for A that corresponds to received SNR of 30dB. Again, all calculated values are given in Table IV. For reference purposes, we include in our comparisons the 8×8 single-symbol decodable STBC in [7]. Since the code in [7] contains only two unique eigenvalues the rotation angle of $tan^{-1}(1/2)$ is PEP-bound optimal for that code; since its rate is 3/4, we select symbols from a 16-QAM constellation to ensure equal spectral efficiency for all codewords under comparison. Our PEP-bound optimized codeword in (196) offers a gain of about 1 dB over the single-symbol decodable STBC in [7]. The minimum eigenvalue optimized version performs almost similarly well. As argued in Section IV.C, due to decreased values of the minimum eigenvalues as compared to the 4-QAM scenario, the maximum diversity (eigenvalue) product optimized system seems to lose diversity over the operable SNR range. Similar performance loss was also observed in [10] when the rotation angles were chosen to maximize the diversity product.

F. Conclusions

We proposed an alternative representation of the 8×8 two-symbol decodable quasi-orthogonal space-time block code (QO-STBC) that can be used on both 8 and 4-transmit-antenna systems. For the 8-transmit-antenna case, we derived three different sets of rotation angle values: maximum diversity-product optimal, maximum minimum-eigenvalue optimal, and minimum maximum-pairwise-error-probability-bound (PEP) optimal.

Most importantly, the proposed codeword doubles the transmit diversity order of a 4-transmit-antenna system. By obtaining new expressions for the PEP-upper-bound for correlated channels we were able to find rotation angles that maximize the diversity product to 4-antenna transmission systems and also proved that the rotation angles are independent of the correlation coefficient. As a by-product, we showed that for the proposed codeword, maximization of the sum of eigenvalues is an irrelevant/non-applicable criterion (for both 8 and 4-antenna transmissions).

Appendix: Derivation of the PEP-upper-bound in (229)

The PEP for a fixed channel realization $\mathbf{H}_e$ is given by [12]

$$Pr(\mathbf{X} \rightarrow \widetilde{\mathbf{X}}|\mathbf{H}_e) = Q\left(\sqrt{\frac{A}{2N_t}}\|\Delta\mathbf{X}\mathbf{H}_e\|_F\right) \tag{234}$$

where $Q(x) = \frac{1}{\sqrt{2\pi}}\int_x^\infty e^{-\frac{y^2}{2}}dy$ and $\Delta\mathbf{X} \stackrel{\triangle}{=} \mathbf{X} - \widetilde{\mathbf{X}}$. Using the approximation $Q(x) \leq \frac{1}{2}e^{-\frac{x^2}{2}}$ we have

$$Pr(\mathbf{X} \rightarrow \widetilde{\mathbf{X}}|\mathbf{H}_e) \leq \frac{1}{2}e^{-\frac{A}{4N_t}\|\Delta\mathbf{X}\mathbf{H}_e\|_F^2}. \tag{235}$$

To evaluate $Pr(\mathbf{X} \rightarrow \widetilde{\mathbf{X}})$ we observe that the channel coefficients are independent and identically distributed (i.i.d) across receive antenna space (columns of $\mathbf{H}_e$ are i.i.d) and

$$\begin{aligned} E_{\mathbf{H}}\{Pr(\mathbf{X} \rightarrow \widetilde{\mathbf{X}})\} &\leq \tfrac{1}{2}E_{\mathbf{H}}\{\textstyle\prod_{j=1}^{N_r} e^{-\frac{A}{4N_t}\|\Delta\mathbf{X}\mathbf{h}_{e_j}\|^2}\} \\ &= \tfrac{1}{2}\left(E_{\mathbf{H}}\{e^{-\frac{A}{4N_t}\|\Delta\mathbf{X}\mathbf{h}_{e_j}\|^2}\}\right)^{N_r} \end{aligned} \tag{236}$$

where $E_{\mathbf{H}}\{\cdot\}$ is the expectation operator over the channel coefficients and $\mathbf{h}_{e_j}, j = 1, \ldots, N_r$, are the columns of $\mathbf{H}_e$. Correlation in space among the four real antennas and the four virtual antennas is given by (199) and denoted by $\mathbf{R}_s$. Performing Cholesky decomposition on $\mathbf{R}_s = \mathbf{Q}\mathbf{Q}^H$, we obtain $\mathbf{h}_{e_j} = \mathbf{Q}\mathbf{v}_j$ where $\mathbf{v}_j \sim CN(0, \mathbf{I}_8)$. From (236) we have

$$\|\Delta\mathbf{X}\mathbf{h}_{e_j}\|^2 = \mathbf{h}_{e_j}^H\Delta\mathbf{X}^H\Delta\mathbf{X}\mathbf{h}_{e_j} = \mathbf{v}_j^H\mathbf{Q}^H\Delta\mathbf{X}^H\Delta\mathbf{X}\mathbf{Q}\mathbf{v}_j.$$

Performing eigen-decomposition on $\mathbf{Q}^H\Delta\mathbf{X}^H\Delta\mathbf{X}\mathbf{Q}$, it can be shown [12]

$$Pr(\mathbf{X} \rightarrow \widetilde{\mathbf{X}}) \leq \frac{1}{2}\left(\prod_{i=1}^{R}\left\{\frac{1}{1+\frac{A\Lambda_i}{4N_t}}\right\}\right)^{N_r} \tag{237}$$

where Λ_i are the eigenvalues of $\mathbf{Q}^H\Delta\mathbf{X}^H\Delta\mathbf{X}\mathbf{Q}$. Since $eig(\mathbf{Q}^H\Delta\mathbf{X}^H\Delta\mathbf{X}\mathbf{Q}) = eig(\mathbf{Q}\mathbf{Q}^H\Delta\mathbf{X}^H\Delta\mathbf{X}) = eig(\mathbf{R}_s\Delta\mathbf{X}^H\Delta\mathbf{X}) = eig(\Delta\mathbf{X}\mathbf{R}_s\Delta\mathbf{X}^H)$ [15], thus we have the PEP-upper-bound in (229).

References

[1] V. Tarokh, H. Jafarkhani, and A. R. Calderbank, "Space-time block codes from orthogonal designs," *IEEE Trans. Inf. Theory*, vol. 45, pp. 1456-1467, May 1999.

[2] O. Tirkkonen, A. Boariu, and A. Hottinen, "Minimal non-orthogonality rate 1 space-time block code for 3+ Tx antennas," in *Proc. IEEE 6th Int. Symp. Spread-Spectrum Techniques and Applications (ISSSTA 2000)*, Parsippany, NJ, Sept. 2000, pp. 429-432.

[3] H. Jafarkhani, "A quasi-orthogonal space-time block code," *IEEE Trans. Commun.*, vol. 49, pp. 1-4, Jan. 2001.

[4] C. B. Papadias and G. J. Foschini, "Capacity-approaching space-time codes for systems employing four transmitter antennas," *IEEE Trans. Inf. Theory*, vol. 49, pp. 726-732, Mar. 2003.

[5] Weifeng Su and X. G. Xia, "Signal constellations for quasi-orthogonal space-time block codes with full diversity," *IEEE Trans. Inform. Theory*, vol. 50, pp. 2331-2347, Oct. 2004.

[6] N. Sharma and C. B. Papadias, "Improved quasi-orthogonal codes through constellation rotation," *IEEE Trans. Commun.*, vol. 51, pp. 332-335, Mar. 2003.

[7] Z. A. Khan, B. S. Rajan, and M. H. Lee, "Rectangular co-ordinate interleaved orthogonal designs," in *Proc. IEEE GLOBECOM*, San Francisco, CA, Dec. 2003, vol. 4, pp. 2004-2009.

[8] C. Yuen, Y. L. Guan, and T. T. Tjhung, "Quasi-orthogonal STBC with minimum decoding complexity," *IEEE Trans. Wireless Commun.*, vol. 4, pp. 2089-2094, Sept. 2005.

[9] N. Sharma and C. B. Papadias, "Full rate full diversity linear quasi-orthogonal space-time codes for any transmit antennas," *EURASIP Journ. Applied Signal Proc.*, pp. 1246-1256, Aug. 2004.

[10] Z. A. Khan, M. H. Lee and, B. S. Rajan, "A rate-one full-diversity quasi-orthogonal design for eight Tx antennas," *Internal Report, TR-PME-2002-15*, available at http://pal.ece.iisc.ernet.in/PAM/tech_rep02.html.

[11] C. Yuen, Y. L. Guan, and T. T. Tjhung, "A class of four-group quasi-orthogonal STBC achieving full rate and full diversity for any number of antennas," in *Proc. IEEE Intl. Symp. on Personal, Indoor and Mobile Radio Commun. (PIMRC)*, Berlin, Germany, Sept. 2005, vol. 3, pp. 1683-1687.

[12] V. Tarokh, H. Jafarkhani, and A. R. Calderbank, "Space-time codes for high data rate wireless communication: performance criterion and code construction," *IEEE Trans. Inf. Theory*, vol. 44, pp. 744-765, Mar. 1998.

[13] J. Yuan, Z. Chen, B. Vucetic, and W. Firmanto, "Performance and design of space-time coding in fading channels," *IEEE Trans. Commun.*, vol. 51, pp. 1991-1996, Dec. 2003.

[14] Weifeng Su, Z. Safar, and K. J. R. Liu, "Diversity analysis of space-time modulation over time-correlated Raleigh fading channels," *IEEE Trans. Inf. Theory.*, vol. 50, pp. 1832-1839, Aug. 2004.

[15] D. Carlson, C. R. Johnson, D. Lay and A. D. Porter, "Gems of Exposition in Elementary Linear Algebra," *College Math. Journal*, vol. 23, no. 4, pp. 299-303, Sept. 1992.

TABLE IV
OPTIMAL ANGLES

QAM	Criterion	(ϕ, θ)	Diversity Product	Min. Eigenvalue
4	Diversity Product	$(37.9, 21.4)$	0.1747	0.0093
4	Min. Eigenvalue	$(30.9, 13.3)$	0.1623	0.0524
4	Max. PEP Bound	$(28.5, 40)$	0.1352	0.0112
8	Diversity Product	$(tan^{-1}(2)/2,$ $tan^{-1}(1/2)/2)$	0.1071	2.35×10^{-4}
8	Min. Eigenvalue	$(3, tan^{-1}(2))$	0.0732	0.0022
8	Max. PEP Bound	$(7.2, 25.1)$	0.0792	2.7×10^{-4}

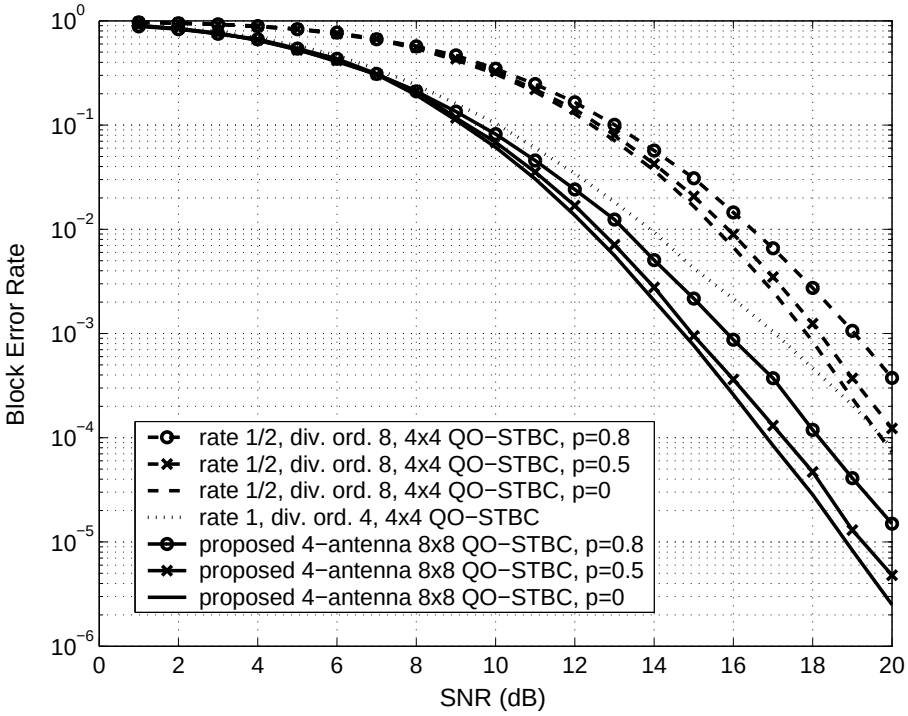

Fig. 31: Block-error-rate versus SNR (4-transmit-antenna system).

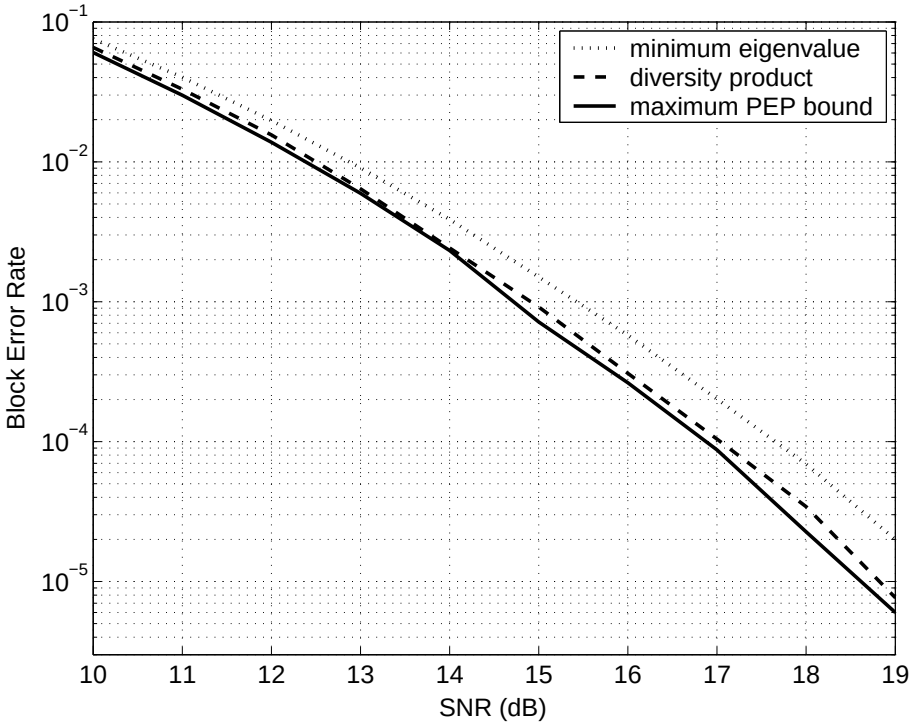

Fig. 32: Block-error-rate versus SNR for 4-QAM constellation (8-transmit-antenna system).

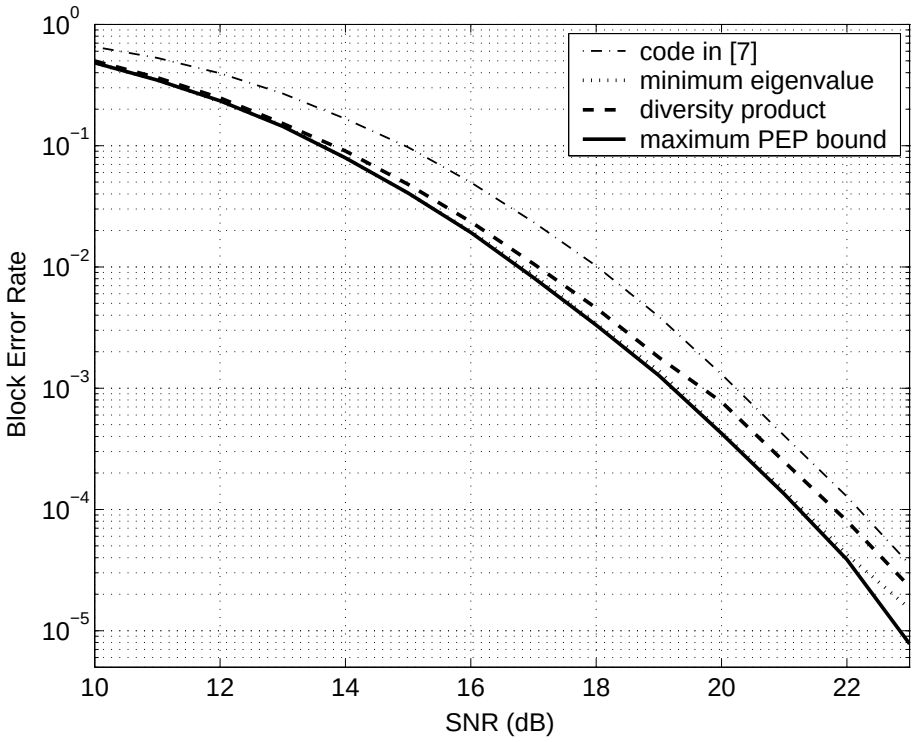

Fig. 33: Block-error-rate versus SNR for non-rectangular 8-QAM constellation and 16-QAM for the rate 3/4 code in [7] (8-transmit-antenna system).

XI. Code-Division MAC in Wireless Sensor Networks by Adaptive Binary Signature Design

This work has been presented at the 2007 SPIE Defense and Security Symposium, Orlando, FL.

Wireless sensor networks (WSN) are characterized by their dense and large node population, severe energy constraints and asymmetric many-to-one data flows [1]−[4] . In terms of node multiplexing for efficient medium sharing, the distributed, decentralized nature and objectives of sensor networks do not favor time-division multiple-access (TDMA) developments. Similarly, frequency-division multiple-access (FDMA), would require broad frequency tuning capabilities of sensor transceivers and may be used for control and data channel separation only. On the other hand, code-division multiple-access (CDMA) seems to serve the particular needs of wireless sensor networks well.

In this work, we focus on CDMA channel design and allocation schemes which allow many sensor nodes to transmit simultaneously over the common shared medium and possibly collaborate with each other. The problem of CDMA signature set optimization over the real/complex field was studied in [5]−[8] . In the context of optimum design of binary signature sets, past work includes the recent developments in [9]−[12] that provide the first designs of binary signature sets that exhibit minimum total-squared-correlation (TSC) for almost all signature lengths and set sizes. The performance of other non-minimum TSC binary signature sets was studied in [13],[14] . In this work, we deal with the problem of pursuing dynamic code division MAC operations via fully adaptive design of binary spreading codes that maximize the signal-to-interference-plus-noise ratio (SINR) at the output of the maximum-SINR receiver. The optimal code is a function of the disturbance autocovariance matrix and its evaluation over the binary field is NP-hard.

A. Code-divison MAC: CDMA Channel Design and Allocation

We consider code-division MAC along the following basic steps (Fig. 34). We note that our focus is on CDMA channel design and allocation; other network services such as organization, synchronization and routing are built at a higher layer.

In step 1, node 1 uses an arbitrarily chosen signature and broadcasts a signal that indicates intention to transmit. The broadcast signal is received by node 2 in the presence of other node interference and noise. Node 2 sends an acknowledgement to node 1 indicating availability to receive (and possibly process and forward) future messages from node 1. In this acknowledgement, node 2 submits an "optimally" designed binary signature ($\mathbf{s}_{opt}$). Subsequent communication from node 1 to node 2 (step 3) is accomplished by means of $\mathbf{s}_{opt}$.

Identifying an appropriate signature at step 2 allows subsequent data transmission/reception that is impaired the least by the present disturbance (other

node interference and noise). The above basic one-hop transmission is generalized later in this paper to various multi-hop network configurations and the performance of such schemes is evaluated in the simulations Section.

In this work we are interested in designing binary signature/spreading codes that maximize the SINR of the output of the max SINR receiver which is an NP-hard optimization problem. We begin our developments by introducing formally the signal model and pertinent notation.

We consider a multinode CDMA-type environment where K nodes transmit asynchronously, simultaneously in frequency and time, over different, in general, multipath fading channels.

Assuming synchronization with the signal of the node of interest k, $k = 1, 2, \ldots, K$ upon carrier demodulation, chip matched-filtering and sampling at the chip rate over a presumed multipath extended data bit period of $L + N - 1$ chips, where L is the signature length and N is the number of resolvable multipaths, the received data vector $\mathbf{r}_k(m) \in \mathbb{C}^{L+N-1}$ takes the following general form,

$$\mathbf{r}_k(m) = \sqrt{E_k}\, b_k(m)\mathbf{H}_k\mathbf{s}_k + \mathbf{z}_k + \mathbf{i}_k + \mathbf{n}_k, \quad m = 0, 1, \ldots \quad . \tag{238}$$

In (238), with respect to kth node, $k = 1, 2, \ldots, K$, $b_k(m) \in \{\pm 1\}$ is the mth data bit, $m = 0, 1, 2, \ldots$, E_k represents transmitted energy per bit period, $\mathbf{H}_k \in \mathbb{C}^{(L+N-1)\times L}$ is the node k channel matrix of the form,

$$\mathbf{H}_{k\ (L+N-1)\times L} \triangleq \begin{bmatrix} h_{k,1} & 0 & \ldots & 0 \\ h_{k,2} & h_{k,1} & \ldots & 0 \\ \vdots & \vdots & & \vdots \\ h_{k,N} & h_{k,N-1} & & 0 \\ 0 & h_{k,N} & & h_{k,1} \\ \vdots & \vdots & & \vdots \\ 0 & 0 & \ldots & h_{k,N} \end{bmatrix} \tag{239}$$

with entries $h_{k,n}, n = 1, \ldots, N$, considered as complex Gaussian random variables to model fading phenomena. $\mathbf{s}_k \in \{\pm 1\}^L$ is the signature vector to be designed. $\mathbf{z}_k \in \mathbb{C}^{L+N-1}$ represents comprehensively multiple-access-interference (MAI) to node k by the other $K - 1$ nodes. $\mathbf{i}_k \in \mathbb{C}^{L+N-1}$ denotes multipath induced inter-symbol-interference (ISI) to node k by its own signal, and $\mathbf{n}_k$ is a zero-mean additive Gaussian noise vector with autocorrelation matrix $\sigma^2\mathbf{I}_{L+N-1}$.

Information bit detection of node k is achieved via linear minimum-mean-square-error (MMSE) filtering as follows (for one-shot detection the data bit index can be suppressed),

$$\hat{b}_k = sgn\left(Re\left\{\mathbf{w}_{MMSE,k}^H\mathbf{r}_k\right\}\right), \quad k = 1, 2, \cdots, K \tag{240}$$

where $\mathbf{w}_{MMSE,k} = c\mathbf{R}_k^{-1}\mathbf{H}_k\mathbf{s}_k \in \mathbb{C}^{L+N-1}$, $\mathbf{R}_k \triangleq E\{\mathbf{r}_k\mathbf{r}_k^H\}$, $c > 0$, $Re\{\cdot\}$ denotes the real part of a complex number, and $E\{\cdot\}$ represents statistical ex-

pectation. We recall that the output SINR of the filter $\mathbf{w}_{MMSE,k}$ is given by

$$\begin{aligned} SINR_{MMSE,k}(\mathbf{s}_k) &= \frac{E\left\{\left|\mathbf{w}_{MMSE,k}^H\left(\sqrt{E_k}b_k\mathbf{H}_k\mathbf{s}_k\right)\right|^2\right\}}{E\left\{\left|\mathbf{w}_{MMSE,k}^H\left(\mathbf{z}_k+\mathbf{i}_k+\mathbf{n}_k\right)\right|^2\right\}} \\ &= E_k\mathbf{s}_k^H\mathbf{H}_k^H\tilde{\mathbf{R}}_k^{-1}\mathbf{H}_k\mathbf{s}_k \end{aligned} \tag{241}$$

where

$$\tilde{\mathbf{R}}_k \stackrel{\triangle}{=} E\left\{\left(\mathbf{z}_k+\mathbf{i}_k+\mathbf{n}_k\right)\left(\mathbf{z}_k+\mathbf{i}_k+\mathbf{n}_k\right)^H\right\} \tag{242}$$

is the autocorrelation matrix of the compound channel disturbance. Since the effect of ISI is practically negligible for CDMA communication systems, in the rest of this paper, we will approximate $\tilde{\mathbf{R}}_k$ by $\tilde{\mathbf{R}}_k \approx E\left\{\left(\mathbf{z}_k+\mathbf{n}_k\right)\left(\mathbf{z}_k+\mathbf{n}_k\right)^H\right\}$. Our objective is to find the signature $\mathbf{s}_k \in \{\pm 1\}^L$ that optimizes (maximizes) $SINR_{MMSE,k}$, i.e.

$$\mathbf{s}_{k,opt} = arg \max_{\mathbf{s}\in\{\pm 1\}^L} \mathbf{s}^H\mathbf{H}_k^H\tilde{\mathbf{R}}_k^{-1}\mathbf{H}_k\mathbf{s}. \tag{243}$$

In the rest of this section we present an algorithm that performs exactly this optimization and, upon eigenvector decomposition, exhibits linear complexity in the signature length.

For notational simplicity we define the $L \times L$ matrix

$$\mathbf{Q}_k \stackrel{\triangle}{=} \mathbf{H}_k^H\tilde{\mathbf{R}}_k^{-1}\mathbf{H}_k \tag{244}$$

Then, the SINR-optimum sequence (cf. (243)) is given by

$$\mathbf{s}_{k,opt} = arg \max_{\mathbf{s}\in\{\pm 1\}^L} \mathbf{s}^H\mathbf{Q}_k\mathbf{s}. \tag{245}$$

The optimization problem in (245) is equivalent to

$$\mathbf{s}_{k,opt} = arg \max_{\mathbf{s}\in\{\pm 1\}^L} \mathbf{s}^H\mathbf{Q}_{kr}\mathbf{s} \tag{246}$$

where $\mathbf{Q}_{kr}$ denotes the real part of the complex, in general, hermitian matrix $\mathbf{Q}_k$ ($\mathbf{Q}_{kr} \stackrel{\triangle}{=} Re\{\mathbf{Q}_k\}$).

If we relax, for a moment, our constraint that the signature (sequence) alphabet is binary and assume, instead, that $\mathbf{s}$ is real-valued ($\mathbf{s} \in \mathbb{R}^L$) with same norm ($\mathbf{s}^H\mathbf{s} = L$), then the corresponding optimization problem becomes

$$\mathbf{s}_{k,opt}^{(r)} = arg \max_{\mathbf{s}\in\mathbb{R}^L, \mathbf{s}^H\mathbf{s}=L} \mathbf{s}^H\mathbf{Q}_{kr}\mathbf{s} \tag{247}$$

where the superscript (r) indicates that $\mathbf{s}_{k,opt}^{(r)}$ is real-valued. The optimization in (247) is carried over a hypersphere in the $\mathbb{R}^L$ space of radius L and centered at the origin.

Let $\{\mathbf{q}_{k,1}, \mathbf{q}_{k,2}, \cdots, \mathbf{q}_{k,L}\}$ be the L eigenvectors of $\mathbf{Q}_{kr}$ and $\{\lambda_{k,1}, \lambda_{k,2}, \cdots, \lambda_{k,L}\}$, the corresponding eigenvalues such that $\lambda_{k,1} \geq \lambda_{k,2} \geq \cdots \geq \lambda_{k,L}$. The real-valued sequence that maximizes the right-hand-side of (247) is well known and equal to the eigenvector that corresponds to the maximum eigenvalue of the matrix $\mathbf{Q}_{kr}$, i.e.

$$\mathbf{s}_{k,opt}^{(r)} = arg \max_{\mathbf{s}\in\mathbb{R}^L, \mathbf{s}^H\mathbf{s}=L} \mathbf{s}^H \mathbf{Q}_{kr} \mathbf{s} = \mathbf{q}_{k,1}. \tag{248}$$

Since $\{\mathbf{q}_{k,2}, \mathbf{q}_{k,3}, \cdots, \mathbf{q}_{k,L}\}$ are orthogonal to $\mathbf{q}_{k,1}$ by definition, the $L-1$ lines defined by

$$\mathbf{q}_{k,1} + \rho \mathbf{q}_{k,i}, \quad i = 2, \cdots, L, \quad \rho \in \mathbb{R} \tag{249}$$

lie on the plane that is tangent to the searching hypersphere, pass through the real maximizer $\mathbf{q}_{k,1}$, and define mutually orthogonal directions of least decrease in the cost function $\mathbf{s}^H \mathbf{Q}_{kr} \mathbf{s}$, $\mathbf{s} \in \mathbb{R}^L$ from the optimum point $\mathbf{s}_{k,opt}^{(r)} = \mathbf{q}_{k,1}$. Projection of the above least decrease lines onto the searching hypersphere results in the slowest descent cords given by

$$\frac{\mathbf{q}_{k,1} + \rho \mathbf{q}_{k,i}}{\sqrt{1+\rho^2}}, \quad i = 2, \cdots, L, \quad \rho \in \mathbb{R} \quad . \tag{250}$$

The slowest descent cords in (250) trace the searching hypersphere, extend from $-\mathbf{q}_{k,i}$ to $\mathbf{q}_{k,i}$, $i = 2, \cdots, L$, and pass through the optimum point $\mathbf{s}_{k,opt}^{(r)}$. On these cords, the function $\mathbf{s}^H \mathbf{Q}_{kr} \mathbf{s}$, $\mathbf{s} \in \mathbb{R}^L$, takes values in $[\lambda_{k,i} L,\ \lambda_{k,1} L]$ respectively. Our objective is to identify the binary sequences that are closest in the l_2 sense to the above least decrease cords. Use of least-decrease-driven search for finite-alphabet solutions has been considered in [15] to convert general maximum likelihood estimates to maximum likelihood decision. Some important observations now follow.

(i) It is straightforward to show that for any given $i \in \{2, 3, \cdots, L\}$, the binary sequences that are closest in the l_2 sense to the cord $\frac{\mathbf{q}_{k,1}+\rho\mathbf{q}_{k,i}}{\sqrt{1+\rho^2}}$, $\rho \in \mathbb{R}$, can be expressed as $sgn(\mathbf{q}_{k,1} + \rho \mathbf{q}_{k,i})$. The set of all binary signatures of the form $sgn(\mathbf{q}_{k,1} + \rho \mathbf{q}_{k,i})$, $\rho \in \mathbb{R}$, has cardinality $L+1$.

(ii) The l_2 distance measure of a binary sequence $\mathbf{x} \in \{\pm 1\}^L$ and a real sequence $\mathbf{y} \in \mathbb{R}^L$ is conventionally defined as $\sum_{i=1}^{L} (x_i - y_i)^2$, where x_i and y_i, $i = 1, \cdots, L$, are the binary and real elements of the vectors $\mathbf{x}$ and $\mathbf{y}$ respectively.

(iii) The binary sequence $\mathbf{x} \in \{\pm 1\}^L$ that is closest in the l_2 sense to a given real sequence $\mathbf{y} \in \mathbb{R}^L$ has elements $x_i = sgn(y_i)$, $i = 1, \cdots, L$.

(iv) The binary sequence $\mathbf{x} \in \{\pm 1\}^L$ that is closest to a cord, e.g. $\frac{\mathbf{q}_{k,1}+\rho\mathbf{q}_{k,i}}{\sqrt{1+\rho^2}}$, $\rho \in \mathbb{R}$, $i \in \{2, \cdots, L\}$, is the sequence that satisfies $\min_{\mathbf{x}\in\{\pm1\}^L} \|\mathbf{x} - (\frac{\mathbf{q}_{k,1}+\rho\mathbf{q}_{k,i}}{\sqrt{1+\rho^2}})\|_2$, $\forall \rho \in \mathbb{R}$, where $\|\cdot\|_2$ denotes l_2-norm.

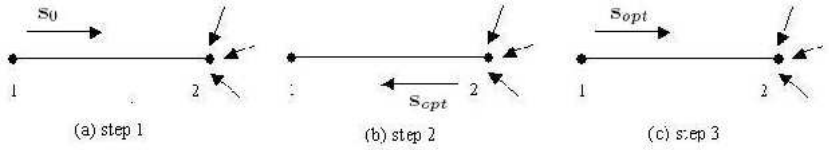

Fig. 34: Code division MAC.

Our proposed binary signature search algorithm is outlined below.

Algorithm
For $i = 2, \cdots, P$ $(P \leq L)$ do :

1. Divide the range of ρ into non-overlapping intervals such that adjacent intervals have opposite signs in exactly one coordinate. The intervals are defined by the points

$$\rho_n = q_{k,1,n}/q_{k,i,n}, \quad n = 1, \cdots, L, \tag{251}$$

where $q_{k,i,n}$, $n = 1, \cdots, L$, is the n-th element of the vector $\mathbf{q}_{k,i}$. Then, arrange $\{\rho_1, \rho_2, \cdots, \rho_L\}$ in ascending order $\{\rho'_1, \rho'_2, \cdots, \rho'_L\}$, $\rho'_1 < \rho'_2 < \cdots < \rho'_L$.

Find the index, say J, of the first positive element in the ordered sequence $\rho'_1, \rho'_2, \cdots, \rho'_L$, i.e. $\rho'_{J-1} < 0 < \rho'_J$, $J \in \{1, 2, \cdots, L\}$.

2. Find the binary sequence that is closest to the line $\mathbf{q}_{k,1} + \rho \mathbf{q}_{k,i}$ for each interval of ρ, i.e. for $\rho \in (-\infty, \rho'_1)$,$(\rho'_1, \rho'_2)$,$\cdots$,$(\rho'_{L-1}, \rho'_L)$, (ρ'_L, ∞). There are $L+1$ binary sequences in total (denoted as $\mathbf{s}_k^0, \mathbf{s}_k^1, \cdots, \mathbf{s}_k^L$) that can be computed recursively,

$$\mathbf{s}_k^0 = sgn[\mathbf{q}_{k,1}] \tag{252}$$

$$\mathbf{s}_k^{l+1} = \mathbf{s}_k^l - 2s_{k,J+l}^0 \mathbf{e}_{J+l}, \quad l = 0, 1, \cdots, L - J \tag{253}$$

$$\mathbf{s}_k^l = \mathbf{s}_k^{l+1} - 2s_{k,J+l}^0 \mathbf{e}_{J+l}, \quad l = -1, -2, \cdots, 1 - J \tag{254}$$

where $s_{k,J+l}^0$ is the $(J+l)$th element of $\mathbf{s}_k^0$ and $\mathbf{e}_{J+l}$ is the $(J+l)$-unit vector in $\mathbb{R}^L$.

3. Evaluate $SINR(\mathbf{s}_k^l)$ for each binary signature $\mathbf{s}_k^l$ returned by Step 2, $l = 0, \cdots, L$, and choose the binary signature that gives maximum SINR. ■

B. Simulation Studies

We consider five basic network configurations (Fig. 35(a)-(e)) to demonstrate the performance of our proposed code division MAC scheme.

In particular, Figs. 35(a) and 35(b) represent a one-hop and a two-hop one-to-one transmission, respectively. Figs. 35(c) and 35(d) represent a one-hop,

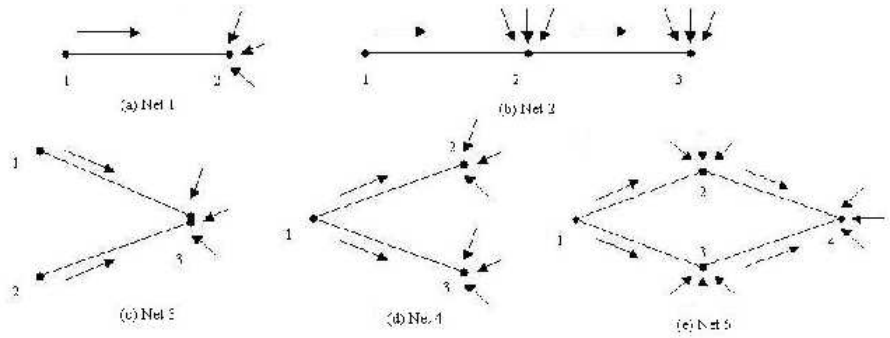

Fig. 35: Sensor network configurations.

two-to-one and a one-hop one-to-two transmission correspondingly, while Fig. 35(e) describes a 4-node network configuration where communication of nodes 1 and 4 is achieved via node 2 and 3 that simply decode and forward. In every network configuration, intended (desired) signals are received in the presence of other node interference and noise.

We compare the performance of the proposed signature optimization algorithm against the following benchmarks: *(i)* The maximum complex eigenvalue eigenvector of $\mathbf{Q}_k$, denoted in the figures as "complex max-EV", which is the theoretical maximum SINR signature solution over the complex, $\mathbb{C}^L$, field and *(ii)* the maximum real eigenvalue eigenvector of $\mathbf{Q}_k$, denoted as "real max-EV", which is the theoretical maximum SINR signature solution over the real, $\mathbb{R}^L$, field.

We consider the multipath DS-CDMA signal model of the previous section with spreading gain $L = 16$ and we assume the presence of $K = 8$ active nodes. Each node signal experiences $N = 3$ independent paths and the corresponding channel coefficients are assumed to be zero-mean complex Gaussian random variables of equal energy. Then, following the notation of the previous section, the total average received SNR for node k is,

$$SNR_k \stackrel{\triangle}{=} \frac{E_k \sum_{n=1}^{N} E\left\{|h_k(n)|^2\right\}}{\sigma^2} = \frac{E_k E\left\{\|\mathbf{h}_k\|^2\right\}}{\sigma^2} \tag{255}$$

We set $SNR_{1-3} = 8dB$, $SNR_{4-6} = 9dB$, and $SNR_{7-8} = 10dB$. We initialize the signature set arbitrarily and execute each signature set design scheme sequentially node-after-node in what we call a *multinode adaptation cycle*. Several multinode adaptation cycles are carried out (all algorithms are seen to converge

in about three cycles). A fixed Walsh-Hadamard signature assignment is also included in the study to challenge, potentially, the notion of signature adaptivity. As we can see from Figs. 36-40, the static (non-adaptive or non-controlled) Walsh-Hadamard signature assignment exhibits rather poor performance, as expected, while the proposed adaptive binary signature design and assignment scheme performs very close to the theoretical complex-EV and real-EV benchmarks.

C. Conclusions

In this work we focused on the problem of CDMA channel design and allocation for code division MAC of wireless sensor networks operating in multipath fading environments. We considered binary signature alphabets and thus pursued digital signature optimization. We proposed and studied a suboptimal CDMA channel design and allocation algorithm that, upon eigenvector decomposition, exhibits linear computational complexity with respect to the signature length.

References

[1] L. F. Akyildiz, W. Su, Y. Sankarasubramaniam and E. Cayirci, "A survey on sensor networks," *IEEE Commun. Mag.*, vol. 40, pp. 102-114, Aug. 2002.

[2] K. Sohrabi, J. Gao, V. Ailawadhi, and G. J. Pottie, "Protocols for self-organization of a wireless sensor network," *IEEE Pers. Commun.*, pp. 16-27, Oct. 2000.

[3] T. van Dam and K. Langendoen, "An adaptive energy-efficient mac protocol for wireless sensor networks," *In Proceedings of ACM Conf. on Embedded Networked Sensor System*, Nov. 2003.

[4] W. Ye, J. Heidemann and D. Estrin, "An energy-efficient mac protocol for wireless sensor networks," *INFOCOM 2002*, Jun. 2002.

[5] L. R. Welch, "Lower bounds on the maximum cross correlation of signals," *IEEE Trans. Inform. Theory*, vol. IT-20, pp. 397-399, May 1974.

[6] P. Viswanath, V. Anantharam, and D. N. C. Tse, "Optimal sequences, power control, and user capacity of synchronous CDMA systems with linear MMSE multiuser receivers," *IEEE Trans. Inform. Theory*, vol. 45, pp. 1968-1983, Sept. 1999.

[7] C. Rose, S. Ulukus, and R. D. Yates, "Wireless systems and interference avoidance," *IEEE Trans. Wireless Comm.*, vol. 1, pp. 415-428, July 2002.

[8] J. Luo, S. Ulukus and A. Ephremides, "Optimal sequences and sum capacity of symbol asynchronous CDMA systems," *IEEE Trans. Inform. Theory*, vol. 51, pp. 2760-2769, Aug. 2005.

[9] G. N. Karystinos and D. A. Pados, "New bounds on the total squared correlation and optimum design of DS-CDMA binary signature sets," *IEEE Trans. Commun.*, vol. 51, pp. 48-51, Jan. 2003.

[10] C. Ding, M. Golin, and T. Kløve, "Meeting the Welch and Karystinos-Pados bounds on DS-CDMA binary signature sets," *Designs, Codes and Cryptography*, vol. 30, pp. 73-84, Aug. 2003.

[11] V. P. Ipatov, "On the Karystinos-Pados bounds and optimal binary DS-CDMA signature ensembles," *IEEE Comm. Letters*, vol. 8, pp. 81-83, Feb. 2004.

[12] G. N. Karystinos and D. A. Pados, "The maximum squared correlation, total asymptotic efficiency, and sum capacity of minimum total-squared-correlation binary signature sets," *IEEE Trans. Inform. Theory*, vol. 51, pp. 348-355, Jan. 2005.

[13] F. Vanhaverbeke and M. Moeneclaey, "Sum capacity of equal-power users in overloaded channels," *IEEE Trans. Inform. Theory*, vol. 53, pp. 228-233, Feb. 2005.

[14] F. Vanhaverbeke and M. Moeneclaey, "Binary signature sets for increased user capacity on the downlink of CDMA Systems," *IEEE Trans. Wireless Communications*, vol. 5, pp. 1795-1804, Jul. 2006.

[15] P. Spasojevic and C. N. Georghiades, "The slowest descent method and its application to sequence estimation," *IEEE Trans. Commun.*, vol. 49, pp. 1592-1604, Sept. 2001.

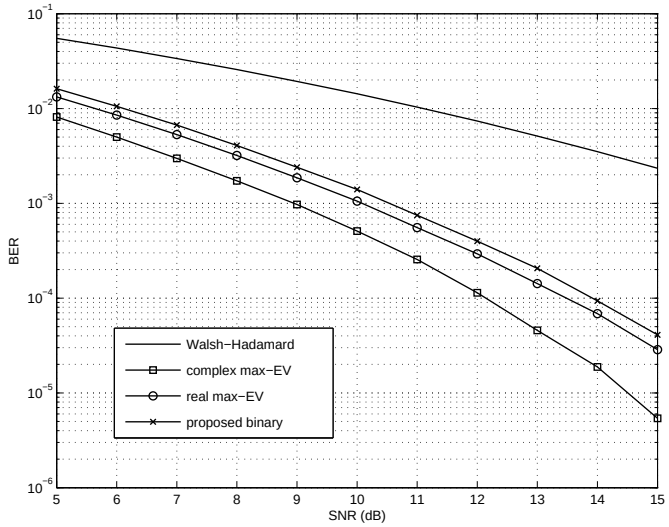

Fig. 36: Net 1: One-hop, one-to-one transmission (L=16, K=8)

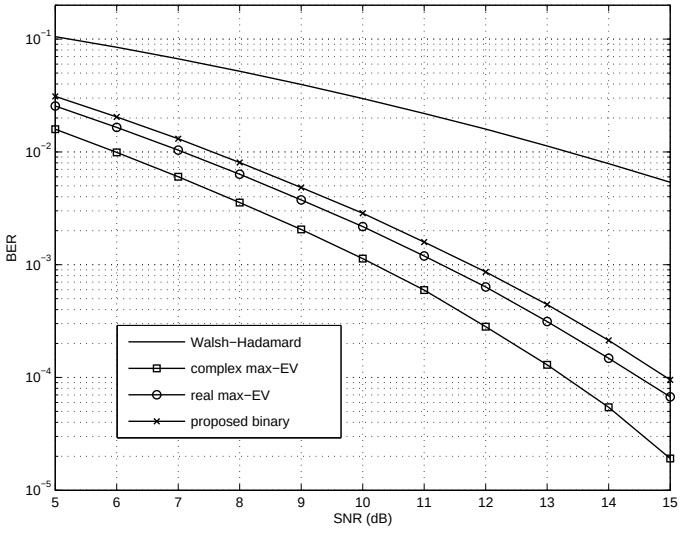

Fig. 37: Net 2: Two-hop, one-to-one transmission (L=16, K=8)

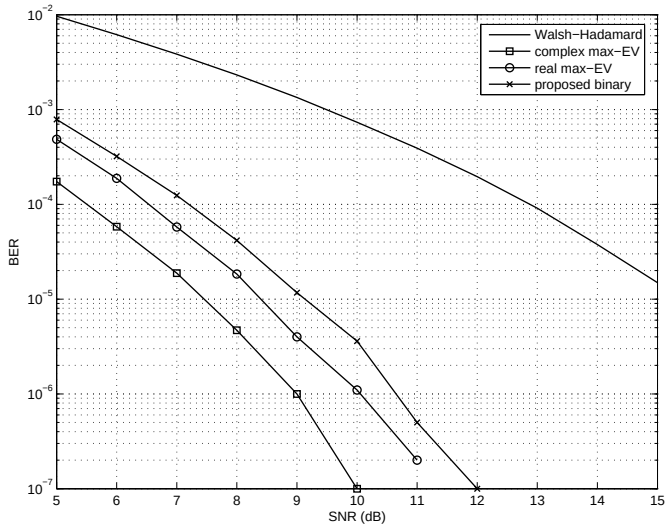

Fig. 38: Net 3: One-hop, two-to-one transmission (L=16, K=8)

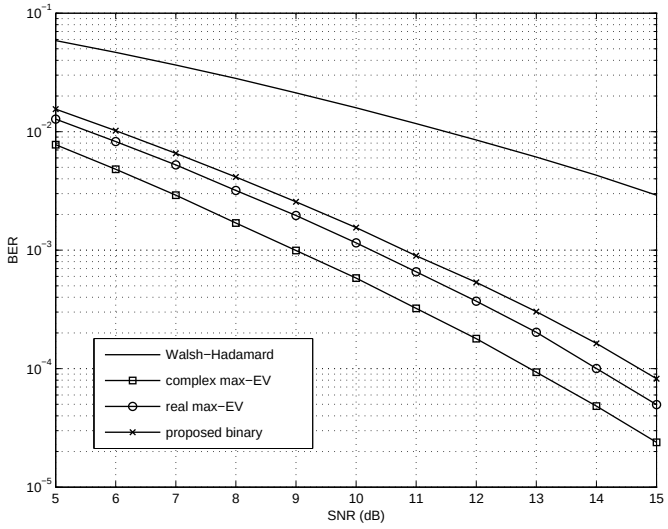

Fig. 39: Net 4: One-hop, one-to-two transmission (L=16, K=8)

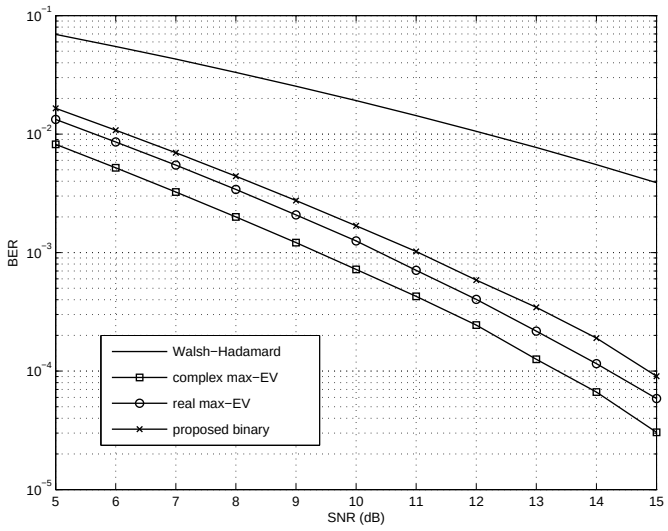

Fig. 40: Net 5: Four node configuration (two decode-and-forward nodes, L=16, K=8)